American Journal of Engineering Research (AJER)

www.ajer.org   ajer.research@gmail.com

CONTENTS

Volume-4 Issue-1

Research Paper   Open Access

"Distinct Revocable Data Hiding In Ciphered Image"

Anamika Patil[1], Mona Pounikar[2], Pooja Bafna[3], Pranjal Badgujar[4]

[1](Computer, University of Pune, India)[2](Computer, University of Pune, India)
[3](Computer, University of Pune, India)[4](Computer, University of Pune, India)

ABSTRACT: *This scheme proposes an authenticated and secure reversible data hiding in cipher images. Nowadays, more attention is paid to reversible data hiding in encrypted images, as the original cover can be reversibly recovered after embedded data is retrieved. In the first stage, the content owner encrypts the original image using an encryption key. Then, a data hider compresses the least significant bits (LSB's) of the encrypted image using a data hiding key to create space to store some additional data. Then, if a receiver has the data hiding key, he can extract the additional data from the encrypted image though he is unaware of the image content. If the receiver has the encryption key with him, then he can decrypt the data to obtain an image similar to the original image. If the receiver has both the data hiding key as well as the encryption key, then he can extract the additional data as well as he can recover the original content.*

KEYWORDS: *Encryption, Steganography, Data Hiding*.

I.   INTRODUCTION

Distinct revocable data hiding in ciphered image also means hiding data reversibly in encrypted image in separable manner. Nowadays data transmission over internet has increased tremendously so image security has become an important factor to be considered for e.g., video surveillance, confidential transmission, medical and military applications. As in medical field the necessity of fast and secure diagnosis is important in the medical world. To reduce the transmission time over network, the data compression is necessary. In the current trends of the world, the technologies have advanced and emerged so much that most of the individuals prefer using the internet as the primary medium to transfer data from one end to another across the world. There are many possible ways to transmit data using the internet: via emails, chats, etc. The data transition is made very simple, fast and accurate using the internet. However, one of the major problem with sending data over the internet is the security threat it poses i.e. the secret or personal data can be stolen or hacked in many ways. Therefore it is very important to take data security into consideration and a matter of concern, as it is one of the most essential factors that need attention during the process of data transferring. The protection of this multimedia data can be done with data hiding and encryption algorithms. In the current trends of the world, the technologies have advanced so much that most of the individuals prefer using the internet as the primary medium to transfer data from one end to another across the world. There are many possible ways to transmit data using the internet through emails, chats or other means.

Data security basically means protection of data from unauthorized users or hackers and providing high security to prevent data being modified. Therefore area of data security has gained more attention over the recent period of time due to the massive increase in data transfer rate over the internet. In order to improve the secret communication and security features in data transfers over the internet, many efficient techniques have been developed like: Cryptography and Steganography.Reversible data hiding (RDH) in images is a technique, in which we can recover the original cover losslessly after the embedded message is extracted. In order to provide security and privacy for images, encryption is an effective and popular means as it converts the original content to incomprehensible one which is not understood. There are some promising applications in RDH that can be applied to encrypted images. The process of extracting data from image requires compression of encrypted images and space for data embedding. Compression of encrypted data can be considered as source code with some information at the decoder, in which the practical method is to generate the compressed data in reversible manner by exploiting the syndromes of parity-check matrix of channel codes [4].In practical aspect, many RDH techniques have evolved in recent years which are helpful in many ways. A general framework have

been constructed for RDH. By first extracting compressible features of original image and then compressing them losslessly,

spare space can be created for embedding data. A more efficient method is dependent on difference expansion (DE) [5], in that the difference of each pixel group is expanded, and the least significant bits (LSBs) of the difference are all zero and can be used for embedding messages and data. The motivation of reversible data embedding can be considered as distortion-free data embedding. Though embedding some data will inevitably change the original content. Even a very small change in pixel values may not be desirable, especially in sensitive images, such as military and medical data. In such situations, every bit of information is important to be considered. Even a small change is going to affect the intelligence of the image, and the access to the original data is always required.

II. REVOCABLE DATA HIDING

Revocable data hiding also known as Reversible data hiding in images is a method that hides data in digital images for secret and secured communication through network. It is a technique to hide additional data into cover media in a reversible way so that the original cover content can be perfectly and accurately recovered after extraction of the hidden data. Traditionally, data hiding is used for secret and secured communication. In many applications that we use, the embedded carriers are encrypted so as to prevent the carrier from being analyzed to reveal the presence of the embedded information. Other applications could be used when the owner of the carrier might not want the other unauthorized person, including data hider, to know and reveal the content of the carrier before data hiding is actually done, such as military or confidential medical images. A major trend is minimizing the computational requirements for secure and secret multimedia distribution by selective encryption where only parts of the data are encrypted. Two levels of security are there for digital image encryption, they are: low level and high-level security encryption. In case of low level security encryption, the image which is encrypted has low visual quality compared to that of the original one, but the content of the image is still visible and easily understandable to the users. In the high-level security encryption, the content of image is completely scrambled and the image will be in random noise format. In this case, the image is not easily understandable to the users at all. Selective encryption aims at avoiding the encryption of all bits of a digital image and also ensures a secure encryption standard [5].

In our proposed method, we first empty out the memory space by embedding LSBs of some pixels into other pixels with a traditional RDH method and then apply encryption on the image, so the positions of these LSBs in the encrypted image can then be used to embed data. Not only does the proposed method separate data extraction from image decryption but also it achieves better performance in a different prospect that is real reversibility is realized, so that we can say data extraction and image recovery are error free. Most of the work on reversible data hiding focuses on the data embedding and data extracting on the plain spatial domain. But, in some applications, the administrator appends some additional message, such as the source information, notation of image or authentication data, inside the encrypted image though he does not know the original image content. And also it is hopeful that the original content should be recovered without any error after image decryption and message extraction on receiver side, that is, the original content must be error free.Reversible data embedding is a secret and secured communication channel since reversible data embedding can be used as a data carrier. Reversible data embedding, which is also called lossless data embedding, embeds data into a digital image in a reversible way. Interesting feature of reversible data embedding is the reversibility that is we can remove the embedded data so as to recover the original image. Reversible data embedding hides some data in a digital image in such a way that any authorized party can decode the hidden information and also recover the image to its original state.

III. EXISTING SYSTEM

In reversible data hiding method the image is compressed and encrypted by using the encryption key. The data to be hidden is embedded inside image by using the data hiding key. At the receiver end, the receiver first need to extract the image using the encryption key in order to extract the data and in order to extract the embedded data he will use a data hiding key. It is a serial process and is not a separable process. Steganography is said to be the art and science of writing hidden messages in such a way that no one, except for the sender and the authorized recipient, can detect the existence of the message. The word Steganography is evolved from Greek origin and it means "covered writing" meaning" protected", Usually, messages will appear to be something else like images or articles or shopping lists, the hidden message may be considered to be invisible ink between the visible lines of a private letter. It is a secure technique for long and secret data transmission. Steganography is the process of hiding some information into other sources of information like text or image so that it is not easily visible to the natural view. Any other person cannot recognize it. There are varieties of stenographic techniques that are available to hide the data depending upon the carriers that we are going to use.
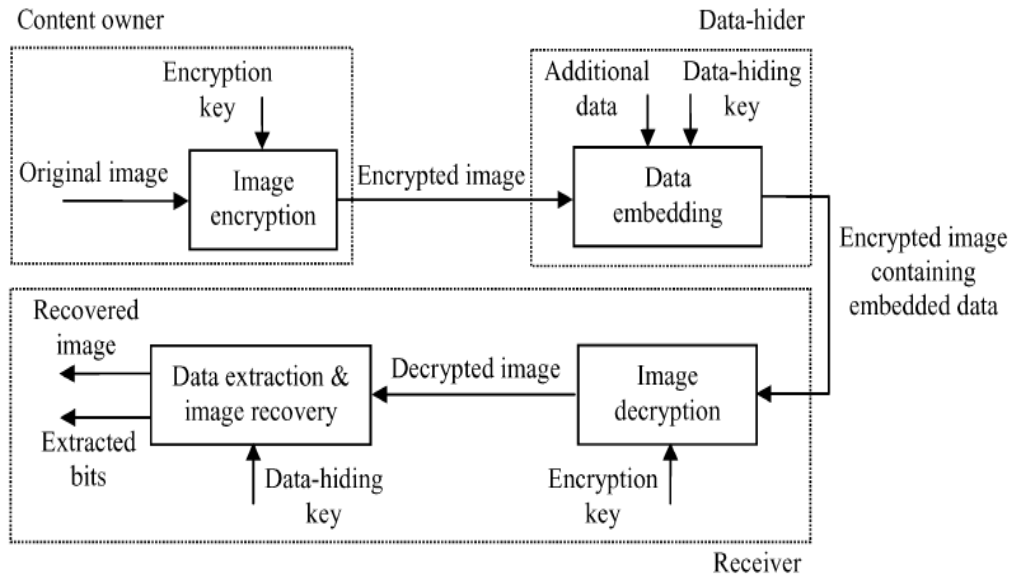
Fig. 1. Sketch of non-separable reversible data hiding in encrypted image.

In the existing system, the image is initially compressed and encrypted using the encryption key and the data which is to be hidden is embedded in to the image using the data hiding key. A content owner encrypts the original image by using an encryption key, the data-hider can then embed additional data into the encrypted image using a data-hiding key though he is not aware about the original one. An encrypted image that contains additional data, a receiver must first decrypt the image according to the encryption key, and then he can extract the additional embedded data and thus recover the original image according to the data-hiding key [2]. In this scheme data extraction is not separable from data decryption. In other way we can say that, the additional data must be extracted from the image which is decrypted, in order to know the principal content of original image before data extraction, and, if anyone does not have the data-hiding key but have the encryption key, then he cannot extract any data from the encrypted image containing additional data but he can decrypt the image as shown in Fig 1.

Disadvantages: The principal content of the image is revealed prior to data extraction.
If anyone has the data hiding key but not the encryption key then he cannot obtain any information from the encrypted image containing additional data.

IV. PROPOSED SCHEME
Our system will have some new features so as to overcome the above issues. Transactions will occur in a secured format between various clients over network. It provides flexibility to the user to transfer the data through the network very easily by compressing the large data in file. It will also recognize the user and provide the communication according to the security standards. The user who is going to receive the file will do the operations like de-embedding, decryption, and uncompressing in their level of hierarchy and get the information which is required. Compressing the data will increase the performance of data transfer and embedding the encrypted data will assure the security while the transferring data over network.

The proposed scheme consists of image encryption, data embedding and data-extraction or image-recovery. The content owner first encrypts the original image using an encryption key to obtain an image in encrypted form. The data-hider compresses the least significant bits (LSB) of the encrypted image using a data-hiding key in order to create a sparse space to accommodate some more amount data. Now at the receiver side, the data embedded in the created space can be easily retrieved according to the data hiding key from the encrypted image. Because the data embedding only affects the LSB, a decryption using an encryption key can then give us an image similar to the original one. By using both the encryption as well as the data-hiding key, the embedded additional data can be successfully retrieved and also the original image can be perfectly recovered [2].
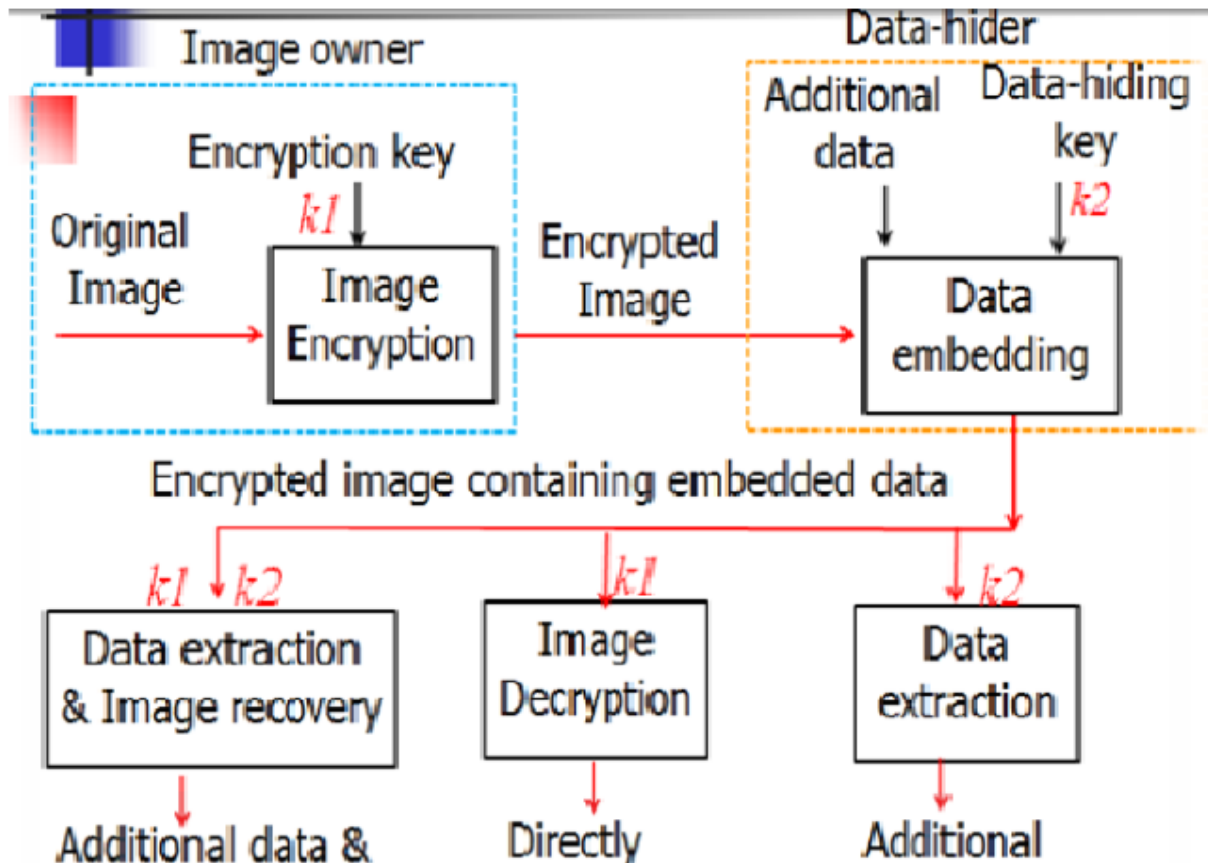
Fig 2. Separable reversible data hiding in encrypted image

This paper proposes a method for distinct revocable data hiding in ciphered image. As shown in Fig. 2, the content owner initially reserve enough space on original image to embed data and then by using an encryption key image is converted into its encrypted form. The data embedding process in encrypted images is inherently reversible for the data hider as he only needs to accommodate data into the created space. The data extraction phase and image recovery phase are similar to that of Framework Vacating room after encryption. In the new framework, we follow the idea that first losslessly compresses the redundant image content and then encrypts in order to protect privacy and maintain security. Next, we consider a practical method based on the Framework "Reserving room before encryption", that has four stages as follows: creating an encrypted image, data hiding in encrypted image, data extraction and image recovery.

Advantages: If the receiver only has the data-hiding key, he can extract the additional data also if he does not know the image content. If he has only the encryption key and not the data hiding key he can decrypt the received data to obtain an image similar to the original image, as data hiding key is absent he cannot extract the additional data. If he receiver has both the data-hiding key as well as the encryption key, can extract the additional data and also recover the original image without any error when the additional data is not too large.

V. IMAGE ENCRYPTION

The user will initially browse the image and encrypt the image, then the system will auto generate an encryption key for encryption. Encryption applies special mathematical algorithms and keys so as to transform digital data into cipher text before they are transmitted further and then decryption applies mathematical algorithms and keys to get back the original data from cipher text. As information privacy becomes a challenging issue thus in order to protect valuable and secret data or image from unauthorized users, data or image encryption or image decryption is important. Consider an original image with a size of $Q1 * Q2$ which is in uncompressed format and each pixel with gray value falling into [0, 255] is represented by 8 bits. We can denote the bits of a pixel as $bij0, bij1,....bij7$ where $1<i<Q1$ and $1<j<Q2$, represent the gray value as $P_{i,j}$ and the number of pixels as Q ($Q= Q1 * Q2$). In encryption phase, we calculate the pseudo-random bits and original bits exclusive-or results, where

$$B_{i,j,u} = b_{i,j,u} \oplus r_{i,j,u}$$

r, i, j, u can be determined by using an encryption key. Then B, i, j, u, are concatenated in an ordered manner as in encrypted data.

VI.   DATA EMBEDDING

User will hide the encrypted data in encrypted image and system will then automatically generate data hiding key. In the data embedding stage, we embed few parameters into a small number of encrypted pixels, and the LSB of the other encrypted pixels are compressed to create a sparse space for so that we can accomodate the additional data and the original data at the positions obtained by the parameters. The data-hider will randomly select Np encrypted pixels using a data hiding key that will be used to carry the parameters for data hiding. Np is a small positive integer, for example, Np=20. The remaining (N-Np) encrypted pixels are permuted and divided into a number of groups, each group will contain L pixels. We can determine the permutation way by using the data-hiding key. For each pixel-group, for L pixels select the M least significant bits, and represent them as B (k,1) , B (k,2) B(k, M*L) where k represents a group index within [1,(N-Np)/L] and M represents a positive integer less than 5. The data-hider generates a matrix G, which is made up of two parts. The left part represents identity matrix and the right part represents pseudo-random binary matrix which is obtained from the data-hiding key. Now for each group, which is product with the G matrix to form a matrix of size (M * L-S), that has a sparse bit of size S, in which the data is embedded and the pixels are then arranged into the original form and re-permutated to form an original image.

$$\begin{bmatrix} B'(k,1) \\ B'(k,2) \\ \vdots \\ B'(k, ML-S) \end{bmatrix} = \mathbf{G} \cdot \begin{bmatrix} B(k,1) \\ B(k,2) \\ \vdots \\ B(k, ML) \end{bmatrix}$$

VI.   IMAGE DECRYPTION

The user will first browse data that he wish to send to receiver and then encrypt the original data and the system will auto generate the data encryption key.The content owner encrypts the original image using an encryption key. Even if the data-hider does not know the original content, he can easily compress the least significant bits of the encrypted image using a data-hiding key to create some space so as to accommodate the additional data. Now with an encrypted image containing additional data, by using a data hiding key receiver can obtain the additional data, or obtain an image similar to the original one using only the encryption key. When the receiver has both of the keys with him, he can extract the additional data as well as he can recover the original content without any error. When having an encrypted image containing embedded data, using encryption key receiver first generate ri,j,k, and calculates the exclusive-or of the received data and ri,j,k so as to decrypt the image. We can denote the decrypted bits as bri,j,k. The original most significant bits (MSB) are retrieved correctly without any errors. Now for a certain pixel, if the embedded bit which is in the block including the pixel is zero and the pixel is belonging to D1, or if the embedded bit is 1 and the pixel is belonging to D0, then the data-hiding will not affect any encrypted bits of the pixel. So, the three LSB which are decrypted must be same as the original LSB, which implies that the decrypted gray value of the pixel is correct. In other way, if the embedded bit in the pixels block is zero and the pixel is belonging to D0, or the embedded bit is one and the pixel is belonging to D1, the decrypted LSB.

$$\begin{aligned} b'_{i,j,k} &= r_{i,j,k} \oplus B'_{i,j,k} \\ &= r_{i,j,k} \oplus \overline{B_{i,j,k}} \\ &= r_{i,j,k} \oplus \overline{b_{i,j,k} \oplus r_{i,j,k}} \\ &= \overline{b_{i,j,k}}, \qquad\qquad k = 0, 1, 2. \end{aligned}$$

VIII. DATA EXTRACTION

As data extraction is totally independent from image decryption, their order implies two different practical applications which are as follows:

First case: Extracting Data from Encrypted Images*:* In order to update some personal information of images which are encrypted for protecting privacy, the database manager will only get access to the data hiding key and will have to calculate data in encrypted domain. Order of data extraction before image decryption will guaranty the feasibility of our work. When the database manager will obtain the data hiding-key, so he will be able to decrypt the LSB-bits of encrypted image of A which is denoted by AE, and then obtain the additional data z by directly reading the decrypted image. When we request for updating information of encrypted images, the database manager, will then update information through LSB replacement and will encrypt updated information according to the data hiding key. Now the entire process is completely operated on encrypted domain, so it will avoid the leakage of original data.

Second case: Extracting Data from Decrypted Images: In 1, embedding and extraction of the data both are calculated in encrypted domain. In other way, there is another situation that the user will want to decrypt the image first and then obtain the data from the decrypted image when it will be required. The following example illustrates an application for such scenario. Consider Alice outsourced her images to a cloud server, and the images are encrypted in order to protect their data into the encrypted images, by embedding some notation the cloud server will mark the images, by including the identity of the images owner and the identity of the time stamps and the cloud server, so as to manage the encrypted images. The cloud server has no authority to do any kind of permanent damage to the images. Only an authorized user, Bob who has the encryption key and the data hiding key with him, downloaded the images and then he decrypted the images. Bob marks decrypted images, so that decrypted images will include the notation, this notation can be used to trace the history and origin of the data. Order of image decryption before data extraction or without data extraction is suitable in this case.

If the receiver has both the data-hiding key and encryption key, he may hope to obtain the embedded data. Now according to the data-hiding key, the values of M,S and L, the LSB of the Np selected encrypted pixels, and the (N-Np) * S/L - Np additional bits can then be obtained from the encrypted image which containing embedded data. Now by placing the Np LSB into their original positions, the data which is encrypted of the Np selected pixels are retrieved, using the encryption keys their original gray values can be appropriately decrypted. We will recover the original gray values of the other (N-Np) pixels. This paper proposes a novel scheme for distinct revocable data hiding, that is, separable reversible data hiding in encrypted image.
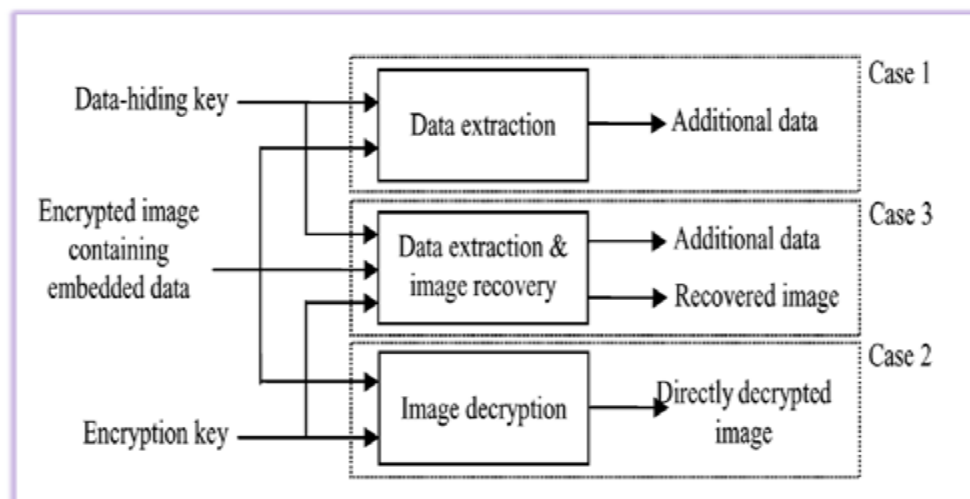
In the proposed scheme, by using an encryption key we can encrypt the original image and by using a data hiding key the additional data can be added in to the encrypted image. Now along with an encrypted image containing additional data, if the receiver only has the data-hiding key, then he can only extract the additional data embedded inside the image even if he is not aware about the image content. If the receiver only has the encryption key, and not the data hiding key then he can decrypt the received data to obtain an image similar to the original image, but then he cannot extract the additional data. In other case, if the receiver has both the data-hiding key as well as the encryption key, then he can obtain the additional data and also recover the original image content without any error when the amount of additional data is considerably small.

IX. CONCLUSION AND FUTURE SCOPE

In this paper, we have proposed a novel scheme for distinct revocable data hiding in ciphered image which consists of 3 phases: image encryption, data embedding and data-extraction or image recovery. In the first stage, the content owner encrypts the original image using an encryption key. Although a data-hider does not know the original content, he can compress the least significant bits of the encrypted image using a data-hiding key so as to create a sparse space to embed the additional data into the encrypted image. With an encrypted image containing additional data, the receiver can extract the additional data using only the data hiding key, or obtain an image exactly similar to the original image using the encryption key. When the receiver has both the keys, the data hiding key as well as encryption key, he can extract the additional data and also recover the original content. If the lossless compression method is used for the encrypted image which contains embedded data, the additional data can still be extracted and the original content can be also recovered since the lossless compression does not change the content of the encrypted image containing embedded data.The reversible compression method is used for the encrypted image containing embedded data, the additional data can be extracted and the original content can be also recovered since the lossless compression does not change the content of the encrypted image containing additional data. Reversible data hiding in encrypted images is a new concept which attracts our attention due to the privacy-preserving requirements from cloud data management. This study helps constructing secure and secret transmission of secrete file in order to prevent any unauthorized party access information and security level of data is increased by encrypting data. We also provide protection for keys during decryption process so that even if any hacker attacks on system it should be secure. In further future we can also use video, audio in case of image as cover for data hiding.

X. ACKNOWLEDGEMENTS

REFERENCES

[1] Study on Separable Reversible Data Hiding in Encrypted Image, International Journal of Advancements in Research & Technology, Volume 2, Issue 12, December-2013 223 ISSN 2278-7763.
[2] Xinpeng Zhang, Separable Reversible Data Hiding in Encrypted Image, IEEE TRANSACTIONS ON INFORMATION FORENSICS AND SECURITY, VOL. 7, NO. 2, APRIL 2012.
[3] Kede Ma, Weiming Zhang, Xianfeng Zhao, *Member, IEEE*, Nenghai Yu, and Fenghua Li, Reversible Data Hiding in Encrypted Images by Reserving Room Before Encryption, IEEE TRANSACTIONS ON INFORMATION FORENSICS AND SECURITY, VOL. 8, NO. 3, MARCH 2013.
[4] Lalit Dhande, Priya Khune, Vinod Deore, Dnyaneshwar Gawade, Hide Inside-Separable Reversible Data Hiding in Encrypted Image, International Journal of Innovative Technology and Exploring Engineering (IJITEE) ISSN: 2278-3075, Volume-3, Issue-9, February 2014.
[5] Jun Tian, Reversible Data Embedding Using a Difference Expansion, IEEE TRANSACTIONS ON CIRCUITS AND SYSTEMS FOR VIDEO TECHNOLOGY, VOL. 13, NO. 8, AUGUST .
[6] M. Johnson, P. Ishwar, V. M. Prabhakaran, D. Schonberg, and K.Ramchandran, On compressing encrypted data," IEEE Trans. Signal Process., vol. 52, no. 10, pp. 2992–3006, Oct. 2004.
[7] C.-C. Chang, C.-C. Lin, and Y.-H. Chen, Reversible data-embedding scheme using differences between original and predicted pixel values, IET Inform. Security, vol. 2, no. 2, pp. 35–46, 2008.
[8] Kede Ma, Weiming Zhang, Reversible Data Hiding in Encrypted Images by Reserving Room Before Encryption, IEEE Trans. VOL. 8, no. 3, Mar 2013.

Research Paper   Open Access

DMP Packet Scheduling For Wireless Sensor Network

Pallavi Sawale[1] , Dr.D.J Pete[2]

[1](Department of Electronics,Datta Meghe College of engineering/Mumbai University,India)
[2](Department of Electronics,Datta Meghe College of engineering/Mumbai University,India)

ABSTRACT : *Most of the existing packet scheduling mechanisms of the wireless sensor network use First Come First Served (FCFS) non pre emptive priority and pre emptive priority scheduling algorithms. The above algorithms have high processing overhead and also long end-to-end data transmission delay. In FCFS concept the data packet which is entering the node first will go out first from the node, and the packet which will enter last will leave at last. But in FCFS scheduling of real time data packets coming to the node have to wait for a long time period.In non pre emptive priority scheduling algorithm there is starvation of real time data packets because once the processor enters the running state, it will not allow remove until it is completed, so there is starvation of real time data packets. In pre emptive scheduling, starvation of non real time data packets, due to continuous arrival of real time data. Therefore the data packets are to be schedule in multilevel queue. But the multilevel queue scheduling scheme is not suitable for dynamic inputs, and hence the scheme is designed for dynamically change in the inputs. The Dynamic Multilevel Priority (DMP) packet scheduling is the scheme for dynamically changes in the inputs. In this scheme each node except the last level of the virtual hierarchy in the zone based topology of wireless sensor network has three levels of priority queues. Real time data packets are placed into highest priority queue and can preempt the data packets in the other queues. Non real time data packets are placed into other two queues based on threshold of their estimated processing time. The leaf node have two queues, one for real time data packet and another for non real time data packet since they do not receive data from other nodes and thus reduces end to end delay. This scheme reduces the average waiting time and end-to –end delay of data packets.*

KEYWORDS : *Data waiting time, FCFS , non-preemptive priority scheduling,non-real-time, packet scheduling, pre-emptive priority scheduling,real-time, Wireless sensor network.*

1. INTRODUCTION

Scheduling of different packets at the sensor nodes is very important as ensures the delivery of the data packet on the priority basis. The sensed data may be real time or non real time. Highest priority should be given to the real time data sense by the node compare to non real time data packet.[1] Sometimes the nodes may be put to sleep mode, when there is no data packet available and as soon as the data packet arrives at the node is putted into wake mode. This reduces the sensor node energy consumption. In FCFS scheduling scheme the data packets are processed in order of their arrival time and therefore the data packet which is entering at the last will require a long time to reach to a base station .However the emergency real time data should be reach to the base station before the deadline expires. Since the emergency real time data packet should reach the base station with shortest possible end-to-end delay. But most of the packets scheduling algorithms are neither dynamic nor suitable for large scale applications as their scheduling is predetermine and they are static. Static means those cannot be change as per the application requirement.[2] In the proposed dynamic multilevel priority packet scheduling scheme hierarchical structure of node is used. The nodes that have same hop distance from the base station will be considered to be located at the same hierarchical level. Processing of the data packets is done by TDMA scheme. In TDMA scheme the time slot is assigned for each data packet. Three levels of priority queues are defined. First priority will be given to real time data packet, second priority will be given to non real time data packets that are sensed by remote node at lower level & third priority will be given to the non real time data packet that are local sensed at the node.

If the non real time data packets with same priority are arrived then they are processed using the shortest job first scheduler scheme. The advantages of wireless sensor networks (WSNs) have lately become interesting for industrial and factory automation, distributed control system, automotive systems and other kinds of network embedded systems. The need for reduced cabling, faster setup times for equipment, reliable communication in harsh areas and added mobility have triggered research on the use of wireless communication in industrial systems. Even if   WSNs provide a lot of benefits in the context of industrial communication, they also suffer from a number of disadvantages. Wireless communication is characterized by its high error probability, leading to the risk of causing severe problems for applications with strict reliability and timing requirements. Lost or delayed data may cause industrial applications to malfunction. Transmission scheduling in the context of time division multiple accesses (TDMA) can achieve robust and collision-free communication. Meanwhile, the TDMA-based medium access control (MAC) protocols can provide quality of service (QoS) access to the wireless network. Therefore a TDMA-based scheme is preferred. In TDMA MAC protocols, time is slotted into intervals of equal length, which are called timeslots. The duration of one timeslot is equal to the time required to transmit a packet and return an acknowledgement (ACK). A collection of timeslots that repeat cyclically are grouped into super frames. The radio spectrum is divided into channels with small frequency bands, which can realize parallel transmissions and enhance network throughput. Although these TDMA-scheduling approaches can find minimum length schedule, minimum energy schedules or a fairness-based schedule, they do not account for reliability. However reliability in the WSNs is particularly significant. Reliability expresses the probability of successful packet delivery from a source node to the destination node. On each wireless link, a packet loss rate (PER) of 10–30% is common, which significantly decreases end-to-end reliability. An example shows that assuming 10% PER and three transmission attempts on each link, 99% packets are received over one hop. After ten hops, success probability is only 76 % [4] .An Energy aware Coverage based Node Scheduling scheme (ECNS) is proposed to provide protection for sensors and guarantees network connectivity and desired coverage level. ECNS enables each node to decide whether it is eligible to turn off to conserve energy through local information exchange with its neighbors. Simulation results show that ECNS improves network performance with respect to energy conservation, load balance and network lifetime. [6]

II. COMPARISON

Comparison of several existing WSN packet or task scheduling algorithms. The existing task scheduling algorithm are based on several factors such as Deadline: - Packet scheduling schemes can be classified based on the deadline of arrival of data packets to the base station (BS), which are as follows First Come First Served (FCFS): Most existing WSN applications use First Come First Served (FCFS) schedulers that process data in the order of their arrival times at the ready queue. In FCFS, data that arrive late at the intermediate nodes of the network from the distant leaf nodes require a lot of time to be delivered to base station (BS) but data from nearby neighboring nodes take less time to be processed at the intermediate nodes. In FCFS, many data packets arrive late and thus, experience long waiting times.

Earliest Deadline First (EDF): -Whenever a number of data packets are available at the ready queue and each packet has a deadline within which it should be sent to BS, the data packet. which has the earliest deadline is sent first. This algorithm is considered to be efficient in terms of average packet waiting time and end-to-end delay. Data, that have travelled the longest distance from the source node to BS and have the shortest deadline, are prioritized. If the deadline of a particular task expires, the relevant data packets are dropped at an intermediate node.

Packet Type: - Packet scheduling schemes can be classified based on the types of data packets, which are as follows.

Real-time packet scheduling: Packets at sensor nodes should be scheduled based on their types and priorities. Real-time data packets are considered as the highest priority packets among all data packets in the ready queue. Hence, they are processed with the highest priority and delivered to the BS with a minimum possible end-to-end delay.

Priority: Packet scheduling schemes can be classified based on the priority of data packets that are sensed at different sensor nodes.

Non-preemptive: In non-preemptive priority packet scheduling, when a packet t1 starts execution, task *t*1 carries on even if a higher priority packet *t*2 than the currently running packet *t*1 arrives at the ready queue. Thus *t*2 has to wait in the ready queue until the execution of *t*1 is complete.

Preemptive: In preemptive priority packet scheduling, higher priority packets are processed first and can preempt lower priority packets by saving the context of lower priority packets if they are already running.

Packet Type: Packet scheduling schemes can be classified based on the types of data packets, which are as follows.

Real-time packet scheduling: Packets at sensor nodes should be scheduled based on their types and priorities. Real-time data packets are considered as the highest priority packets among all data packets in the ready queue. Hence, they are processed with the highest priority and delivered to the BS with a minimum possible end-to-end delay.

Non-real-time packet scheduling: Non-real time packets have lower priority than real-time tasks. They are hence delivered to BS either using first come first serve or shortest job first basis when no real-time packet exists at the ready queue of a sensor node. These packets can be intuitively preempted by real-time packets.

Number of Queue: - Packet scheduling schemes can also be classified based on the number of levels in the ready queue of a sensor node. These are as follows.

Single Queue: Each sensor node has a single ready queue.

All types of data packets enter the ready queue and are scheduled based on different criteria: type, priority, size, etc.

Single queue scheduling has a high starvation rate.

Multi-level Queue: Each node has two or more queues. Data packets are placed into the different queues according to their priorities and types. Thus, scheduling has two phases: (i) Allocating tasks among different queues, (ii) scheduling packets in each queue. The number of queues at a node depends on the level of the node in the network. For instance, a node at the lowest level or a leaf node has a minimum number of queues whilst a node at the upper levels has more queues to reduce end-to-end data transmission delay and balance network energy consumptions. Figure 1 illustrates the main concept behind multi-level queue scheduling algorithms
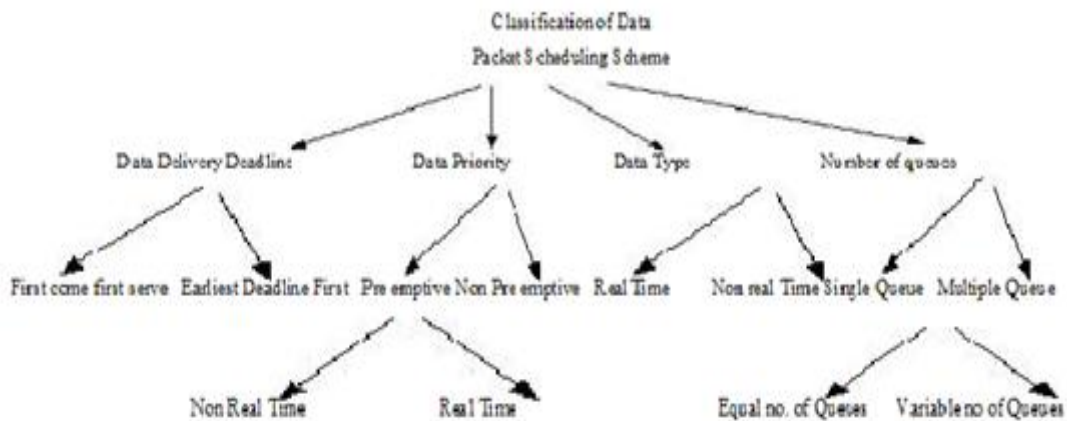

Fig.1 Classification of Packet Scheduling Schemes.

III.   ASSUMPTIONS

The following assumptions are made to design and implement
DMP packet scheduling scheme.

• Data traffic comprises only real-time and non-real-time data, e.g., real-time health data sensed by body sensors
and non-real-time temperature data.

• All data packets (real-time and non-real-time) are of same size.

• Sensors are time synchronized.

• No data aggregation is performed at intermediate nodes for real-time data.

• Nodes are considered located at different levels based on the number of hop counts from BS.

• Timeslots are allocated to nodes at different levels using TDMA scheme.

• The ready queue at each node has maximum three levels or sections for real-time data (pr1) non-real-time
remote data (pr2) and non-real-time local data (pr3). The length of data queues is variable. For instance, the
length of real-time data queue (pr1) is assumed to be smaller than that of non-real-time data queues (pr2 and
pr3). However, the length of the non-real-time pr2 and pr3 queues are same.

• DMP scheduling scheme uses a multichannel MAC protocol to send multiple packets simultaneously.

IV.   TERMINOLOGIES

In this section, we define the following terminologies and factors that are used in designing the DMP
packet scheduling scheme.Routing Protocol: For the sake of energy efficiency and balance in energy
consumption among sensor nodes, we envision using a zone-based routing protocol [8,9]. In a zone based
routing protocol, each zone is identified by a zone head (ZH) and nodes follow a hierarchical structure, based on
the number of hops they are distant from the base station (BS). For instance, nodes in zones that are one hop and
two hops away from the BS are considered to be at level 1 and level 2, respectively. Each zone is also divided
into a number of small squares in such a way that if a sensor node exists in square S1, it covers all neighboring
squares. Thus, this protocol reduces the probability of having any sensing hole in the network even if the
neighboring squares of a node do not have any sensor node.TDMA Scheme: Task or packet scheduling at each
nodal level is performed using a TDMA scheme with variable-length timeslots. Data are transmitted from the
lowest level nodes to BS through the nodes of intermediate levels. Thus, nodes at the intermediate and upper
levels have more tasks and processing requirements compared to lower-level nodes. Considering this
observation, the length of timeslots at the upper-level nodes is set to a higher value compared with the timeslot
length of lower-level nodes. On the other hand, real-time and time critical emergency applications should stop
intermediate nodes from aggregating data since they should be delivered to end users with a minimum possible
delay. Hence, for real-time data, the duration of timeslots at different levels is almost equal and short.Fairness:
This factor ensures that tasks of different priorities get carried out with a minimum waiting time at the ready
queue based on the priority of tasks. For instance, if any lower priority task waits for a long period of time for
the continuous arrival of higher-priority tasks, fairness defines a constraint that allows the lower-priority tasks to
get processed after a certain waiting time.Priority: The priority of non-real-time data packets is assigned based
on the sensed location (i.e., remote or local) and the size of the data. The data packets that are received by node
x from the lower level nodes are given higher priority than the data packets sensed at the node *x* itself. However,
if it is observed that the lower priority non-real-time local data cannot be transmitted due to the continuous
arrival of higher priority non-real-time remote data, they are preempted to allow low-priority data packets to be
processed after a certain waiting period. Nevertheless, these tasks can be preempted by real-time emergency
tasks. In case of two same priority data packets the smaller sized data packets are given the higher priority.

V.   PROPOSED DMP PACKET SCHEDULING SCHEME

In non-preemptive packet scheduling schemes real-time data packets have to wait for completing the
transmissions of other non-real-time data packets. On the other hand, in preemptive priority scheduling, lower-
priority data packets can be placed into starvation for continuous arrival of higher priority data. In the multilevel
queue scheduling algorithm [], each node at the lowest level has a single task queue considering that it has only

local data to process. However, local data can also be real-time or non-real time and should be thus processed according to their priorities. Otherwise, emergency real-time data traffic may experience long queuing delays till they could be processed. Thus, we propose a Dynamic Multilevel Priority (DMP) packet scheduling scheme that ensures a tradeoff between priority and fairness.

Working Principle: Scheduling data packets among several queues of a sensor node is presented in Figure 2. Data packets that are sensed at a node are scheduled among a number of levels in the ready queue. Then, a number of data packets in each level of the ready queue are scheduled. For instance, Figure 2 demonstrates that the data packet, *Data*1 is scheduled to be placed in the first level, Queue1. Then, *Data*1 and *Data*3 of Queue1 are scheduled to be transmitted based of different criteria. The general working principle of the proposed DMP scheduling scheme is illustrated in Figure 3.
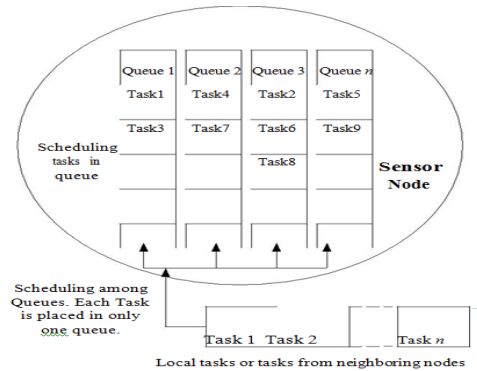
Fig. 2 Scheduling data among multiple queues.

The proposed scheduling scheme assumes that nodes are virtually organized following a hierarchical structure. Nodes that are at the same hop distance from the base station (BS) are considered to be located at the same level. Data packets of nodes at different levels are processed using the Time-Division Multiplexing Access (TDMA) scheme. For instance, nodes that are located at the lowest level and the second lowest level can be allocated timeslots 1 and 2, respectively. We consider three-level of queues, that is, the maximum number of levels in the ready queue of a node is three: priority 1 ($pr1$), priority 2 ($pr2$), and priority 3 ($pr3$) queues. Real-time data packets go to $pr1$, the highest priority queue, and are processed using FCFS. Non-real-time data packets that arrive from sensor nodes at lower levels go to $pr2$, the second highest priority queue. Finally, non-real time data packets that are sensed at a local node go to $pr3$, the lowest priority queue. The possible reasons for choosing maximum three queues are to process (i) real-time $pr1$ tasks with the highest priority to achieve the overall goal of WSNs, (ii) non real-time $pr2$ tasks to achieve the minimum average task waiting time and also to balance the end-to-end delay by giving higher priority to remote data packets, (iii) non-real-time $pr3$ tasks with lower priority to achieve fairness by preempting $pr2$ tasks if $pr3$ tasks wait a number of consecutive timeslots processed using FCFS. Non-real-time data packets that arrive from sensor nodes at lower levels go to $pr2$, the second highest priority queue
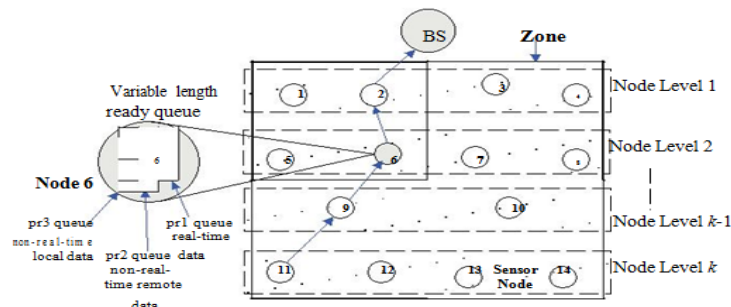
Fig.3. Proposed dynamic multilevel priority scheduling scheme.

Finally, non-real time data packets that are sensed at a local node go to $pr3$, the lowest priority queue. The possible reasons for choosing maximum three queues are to process (i) real-time $pr1$ tasks with the highest priority to achieve the overall goal of WSNs, (ii) non real-time $pr2$ tasks to achieve the minimum average task waiting time and also to balance the end-to-end delay by giving higher priority to remote data packets, (iii) non-real-time $pr3$ tasks with lower priority to achieve fairness by preempting pr2 tasks if $pr3$ tasks wait a number of consecutive timeslots. In the proposed scheme, queue sizes differ based on the application requirements. Since preemptive priority scheduling incurs overhead due to the context storage and switching in resource constraint sensor networks, the size of the ready queue for preemptive priority schedulers is expected to be smaller than that of the preempt able priority schedulers. The idea behind this is that the highest-priority real-time/emergency tasks rarely occur. They are thus placed in the preemptive priority task queue ($pr1$ queue) and can preempt the currently running tasks. Since these processes are small in number, the number of preemptions will be a few. On the other hand, non real time packets that arrive from the sensor nodes at lower level are placed in the pre emptable priority queue ($pr2$ queue). The processing of these data packets can be preempted by the highest priority real-time tasks and also after a certain time period if tasks at the lower priority $pr3$ queue do not get processed due to the continuous arrival of higher priority data packets. Real-time packets are usually processed in FCFS fashion. Each packet has an ID, which consists of two parts, namely level ID and node ID. When two equal priority packets arrive at the ready queue at the same time, the data packet which is generated at the lower level will have higher priority. This phenomenon reduces the end-to-end delay of the lower level tasks to reach the BS. For two tasks of the same level, the smaller task (i.e., in terms of data size) will have higher priority. Moreover, it is expected that when a node x senses and receives data from lower-level nodes, it is able to process and forward most data within its allocated timeslot; hence, the probability that the ready queue at a node becomes full and drops packets is low. However, if any data remains in the ready queue of node x during its allocated timeslot, that data will be transmitted in the next allocated timeslot.

VI.   PERFORMANCE EVALUATION

The simulation model is implemented using the java programming. It is used to evaluate the performance of the proposed DMP packet scheduling scheme, comparing it against the FCFS, and Multilevel Queue scheduling schemes. The comparison is made in terms of average packet waiting time, and end-to-end data transmission delay. We use randomly connected Unit Disk Graphs (UDGs) on a surface of 100 meter $\times$ 100 meter as a basis of our simulations. The number of simulated zones varies from 4 to 12 zones. Nodes are distributed uniformly over the zones. The ready queue of each node can hold a maximum of 50 tasks. Each task has a Type ID that identifies its type. For instance, type 0 is considered to be a real-time task. Data packets are placed into the ready queue based on the processing time of the task. Moreover, each packet has a hop count number that is assigned randomly, and the packet with the highest hop count number is placed into the highest-priority queue. We run the simulation both for a specific number of zones, and levels in the network until data from a node in each zone or level reach BS. Simulation results are presented for both real-time data and all types of data traffic. Table I presents simulation parameters, and their respective values.

TABLE I
Simulation Parameters And Their Values

Parameter	Value
Network Size	100m X 100m
Number of Nodes	Maximum 200
Number of Zones	4 - 12
Base station position	55m X 101m
Transmission Energy Consumptions	50 n Joule/bit
Energy Consumption in free space or air	0.01 n Joule/bit/m2
Initial Node Energy	2 Joule
Transmission Speed	$250Kbps$
Propagation Speed	198×106 meter/sec

VII.   RESULT

End-End delay of real time data
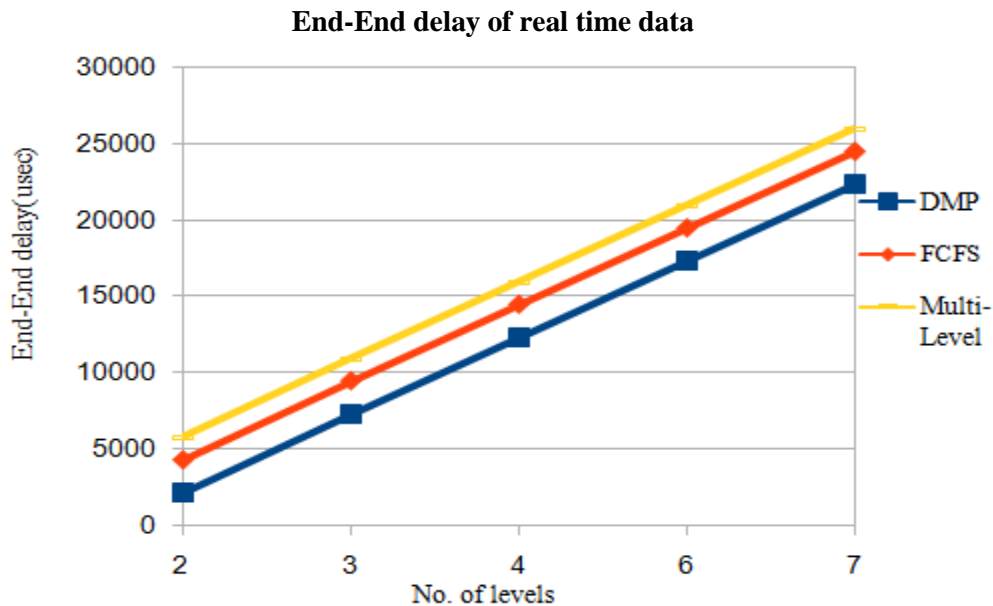
Figure 4. End-to-end delay of real-time data over a number of zones

Figures 4. Demonstrates the end-to-end delay of all types of data traffic over a number of zones and levels. From these results, we find that the DMP task scheduling scheme outperforms FCFS, and Multilevel Queue scheduler in terms of end-to-end data transmission delay. This is because in the proposed scheme, the tasks that arrive from the lower level nodes are given higher priority than the tasks at the current node. Thus, the average data transmission delay is shortened. Furthermore, the average waiting time of a task contributes largely to the experienced end-to-end data transmission delay. We are assigning task priority based on task deadline instead of the shortest task processing time. To reduce processing over-head and save bandwidth, we could also consider removing tasks with expired deadlines from the medium.

VIII. CONCLUSION AND FUTURE WORK

DMP task scheduler has better performance than the FCFS, and Multilevel Queue scheduler in terms of average task waiting time, both for real-time tasks, and all types of tasks. Using the concept of three-level priority queues at each node, the proposed DMP task scheduling scheme allows different types of data packets to be processed based on their priorities. Since real time and emergency data should be processed with the minimum end-to-end delay, they are processed with the highest priority, and can preempt tasks with lower priorities located in the two other queues. On the other hand, in existing multilevel queue schedulers, a task with the highest hop count is given the highest priority. Hence, real-time tasks are prioritized over other task types only if their hop counts are higher than those of non-real-time tasks. Moreover, in FCFS and multilevel queue schedulers, the estimated processing time of a task is not considered when deciding the priority of a task. Thus, FCFS and Multilevel Queue schedulers exhibit longer task waiting times and end-to-end delays, in comparison to the DMP task scheduling scheme. If a real-time task holds the resources for a longer period of time, other tasks need to wait for an undefined period time, causing the occurrence of a deadlock. This deadlock situation degrades the performance of task scheduling schemes in terms of end-to-end delay. Hence, we would deal with the circular wait and preemptive conditions to prevent deadlock from occurring.

REFERENCES

[1]   Nidal Nasser, Lutful Karim, and Tarik Taleb "Dynamic Multilevel Priority Packet Scheduling Scheme for Wireless Sensor Network", IEEE Transactions On Wireless Communications, VOL. 12, NO. 4, APRIL 2013, pp. 1448-1459.
[2]   Ali Sharifkhani, and Norman C. Beaulieu, "A Mobile-Sink-Based Packet Transmission   Scheduling Algorithm for Dense Wireless Sensor Networks", IEEE Transactions On Vehicular Technology, VOL. 58, NO. 5, JUNE 2009, pp. 2509-2518.
[3]   Nilesh Khude, Anurag Kumar, Aditya Karnik, "Time and Energy Complexity of Distributed Computation of a Class of Functions in Wireless Sensor Networks", IEEE Transactions On Mobile Computing, VOL. 7, NO. 5, MAY 2008, pp. 617-631.
[4]   Xiaoling Zhang, Wei Liang, Haibin Yu, Xisheng Feng, "Reliable transmission scheduling for multi-channel wireless sensor

networks with low-cost channel estimation", IET Communications, ISSN1, 2013, Vol. 7, pp. 71–81.

[5]   F. Liu, C. Tsui, and Y. J. Zhang, "Joint routing and sleep scheduling for lifetime maximization of wireless sensor networks," IEEE Trans. Wireless Communication, vol. 9, no. 7, pp. 2258–2267, July 2010.

[6]   J.Liu, N.Guo, and S. He, "An energy-aware coverage based node scheduling scheme for wireless sensor networks," in Proc. 2008 International Conf. Young Comput. Scientists, pp. 462–468.

[7]   S. Paul, S. Nandi, and I. Singh, "A dynamic balanced-energy sleep scheduling scheme in heterogeneous wireless sensor network," in Proc. 2008 IEEE International Conf. Netw., pp. 1–6, 2008.

[8]   O. Khader, A. Willig, and A. Wolisz, "Distributed wakeup scheduling scheme for supporting   periodic traffic in wsns," in Proc. 2009 European Wireless Conf., pp. 287–292.

[9]   B. Nazir and H. Hasbullah, "Dynamic sleep scheduling for minimizing delay in wireless sensor network," in Proc. 2011 Saudi International Electron., Communications Photon. Conf., pp. 1–5.

[10]   D. Shuman and M. Liu, "Optimal sleep scheduling for a wireless sensor network node," in Proc. 2006 Asilomar Conf. Signals, Syst. Comput., pp 1337–1341.

Unmanned Aerial Vehicle and Geospatial Technology Pushing the Limits of Development

Anuj Tiwari[1], Abhilasha Dixit[2]
[1](Department of Civil Engineering, Indian Institute of Technology –Roorkee, India)
[2](School of Electronics, DAVV, Indore, India)

ABSTRACT: *Often referred to as unmanned aerial vehicles, or UAVs, drones were most commonly associated with military or police operations but with advancement in information technology in last two decades, cheaper and smaller sensors, better integration and ease-of-use options this tool is start revolutionizing the way geospatial data is collected in many countries, monitoring large, rugged areas, tracking down criminals, observing forest fires and disaster areas. Beyond just viewing the result, with the use of photogrammetry, image processing and ground control points, the captured imagery could provide a base for collecting all the 2D and 3D features that are the last-mile problem in modeling and visualizing the whole world. The research aims to understand various characteristics of this emerging technology that makes it the most promising geospatial and attribute data collection tool in GIS community. Second aim of this paper is to explore the possible applications of UAV in the developing country like India.*

KEYWORDS: *UAV, Drone, Photogrammetry, GIS, 3D Model, Geospatial.*

I.   INTRODUCTION

UAVs commonly referred to as drones, are remotely piloted aircraft or systems. They range from simple hand-operated short-range systems to long endurance, high altitude systems that require an airstrip [1]. UAVs have been in use by the military for a long time, mainly as shooting targets, and for surveillance. In the past years, there has been considerable activity in the development of UAVs of all possible kinds, and this is well documented on the UVS-International website [2]. The potential benefits like ease of use, monitoring large rugged areas, tracking down illegal activities, observing forest fires and disaster areas these systems are now extended well beyond defense use to a variety of domestic and personal applications that will improve the safety of our communities, strengthen public services and achieve countless additional benefits to a broad variety of commercial and government organizations. The UAVs not only open up the gateway of new markets but will greatly broaden current markets. In south Mumbai a restaurant 'Francesco Pizza' recently delivered one of their Pizza's using a drone to a location nearby (Worli).

Figure1. Drone to deliver Pizza in Mumbai, India

GIS was developed as a computer system for capturing, storing, querying, analyzing and displaying geographically referenced data [3] but with the advancement in information and computational technology, GIS emerged as a broad term and a complete package, which can refer to a number of modern technologies and advance processes and became mainstream that expands knowledge and connections among people [4]. When working on a GIS project, the very first issue is 'data collection'. The fact that the data collection is one of the

most time consuming step in GIS, turns the decision on how to collect data, one of the most important factor, since the cost of this part of the project may become a great burden for the rest of the future analysis that is going to be performed with this data. GIS users have always craved high-quality, near real-time imagery. Over the years, expectations for resolution and fast delivery have been significantly raised. As the market for UAVs continues to expand from last two decades, they have transformed into data-gathering tools for GIS. Today UAV has become a primary resource to acquire remotely-sensed GIS data.
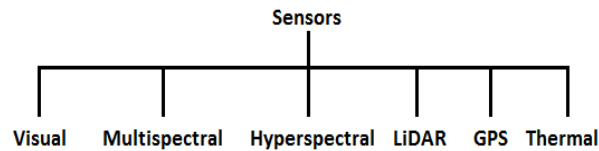
Figure2. Types of Sensors

a. **3D POINT CLOUD**: Traditionally, DEMs have been produced by survey methods or by stereo photogrammetry [5] [6]. Since the introduction of LiDAR in the mapping industry, its applications in GIS and other areas has increased exponentially and diversified innovatively. LiDAR has become the natural choice to provide data for Digital Surface Models (DSM) and Digital Elevation Models (DEM) in different applications. However, instrument cost and point cloud acquisition costs often prohibit LiDAR use solely for various projects in developing countries like India.

Low operation and hardware costs with high quality mapping sensors UAVs have become an attracting choice for aerial photogrammetry [7]. Automatic generation of high-quality, dense point clouds from digital images by image matching is a recent, cutting-edge step forward in digital photogrammetric technology [8].

b. **DIGITAL AERIAL IMAGERY (DAI)**: Recent technological developments in both hardware and software allow UAVs to capture high-resolution, georeferenced still photograph of study area. Acquired images of study area can be successfully processed to produce digital ortho-photo and digital map.

c. **REAL TIME MOTION PICTURE (VIDEO)**: Currently, UAVs are primarily used for capturing and down-linking real-time video. High definition low cost video camera is used to acquire video streams in software friendly format. Aerial video, collected by visible video cameras deployed on small UAV platforms, is rapidly becoming low-cost and up-to-date source to solve many hard real time challenges like natural disaster remediation [9].

d. **OBLIQUE IMAGES**: Oblique imagery is an aerial photography that is captured at specific angle with the ground and allows us to obtain an aerial perspective of the object. For underlying scene/feature oblique imagery helps to extract three major components (i) 3D geometry, (ii) appearance texture/facade, and (iii) properties/attributes. UAV provides cost effective and a quick alternative with an additional feature to capture building texture /façade at all possible angles. This will boost the hope of much awaited 3D GIS system development.

e. **THERMAL IMAGES**: Thermal imaging is a method of improving visibility of objects in a dark environment by detecting the objects' infrared radiation and creating a crisp image based on energy fluxes and temperature variations. Thermal camera is an electro-optical device that can be attached to drones to carry out thermographic surveys. They are used as a perfect solution for defect analysis of solar panels, wind turbines, buildings, and other difficult-to-access structures.

f. **GPS/INS LOCATION**: Many applications like surveillance, surveying and mapping, spatial information acquisition require precise navigation. Currently, the most widely used navigation technologies for the UAVs are GPS receivers and INS devices, alone or in combination. INS is a self-contained device which operates independently of any external signals or inputs, providing a complete set of navigation parameters, including position, velocity and altitude, with a high data rate. In contrast to INS's short-term positioning accuracy, satellite-based GPS navigation techniques can offer relatively consistent accuracy if sufficient GPS signals can be tracked during entire UAV mission [10].

II. APPLICATION OF UAVS IN DEVELOPING COUNTRIES

Developing countries, also known as third and fourth world countries; face economic challenges that first world countries do not, on a large scale. Poverty, Agriculture, low literacy rates, interrupted medicine supply; poor nutrition and lower energy production have become the common constraints on development. These factors must be broken for countries to develop. Technology is the only answer to these challenges. From high definition georeferenced images, oblique photographs, point cloud models to real time motion pictures, UAVs has opened up a world of possibilities for developing countries. Here we are presenting some of the core applications of drone/UAVs to improve the pace of development and level of life in the developing countries like India.

III. DRONES FOR AGRICULTURAL CROP SURVEILLANCE

Slow agricultural growth is major concern in countries like India where agriculture is demographically the broadest economic sector and plays a significant role in the overall socio-economic fabric. Higher cost and tuff handling of modern technology is the major problem in the use of technology in agriculture and yet farmers are forced to use conventional way of farming. Today 'walking the field' is the only way farmers monitor their crops. But this method often can be incomplete or time consuming, and collected data take long time to process and analyze. As a result, it can be difficult or impossible for the farmer to react to a problem like a disease outbreak before its too late or the costs to treat it have soared. Using drones for crop surveillance can drastically increase farm crop yields while minimizing the cost of walking the fields. Various drone enabled Crop Health Imaging systems at very low cost available that helps to have a composite video showing the health of crops. The Benefits of Drones in Farming are

- **Save Time**: While all farmers know the value of scouting their crops few actually have time to cover the acres on foot.
- **Increase Yield**: The precision application of pesticides, water, and fertilizers only where it is needed for specific crop increase the yield.
- **Crop Health Imaging**: Seeing the true health of your field in a color contrast allows you to see how much sunlight is being absorbed by the crop canopy.
- **Integrated GIS mapping**: Draw field borders for flight pattern

GIS technology has already proved its importance throughout the agricultural industry to manage resources, increase yields, reduce input costs, predict outcomes, improve business practices, and more [11]. GIS has a significant role to play in agriculture at several scales from local to global. The arrival of small and compact UAVs at regional and larger scales provide continuous data and when collected data is processed using thematic mapping system (GIS) at farm scale, produce maps based on themes such as soils or hydrology. Multiple layers of maps can be quickly displayed in a variety of overlap, scales, and combinations to fit the needs of the farmers.

Figure3. Drone over agriculture land.

IV. DRONES FOR DIASTER MANAGEMENT
(SEARCH AND RESCUE OPERATIONS)

There is a great need for information gathering from air, at sites of natural disaster and accidents. After disaster strikes it is critical to analyze situation and prepare immediate relief and rescue plans. At the same time it is too expensive, tuff and risky (environmental conditions) for a manned aircraft to acquire information. UAV is attracting a great deal of attention as a safe and efficient means of acquiring information in a region that are difficult for rescue teams to access and get a basic idea about situation such as flooded areas, tsunami, volcano sites or cultural riots. Drones are used to ascertain status of damages and provide information about its impact.

Benefit of UAV in disaster operations are:

- Food and Medical supply: Drones can be used to supply food and medical at disaster site that are not easily accessible.
- Search and rescue operation: After the disaster situation UAVs are used to search for missing people, and rescue people which got stuck.
- Monitoring relief and rehabilitation operations and make them enough to serve persons in trouble.

GIS can be a very useful tool to complement conventional methods involved in Disaster Management Mitigation of natural disaster management can be successful only when detailed knowledge is obtained about the expected frequency, character, and magnitude of hazard events in an area [12] [13]. GIS when integrated with UAV provide layers of information on various themes to enable the managers to take the most appropriate decisions under the given circumstances at run time.

Figure4. Drone over a disaster area.

V.   DRONES FOR SUPPLYING MEDICINE AND FOOD IN REMOTE/INACCESSIBLE AREAS

Access to healthy food and full medical support is a basic human right. The policies that affect our food and medical system should be enacted to ensure that everyone has access to these life support services. There have been numerous methods used to identify and analyze food access and medical supplies. Mapping patterns of access to food stores, hospitals, medical centers using GIS is becoming more prevalent and increasingly effective. In India, major percentage of total population is living in rural areas and among them there are many villages that are inaccessible by road for at least part of the year. The only reasonably fast way of getting medicine and other essential goods to these locations is to fly them in by military helicopters. At the same time in India 1.3 million children die every year from malnutrition, it is because of improper diet and interrupted supply of medication. Small UAVs, which would inexpensively deliver payloads to remote communities can bring smile on the face of people who feels disconnected and solve basic problems related to food and medical. Use of drones together with GIS can solve many problems in remote areas like

- Virus affected Areas: In that particular areas which has been affected by virus or infectious diseases and where external man force cannot be entered drone can fulfill the requirement of medicine.
- Tribal and naxalite areas: Areas where life is too hard to survive, where basic need of people is food and where external man force cannot be allowed to enter because of political or security reasons, drone can maintain the supply for basic need of life.

Figure5. Drone for rescue and rehabilitation.

VI. DRONES FOR ENERGY

Setup and maintenance for both the conventional and unconventional energy source is too costly and always a time consuming task. So there is a requirement of continuous monitoring of these systems. In power plants and transmission lines some factor which have to be monitored on periodically/regular basis are cracked insulator string ,frayed power conductor, degraded conductor splices, tower corrosion, tree growth ground clearance, conductor space/damper condition and critical thermal spans along transmission line. Manned helicopter are dangerous to fly along EHV power transmission line during inclement weather. Benefits of Drones in energy sectors are as follows:

- Storm damage inspection: After natural calamities, drones with high resolution imagery and ultra violet sensors used to collect information about status of transmission lines, cracked insulators and connections. This information essential for maintenance operations and in order to restart power transmission.
- Monitor the height of tree around the transmission lines: Drones are main source to monitor status of trees around transmission line and collect information to ascertain need of trimming.

In order to cater the increasing energy requirement another important option is nuclear energy which is rapidly adopted by growing countries all over the world. It is always critical to manage nuclear power plants and nuclear radiations. Because drones are able to fly at low altitudes, they can measure radiation in greater detail than a helicopter or other aircraft. GIS is a potential tool for planning and monitoring both conventional and non-conventional power generation resources. Sophisticated spatial analysis tools when integrated with real time monitoring methods are used for determining optimum generation potential, formulating what-if scenarios, studying environmental impact, and managing facility assets. Geo-database developed with continuous inflow of data is key component for maintaining and managing accurate transmission asset data such as substations, lines, and associated structures.

Figure6. Surveillance Drone over power line masts.

VII. DISCUSSION

There is growing interest in unmanned aircraft at the beginning of 21st century in almost all developed countries. There is no way question or doubt regarding technical viability or operational utility of UAVs. Success of UAVs in developed countries represents a historic opportunity to exploit transformational capabilities of this leading technology to support life services. Four major factor which are the symbol of economic growth for any developing country is: Agriculture, Energy, living standard, ability to mitigate natural calamities. UAV can help in many ways to increase and to sustain the development of countries whose economy majorly dependent up on agriculture. Drones fitted with payloads such as cameras, enable farmers to get a bird's eye-view of their crop by flying at low altitudes. Using much advanced sensors like hyper spectral, Infra-red imaging, drones can also detect the health condition of the plants. Spray of pesticides, fertilizers or any other beneficial substance can also be efficiently covered with UAVs. Energy is directly linked with the key global challenges that world faces - poverty alleviation, climate change, global environmental and food security. Ensuring access to sustainable and cleaner energy is a key objective for international community. Many fast-growing developing countries will make their major energy-related investments in next decade [United Nations: Ban Ki-moon Secretary-General of the United Nations]. To ensure supply of electricity, gas and oil, regular inspections of installations are imperative. Because of their size and structure, they are often inspected from the air. Instead of contracting an independent organization/firm, the inspections can be carried out with UAVs.

Natural disasters frequently occur across the world, affecting both developed and developing countries. For people in developing countries where humanitarian impact is often devastating, natural disasters present a larger problem than rest of the world may realize [14] [15]. UAVs equipped with remote sensing instrumentation offer numerous opportunities in disaster related situations. The low flying UAVs can be autonomously redirected to location of interest selected in the high flying UAV images by the user [16]. Video and GPS coordinates can be sent through a network to other responders in the area. The use of UAV imagery for post-disaster assessments has been explored in the capacity of both automatic and manual imagery assessments [17]. In 2012, Food and Agriculture Organization of United Nations (FAO) concluded that, food insecurity is still a major global concern as 1 billion people are suffering from starvation and malnutrition around the world. Rural and remote areas also share common traits such as older population, higher level of health risks and higher rates of diseases, chronic disease and injuries. People living in these areas generally have less access to health services with shortages of almost all health professions and health-related infrastructure. Use of UAVs can speed up the delivery of food, medicines and other supplies to remote areas, and even provides a cheaper alternative to develop a road network rather than other costly alternatives.

VIII.   CONCLUSION

As the market for UAVs continues to expand from last two decades, they have transformed into data-gathering tools for GIS. Today UAV has become a primary resource to acquire remotely-sensed GIS data. This study investigated the four basic requirements of developing countries and concluded that there is no doubt regarding the technical viability or operational utility of UAVs in integration to geospatial analysis tools to support life services. This paper finally present UAVs as more reliable, economical, autonomous and easier to use technology with great potential to conduct essential ground operations in a more efficient way.

REFRENCES

[1].   Louisa Brooke-Holland, Unmanned Aerial Vehicles (drones): an introduction (United Kingdom House of Commons International Affairs and Defence Section, Standard Note SN06493, 5 December 2012), online: United Kingdom Parliament
[2].   UVS-International, 2014. http://www.uvs-international.org/ (accessed 15 Sep 2014)
[3].   I. Getting. The global positioning system. IEEE Spectrum, 30(12):36–47, December 1993.
[4].   Online Source: http://www.opengeospatial.com.
[5].   Sties, M; Kruger, S; Mercer, J; Schnick, S. 'Comparision of digitial elevation data from airbourne laser and interferometric SAR systems'. International Society for Photogrammetry and Remote Sensing 2000; 33.
[6].   Kunapo, J. (2005) Spatial data integration for classification of 3D point clouds from digital photogrammetry. Applied GIS, vol. 1, pp. 26.1-26.15.
[7].   Everaerts, J. NEWPLATFORMS—Unconventional Platforms (Unmanned Aircraft Systems) for Remote Sensing; Official Publication No. 56; Gopher: Amsterdam, Netherlands, 2009.
[8].   Rosnell, Tomi; Honkavaara, Eija. 2012. "Point Cloud Generation from Aerial Image Data Acquired by Quadrocopter Type Micro Unmanned Aerial Vehicle and Digital Still Camera." Sensors 12, no. 1: 453-480.
[9].   Moore, M., C. Rizos, and J. Wang. 2003: Issues concerning the implementation of a low cost attitude solution for an unmanned airborne vehicle (UAV), Presented at SatNav 2003 The 6th International Symposium on Satellite Navigation Technology Including Mobile
[10].   Wang, Jinling, et al. "Integration of GPS/INS/Vision sensors to navigate unmanned aerial vehicles." International Society for Photogrammetry and Remote Sensing (ISPRS) Congress. 2008.
[11].   ESRI Farming Future August 2013 cover photography courtesy of Derek Tickner GIS for Agriculture, Vol 2
[12].   Cova, T.J. GIS in emergency management. In: Geographical Information Systems, management and applications. Longley, P.A.; Goodchild, M.F.; Maguire, D.J. and Rhind, D.V.
[13].   Pearson, E, Wadge, G, And Wiscoski, A.P. An integrated expert system/GIS approach to modeling and mapping hazards. Proc European conference on GIS, session 26, pp 763-771.
[14].   Beck, U. 1995. Ecological Politics in an Age of Risk. Cambridge, England: Polity Press.
[15].   Beck, U. 1999. World Risk Society. Cambridge, England: Polity Press.
[16].   Pedro A. Rodriguez, William J. Geckle, MS, Jeffrey D. Barton, MS John Samsundar, PhD, Tia Gao, Myron Z. Brown, MS, Sean R. Martin Johns "An Emergency Response UAV Surveillance System" AMIA 2006 Symposium Proceedings Page – 1078.
[17].   Adams, S., C. Friedland, M. Levitan (2010). Unmanned Aerial Vehicle Data Acquisition for Damage Assessment in Hurricane Events. 8th International Workshop on Remote Sensing for Disaster Management. Tokyo, Japan: 7.
[18].   Anuj Tiwari, Dr. Kamal Jain (2014), "GIS Steering Smart Future for Smart Indian Cities", International Journal of Scientific and Research Publications (IJSRP), vol 4, issue 8 (2014): 60, ISSN 2250-3153.

Research Paper   open Access

WHY JESUS CHRIST CAME INTO THE WORLD?... (A New theory on "TIE MINISTRY")

M.Arulmani, B.E.
(Engineer)

V.R.Hema Latha, M.A., M.Sc., M.Phil.
(Biologist)

ABSTRACT:
"JESUS CHRIST" came into the world….

[1]   **To Promote "violence"?...**

[2]   **To Promote "Racism and Castism"?...**

[3]   **To Promote his personality by doing "Wonders"?...**

[4]   **NO…**   **NO…**   **NO…**

This scientific research focus that "**JESUS CHRIST**" came into the world to translate meaning of

"**TIE MINISTRY**" rather than doing emotional sermon. The philosophy of "**TIE Ministry**" shall mean…

[1]   Translating the meaning of **"EVERLASTING LIFE"**
[2]   Emphasizing the meaning of **"HUMAN VALUE"**
[3]   Focusing the meaning of **"PEACE"**

According to **BIBLE** there were so many Commandments, Covenants were given to the ancient human populations by "**HEAVENLY FATHER**" right from **"ADAM", "EVE**" to the period of "**JOESPH" "MARY"** through various lineage of **NOAH, ABRAHAM, JACOB MOSES, DAVID, DANIEL, SOLOMON, ISAIAH, JEREMIAH** etc.

"THEN WHY JESUS CHRIST NEED

TO COME INTO THE WORLD"?...

(i)

(LIFE LOGO)

TIE
(New Covenant)
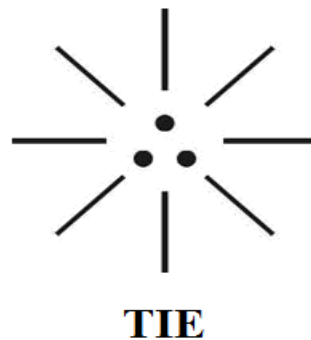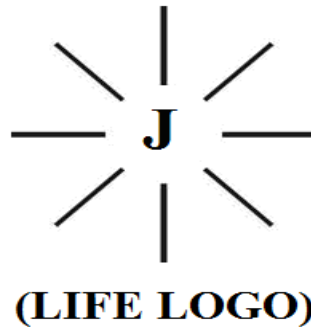
(ii)

[1]   Right dot is "**LOVE**"

[2]   Left dot is "**MERCY"**

[3]   Centre dot is **"HOPE"**

---

[4]   *"**TIE**" shall mean **three-in-one** element in the Divine plan of Heavenly Father which can't be separated. TIE shall mean "**JESUS**" or "**NEW COVENANT**". "**MINISTRY"** shall mean Transformation of TIE into **DEEDS** and **PEACE**.*

                                                                        [5]   - Author

---

                                                                                        KEY

WORDS:

a.   Philosophy of word "**TIE**"?...

b.   Philosophy of word "**MINISTRY**"?...

c.   Philosophy of word "**JESUS**"?...

I.   INTRODUCTION:

According to **"BIBLE**" prophecy was given through prophet ISAIAH that "Behold the virgin shall conceive and bear son and shall call this name "**IMMANUEL"** even long before birth of "**HOLY SON".**

> *[6]   "Then why the son was called as "JESUS" instead of "IMMANUEL"?...*

[7]   Do **JESUS** differs from **IMMANUEL**?...

[8]   Do **IMMANUEL** differs from **CHRIST**?...

[9]   Do **CHRIST** differs from **JESUS**?...

a.   This scientific research focus that the origin of **ADAM** shall be considered as the Natural product of **"J-RADIATION"** (Zero hour radiation) composed of **three-in-one** fundamental particles **photon, proton, Electron.**   It is speculated that the Heavenly Father (Super natural spirit) probably shall be called as **"JESUS"** as per Author's understanding.
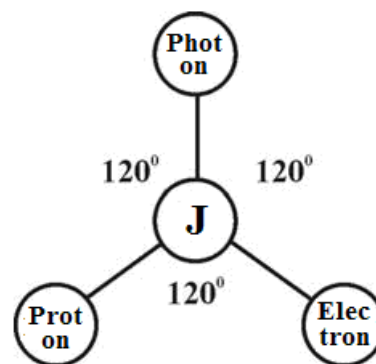
JESUS
(New Covenant)

[10]   Proton is like **LOVE (Son)**?...

[11]   Electron is like **MERCY (Mother)**?...

[12]   Photon is like **HOPE (Father)**?...

It is further speculated that the "**HOLY ADAM**" probably failed to obey and do **"good deeds"** according to law of Heavenly Father and thus HOLY ADAM might become **"ADAM" (HUMAN)**.

> *[13]   "JESUS"* shall mean *"SUPERNATURAL SPIRIT".*
>
> *[14]   "IMMANUEL"* shall mean *"DIVINE PRODUCT".*
>
> *[15]   - Author*

[16]   **Hypothesis and Narrations**

[17]   **Philosophy of word "JESUS"?...**

a.   It is hypothesized that the philosophy of "**JESUS**" shall be considered as **"TIE"** (New covenant) descended from supernatural spirit (Heavenly Father). Alternatively "**JESUS**" shall be called as **"IMMORTAL SOUL"** as described below.
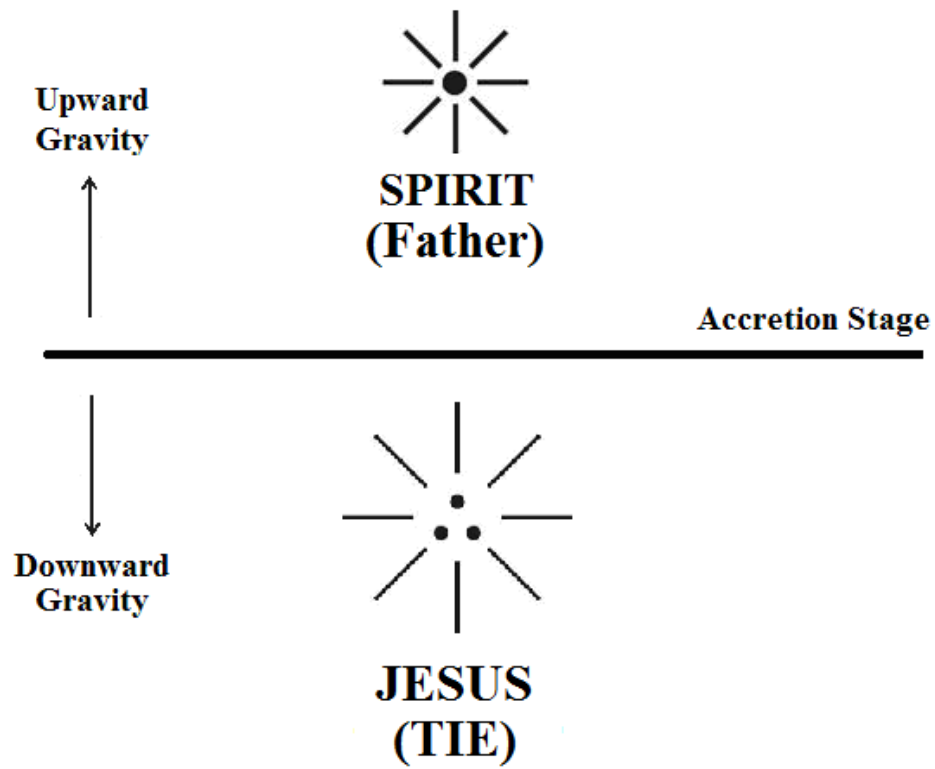
[18]

[19] **Philosophy of Immanuel?...**

    a.   It is hypothesized that the philosophy of Immanuel shall be considered as **"Transformed soul"** of **JESUS**. In other words Immanuel shall be considered as Image of **JESUS** as described below.

Upward Gravity

JESUS (Real)

Transformation & Plasma barrier

Downward Gravity

IMMANUEL (Image)
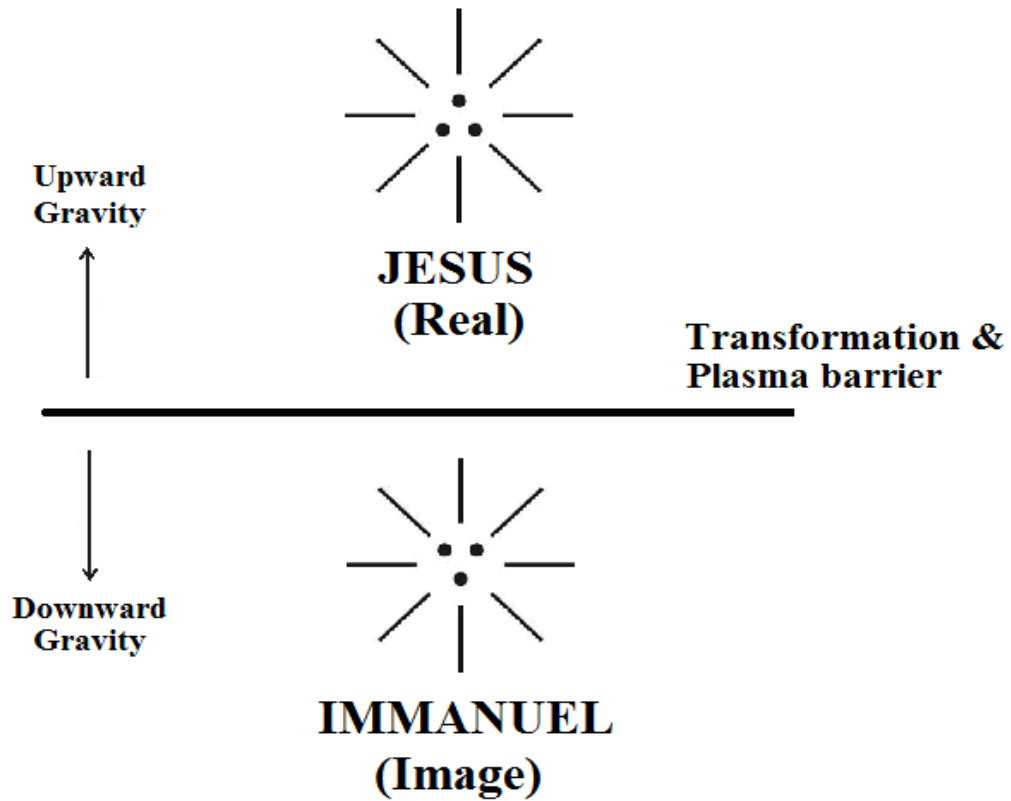
[20]

[21] "CHRIST" different from "Immanuel"?...

    a. It is hypothesized that "**Christ**" shall been mean **"good deeds"** derived from transformed soul of Immanuel.

    b. It is further focused that In the **"Divine plan"** of Heavenly Father, **"JESUS"**, **"IMMANUEL"**, **"CHRIST"** shall be considered as three distinguished persons having genetically varied characteristics as narrated below. In other words Heavenly Father become "**good deeds**" of Earth planet through **JESUS, IMMANUEL, CHRIST.**

SPIRIT (Super Nature)

[22]
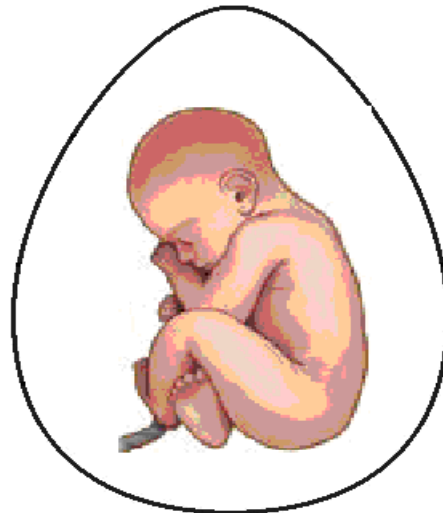
TIE
(Jesus)

[23]
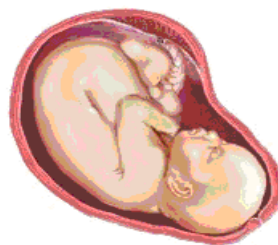
MINISTRY
(Immanuel)

[24]

DEEDS & PEACE
(Christ)

[25]

> *[26]*   *"JESUS"* shall mean *"SON OF GOD"*
> *[27]*   *"IMMANUEL"* shall mean *"SON OF MAN"*
> *[28]*   *"CHRIST"* shall mean *"LORD"*
>
>   -   *M. Arulmani,*
>
>   *[29]*   *Tamil Based Indian*

[30]   **Philosophy of "Heavenly Father"?...**

a. From biblical understanding it is hypothesized that "**Heavenly Father**" also called as **"GOD"** shall be considered as "**Supernatural Human**". In proto Indo Europe language "**GOD**" shall mean "**KARI THIRI**".
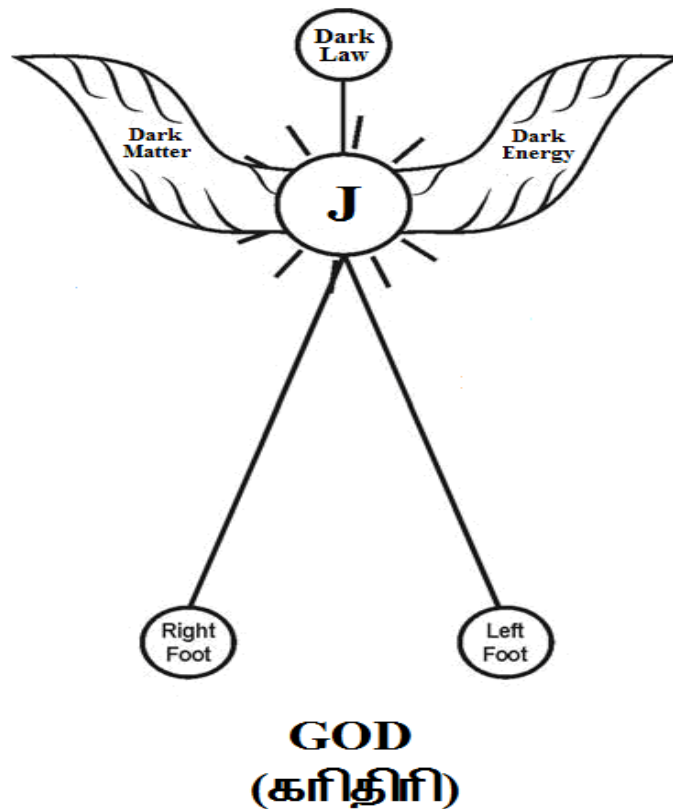
[31]

[32]   **Etymology of word SATAN?...**

a. Case study shows that the word Satan refers to **devil** or **evil person.** From biblical understanding It is hypothesized that Satan shall be considered as **HOLY PERSON.** The **HOLY ADAM** (before eating forbidden fruit) shall be called as **SATAN.** The etymology of English word Satan might be derived from the proto Indo-Europe root word **Sathian, Sathiya.** Further the English word Sat, Satyr, Saturation might be derived from the proto Indo-Europe root word.
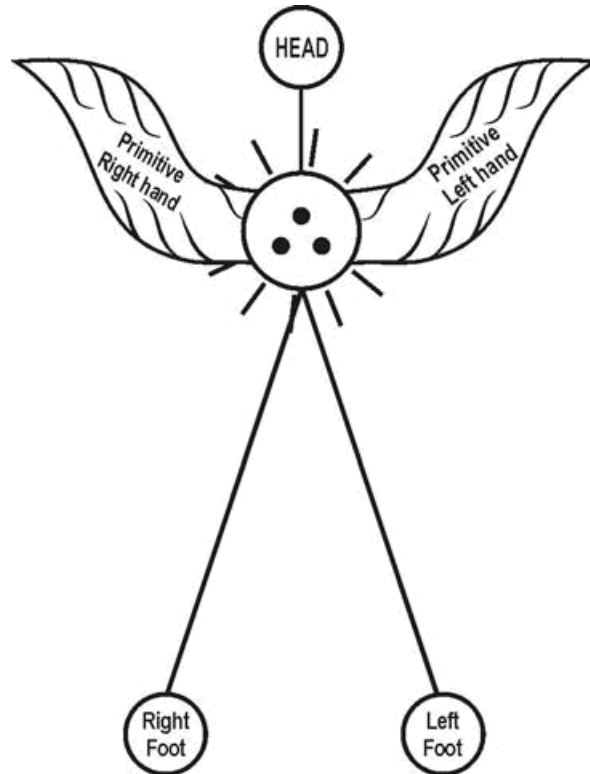
HOLY ADAM
(Sathian)

[33]

HOLY EVE
(Sathiya)

[34]

II. CONCLUSION:

a. The philosophy of "**CHRIST**" shall mean "**GOOD DEEDS**". "**CHRISTIAN**" shall mean person **translating** his Soul into Good deeds. **Christianity** shall mean focusing **human value** rather than **religion.**

KACHCHA THEEVU!...
(TIE 2015)

[35]

[36]   **TIE** *shall alternatively mean* **PEACE**. *TIE ministry shall mean translation of* **soul** *into* **good deeds and peace.**

[37]   *- Author*

[38]

[39]   <u>**Previous Publication:**</u>

The philosophy of origin of first life and human, the philosophy of model Cosmo Universe, the philosophy of fundamental neutrino particles have already been published in various international journals mentioned below. Hence this article shall be considered as **extended version** of the previous articles already published by the same author.

[1]   Cosmo Super Star – IJSRP, April issue, 2013

[2]   Super Scientist of Climate control – IJSER, May issue, 2013

[3]   AKKIE MARS CODE – IJSER, June issue, 2013

[4]   KARITHIRI (Dark flame) The Centromere of Cosmo Universe – IJIRD, May issue, 2013

[5]   MA-AYYAN of MARS – IJIRD, June issue, 2013

[6]   MARS TRIBE – IJSER, June issue, 2013

[7]   MARS MATHEMATICS – IJERD, June issue, 2013

[8]   MARS (EZHEM) The mother of All Planets – IJSER, June issue, 2013

[9]   The Mystery of Crop Circle – IJOART, May issue, 2013

[10]   Origin of First Language – IJIRD, June issue, 2013

[11]   MARS TRISOMY HUMAN – IJOART, June issue, 2013

[12]   MARS ANGEL – IJSTR, June issue, 2013

[13]   Three principles of Akkie Management (AJIBM, August issue, 2013)

[14]   Prehistoric Triphthong Alphabet (IJIRD, July issue, 2013)

[15] Prehistoric Akkie Music (IJST, July issue, 2013)

[16] Barack Obama is Tamil Based Indian? (IJSER, August issue, 2013)

[17] Philosophy of MARS Radiation (IJSER, August 2013)

[18] Etymology of word **"J"** (IJSER, September 2013)

[19] NOAH is Dravidian? (IJOART, August 2013)

[20] Philosophy of Dark Cell (Soul)? (IJSER, September 2013)

[21] Darwin Sir is Wrong?! (IJSER, October issue, 2013)

[22] Prehistoric Pyramids are RF Antenna?!... (IJSER, October issue, 2013)

[23] HUMAN IS A ROAM FREE CELL PHONE?!... (IJIRD, September issue, 2013)

[24] NEUTRINOS EXIST IN EARTH ATMOSPHERE?!... (IJERD, October issue, 2013)

[25] EARLY UNIVERSE WAS HIGHLY FROZEN?!... (IJOART, October issue, 2013)

[26] UNIVERSE IS LIKE SPACE SHIP?!... (AJER, October issue, 2013)

[27] ANCIENT EGYPT IS DRAVIDA NAD?!... (IJSER, November issue, 2013)

[28] ROSETTA STONE IS PREHISTORIC "THAMEE STONE" ?!... (IJSER, November issue, 2013)

[29] The Supernatural "CNO" HUMAN?... (IJOART, December issue, 2013)

[30] 3G HUMAN ANCESTOR?... (AJER, December issue, 2013)

[31] 3G Evolution?... (IJIRD, December issue, 2013)

[32] God Created Human?... (IJERD, December issue, 2013)

[33] Prehistoric "J" – Element?... (IJSER, January issue, 2014)

[34] 3G Mobile phone Induces Cancer?... (IJERD, December issue, 2013)

[35] "J" Shall Mean "JOULE"?... (IRJES, December issue, 2013)

[36] "J"- HOUSE IS A HEAVEN?... (IJIRD, January issue, 2014)

[37] The Supersonic JET FLIGHT-2014?... (IJSER, January issue, 2014)

[38] "J"-RADIATION IS MOTHER OF HYDROGEN?... (AJER, January issue, 2014)

[39] PEACE BEGINS WITH "J"?... (IJERD, January issue, 2014)

[40] THE VIRGIN LIGHT?... (IJCRAR, January issue 2014)

[41] THE VEILED MOTHER?... (IJERD, January issue 2014)

[42] GOD HAS NO LUNGS?... (IJERD, February issue 2014)

[43] Matters are made of Light or Atom?!... (IJERD, February issue 2014)

[44] THE NUCLEAR "MUKKULAM"?... (IJSER, February issue 2014)

[45] WHITE REVOLUTION 2014-15?... (IJERD, February issue 2014)

[46] STAR TWINKLES!?... (IJERD, March issue 2014)

[47] "E-LANKA" THE TAMIL CONTINENT?... (IJERD, March issue 2014)

[48] HELLO NAMESTE?... (IJSER, March issue 2014)

[49] MOTHERHOOD MEANS DELIVERING CHILD?... (AJER, March issue 2014)

[50] E–ACHI, IAS?... (AJER, March issue 2014)

[51] THE ALTERNATIVE MEDICINE?... (AJER, April issue 2014)

[52] GANJA IS ILLEGAL PLANT?... (IJERD, April issue 2014)

[53] THE ENDOS?... (IJERD, April issue 2014)

[54]   THE "TRI-TRONIC" UNIVERSE?... (AJER, May issue 2014)

[55]   Varied Plasma Level have impact on "GENETIC VALUE"?... (AJER, May issue 2014)

[56]   JALLIKATTU IS DRAVIDIAN VETERAN SPORT?... (AJER, May issue 2014)

[57]   Human Equivalent of Cosmo?... (IJSER, May issue 2014)

[58]   THAI-e ETHIA!... (AJER, May issue 2014)

[59]   THE PHILOSOPHY OF "DALIT"?... (AJER, June issue 2014)

[60]   THE IMPACT OF HIGHER QUALIFICATION?... (AJER, June issue 2014)

[61]   THE CRYSTAL UNIVERSE?... (AJER July 2014 issue)

[62]   THE GLOBAL POLITICS?... (AJER July 2014 issue)

[63]   THE KACHCHA THEEVU?... (AJER July 2014 issue)

[64]   THE RADIANT MANAGER?... (AJER July 2014 issue)

[65]   THE UNIVERSAL LAMP?... (IJOART July 2014 issue)

[66]   THE MUSIC RAIN?... (IJERD July 2014 issue)

[67]   THIRI KURAL?... (AJER August 2014 issue)

[68]   THE SIXTH SENSE OF HUMAN?... (AJER August 2014 issue)

[69]   THEE… DARK BOMB?... (IJSER August 2014 issue)

[70]   RAKSHA BANDHAN CULTURE?... (IJERD August 2014 issue)

[71]   THE WHITE BLOOD ANCESTOR?... (AJER August 2014 issue)

[72]   THE PHILOSOPHY OF "ZERO HOUR"?... (IJERD August 2014 issue)

[73]   RAMAR PALAM?... (AJER September 2014 issue)

[74]   THE UNIVERSAL TERRORIST?... (AJER September 2014 issue)

[75]   THE "J-CLOCK"!... (AJER September 2014 issue)

[76]   "STUDENTS" AND "POLITICS"?... (IJERD October 2014 issue)

[77]   THE PREGNANT MAN?... (AJER September 2014 issue)

[78]   PERIAR IS ATHEIST?... (IJSER September 2014 issue)

[79]   A JOURNEY TO "WHITE PLANET"?... (AJER October 2014 issue)

[80]   Coming Soon!... (AJER October 2014 issue)

[81]   THE PREJUDICED JUSTICE?... (IJERD October 2014 issue)

[82]   BRITISH INDIA?... (IJSER October 2014 issue)

[83]   THE PHILOSOPHY OF "HUMAN RIGHTS"?... (IJERD October 2014 issue)

[84]   THE FOSTER CHILD?... (AJER October 2014 issue)

[85]   WHAT DOES MEAN "CRIMINAL"?... (IJSER October 2014 issue)

[86]   1000 YEARS RULE?... (AJER November 2014 issue)

[87]   AM I CORRUPT?... (IJSER November 2014 issue)

[88]   BLACK MONEY?... (AJER November 2014 issue)

[89]   DEAD PARENTS ARE LIVING ANGELS?... (IJERD November 2014 issue)

[90]   MICHAEL IS CHIEF ANGEL?... (AJER November 2014 issue)

[91]   LONG LIVE!... (IJERD November 2014 issue)

[92]   THE SOUL OF THOLKAPPIAM (AJER December 2014 issue)

[93]   SENTHAMIL AMMA!... (IJERD December 2014 issue)

[94]   THE LAW OFLYRICS?... (IJERD December 2014 issue)

REFERENCE

[1]   Intensive Internet "e-book" study through, Google search and wikipedia
[2]   M.Arulmani, "3G Akkanna Man", Annai Publications, Cholapuram, 2011
[3]   M. Arulmani; V.R. Hemalatha, "Tamil the Law of Universe", Annai Publications, Cholapuram, 2012
[4]   Harold Koontz, Heinz Weihriah, "Essentials of management", Tata McGraw-Hill publications, 2005
[5]   M. Arulmani; V.R. Hemalatha, "First Music and First Music Alphabet", Annai Publications, Cholapuram, 2012
[6]   King James Version, "Holy Bible"
[7]   S.A. Perumal, "Human Evolution History"
[8]   "English Dictionary", Oxford Publications
[9]   Sho. Devaneyapavanar, "Tamil first mother language", Chennai, 2009
[10]   Tamilannal, "Tholkoppiar", Chennai, 2007
[11]   "Tamil to English Dictionary", Suravin Publication, 2009
[12]   "Text Material for E5 to E6 upgradaton", BSNL Publication, 2012
        Nakkiran, "Dravidian mother", Chennai, 2007
[13]   Dr. M. Karunanidhi, "Thirukkural Translation", 2010
[14]   "Manorama Tell me why periodicals", M.M. Publication Ltd., Kottayam, 2009
[15]   V.R. Hemalatha, "A Global level peace tourism to Veilankanni", Annai Publications, Cholapuram, 2007
[16]   Prof. Ganapathi Pillai, "Sri Lankan Tamil History", 2004
[17]   Dr. K.K. Pillai, "South Indian History", 2006
[18]   M. Varadharajan, "Language History", Chennai, 2009
[19]   Fr. Y.S. Yagoo, "Western Sun", 2008
[20]   Gopal Chettiar, "Adi Dravidian Origin History", 2004
[21]   M. Arulmani; V.R. Hemalatha, "Ezhem Nadu My Dream" - (2 Parts), Annai Publications, Cholapuram, 2010
[22]   M. Arulmani; V.R. Hemalatha, "The Super Scientist of Climate Control", Annai Publications, Cholapura

Research Paper   open Access

Statistical Method of Estimating Nigerian Hydrocarbon Reserves

[1]Jeffrey O. Oseh; [2]Ifeanyi A. Oguamah; [3]Charles U.Omohimoria; [4]Omotara O. Oluwagbenga

[1,2,3,4]C & PE, COE, Afe Babalola University,Ado – Ekiti,

ABSTRACT:- *Hydrocarbon reserves are basic to planning and investment decisions in Petroleum Industry. Therefore its proper estimation is of considerable importance in oil and gas production. The estimation of hydrocarbon reserves in the Niger Delta Region of Nigeria has been very popular, and very successful, in the Nigerian oil and gas industry for the past 50 years. In order to fully estimate the hydrocarbon potentials in Nigerian Niger Delta Region, a clear understanding of the reserve geology and production history should be acknowledged. Reserves estimation of most fields is often performed through Material Balance and Volumetric methods. Alternatively a simple Estimation Model and Least Squares Regression may be useful or appropriate. This model is based on extrapolation of additional reserve due to exploratory drilling trend and the additional reserve factor which is due to revision of the existing fields. This Estimation model used alongside with Linear Regression Analysis in this study gives improved estimates of the fields considered, hence can be used in other Nigerian Fields with recent production history.*

KEYWORDS:*Additional Reserves, Completed Wells, Estimation Model, Linear Squares Regression, Nigerian Hydrocarbon Reserves).*

I.   INTRODUCTION

The process of estimating oil and gas reserves for a producing field continuesthroughout the life of the field. There is always uncertainty in making such estimates. The level of uncertainty is affected by the following factors: Reservoir type, source of reservoir energy, quantity and quality of the geological, engineering, and geophysical data, assumptions adopted when making the estimate, available technology, and experience and knowledge of the evaluator *Arps, (1956)*. The magnitude of uncertainty, however, decreases with time until the economic limit is reached and the ultimate recovery is realized *Arps, (1956)*. Petroleum (or any other natural resource) reserves cannot be measured directly. They are estimates of future production under certain conditions which may or may not be well specified, but which include economic assumptions, knowledge of the feasibility of projects to extract the resources, and geological information. Judgment is involved and different estimates for the same field are legitimately possible*Ross, (2001)*.

Statistical estimation of oil and gas reserves is the estimation of petroleum reserves using historical records of production, exploratory drilling, pressure history and other factors that influence reserves *SPE, (1979)*. Reserve estimation is useful in evaluation of exploration and development expenditures, to determine the market value of a field in connection with possible purchase or sale. It is also used to determine the feasibility of secondary recovery projects and other special recovery projects. Reserves can be divided into primary and secondary reserves. Primary reserves is the estimated future commercial production recoverable by normal or primary method as a result of energy availability in the reservoir while secondary reserve is the estimated future commercial production which will be recovered in addition to the primary reserves as a result of pressure maintenance, water flooding or other secondary methods *Cronquist, (2001)*. Unproved reserves are less certain to be recovered than proved reserves and may be sub-classified as probable or possible to denote increasing uncertainty. Proved reserves can be estimated with reasonable certainty to be recoverable under current economic conditions which include prices and costs prevailing at the time of the estimate *SPE/WPC/AAPG, (2001)*. Proved reserves may be developed or under developed. It must have facilities to process and transport those reserves to markets that are operational at the time of the estimate or there is commitment or reasonable expectation to install such facilities in the future *SPE/WPC/AAPG, (2001)*..

The additional reserve each year is dependent on reserves found by exploratory drilling in new pools, in new fields and reserves done to re-evaluate the basic geological and engineering data of existing fields. A discovery during one year will result in the drilling of additional wells during subsequent production and these wells add productive acreage to the previously estimated proved area *Jacks, (1990).* Other reserves estimation methods includes: Analogy, Volumetric, Decline analysis, Material balance, and Reservoir simulation *Dake, (1989)*. Most of the field data required are not obtainable until the reservoir has produced for substantial period, therefore evaluated reserve of new field using other reserves estimation methods are not reliable.

Aims of the study : The aims of this study are to Estimate the Nigerian hydrocarbon reserve and to measure the crude oil potential of Nigerian fieldsusing Least Squares Regression (LSR).

Objective of the study : A mathematical model "(Estimation Model) for petroleum reserves estimate based on extrapolation of exploratory drilling trend was developed. Additional reserve factor due to revision of existing field is included in the model. Method of Least Square Regression is employed to solve the constants in the developed model and to compare the estimated reserves from the actual reserves.

Geological Settings of the Niger Delta Region of Nigeria : Niger Delta is a large arcuate Tertiary prograding sedimentary complex deposited under transitional marine, deltaic, and continental environments since Eocene in the North to Pliocene in the South. Located within the Cenozoic formation of Southern Nigeria in West Africa, it covers an area of about 75,000 Km *Arps, (1967)*from the Calabar Flank and Abakaliki Trough in Eastern Nigeria to the Benin Flank in the West, and it opens to the Atlantic ocean in the South where it protrudes into the Gulf of Guinea as an extension from the Benue Trough and Anambra Basin provinces *Burke et al.,* **(1972).** The Niger Delta as a prograding sedimentary complex is characterized by a coarsening upward regressive sequences. The overall regressive sequence of clastic sediments was deposited in a series of offlap cycles that were interrupted by periods of sea level change *Etu-Efeotor, (1997).* These periods resulted in episodes of erosion or marine transgression. Stratigraphically, the Tertiary Niger Delta is divided into three Formations, namely Akata Formation, Agbada Formation, and Benin Formation *Ekweozor et al, (1984).* The Akata Formation at the base of the delta is predominantly undercompacted, overpressured sequence of thick marine shales, clays and siltstones (potential source rock) with turbidite sandstones (potential reservoirs in deep water). It is estimated that the formation is up to 7,000 meters thick *Bouvier et al, (1989).* The Agbada Formation, the major petroleum-bearing unit about 3700m thick, is alternation sequence of paralic sandstones, clays and siltstone and it is reported to show a two-fold division *Doust, and Omatsola, (1990).* The upper Benin Formation overlying Agbada Formation consists of massive, unconsolidated continental sandstones.

Why "Linear Regression Analysis (LRA)" for Hydrocarbon Reserves? : The "Method of Least Squares" that is used to estimate parameters estimates was independently developed in the late 1700's and the early 1800's by the mathematician Karl Friedrich Gauss, Adrien Marie Legendre and Robert Adrain *Stigler, (1978)], Harter, (1976), Stigler, (1986)* working in Germany, France and America respectively. In the least squares method the unknown parameters are estimated by minimizing the sum of the squared derivatives between the data and the model. The minimization process reduces the over-determined system of equations formed by the data to a sensible system of p (where p is the number of parameters in the functional part of the model) equations in p unknowns. This new system of equations is then solved to obtain the parameter estimates *Stigler, (1986)*. Linear Regression Analysis (LRA) is by far the most widely used modeling method adapted to a broad range of situations that are outside its direct scope. It plays a strong underlying role in many other modeling methods like Non Linear Least Squares Regression Method, Weighted Least Squares Regression, and LOESS *Stigler, (1978).* Linear Regression Analysis (LRA) can be used directly with an appropriate data set to fit complex data. It has earned its place as the primary tool for process modeling because of its effectiveness and completeness. Though there are types of data that are better described by functions that are non-linear in the parameters, many process in science and engineering are well described by linear models. This is because either the processes are inherently linear or because, over short range, any process can be well-approximated by a linear model. The estimates of the unknown parameters obtained from linear regression are the optimal estimates from a broad class of possible parameter estimates under the usual assumptions used for process modeling. Practically speaking, Linear Regression Analysis (LRA) makes very efficient use of the data. Good results can be obtained with relatively small data sets *Larry, (1998).*

II.   RESEARCH METHODOLOGY

a). Model Development Procedure : The model is based on the principle that the reserve at the end of any year will be the sum of the reserve at the beginning of that year and additional reserve minus productions during that year. Additional reserves of hydrocarbons in any year are broken down into two established categories: Those

attributable to recoveries as a result of exploratory effort in new pools in new fields. Reserves attributed to revisions as a result of re-evaluation on the existing fields. Newly discovered petroleum reservoirs, even in existing fields are always fully developed during the year of recovery *John, (2004).* Therefore, the year and reserve estimates of discoveries generally represent only a part of the reserves that will ultimately be assigned to these new reservoirs. A discovery during one year will usually result in the drilling of additional wells during subsequent years and generally these new wells will increase the previously estimated productive area *Mistrot, (1998).* Additional producing wells in a reservoir not only add to the estimated productive area but also help to improve the basic geologic and engineering data. Early estimates of porosity, interstitial water, pay thickness and other important reservoir factors may be reviewed therefore from future wells. As field development continues, production history accumulates and the most accurate methods of pressure maintenance and secondary recovery factor are formulated *McMichael, and Spencer, (2001).*

b). Estimation Model Derivation
Reserve at the end of any year is defined as:
$$R_x = R(x-1) + R_x^+ - Q_x + A_x \tag{1.1}$$
Where,
X is the number of terms in years
R_x is the estimated reserve at the end of xth year.
$R(x-1)$ is the estimated reserve at the end of (x–1)th year.
R_x^+ is the additional reserve during the xth year due to exploratory drilling.
Q_x is the production in the xth year
A_x is the additional reserve in the xth year due to revision of existing fields.
Additional reserve due to exploratory drilling R_x^+ based on historical trend is defined as:
$$R_x^+ = (m + nP_x) - C_{x-1} \tag{1.2}$$
Where,
m is the intercept of regression line of plot of cumulative additional reserve against cumulative number of completed wells.
n is the rate of change of cumulative additional reserve with cumulative number of completed wells.
P_x is the cumulative number of completed wells at the end of xth year.
C_{x-1} is the cumulative additional reserve at the end of (x-1)th year.
In general, $(m + nP_x)$ represents cumulative additional reserve due to exploratory effort in the xth year. Thus, it can be represented by C_x.
$$C_x = m + nP_x \tag{1.3}$$
Where,
C_x is the cumulative additional reserve in the xth year. The Estimation Model can therefore be approximated as:
$$R_x = R(x-1) + C_x - C_{x-1} - Q_x + A_x \tag{1.4}$$
$$= R(x-1) + (m + nP_x) - C_{x-1} - Q_x + A_x \tag{1.5}$$
$$= R(x-1) + (m + nP_x) + A_x - (C_{x-1} + Q_x) \tag{1.6}$$
Constants m and n can be calculated by Linear Regression Analysis (LRA). **Equation (1.6)** represents the general form of the Estimation Model.

c). Linear Regression Analysis (LRA)
The concept of linear regression is concerned with an investigation of the dependence of one variable on a linear combination of independent variable. When the dependent variable is expressed linearly in terms of one independent variable, the linear expression is said to be simple while it is said to be multiple when the dependent variables is expressed linearly in terms of several independent variables. In this study, the linear regression is simple since only one independent variable is involved.
From **Equation (1.3):**
$$C_x = m + nP_x$$
C_x from this equation is the calculated C_x which may not correspond to the observed C_x.
Let $C_x' =$ observed C_x.
Then the error term, T_x is calculated as:
$$T_x = C_x - C_x' \tag{1.7}$$
$$T_x = (nP_x + m) \tag{1.8}$$
To minimize the error, a relation of the form is introduced:
$$S = \sum T_x^2 \tag{1.9}$$
Using least squares to minimize S, so that
$$\frac{ds}{dT} = 0; \frac{ds}{dm} = 0$$

$\frac{ds}{dn} = 2\sum t \frac{dTx}{xdn} = 0$

$= 2\sum(nP_x + m - C_x)P_x = 0$

$= n\sum P_x{}^2 + m\sum P_x - \sum C_x P_x = 0$

Therefore,

$\sum C_x P_x = m\sum P_x + n\sum P_x{}^2$ (2.0)

Similarly,

$\frac{ds}{dm} = 2\sum T_x \frac{dTx}{xdn} = 0$

$= 2\sum(nP_x + m - C_x) \times 1 = 0$

$= n\sum P_x + m - \sum C_x = 0$

$= n\sum P_x + km - \sum C_x = 0$

Therefore,

$\sum C_x = km + n\sum P_x$ (2.1)

Where,

k is the number of data used in trend analysis. **Equations (2.0) and (2.1)** can then be solved simultaneously to obtain **m** and **n.**

$\sum C_x = km + n\sum P_x$

$\sum C_x P_x = m P_x + n\sum P_x + n\sum P_x^2$

Or

$\sum P_x C_x = m\,k\sum P_x + n\,(\sum P_x)^2$ (2.2)

$k\sum C_x P_x = m\,k\sum P_x + n\sum P_x{}^2$ (2.3)

$k\sum C_x - (\sum P_x)(\sum C_x) = (k\sum P_x{}^2 - (\sum P_x)^2)$

$n = \frac{k\sum CxPx - \sum PxCx}{(k\sum Px{}^2 - (\sum Px){}^2)}$ (2.4)

Substitute **equation (2.4) in equation**   (2.1)

$\sum C_x = km + \frac{k\sum Px \sum CxPx - (\sum Px){}^2 \sum Cx}{(k\sum Px{}^2 - (\sum Px){}^2)}$

$m = \frac{\sum Cx}{k} - \frac{1}{k} \frac{k\sum Px \sum CxPx - (\sum Px){}^2 \sum Cx}{(k\sum Px{}^2 - (\sum Px){}^2)}$ (2.5)

$C_x = m + nP_x$ represents equation of regression line on C_x and P_x.

d). Estimated Model Equation Application in Nigerian Fields

The developed estimation model can be used to evaluate the total petroleum reserves in Nigeria.

Recall that:

$R_x = R(x-1) + (m + nP_x) + A_x - (C_{x-1} + Q_x)$ (1.6)

Assuming $A_x = 0$, that is no revision of the existing fields used in the reserve estimation, the estimation model will reduce to:

$R_x = R(x-1) + (m + nP_x) + (C_{x-1} + Q_x)$ (2.6)

e). Concept of Correlation and Standard Error of Estimate

Correlation is the degree of relationship between variables, in this case, the cumulated additional reserves and cumulated number of completed wells. The coefficient of correlation can be determined using the Pearson's Product-Moment Method.

$R = k\frac{k\sum PxCx - (\sum Px)\sum Cx}{\sqrt{(k\sum Px{}^2 - (\sum Px){}^2)(k\sum Px{}^2 - (\sum Cx){}^2)}}$ (2.7)

Standard error of estimate S is a measure of the scatter about the regression line and is supplied by the quantity.

$S = \sqrt{\frac{\sum Cx{}^2 - m(\sum Cx) - n\sum CxPx}{k}}$ (2.8)

III. RESULTS AND DISCUSSION

Results

The general form of the estimation model is given by:

$R_x = R(x-1) + C_x - C_{x-1} - Q_x + A_x$

Where,

R_x = Estimated reserve at the end of xth year.

$R(x-1)$ = Estimated reserve at the end of (x–1)th year.

C_x = Cumulative additional reserve during the xth year due to exploratory drilling at the end of xth year.

C_{x-1}= Cumulative additional reserve at the end of (x-1)th year.
Q_x= Production during the year.
A_x= Additional reserve in the xth year due to revision of existing fields.
$C_x = (m + nP_x)$
Where,
P_x is the intercept of regression line of plot of cumulative additional reserve against cumulative number of completed wells.
m and n are constant determined from linear regression model.

Estimation of Fields X and Y Reserves in Nigeria
Two fields considered in Nigeria were assigned X and Y fields due to the sensitive nature of the data*(DPR, 2014).* The generalized form of the estimation model is:
$R_x = R(x–1) + (m + nP_x) + A_x – (C_{x-1} + Q_x).$
A_x was assumed to be zero, i.e. no revision of the existing fields used in the reserve estimation.
The above equation reduces to:
$R_x = R(x–1) + (m + nP_x) - (C_{x-1} + Q_x).$ (2.6)

Coefficient of Correlation
The correlation between the cumulative additional reserve and cumulative number of completed wells can be estimated from **equation (2.6)** using the data shown in **Tables 2** and **3.**

Table 1: Coefficient of Correlation for Field X and Y (2014)

Field	Coefficient of Correlation, r
X	0.999817
Y	0.993728

The result from **Table 1** shows that there is a perfect correlation between cumulative additional reserve and cumulative number of completed wells in the positive direction for both fields.

Table 2: Production History of Field X (2014)

Year	Annual Production (mmmbbls)	Reserves (mmmbbls)	Additional Reserve (mmmbbls)	Cumulative Additional Reserve (mmmbbls)	Cumulative No. of Completed Wells
1978	0.0301	0.615	0.0348	0.3048	18
1979	0.0304	0.594	0.0098	0.0446	24
1980	0.0363	0.560	0.0022	0.0468	25
1981	0.0217	0.597	0.0587	0.1055	55
1982	0.0318	0.571	0.0053	0.1108	58
1983	0.0258	0.554	0.0090	0.1198	62
1984	0.0286	0.529	0.0041	0.1239	64

Table 3: Production History of Field Y (2014)

Year	Annual Production (mmmbbls)	Reserve (mmm bbls)	Additional reserves (mmmbbls)	Cumulative additional reserve (mmmbbls)	Cumulative No. of completed wells
1978	0.0150	0.116	0.0201	0.0201	1.0
1979	0.0153	0.142	0.0413	0.0614	31

19980	0.0133	0.144	0.0148	0.0762	38
1981	0.0088	0.138	0.0026	0.0788	41
1982	0.0057	0.133	0.0009	0.0797	42
1983	0.0064	0.128	0.0012	0.0809	44
1984	0.0054	0.123	0.0008	0.0817	45

Determination of constants n and m from Table 2 and 3 using equation (2.4) and (2.5) respectively

Field	n	m
X	0.1949×10^7	-0.1440×10^7
Y	0.1807×10^7	0.3607×10^7

Applying the constants generated from **equation (2.4)** and **(2.5)** respectively to the developed estimation model of **equation (1.6)** for **Field X** and **Y** gives the results in **Tables 4** and **5** respectively.

Table 4: Annual Estimated Reserves and Actual Reserves for Field X (2014)

Year	Estimated Reserve (mmmbbls)	Actual Reserves (mmmbbls)	Difference
1979	0.596092	0.59420	0.001892
1980	0.561740	0.56010	0.001640
1981	0.598499	0.59710	0.001399
1982	0.527544	0.57060	0.000739
1983	0.554539	0.55380	0.000739
1984	0.529836	0.52930	0.000536

Table 5: Annual Estimated Reserve and Actual Reserve for Field Y (2014)

Year	Estimated Reserve (mmmbbls)	Actual Reserves (mmmbbls)	Difference
1979	0.138946	0.142300	0.003354
1980	0.138295	0.143300	0.005505
1981	0.134915	0.137600	0.002684
1982	0.131022	0.132800	0.001778
1983	0.128236	0.127600	0.000636
1984	0.124643	0.123000	0.001643

Concept of Correlation Coefficient and Standard Error of Estimate : The correlation between the cumulative additional reserve and cumulative number of completed wells as well as standard error of estimate were evaluated from **equation (2.7)** and **(2.8)** respectively using the data in **Table 6:**
The obtained results of **r = 0.9996208 and S = 0.6980×10^6 for Field X**, and **S = 0.2323×10^7 for Field Y** shows that there is perfect correlation between cumulative additional reserve and cumulative number of completed wells in the positive direction.

Determination of constants n and m for Nigerian hydrocarbon reserves

Applying data in **Table 4** to constants n and m expressions gives:

n = 0.7527 × 10^7 bbls/well and m = 0.3128 × 10^9 bbls/well

The general equation of estimated model therefore becomes:

R$_x$ = R (x–1) + (0.3128 × 10^9 + 0.7527 × 10^7 P$_x$) $_–$ (C$_{x-1}$ + Q$_x$). (2.9)

The result obtained from **equation (2.9)** using data in **Table 6** is shown in **Table 7.**

Table 6: Production History of a Named Nigerian field (2014)

Year	Annual Production (mmmbbls)	Reserve (mmmbbls)	Additional reserve (mmmbbls)	Cumulative additional reserve (mmmbbls)	Cumulative no. of completed wells (mmmbbls)
1970	0.3958	10.400	0.4458	0.4958	105
1971	0.5596	11.200	1.3596	1.8554	223
1972	0.6666	12.100	1.5666	3.420	368
1973	0.7484	12.700	1.3484	4.7704	520
1974	0.8231	12.800	0.9231	5.6935	652
1975	0.6514	13.000	0.8514	6.5449	819
1976	0.7568	12.800	0.5568	7.1017	936
1977	0.7646	12.600	0.5648	7.6665	1033

Table 7: Annual Estimated Reserves and Actual Reserves for Nigeria (2014)

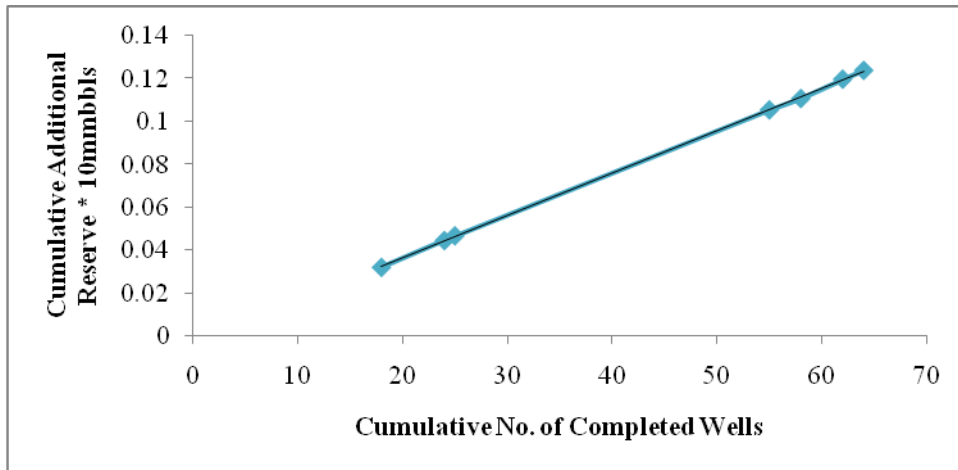| Year	Estimate Reserves (mmmbbls)	Actual Reserves (mmmbbls)	Variation
1971	10.728625	11.20000	0.471375
1972	11.153489	12.10000	0.946511
1973	11.549245	12.70000	1.150755
1974	11.719751	12.80000	1.080249
1975	12.325417	13.00000	0.674583
1976	12.449317	12.80000	0.350683
1977	12.414868	12.60000	0.185132

Fig. 1: Cumulative Additional Reseves vs. Cumulative No. of Completed Wells for Field X
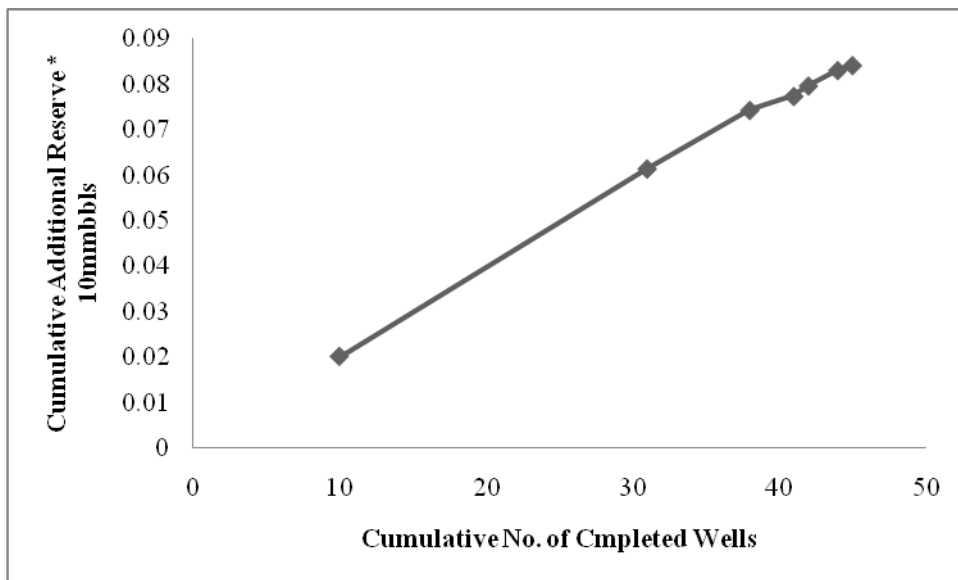

Fig. 2: Cumulative Additional Reseves vs. Cumulative No. of Completed Wells for Field Y
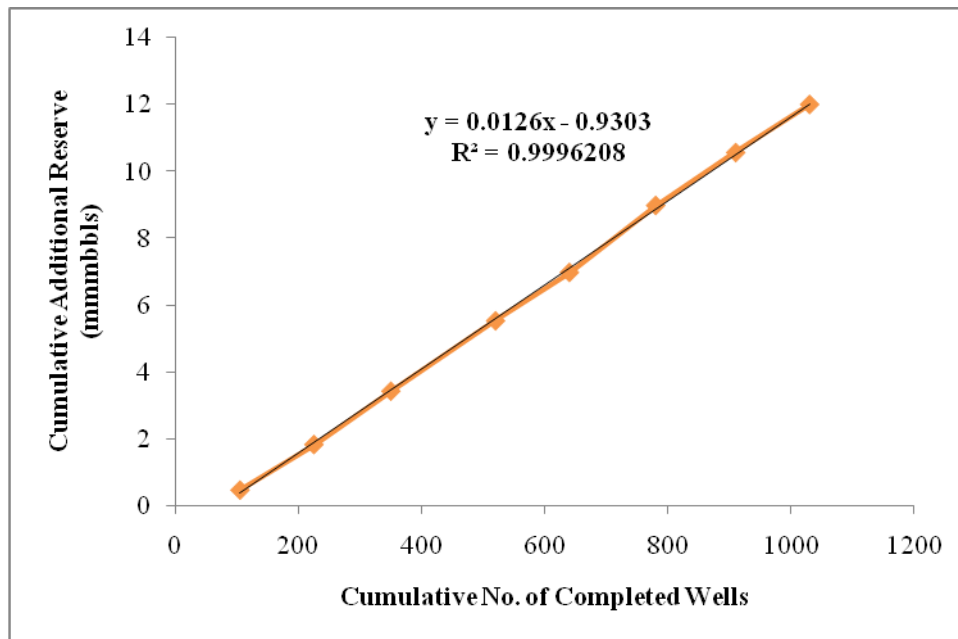
Fig. 3: Cumulative Additional Reseves vs. Cumulative No. of Completed Wells for Nigeria

III. DISCUSSION

Thecumulative additional reserve with cumulative number of completed wells varies from one field to the other and it is a function of hydrocarbon potential of each field. A field with high hydrocarbon potential has a high rate of change of cumulative number of completed wells. For example the rate of change of cumulative additional reserves with cumulative number of completed wells of **Field Y** is larger than that of **Field X**. It shows that **Field Y** has a huge crude oil potential than **Field X**. Therefore the developed Estimation Model could be used as a benchmark to measure the hydrocarbon potential of a given field.The variation between the estimated reserve and the actual reserve could be attributed to the assumption made in the application of the estimation model that no revision of the field samples has been used which makes the additional reserve due to the revision of the field to be zero. The additional reserve when added by way of revision could alter the reserve potential when increased knowledge of the field changes the field fractional recovery.

IV. CONCLUSION AND RECOMMENDATIONS

Conclusion

The following conclusions could be drawn from the findings:

- The Estimation model is useful in that better and more reliable reserve estimates are evaluated since the most recent data are used.
- The model gives an improved performance when compared between cumulative additional reserve and cumulative number of completed wells.
- The model depends on sound, accurate and up to date production data. Direct estimation of reserves in future will not be possible without first estimating the production during the year and reserve at the end of the preceding year.
- Reserves estimates of some existing fields could be considerably improved upon if such fields are revised by way of re-evaluating their basic geology and engineering data.

Recommendations

- The model only investigated the reserves in existing wells. Effort should be geared towards evaluating reserves of unexpected fields.
- A mathematical expression that would relate the rate of change of cumulative additional reserve to cumulative number of completed wells be developed and incorporated into the model to replace the one evaluated from linear regression analysis.

V. ACKNOWLEDGEMENTS

The author acknowledges Prof. A. I. Igbafe and the entire staff in the Department of Petroleum engineering, Afe Babalola University, Ado-Ekiti, Nigeria for the contribution and assistance in this research work. I am equally grateful to Engr. Rotimi Osho (SPE NAICE, 2008 TPC Chairman) for given me much courage in this technical paper. I am grateful to Engr. T. A. Ibeh (DPR Data Analyst) and Dr. A. I. Suleiman for all that they contributed in this paper.

REFERENCES

[1]   "Standards Pertaining to the Estimating and Auditing of Oil and Gas Reserve Information," SPE, Richardson, Texas (1979).

[2]   **Arps, J. J., & Ertekin, T. (1967).** "Statistical Analysis of Crude Oil Recovery and Recovery Efficiency," Bulletin D14, American Petroleum Institute, Washington D.C.

[3]   **Arps, J.J., (1956).** Estimation of primary oil reserves: Transactions AIME (Journal of Petroleum Technology), vol. 207, pp. 182-191.

[4]   **Bouvier, J. D., Kaars-Sijpesteijn, C. H., Kluener, D. F., & Onyejekwe, C. C. (1989).** "Three-dimensional Seismic Interpretation and Fault sealing Investigations". Nun River Field, Nigeria. AAPG Bulletin 73(11): 1397-1414.

[5]   **Burke, R. C., Desauvagie, T .F. J., & Whiteman, A. J. (1972).** Geological History of the Benue Valley andadjacent areas. University press: Ibadan.

[6]   **Cronquist, C. (2001).** Estimation and Classification of Reserves of Crude Oil, Natural Gas, and Condensate. Richardson, Texas: SPE.

[7]   **Dake, L. P. (1989).** The Practice of Reservoir Engineering. Amsterdam: Elsevier Scientific Publishing Co. pp. 23-44.

[8]   **Department of Petroleum Resources (2014),** No. 7, Kofo Abayomi Street, Victoria Island, Lagos State, Nigeria.

[9]   **Doust, H., & Omatsola, E. (1990).** Niger Delta. "Divergent/passive Margin Basins". AAPG Memoir 48: 239-248.

[10]   **Ekweozor, C. M., & Daukoro, E. M. (1984).** Petroleum source bed evaluation of Tertiary Niger Delta-reply: American Association of Petroleum Geologists Bulletin, vol. 68, pp. 390-394.

[11]   **Etu-Efeotor, J. O. (1997).** Fundamentals of Petroleum Geology. Paragraphics: pp. 21-23, Port Harcourt, Rivers State, Nigeria.

[12]   Guidelines for the Evaluation of Petroleum Reserves and Resources.A Supplement to the SPE/WPC Petroleum Reserves Definitions and theSPE/WPC/AAPG Petroleum Resources Definitions (2001), pp. 1-7, 131-137.

[13]   **Harter, H. L. (1976).** The method of Least Squares and some alternatives. International Statistical Review 42: 147-174, 235-264, 282.

[14]   **Jacks, H.H. (1990).** Forecasting Future Performance. Reservoir Simulation, C.C. Mattox and R.L. Dalton eds., Vol. 13, pp. 99-110. Richardson, Texas: Monograph Series, SPE.

[15]   **John, M. (2004)**. *"*Petroleum Reserves in Question" Sustainable Development Programme SDP BP 04/03, pp. 23-56.

[16]   **Larry, J. S. (1998).** "Theory and Problems of Beginning Statistics" (Schaum's Outline Series), McGraw Hill, pp. 309-330.

[17]   **McMichael, C. and Spencer, A. (2001).** "Operational Issues" The Guidelines for the Evaluation of Petroleum Reserves and Resources, pp. 5-10, 21-26. Society of Petroleum Engineers, 222 Palisades Creek Drive Richardson, TX 75080-2040, USA.

[18]   **Mistrot, Gus A. (1998).** Reserves Estimating-Common Errors and How to Avoid Them. pp. 39-44, Richardson, Texas: SPE Short Course, SPE.

[19]   **Ross, J.G. (2001).** Petroleum Resources Classification and Definitions. The Guidelines for the Evaluation of Petroleum Reserves and Resources, pp. 6-11. 25 Richardson, Texas: SPE.

[20]   **Stigler, S. M. (1978)**. "Mathematical Statistics in the early state". The Annals of Statistics, vol. 6, pp. 239-265

[21]   **Stigler, S. M. (1986).** The History of Statistics. The measurement of Uncertainty Before 1900, The Belknap Press of Harvard University Press, Cambridge, Massachusetts, pp. 56-87.

Eye State Detection Using Image Processing Technique

Vijayalaxmi[1], D.Elizabeth Rani[2]

[1] *Electronics & Communication Engineering Department, Vignan Institute of Technology and Science, Hyderabad, India;*
[2] *Electronics & Instrumentation Engineering Department, Gitam Institute of Technology, GITAM University, Vishakapatnam, India;*

ABSTRACT: *Estimation of driver fatigue is a significant factor in driver assistance system. Recent statistics shows that annually 1,550 deaths and 71,000 injuries are attributed to fatigue related accidents. Because of the hazard that drowsiness present on the road, methods need to be developed for counteracting its affects. The focus may be placed on designing a system that will accurately monitor the open or closed state of the driver's eyes. In this paper, an algorithm is proposed for determining the state of an eye, based on the mean and standard deviation of eye image. In the proposed algorithm, Skin segmentation and Lab transform is used to detect face and Eye. To know the state of eye, mean and standard deviation of eye area is determined. It is found from a result that if mean is >0.2 and standard deviation is <0.02 then the state of the eye is open otherwise closed. This method is tested on face database from M/s. Audio Visual Technologies Group (GTAV) and also a new database is created in-house for the testing purpose. The overall success rate of the algorithm is 89.5%.*

KEYWORDS: *Face Extraction, Eye State, Mean, Standard Deviation*

I. INTRODUCTION

Many accidents occur due to the manual error and more so due to fatigue. While many of the drunken driving may be highly publicized, the major contributing factor in most accidents particularly fatal is due to driver fatigue. According to the Road Safety Authority, driving tired is as lethal as driving drunk. up to 20% of fatal crashes may be linked to driver fatigue, later research indicates that driver fatigue could be a contributory factor up to a fifth of driver deaths. This calls for the development of a device to alert the driver, if not control the vehicle automatically. In the recent years, many researchers worked on these devices and few approaches have been reported [3-12]. One of the suggested methods is to monitor the movement of the vehicle to detect drowsiness of the driver [3]. However this method has limitations as the results are influenced by the type of vehicle and the condition of road. Another method is to process the electrocardiogram (ECG) signals of driver [4]. This approach also has limitations as ECG probes shall always be connected to the driver's body. That would disturb the driver. Few researches tried to assess the fatigue factor by monitoring the eye blink rate of the driver [5-11].

Successful detection of eye blink rate has been the interest of many researchers. H Wen-Bing, et.al. [5] proposed methods based on combination of projection and the geometry feature of iris and pupil. T. D'Orazio, et.al. and Z.Zhang, et.al. [6,7] use the fact that the iris and pupil are darker than skin and white part of the eye. Y.Lei, et.al. [11] proposed an algorithm based on the cascade AdaBoost classifier. T.Hong, et.al.[12], a gray level image of an eye is converted to a binary image, using a predetermined threshold. Then, based on the number of black and white pixels of this binary image, state of the eye is determined. The algorithm presented by Ms.Devi, et.al. [8] used the Hough Transform to detect the iris and to determine openness of the eye. Some researchers are based on the projection of the image, to determine the state of an eye. Z.Liu, et.al. [9], the vertical projection of the image of both eyes is used. J.Wu, T.Chen, et.al. [10], horizontal projection image of an eye is used to determine the interval between eyebrows and eyelids and to recognize the state of an eye. MJ Flores, et.al. [14], the horizontal projection of the image of a face is calculated to determine state of an eye. Some works also are based on "Support Vector Machine" (SVM) classifier. P.Viola, et.al. [15], the SVM classifier is used to detect state of the eye. F Smach, et.al.[16] used SVM classifier and Gabor filter to extract eye characteristic. In the above methods, the authors used some conditions which make some difficulties in the eye state recognition.
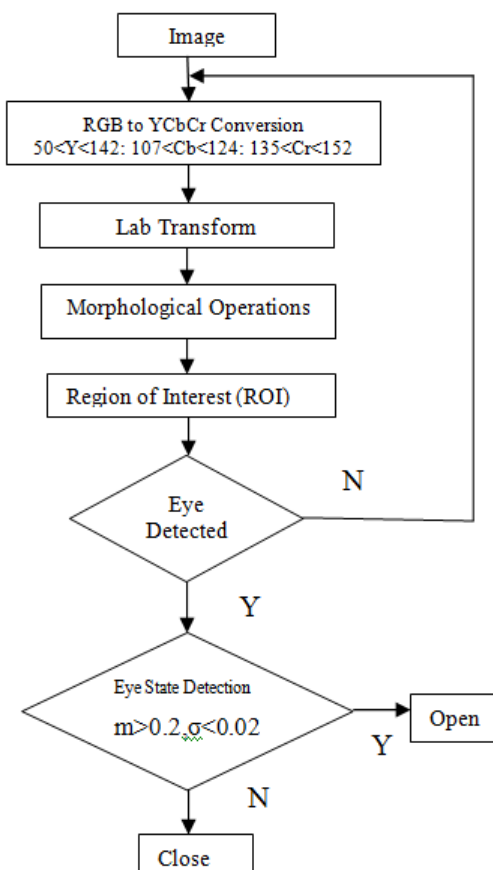
Fig.1. Flow Chart of proposed algorithm

A new algorithm is now proposed to learn the eye status that takes all the earlier stated constrains, thus enhances the reliability. This algorithm does not need training and hence easily handles varying light conditions. In order to verify the correctness of the proposed algorithm, a computer simulation is developed. The algorithm is verified for its accuracy with images available in different data bases.

The rest of this paper is organized as follows. The proposed algorithm is discussed in Section II. Section III describes face extraction, the eye state detection and tracking is described in Section IV, Section V discusses results and conclusions are drawn in section V.

II.   PROPOSED ALGORITHM

The proposed algorithm is implemented on SIMULINK and all the required functions are developed using MATLAB routines. The first step is face extraction and then the localization of the eyes. This is done by following one of the methods proposed by Dr.P.Sudhakar Rao, et.al.[24]. Subsequently the algorithm learns the status of each eye as 'CLOSE' or 'OPEN'. The proposed algorithm is shown in Fig.1. This proposed algorithm extracts the face and eyes using skin segmentation and state of eyes is recognized based on mean and standard deviation.The eye state detection algorithm is divided into three steps i) face detection and extraction ii) eye detection and iii) eye tracking. The performance of each step is highly dependent on the previous steps as the results obtained in each step are passed on to the next step as input.

Face Extraction : Given an arbitrary image, the goal of face detection is to determine whether or not there are any faces in the image and if so return the image location . The common approach of face region detection is by using the characteristic of the skin colour.

Algorithm for face extraction: The following is the sequence of steps followed for the face extraction.
[1]   i. Convert the given image in RGB colour space into YCbCr colour space.
[2]   ii.The Y, Cb and Cr ranges for skin region are: $50<Y<142$, $107<Cb<124$ and $135<Cr<152$. Each pixel of YCbCr is compared against the limits of Y, Cb and Cr to determine if the skin is present and if so by

means of thresholding, the face is identified and segmented. In order to eliminate non-skin regions in the image, it is required to erode and dilate the image using a structured element. Subsequently do filling operation to fill the area defined by locations with connectivity.

[3]   iii.Compare the dimensions with certain thresholds for each region and percentage of skin in each region, which will help in removing non -face object.

[4]   iv.For each region if height and width are within the range then the processed image is a face and otherwise it is not a face.

An example of an original image and the face extracted image are shown in Figure 2(a) and (b).

| Original Image | Extracted face |

Fig.2.Face Extraction

III. EYE STATE DETECTION

After the face detection, the next step is to determine the location of the eyes. In this process, the area where both eyes are located is found or two eyes individually localized. Eye areas are marked by a rectangle after successfully locating. The steps followed to find and track eyes are

[1]   Apply Lab transform to the extracted face to eliminate unwanted portion.

[2]   ii.Apply morphological operations on the output of transformed image to remove noise.

[3]   iii.Determine the region of interest which locates eyes.

[4]   iv.Apply region properties to track the eye pair.

Before eyes are tracked, eyes must be first located. Eyes should also be relocated periodically during the tracking in order to make sure that the correct feature is being considered. The face is divided into 6 quadrants. The region of eyes will be in the uppermost 2 quadrants. Lab transform is applied on the extracted face to locate the eyes. Connected component analysis is applied to detect the eyes. The result of Eye Detection is shown in Figure 3.
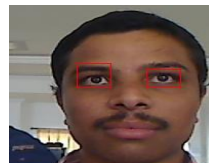
Fig.3. Results of Eye Detection

The image of an open human eye has three different regions, pupil/iris in the middle and two white parts in the left and right sides. However, in the image of a closed eye, these areas can't be discriminated. The effect of this observation is the basis of our proposed algorithm to determine the state of the eye. The vector of the pupil and iris area has less gray values than two other white areas. As a result, the mean and standard deviation of the 'OPEN' are found and concluded that mean is always >0.2 and standard deviation is always <0.02. If the mean is <0.2 and standard deviation is >0.02, then the state of the eye is concluded as 'CLOSE'. Both cases are shown in Figures 4.a. and 4.b.

| Closed eye (μ=0.179 & σ = 0.01742) | Open eye (μ=0.3366 & σ = 0.2243) |
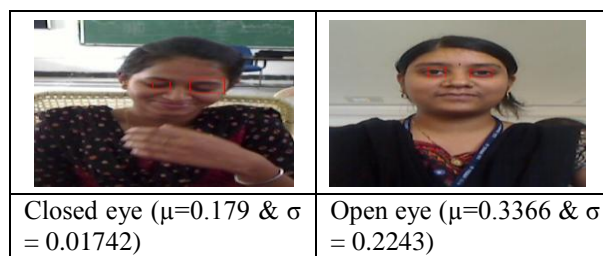
Fig.4.Closed & Open Eyes

IV. RESULTS

The results obtained after testing on GTAV database and in-house database images are tabulated in Table 1.

Table 1: Result Analysis

S. N.	μ	Σ	Output	Status of Eye
1.	0.179	0.01742	0	CLOSE
2.	0.3366	0.2243	1	OPEN
3.	0.2931	0.0166	0	CLOSE
4.	0.2747	0.01384	0	CLOSE
5.	0.4611	0.05534	1	OPEN
6.	0.3534	0.01691	0	CLOSE
7.	0.3189	0.03361	1	OPEN
8.	0.1999	0.04755	1	OPEN
9.	0.3624	0.01552	0	CLOSE
10	0.3281	0.03449	1	OPEN

For most of the cases this algorithm works to the satisfaction. However, in some cases the algorithm fails and 3 such cases are shown in Figure 5,6,7.

Case 1: The case where the algorithm failed

Fig. 5: Failure case1

The left eye is not covered in the region of interest as shown in the figure 5. The eyebrows are covered within ROI hence not detected.

Case 2: The case where the algorithm failed

Fig. 6: Failure case2

The right eye is covered in the ROI but its area is too small to be in the range and hence not detected.

Case 3: The case where the algorithm failed

Fig.7: Failure Case3

The right eyebrow is covered in the ROI and hence eyebrows are also detected.

V. CONCLUSION

A new approach for Eye state detection is presented in this paper. Simulation results shows that the proposed algorithm works successfully on different images under different illumination conditions. A total of 36 different images from GTAV database [25] and 30 images from local database have been tested in the laboratory. The success rate of the proposed algorithm is 89.5%. The purpose of this research work is to develop a driver fatigue detection system using vision based approach based on eye blink rate.

REFERENCES

[1]   P Boyraz, JHL Hansen, Active accident avoidance case study: integrating drowsiness monitoring system with lateral control and speed regulation in passenger vehicles. IEEE International Conference on Vehicular Electronics and Safety, ICVES 2008, 293–298 (2008) .

[2]   K Yun Seong, L Haet Bit, K Jung Soo, B Hyun Jae, R Myung Suk, P Kwang Suk, ECG, EOG detection from helmet based system. 6th International Special Topic Conference on Information Technology Applications in Biomedicine, 2007. ITAB 2007, 191–193 (2007)

[3]   PR Tabrizi, RA Zoroofi, Drowsiness detection based on brightness and numeral features of eye image. Fifth International Conference on Intelligent Information Hiding and Multimedia Signal Processing, 2009. IIH-MSP'09, 1310–1313 (2009)

[4]   WB Horng, CY Chen, Improved driver fatigue detection system based on eye tracking and dynamic template matching ICS, 11–2.

[5]   H Wen-Bing, C Chih-Yuan, C Yi, F Chun-Hai, Driver fatigue detection based on eye tracking and dynamic template matching. Proceeding of the 2004 IEEE International Conference on Networking, Sensing & Control (Taipei, Taiwan, 2004)

[6]   T D'Orazio, M Leo, C Guaragnella, A Distante, A visual approach for driver inattention detection. Pattern Recogn 40, 2341–2355 (2007).

[7]   Z Zhang, J-S Zhang, Driver fatigue detection based intelligent vehicle control. Paper presented at The 18th IEEE International Conference on Pattern Recognition (2006)

[8]   MS Devi, PR Bajaj, Driver fatigue detection based on eye tracking. First International Conference on Emerging Trends in Engineering and Technology, 649–652 (2008)

[9]   Z Liu, H Ai, Automatic eye state recognition and closed-eye photo correction. 19th International Conference on Pattern Recognition, 1–4 (2008)

[10]   J Wu, T Chen, Development of a drowsiness warning system based on the fuzzy logic images analysis. Expert Syst Appl 34(2), 1556–1561 (2008).

[11]   Y Lei, M Yuan, X Song, X Liu, J Ouyang, Recognition of eye states in real time video. International Conference on Computer Engineering and Technology, ICCET'09, 554–559 (2009)

[12]   T Hong, H Qin, Q Sun, An improved real time eye state identification system in driver drowsiness detection. IEEE International Conference on Control and Automation 0, 1449–1453 (2007)

[13]   Y-S Wu, T-W Lee, Q-Z Wu, H-S Liu, An eye state recognition method for drowsiness detection. IEEE 71st Vehicular Technology Conference, 1–5 (2010)

[14]   MJ Flores, JM Armingol, A de la Escalera, Driver drowsiness warning system using visual information for both diurnal and nocturnal illumination conditions. EURASIP J Adv Signal Process 2010, 1–20 (2010) .

[15]   P Viola, M Jones, Rapid object detection using a boosted cascade of simple features. Proceedings of the 2001 IEEE Computer Society Conference on Computer Vision and Pattern Recognition, CVPR 2001 1, I-511–I-518 (2001).

[16]   F Smach, M Atri, J Mitéran, M Abid, Design of a neural networks classifier for face detection. Eng Technology, 124–127 (2005)

[17]   C Huang, H Ai, Y Li, S Lao, High-performance rotation invariant multi view face

[18]   P Zhang, A video-based face detection and recognition system using cascade face verification modules. Proc of the 2008 37th IEEE Applied Imagery Pattern Recognition Workshop (Washington DC, 2008), pp. 1–8

[19]   V Vezhnevets, A Degtiareva, Robust and accurate eye contour extraction. Proc Graphicon-2003 (Moscow, Russia, 2003), pp. 81–84

[20]   Caltech vision lab

[21]   [http://www.vision.caltech.edu/html/files/archive.html].

[22]   Eye SBU database http://faculties.sbu.ac.ir/~eshghi /sbu-database-9008/one_eye.rar.

[23]   Dr.P.Sudhakar Rao, Ms.Vijayalaxmi, Mr.S.Sreehari, "A new procedure for segmenting eyes for human face", ISSN: 0974-3588 JULY '11 – Dec '11| Volume 4: Issue 2, IJ-ETA-ETS.

[24]   http://gps-tsc.upc.es /GTAV /Research Areas /UPC FaceDatabase /GTAV FaceDatabase. htm

ABOUT AUTHORS

First Author Ms.Vijayalaxmi, received her B.E (E&CE) degree from GNDEC, Visveswaraiah Technological University, Belgaum, Karnataka, India in 2003. M.Tech (DE&CS) from JNT University, Hyderabad, Andhra Pradesh, India in 2008. She is pursuing her Doctorate from Gitam Institute of Technology, Gitam University, Vishakapatnam,Andhra Pradesh, India. Her area of research is Digital Image Processing. She has published 2 Journal papers, 3 International Conference papers and 2 National Conference papers. She received Best Paper award in August 2013 in IEEE International conference organized by Saveetha University, Chennai, India. She is the Life Member of ISTE and Member of IEEE.

Second Author Dr. D.Elizabeth Rani Completed Ph.D.,Electronics and Communication Engineering in 2003 from Anna University, India, Masters in Communication Systems in 1984 from Bharathiar University, India, Bachelors in Electronics and Communication Engineering in 1982 from Madurai Kamaraj, University, India. Presently she is Head of the Department of Electronics and Instrumentation branch in Gitam University, Vishakapatnam, India .She has 25 technical publications/ conference papers to her credit. She is a member of MISTE, IETE, SEMCE (I). She has 26 years of teaching experience and 15 years of research experience. Her area of interest are Signal processing, Communication systems, Network theory, Image processing.

Urbanization and the Risk of Flooding In the Congo; Case of The City Of Brazzaville

Nzoussi Hilaire Kevin [1] Prof Li Jiang Feng [2]

1 School of Public Administration, China University of Geosciences, Wuhan, 430074 China
2 School of Public Administration, China University of Geosciences, Wuhan, 40074 China

ABSTRACT : *Urbanization is the process by which cities grow. For over a decade, African cities in general have had a very significant population growth. And Brazzaville, the political capital of the Republic of Congo has not remained on the sidelines of this exponential growth. This is probably due to the political and economic stability singularly marked by oil upturn. This rapid urbanization contributes to defy all the forecasts made in terms of urbanization and poses many problems. Population growth leads to an occupation with no real urbanization standards of public space in the city which causes uncontrolled building, with major flooding during rainy periods to disproportionate consequences.*

KEYS WORDS; *Urbanization, risk, flooding, Congo, city, Brazzaville*

I. INTRODUCTION

Urbanization is a very old phenomenon that dates back several years. Congo particularly population growth is the major causes of migration to urban centers (Mauriac and al, 1988) .This impressive urban growth that has its roots in the rural exodus (Vennetier, 1990) .The city is a place of concentration, communication node (Lacour, 1999) .The city is also a gifted place, with logs (Trion, 1997) . Massive arrival of urban neo-urbanites requires coaching and social integration to address urban needs .Drop-off window However, the city still has the realities that we sometimes seems to ignore. Urban development works for town planning reasons, the anarchic occupation of space, high rainfall and the special extension are all problems that are the cause of flooding in the city of Brazzaville. This article aims to study urbanization and the risk of flooding in the city of Brazzaville, and offers appropriate solutions in order to remedy situations of flooding as floods are still a concern in recent years the population of Brazzaville.

II. STUDY AREA

The city in our study is that of the city of Brazzaville. Brazzaville is the political capital of the Republic of Congo, and the first agglomeration of the country .It is located on the right bank of the Congo River. Brazzaville was divided administratively in 2011 in 7 districts which are; Makélékélé, Bacongo, Poto-Poto, Ouenzé, Talangai, Moungali and Mfilou as shown in this figure (Fig.**1).**
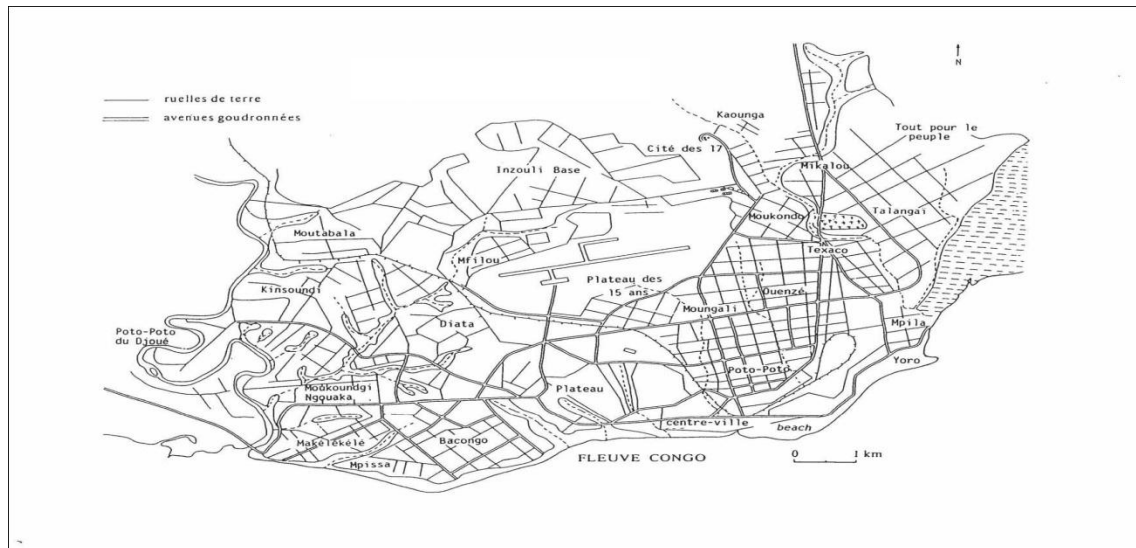
Fig 1; the map of Brazzaville city

But due to the spatial growth of the city other two additional districts were born towards the end of 2011. They are Djiri and Madibou .As city with multiple functions, Brazzaville attracts many neo-urbanites who come from everywhere. It is located in the pool of the department. It is bounded to the north and south by the pool of the department, to the east by the Congo River and to the west by the pool of the department. Geographic coordinates of the city of Brazzaville; Latitude 4 degrees 16 south, longitude 15degrés16 East. His current area of 263.9 km ^{2} with a population of 1 .373 .382. Inhabitants (CNSEE 2007)), a 5204hab / Km2 density.

III.   CAUSES OF URBAN GROWTH

" In urban areas, the demo-economic approach invites to remember that cities have the function to attract as many people as compatible with basic needs in urban areas. A city without poor would be comparable to an apartheid city, trying to put the shelter of migratory pressures. It is not the presence of the urban poor need to worry, but the average time that new citizens bring to a level compatible with productivity and income of the living conditions in the middle of Home '(Tchawe, 2003).For this author, the city has an attractive character, and does not worry about the role of the city but the time take neo-urbanites to easily integrate. So there is no city without poor.

The rural exodus : Several causes are at the root of urban growth of the city of Brazzaville. These causes are both endogenous and exogenes.The endogenous factors are of two types. This is particularly the rural exodus and population dynamics (Vennetier, 1990). Increase of the population of Brazzaville foreshadows an increase in demand for services and goods (Nzoussi, 2014d).Rural-urban migration can be defined as the mass displacement of country people to the city. It is the cause of the swelling population of the city of Brazzaville.
Indeed, several neo-urban is coming to town in search of work or to continue studies (academic secondary education, skills training   ...), or in search of better material being. According to them, the city has all the possibilities consisting having money and achieve a social life worthy of the name. This movement of the population is favored today by the establishment of transport networks which have intensified in recent years .We are witnessing a suburbanization of the city of Brazzaville. This movement is quite opposite in developed countries or peoples densely central areas with cities are gradually emptied of their inhabitants because of several factors; pollution, saturation of transport networks, rental constraints the cost of living .

The city is the environment that has a large monetary possibility due to the diversification of jobs and provides money. Gold and silver have become indispensable in the countryside with the spread of the monetary economy (Idem) .It allows the empowerment of young people and connect them to other lands especially with the development of new information technologies and communication. Rural-urban migration contributes 2.5% of the growth of the city of Brazzaville .This phenomenon is not new even if it has become increasingly recurrent. It dates even before independence of the Congo in 1960. when more work had been undertaken to modernize the city of Brazzaville particularly funded FIDES (Investment Fund for Economic and Social Development) .We have witnessed massive displacement of villagers to the city a labor-intensive for the modernization of the city of Brazzaville. Several national and foreign researchers were then boards on the

issue. Among them Vennetier (1963), the rural exodus the Phenomenon of significant scale and has had a negative impact on the development of an urban hierarchical structure. Auger (1968) has observed that the rural exodus hampers the development of agricultural production due to the imbalance between town and country. Balandier (1954) already noted in 1955 that is to say a- 5 years before independence, the negative side of the rural exodus and said that has more disadvantages than advantages. The future of the city in food becomes uncertain because of the explosive urban growth coming from rural areas. The rural exodus leads to negative consequences in both urban and rural areas. In rural areas, rural lose bodied men actually had to work hard to feed the urban populations. Some villages also disappear because of the rural exodus. In urban areas, the increase in population leads to many evils (theft, rape, robbery ...).

The spatial dynamics : Spatial dynamics is the most visible phenomenon of urban growth. Just as the rural exodus, this phenomenon is not new and dates back several decades. Neo-urbanites who settle in the city do not occupy the central districts because of the high cost of living rises .They thereby occupy the outskirts of a growing neighborhoods disproportionate. These way are as marginalized due to lack modern urban amenities (schools, roads, hospitals, electricity, market ...) and are victims of several evils. Like most African cities, Brazzaville bears the mark of a colonial past. The true downtown residential area is the home of the rich men, and the suburb is the materialization of the poor areas. The spatial dynamics of the city of Brazzaville is very chaotic and unplanned. This is caused both by landowners and public authorities that city dwell in the city.

The population growth of the city of Brazzaville, which is 7% per year has distorted all expectations that were established in the master plan of the city of Brazzaville (Brazzaville Act of Symposium, 1986) .In 1974 had 321,000 inhabitants Brazzaville in 1985 it had 590,000 inhabitants, 611,000 inhabitants in 1986,760.000 inhabitants in 1990, 1242.000 in 2000.In 2007it was estimated at 1,337,382 inhabitants (CNSEE, 2013). Between 1974 and 1984, for example, the population of Bacongo increased from 38,500 to 56,500 inhabitants per hectare, that of Moungali and mud built from 117, 000 to 145 000 people per hectare.
The increase in the population contributes to the densification of old neighborhoods and especially the extension of the peripheral areas. Thus, all the forecasts of the limits of the city of Brazzaville today require a redesign of the public authority's .This is why, on 17 May 2011 other two other districts were created (Madibou and Djiri). Spatial dynamics has brought many consequences both socially and environmentally.

IV. MIGRATION

The Republic of Congo Brazzaville in general and in particular is also a land of immigration. As a capital city that she takes strangers from several horizons.Indeed, immigration is not a new phenomenon. During the industrialization of the country around 1960, Brazzaville during the colonial period Brazzaville played a major role by receiving immigrants neighboring countries. The latter were either for studies (in the case of the National Institute of Education of Central Africa built only in the Congo, and to receive all the peoples of Central Africa studying in the goal of becoming teachers) is looking for employment. Thus, the people of Chad, DRC, Gabon and RCA have long stayed in Congo and others remain to this day there. Added to this are people coming from West Africa.Obviously, Brazzaville attracts a large population of West Africa. The latter came for lucrative reasons. A mud built and Moungali for example, West Africans hold the bulk of trade. All these migrations are juvenile's majority. It is young people who participate in this migration which has become inevitable today. This is caused by the growing phenomenon of unemployment (Augier, 1972).

The natural movements : The natural movements are characterized by three main factors that determine the evolution of the population of the city of Brazzaville. This is the birth rate, mortality and natural increase.

The birth rate : The birth rate is the ratio of the total number of births per thousand inhabitants. Its formula is as follows;
Number of birth
TN = --------------------------- X1000

Total population
Indeed, in 1984, recorded a civil Brazzaville 19812.L'état birth records the following births; 1999.17945 13210 in 2000 and 21295 in 2001 (Balkiabiya, 2008) .With a high birth rate, around 42%0.Also, Brazzaville she carries the causes of population growth with high birth as shown in the above totaled. The population pyramid of Brazzaville would be a pyramid with a wide base with a tapered top. This is the type of underdeveloped countries of the pyramids with a very important youth, dynamic economic activities, so having a large workforce. But the summit would be tapered, symbolizing few. Life expectancy (the average number that a person is supposed to last on earth before dying) in the country is 50 years for men and 55 years for

women. Women who are of childbearing age in Brazzaville are growing. This explains high fertility. The Brazzaville fertility rate declined from 5.8% 0 in 1984 to 3.5 in 2005.

Mortality : The mortality rate is the average number of deaths per thousand inhabitants. Its formula is as follows;

Number of deaths

TN = --------------------------- X1000

Total population

1,555 deaths was recorded in the 1984 census, Brazzaville noted 1999.6072 6090 deaths in 2000 and 6132 in 2001 (Balkiabiya, 2008) .The proportion of deaths under 5 years was 12.3% 0 in 1984. In 1999, fewer deaths a year were evaluated in 1090 (ibid).

But following a land of investigations, it has been shown that infant mortality is down today with very low rates. This is justified by the fact that national public health policy made a considerable effort in fighting against epidemics and other diseases related to mortality. In 2005, for example, infant mortality was 69% .This decrease in mortality is also explained by the schooling of the young woman who has reached a level of education and higher education and health progress.

Life expectancy : The rate of natural increase is the difference between the birth rate and death rate. Its formula is as **follows;**

TAN = TN-TM : The Brazzaville natural growth rate even symbolizes the evolution of the population of the city proper. In other words, it is indeed the excess of births over deaths.

V.   CAUSES FLOODING

There are several causes are the cause of flooding in the city of Brazzaville. These are;

Climate change : The city of Brazzaville is built on a soft rock, and has existed for several years. It was founded in 1880 date at which the King Makoko and De Brazza had signed the friendship treaty that allowed the Congo to pass under French protection. Since then the city has always existed and displays the shape of a city in which to live. However, climate changes in recent years arouse much dissatisfaction and dismay regarding the population of Brazzaville. Urban water these days are the subject of reflection well advanced by economists, management scientists and planners on urban water services management methods, their actors (public / private), regulations Land and overlays generated by the managements of urban water (Barraqué and Nahrath, 2009; Renaud-Hellier, 2006)

The spatial growth and development works in the city : Urban growth is apprehended from the notion of urban fabric which describes the city and its Changes over time. The location of cities and their development has led to extensive legislation. It allows urban planning at various levels to avoid uncontrolled growth (Valey, 2011) .But, in the city of Brazzaville, there is an illegal occupation of urban space without genuine rule of urbanization.The suburbs who are marginalized and lack infrastructure (Dureaud et al, 2000) .The habitat types, tenure of land to build in Brazzaville and horizontal building pose serious problems. (Moutsara, 1986). Estimated at 122,000 inhabitants in 1961,420.000 in 1981, around 900,000 in 1998 and in 2007 1. 373 .382 (Yekoka 2008), the population growth poses real not only administrative problems, but as the management of space and population (Nzoussi, 2014b).

Rainfall : Located in the tropics, Brazzaville has an inter tropical climate. Maximum temperatures are around 35 degrees .To be convinced, observe the outlined below **(Fig .2).**
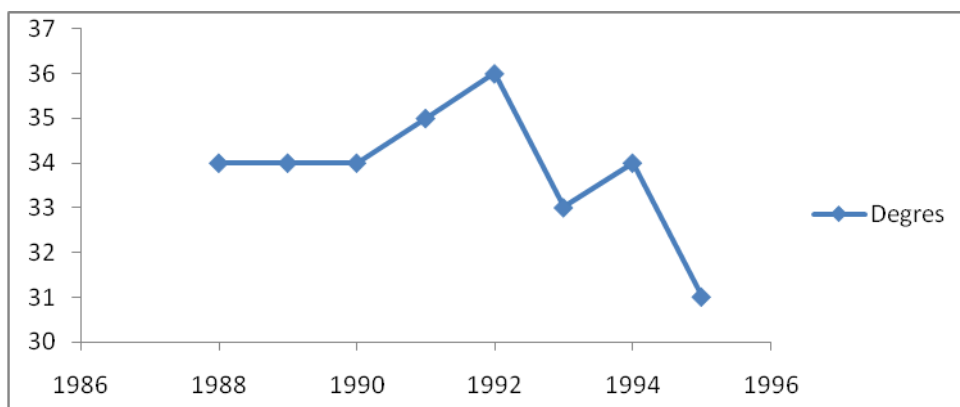
Figure 2; Maximum temperatures in the city of Brazzaville from 1988 to 1995

During the rainy season, for against the dry season temperatures reach sometimes15 degrees. The figure below illustrates this **(Fig 3).**

Degres
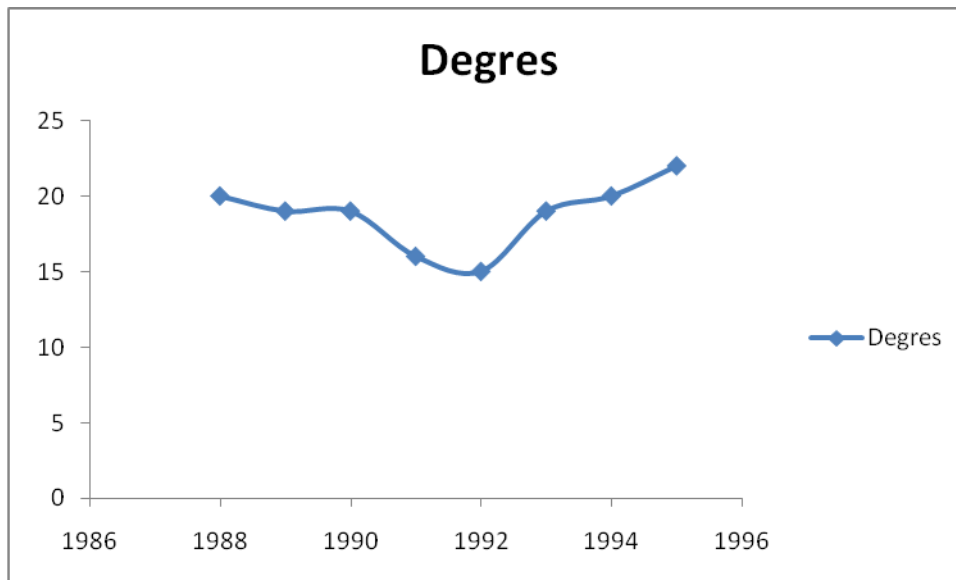
Figure3 minimum temperatures of the city of Brazzaville from 1988 to 1996

Rainfall formerly ranged between 1500 and 1800mm of water / year. But now with climate change that threatens the planet besides, rainfall in the city of Brazzaville is now above average 1500mm of water, and cause significant damage to the topography of the city. We must not forget that the city is built on a soft rock which is the sand. For proof, just watch the figures below **(see Fig. 4, Fig. 5 for evidence)**.From these days the emphasis of this scourge is becoming increasingly shrill and is criticized by more than one Brazzaville because of the disaster and devastation that continues to inflict on the populations most affected are the poor layers.

Fig, 4 flooding in the city center of Brazzaville in November 2014

Fig; 5The flooding in the northern districts of Brazzaville (Talangai and Ngamakosso)

The floods and their consequences : The population growth implies (...), good governance to better meet the needs of the population (Nzoussi, 2014b) .This why the flood issue challenges the government consciousness. Flooding causes very dangerous consequences. Water levels in some neighborhoods sometimes reach the knees, with the first victims schoolchildren who arrive late to school, some students may flee during the day. Officials and traders sometimes have difficulty moving because of transport that have already become so problems. The climate change will be at the origin of these overflows waters of the flooding. Neophytes think it raises the pipe problem. Roads are made without pipes and without landscaped sidewalk. While pioneer roads that the Romans had already understood the importance of pipes to drain the water. These waters flowing train with them a lot of debris and harmful bacteria to human health. So the poor vulnerable are often the most affected. Brazzaville is a real devastation to the difficult conditions of urban life is added the phenomenon of flooding. In 2013 several families were afflicted by floods Bacongo Mfilou and Talangai In November 2014, for example, some 600 families in Brazzaville have become homeless in the northern districts of Brazzaville because of the phenomenon of flooding. Hundreds if not thousands of families who once lived in their homes are now in the street begging which leads to urban poverty.

VI.   CONCLUSION AND RECOMMENDATIONS

At present the issues of flooding in ASS (Africa South of the Sahara) cities general in Congo in particular should concern any urban who would live in an environment and peaceful city. The urbanization of Brazzaville is partly responsible for the observed floods in the city, accompanied collateral damage and all the attendant evils. So to solve this problem, the authorities who are in charge of managing the territory and people should make healthy and enforcement measures in order to find a lasting solution to this thorny issue that is becoming increasingly worrying.Thus it is the duty of the state to prohibit the Brazzaville to build on wetlands, which are dangerous to their lives. Build quality urban roads in order to guide rain water. Enforce action with respect to any resident who tried to settle in areas at risk. Post a law of the land use which is to ban the sale of plots in swampy areas. Since the city is built on a soft rock which is the sand, the state must build for vulnerable population's quality of social housing in order to save their lives from the dangers of flooding. Prohibit landowners to sell land in hazardous environments without measurement Subdivision and Development beforehand. Implement the project co-led between Congo and the World Bank to identify all parcels in areas in danger of flooding in order to bring tangible solutions.

ACKNOWLEDGEMENT

REFERENCES

[1]   Auger, A., the study of relationships towns and countryside in developing countries, Paris, ORSTOM, pp 738 to 741.1968.
[2]   Auger A., Traditional food supplies to the population of Brazzaville. Contribution to the urban-rural geographic scale in tropical Africa in urban growth in black Africa and Madagascar NCRS, Paris, pp273-298, 1972.
[3]   Balandier G., Black Brazzaville Sociology, Paris, A. Colin, 274p, 1955.
[4]   Balkiabiya K.D.S Spatial dynamics and environmental problems in Brazzaville, UMNG, 54p, 2008.
[5]   Barraqué et al, uses and regulation of urban water, spaces and societies in magazines, Vol, 139, eras Editions, Paris, 244 p., 2009
[6]   Dureaud and al, movements in Metropolis, Paris, Anthropos IRD 2000.
[7]   Lacour C.et al Metropolisation -Growth, diversity and fractures, Paris, Economica, 1999 194p.
[8]   Mauriac F. and al, The African politics 31 Congo Brazzaville suburb, Paris, Karthala, 140 p 1988.
[9]   Motsara A., Conference Proceedings, 25-28 April 1986 Brazzaville, 12p, 1986
[10]   Nzoussi H.K , Decentralization, local governance and types of transportation in Brazzaville, International Journal of Science and Research (ISJR) vol 3 (8) (eISSN2319-7064), p146-149, August 2014b.
[11]   Nzoussi H.K and al, The issues of residential mobility in the Congo case of the city of Brazzaville, American Journal of Educational Research (AJER) Vol.2 n0 10 (eISSN, 2327-6150), p.906- 910 October 2014c.
[12]   Nzoussi H.K, Management of the urban environment in Brazzaville, Problems and Prospects, European Scientific Journal (ESJ) Vol 10 N0 29 (eISSN1857-7431), pp 209-2016, october 2014d,
[13]   Tchawe E. The supply and food distribution in Douala (Cameroon); social logic and spatial practices of actors, University Sorbonne, PhD Thesis, 455p, 2003.
[14]   Troin J., 1997 the cities of the Mediterranean, Paris, Edisude, 110p
[15]   Valy J., Urban Growth and the risk of flooding in Brittany, Rennes 2 University, PhD Thesis, 544p, 2011.
[16]   Vennetier P., Urbanization and its consequences in the Congo in the books overseas, Paris, n063 p.263-280, 1963.
[17]   Vennetier P, what cities in tropical Africa? But problems of rapid urbanization newsletter Geographical Society of Liège, PP63-75 1990.
[18]   Yekoka F. spatial practices and urban imbroglio in Brazzaville, analysis of public administration dysfunction of space Condersia 2008.

Research Paper   Open Access

Utilization of "Marble Slurry" In Cement Concrete Replacing Fine Agreegate

Er: Raj.p.singh kushwah[1], Prof (Dr.) Ishwar Chand Sharma[2], Prof (Dr.) PBL Chaurasia[3]

1.Scholar, SGV University Jaipur(India). 2. Professor Civil and Principal Arya college of engineering Jaipur(India), 3. Dean engineering and Centre of excellance SGV University Jaipur(India).

Abstract*: The wastage of marble industry are responsible for many environmental problems because 70% wastes and only 30% recovery of main product contribute to the maximum wastes which are indestructible. Dumping sites give dirty look. Contaminate top fertile soil cover, along with rivers/water bodies affecting irrigation and drinking water resources and air as well as loss to flora and fauna.*
The most efficient Solution of marble slurry pollution is utilization in Bulk. The only industry which can consume marble slurry at so large level is only the construction industry. Different properties of marble slurry determined in the laboratory. Sp. gravity 2.61, Fineness modulus was found to be 0.91 and Utilization of marble slurry in Cement Concrete replacing Sand is 30% which shows equal strength as of Control i,e. 1:2:4 Cement Concrete 0% Marble slurry. Marble slurry can be easily utilized in construction industry in preparing Cement Concrete.
Key words:- *Cement Concrete, Fineness modulus, Marble slurry, Specific gravity.*

I.   Introduction

Marble occur abundant in nature. It is used and mined many places in the world since early time. Around 90% of the world's production of marble comes from India and approx 85% of India's production is received from Rajasthan and almost all mining and processing activities are concentrated around **Makrana**, where the proposed study is planned to undertake. Rajasthan has more than 4000 marble mines and about 1100 marble gang saws (processing units). At the same time it leads to growth of many processing units in respective areas. These two activities in Rajasthan have been extended in 20-25 years and have played important role in the economy of the state providing direct and indirect employment to majority of people and therefore also raising their living standard.

The industry involves mining and processing units for the production of tiles for walls and floors, articles, waste production and other ancillary works. The marble mining and the industry as a whole are different from other industries to the ver y fact that, the marble is a "Dimensional Stone", which means the stone is sold by size not by weight (In other words in sqm not by tonnes). Since the selling price increases manifolds with size, all the operations involving mining and processing are aimed to get slabs as big as possible.

Marble slurry generation:-
Marble Slurry is a suspension of marble fines in water, generated during processing and polishing, etc.

Environmental Hazards due to waste.
It is shaping to major threat of the Environment in the state by mining and processing activities. Nearly one thousand Gang saws and thousands of cutters are producing 15-20 lac tons of marble slurry waste which is indestructible waste and harm to general Public. Some of effects of the marble slurry may be listed as under: -
1. The waste is indestructible.
2. The sites which can be used as dumping ground are limited and gives repulsive dirty look.
3. Contamination of top fertile soil cover.
4. Contamination of the rivers and other water bodies there by adversely affecting irrigation and drinking water resources.
5. Contamination of air.

Public resistance, Law & order and prevention (Banning) can give a deathblow to the growth of the marble industry. It is therefore a social responsibility of Public, and scientific & engineering responsibility of government and industry to solve the problem of marble slurry pollution.

Fraction of Total Marble Production : -
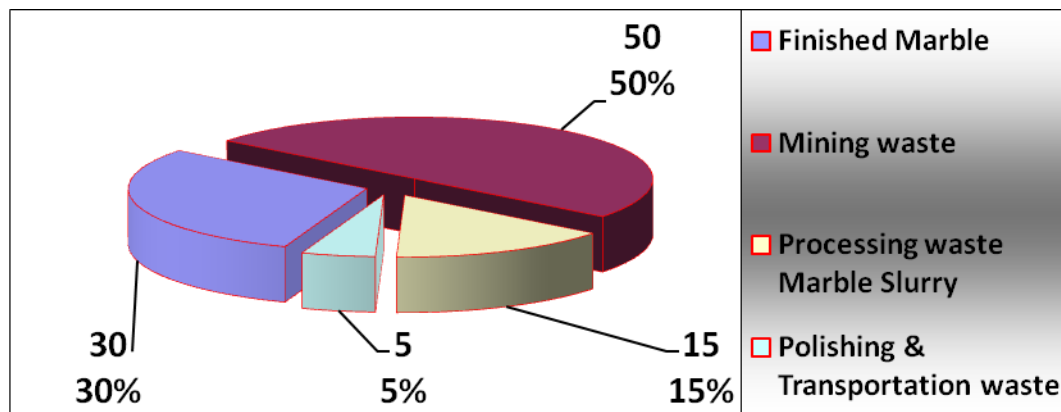
However, the development of country is only possible by sustainable and balanced industrialization.

(a) Conservation of Natural Resources.
> The valuable national wealth is getting wasted mainly due to lack of management and technology. This waste, if used, can change perhaps the entire scenario of the industry.

(b) Air pollution.
> This is the most hazardous impact of the marble industry. It is clear from the table 1, slurry is produced at almost every operation and it is a great problem. When it gets dry, it causes air pollution and related problems.

(c) Water pollution.
> Like any other industry, the marble industry needs water in its different operations for cutting, cooling and flushing. In these operations water gets contaminated by marble slurry.

(d) Visual impacts.
> Abandoned mines, dumping sites, slurry waste sites, deposition of dried slurry over almost every structure in surrounding areas gives a very bad, dirty look and aesthetic problem.

(e) Accidents due to unscientific dumping.
(f) Dry Slippery road
> Due to dumping of mine waste and marble slurry on road side causing dust in air(polluting air) and creating less visibility, due to less visibility number of accidents occurs.

(g) Wet slippery road
> In raini season marble slurry flows over road. Due to marble slurry road becomes slippery and many accidents takes place.

(h) Loss to flora & fauna
> Already grown trees and bushes die out and new ones do not grow due to deposition of marble slurry. Animals also suffer for their food and shelter.

II. AIMS AND OBJECTIVES:-
Utilization of the Marble slurry is the only complete solution of the Marble slurry Pollution. For this purpose the most useful steps can be:
> (A) Re-utilization of water after separating the Marble slurry.
> (B) Utilization of Marble slurry.

(A) Re-utilization of water after separating the Marble slurry.

Proper separation of water is essential. 5000,000 tons slurry is generated annually which contains 4000,000 tons of water. Hence an effort should be made to get the maximum possible water out of it and slurry be converted in the form of cakes. These cakes can far more easily be transported for utilization at distance sites. This will help in saving the natural resources of water and also the sand lowering the damage to eco-system.

(i)   **Natural process:-** Naturally separating water from marble slurry by settling process and drying in different settling and drying tanks separated water will available for reuse.

(ii)   **Mechanical process:-** In this process by a mechanical filter press water is separated and cakes of slurry are formed and dried in air.

(B) Utilization of marble slurry:-

Even minimizing waste/slurry production the problem could only be partially solved. Therefore it is needed to develop modes of utilization of waste/slurry. Since other applications cannot consume such a bulk amount of slurry, efforts are being made to utilize slurry for different civil works.

It is essential to explore possibilities of alternative uses. To arrive at technically sound and financially viable technologies to utilize marble slurry / waste and also work out a framework for long term waste management in Industrial Areas.

The areas where the utilization of marble waste and marble slurry needs to be explored as a substitute for conventional raw materials are as follows:
1. **As a filler material for roads and embankments**
   (As per Khadi Board of India ItemNo 31 from sr no. 1 to 9 of this chapter)
2. **For manufacture of bricks**
   Central Brick Research Institute (CBRI), Roorkee.
3. **Manufacture of Portland Cement**
4. **Manufacture of Ceramic Tiles**
5. **Manufacture of Thermoset Resin Composites**
   The Macromolecular Research Centre at Jabalpur.
6. **Manufacture of lime**
7. **Manufacture of Activated Calcium Carbonate**
8. **Hollow Blocks and Wall Tiles**
9. **Manufacture of Ground Calcium Carbonate**
10. **Making Cement mortar (Partially replacing sand)** and
11. **Making Cement concrete (Partially replacing sand)**.

Properties of marble slurry:-

a. Colour   White.
b. Texture   Powder.
c. Taste   None
d. Particle Size   4.75mm-75micron
e. Fineness Modulus   0.91
f. Natural moisture content
                           0%(if under roof)
g. Solubility in Water   Totally in soluble.
h. Densification   Lesser (Compare to Cement)
i. Specific gravity   2.56

11.Optimum quantity of Marble slurry for same strength as of Control for M20 Cement Concrete Without distorting standard designed mix. Many researchers made their efforts distorting standard design mix.

Compressive Strength   28 Days Curing

Slurry Mixed
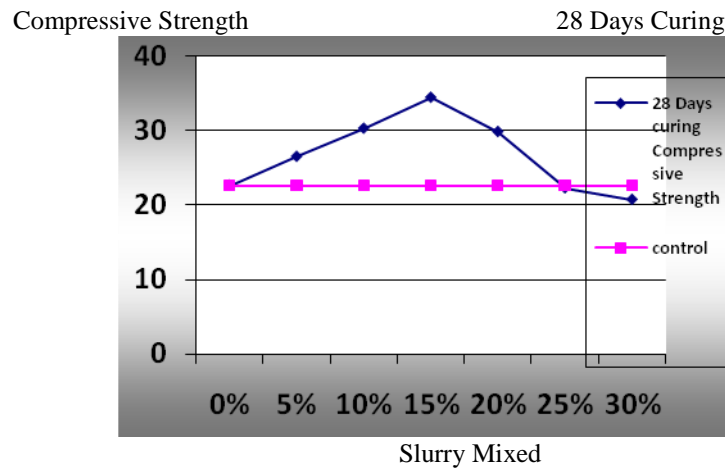
III. Conclusion based on Examination

AS per results of Practical examination this material Marble slurry shows a good and acceptable strength when added in Cement Mortar and Cement Concrete Both (replacing sand). It can be used as a filler material (upto 30% replacing sand) showing same strength as of controll.

IV. Acknowledgement

This paper is Acknowledged to Late Prof(Dr.) N.C. Saxena. He was HoD Civil Engineering department JECRC University Jaipur (India) prior to this was Professor Civil Engineering department in **Ohaiyo State University USA.**

References

[1]   Ameida, N, Branco, F. &Santo, J.R.(2007, "Recycling of stone slurry in industrial activities: Application to concrete mixture". Building and environment, 42 (2007) pp810 - 819 Portugal (IST).
[2]   Fakher J. Aukour "Incorporation of Marble Sludge in Industrial Building Eco-blocks or Cement Bricks Formulation" 1) Faculty of Natural Resources and Environment, The Hashemite University, Zarqa, Jordan,
[3]   Postal Code 13115, P.O.Box 150459, Tel: +962-5-3903333 Etx. 4694, Email: fakagr67@hu.edu.jo.
[4]   Jordan Journal of Civil Engineering, Volume 3, No. 1, (2009).
[5]   Hanifi Binici, Hasan Kaplan and Salih Yilmaz, "Influence of marble and limestone dusts as additives on some mechanical properties of concrete"Scientific Research and Essay Vol. 2 (9), pp. 372-379, (2007).
[6]   H. Binici, H kaplan. And S. Yilmaz 'Influence of marble and limestone dusts as additives on some mechanical properties of concrete', Scientific Research and Essay, Vol.2 (9), 372-379, Full Length Research Paper (2007).
[7]   Karasahin, M. and S. Terzi, "Evaluation of marble waste dust Mixture of asphaltic concrete". Construct. Build. Mater., 21: 616-620. (2007).
[8]   Mathur R, Misra A K & Goel P, "Marble slurry dust and wholastonitenert mineral admixture for cement concrete"Indian highway (2007).
[9]   M. Belachia and H. Hebhoub, "Use of the Marble wastes in the Hydraulic Concrete" 6th International Advanced Technologies Symposium (IATS'11), (2011).
[10]   M. E. TAWFIK, S. B. ESKANDER, "Polymer Concrete from Marble Wastes and Recycled Poly (ethylene terephthalate)" Journal of Elastomers and Plastics (2005).
[11]   Rania Hamza, Salah El-Haggar, Safwan Khedr, "Utilization of Marble and Granite Waste in Concrete Bricks" International Conference on Environment and BioScience IPCBEE vol.21 (2011).
[12]   Valeria Corinaldesi, Giacomo Moriconi, and Tarun R. Naik, "Characterization of marble powder for its use in mortar and concrete" For Presentation and Publication at the CANMET/ACI Three-Day International Symposium on Sustainable Development of Cement and Concrete, October 5-7, (2005).

| Research Paper | Open Access |

Minimizing Household Electricity Theft in Nigeria Using GSM Based Prepaid Meter

Damian O. Dike[1], Uchechukwu A. Obiora[1], Euphemia C. Nwokorie[2],
Blessing C. Dike[1]

[1]*(Department of Electrical & Electronic Engineering, Federal University of Technology Owerri Nigeria), and*
[2]*(Department of Computer Science, Federal University of Owerri Imo State University Owerri Nigeria)*

ABSTRACT: *Many households indulge in different forms of electricity theft and illegal tampering of electric metering devices. These lead to distribution system faults and overload as well as loss of revenue by the distribution companies,this paper envisages the utilization of the global system for mobile communication (GSM) into the prepaid energy meter for increased generation of revenue in developing countries like Nigeria. The proposed meter is set to carry a unique identification number such as the consumer's phone number which may be encrypted into the memory of the microcontroller. Electricity theft is being detected as the GSM module sends message to the distribution company. Revenue generated can be increased through the use of the proposed meter as unaccountability by utility workers and billing irregularities are eliminated. The results obtained from the simulation shows that immediately an illegal load is connected to the utility system either within the residential meter jurisdiction or otherwise stated, the GSM module alerts the utility company no matter how small the illegal load is.*

Keywords -/ Electricity theft, GSM networks, Prepaid meter, Short message service and Revenue generation.

I.   INTRODUCTION

Meters in the past and today in a few countries, were electromechanical devices with poor accuracy and lack of configurability. The present billing system is minimally able to detect power theft and even when it does that it is at the month. The distribution company is unable to keep track of the changing maximum demand for the domestic consumer while the consumer is faced with problems like receiving due bills for bills paid for and also poor reliability of electricity supply and quality [1]. Prior to the introduction of prepaid meter, various methods were proposed to detect electricity theft which includes: inspection of suspicious load profile, though the method was good certain drawbacks accruing to this method are the requirement of large manpower and huge labour, this failed due to dishonesty of the service workers. A huge amount of money is lost due to theft, in some countries; the government has to provide subsidies to the power sector to maintain a reasonable price of electricity [2]. The major problem facing the electricity industry in many developing countries is poor revenue generation. This arises from illegal consumption of electricity via mostly meter tampering and bypassing as well as direct connection to the low voltage distribution lines. In order to solve all the problems of the traditional meter reading, the consumer load should be tracked on a regular basis as this will help ensure accurate billing, keep track of the maximum demand and detect theft.

The prepaid meter enables the distribution companies to collect electricity bills from the consumers prior to its consumption. This meter is not only limited to automated meter reading but is also attributed with recharging ability and exchanging information with the power sector pertaining the details of the consumers' consumption [3]. This paper is aimed at creating a design that will regulate the listed problem as well as increase revenue collection via payment by SMS. It shows the embedded features combination of the hardware and software to implement the desired goals. In smart meters provide an opportunity to better monitor and control household energy consumption by both consumers and utility without persons visiting each house.

The design and implementation of a Bluetooth-based energy meter where several meters are in close proximity, communicated wirelessly with a Master PC was presented in [4]. Distance coverage is the major limitation for this kind of system because the Bluetooth technology works effectively at close range. [5] In their paper, proposed the use of Automatic Meter Reading (AMR) using wireless networks. Certain AMRs utilized

the internet for data transmission. Moreover, the design and implementation of an SMS-based control for monitoring the complex applications where the SMS is used for status reporting such as the occurrence of power failure.

Many issues involving billing systems for electricity board usage were considered in [6]. This paper discussed the remote control of home appliances with in-built security scheme when the user is away. Maheswari and Sivakumar [7], developed an energy efficient and low cost solution for street lighting system using Global System for Mobile Communication (GSM) and General Packet Radio Service (GPRS). The experimental set-up allowed the operator to turn off the lights when not required, regulate the voltage supplied to the street-lights and prepared daily reports on glowing hours. A prepaid energy meter like-mobile phone was proposed in [3]. It contained a prepaid card analogous to mobile SIM card. This card communicates with the power company using mobile communication infrastructure. If the card is out of balance, the consumer load is disconnected from the utility supply by the contactor. The distribution company can recharge the prepaid card remotely through mobile communication based on customer requests.

II.　ELECTRICITY THEFT MECHANISMS

2.1.　Different Types of Illegal Electricity Theft

Electricity thefts may occur in different forms. From available literature and practical daily reports in Nigeria [8] – [12], the common ways include bypassing (illegal tapping of electricity from the feeder), meter tampering (by grounding the neutral wire as it does not measure readings) and physical methods to evade payment of bills. The basic method of stealing electricity is a direct wire-connection to a main power route passing a shop or a house so that electricity can flow to the consumer without crossing the electric meter installed by a government agency which is responsible for providing electrical services to customer. There are different types of theft done all over the world. Huge amount of power theft are done by tapping from line or bypassing the meter, According to a study 80% of the total theft detected all over the world is from residential buildings and 20% from commercial and industrial premises [8].

(A) *Meter Tampering*: Customers tamper the meter by grounding the neutral wire, this causes the meter to assume an incomplete circuit and it does measure the meter reading.

(B) Meter bypass: The input terminal and output terminal of the energy meter has been shorted by a wire. This act prevents energy from been registered in the meter [9].

(C) Illegal terminal taps of overhead lines on the low tension side of the transformer: Primarily, electricity theft affects the power sector as a whole, tapping of the low tension side of the transformer result in overloading which causes tripping and can lead to blackout.

(D) *Illegal tapping to bare wires or underground cables*: This is the most used method for theft of power. 80% of total power theft all over the world is done by direct tapping from line. The consumer taps into a direct power line from a point ahead of the energy. This energy source is unmeasured in its consumption and procured with or without switches.

(E) Unpaid bills: Non-payment of bills by individuals, government institutions and untouchable VIPs results in utility running at a loss and a must continually increase in electricity charges.

(F) Billing irregularities: This incorporates the inaccurate meter reading taken by bribed servicemen and intentional fixing of the bill by office staffs in exchange of illicit payments from the consumers.

2.2.　Causes of Electricity Theft

All energy distribution companies operate with some accepted degree of losses. This is no different from the scenario of Nigeria. The losses incurred are subdivided into two namely; Technical losses and Non-technical losses.

(A) Technical losses: These are naturally occurring losses and consist mainly of power dissipation in electrical system components such as transmission lines, power transformers, measurement systems, etc. They are caused by the physical properties of the components of power systems [9]. *Non-technical losses*: These refer to those losses that are independent of technical losses in the power system. The most prominent forms of non-technical losses in Nigeria are electricity theft and non-payment of bills. It can also be viewed as undetected load [10]

Theft is a serious crime, it creates short fall, increase of load, decrease of frequency, which is not acceptable, causing load shedding and increase of tariff on the legal consumers [11]. Some may argue that the distribution companies providing services give; over-voltage, poor service and make excess money thus, some theft will not affect its operations and profitability. Nigeria's power system is an illustration of a worst-case situation prior to its privatization in 2013. The distribution companies have not upgraded their systems to meet

the technological trends in advanced countries. In certain cities, however, the post-paid energy meters are gradually being replaced with the prepaid meters, the issue of constant electricity continually plague the country as this has not been achieved prior to its privatization in the last ten months.

Some localized catalyzing factors influencing electricity theft in Nigeria include lack of accountability in electricity market system, political protection of employees involved in corruption, influential customers who do not pay their bills, absence of effective laws to abate electricity related crimes and inadequate and ineffective enforcement of existing weak laws and generally negative attitude of electricity customers. Electricity pilferage has its root in corruption and bad governance. Customers attitude contribute a great deal to revenue losses. These attitudes range from their ill-conceived feelings that electricity should be a welfare commodity and therefore legitimate to steal from the state, to the generalization that the state is not incurring losses. They do not have the fore-knowledge that the money realized from the payment of bills are re-instated into the power sector for its improvement and development.

2.3. Existing Ways of Tackling Electricity Theft

The first step in electricity theft reduction is to become knowledgeable about the theft problem. Unless the nature and extent of power theft is known in great details, any attempts to deal effectively with the problem are prone to fragmented and limited action that has little over-all success [12]. Corruption is one of the difficult problem areas for electricity organizations because power theft occurs with the connivance of employees of the power sector. Employees should hence, be paid adequately so that the issue of bribe collection will not be their last resort. Power companies are combating theft through the use of smart meters and sophisticated software that continuously records consumption and send the data back to them. One advantage of using the smart meter is that it eliminates contact between the consumers and the power provider's employees thus preventing the issue of bribery [13].

The already existing methods which may be utilized in tackling electricity theft in some countries where practiced include proper enforcement of electricity regulatory laws, periodic and impromptu checks of consumer homes, electronic tampering detection meter and use of prepaid meter. The limitations of using the smart meters is that: consumers feel it discloses privacy of their homes which is not ethically true and that it interferes with radio frequency and create problems in radio transmission profile [14]. Periodic checks are not 100% efficient due to its laborious and sluggish nature. Adopting this kind of method in electricity theft reduction will delay accurate and effective reading of the meters in remote areas that are non-accessible. Moreover, as result of the ever-increasing rate of corruption (such as greed and bribes) in the Nigeria, the proper enforcement of laws would take a drastically longer time than stipulated. In the past, committees that were set-up see it as an avenue to amass wealth rather than strictly punish defaulters thus all these reasons have hindered the growth of our power sector.

2.4 Merits of Proposed Methodology

The proposed methodology has the following advantages over the existing schemes, which are outlined hereunder.

(A) In the Existing Meters, manual billing is often restricted and delayed by bad weather condition in other cases the printed billing may even get lost whereas the proposed meter, prevents house to house visitation in order to issue bills as it requires consumers to pay for the consumption before its usage.

(B) The need for the disconnection of power supply before is no longer taken care of by the electrical workers because the proposed meter automatically disconnects it when the consumers units have been used up.

(C) In using the prepaid, the consumer pays for the units needs. It also manages the customer's consumption as it provides credit control and facilitates affordability [15].

(D) GSM application in system monitoring: Nowadays, GSM modules are used to transmit the meter reading from one end to the other. The main aim of this work is to use the GSM network alongside the prepaid meter in reducing theft and losses. It is also used in remote monitoring and records the energy meter reading. This also can be used to disconnect the power supply to the house in case of non-payment of electricity bills. The GSM modem with SIM card is required for each energy meter which aids continuous reading. In case of tampering, it immediately sends signal to the central server of the utilities. Another advantage of the GSM is that it enables the utility engineers efficiently plan for network expansion while delivering a higher quality of supply [16], 17].

(E) Mobile Phone Based Recharging: In this work

Prepaid Energy meter may be recharged from a remote location by using a mobile phone. The user transfers the amount to the service provider bank account and the service provider makes a call to the system, and recharges by entering digits from its key pad. The recharging can be done from any mobile set but the system access code must be put in to the system to log into the energy meter. The energy meter sends a pulse to the microcontroller indicating a unit is consumed.

III. SYSTEM DESIGN

The design of the project consists of the hardware design and software design. A Computer Aided Instruction (CAI) was first used to create a circuit model of the design before it was built and the software was implemented.
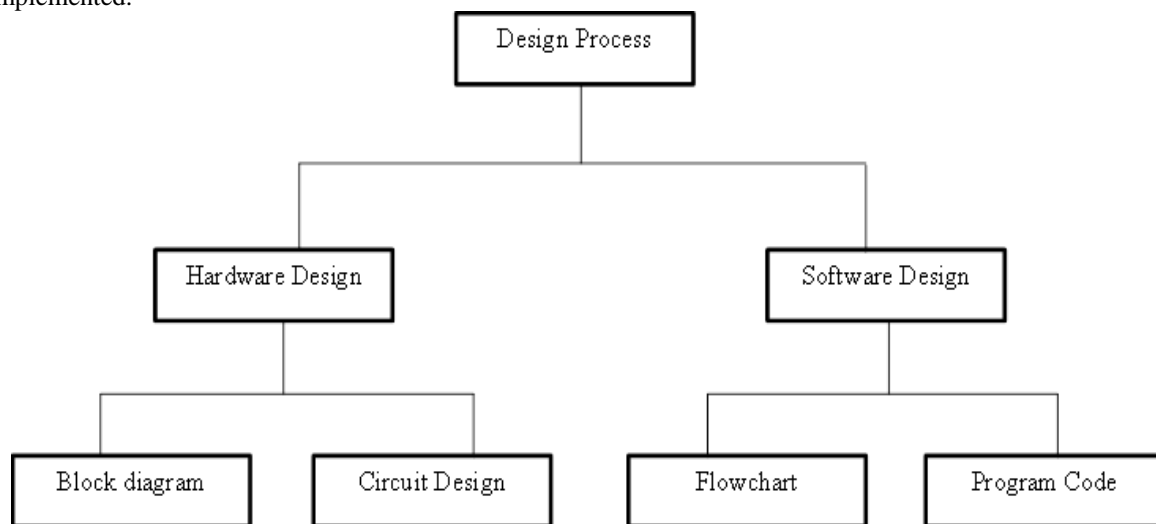

Figure1: Design process for the GSM-based prepaid meter

3.1. Composition of Hardware

The hardware comprises of the following electronic components.

(A) GSM modules (SIM 300): It is used specifically for the purpose of sending messages although various tasks can be performed with it. For the purpose of this project the GSM module used is the SIM 300. It also helps in long duration communication.

(B) Microcontroller: This is a chip which contains a processor, having a non-volatile programming memory called a flash or ROM (Read Only Memory) and also a volatile memory for input and output called RAM (Random Access Memory). The brand used is an AT89C52, a high performance, and low power CMOS (Complimentary Metal-Oxide Semiconductor) family controller. The programs are encoded in the microcontroller. Its functions include:

(i) Transmission of the consumption amount to the GSM module.

(ii) Taking the pulses from the energy meter and incrementing the unit.

This depends upon the calculation and stores in memory.

(C) EEPROM: This is known as Electrically Erasable Programmable Read Only Memory. It is a type of non-volatile memory used in computers and other electronic devices to store small amounts of data that must be saved when power is removed. It can be programmed and erased in circuit by applying specially programming signals. It does not require a power source to maintain its data. It is limited to applications that require infrequent reprogramming sessions. The code name of the EEPROM used is AT-24C02C.

(D) Buzzer: This is the sound output; it produces alarm or sound when an illegal load is added to the meter.

(E) Liquid crystal controller (LCD):This is a thin flat panel device made up of the LCD driver and the glass; it is used for displaying information such as text, images and moving pictures. Also, the pulse count, unit price and meter reading are displayed. It is an electronically-modulated optical device made up of several pixels filled with liquid crystals and arrayed in front of a light source (backlight) or reflector to produce images or text either in monochrome or colour. Its advantages include its lightweight construction, portability and low power consumption which makes it more feasible for battery powered electronic equipment. The kind used is the LM016L, 16*2 LCD which means it has 2 line displays with each line having 16 characters. It has 14 pins and is powered from a 5V dc supply.

(E) Pull-up resistor**:** This is added in the circuit because it helps to send the appropriate signal to the LCD. It is also used because the port O of the microcontroller is below 0.6V which is quite low.

(F) The power supply: Every electronic circuit needs appropriate power supply for its operation. Basically microcontrollers, energy meters, LCD and relays operate on + or -5V supply. For this reason a 5V power supply is used.

(G) Crystal oscillator: The AT89C52 microcontroller has on-chip crystal oscillator, but requires an external crystal oscillator to run it. It is often times connected to inputs pin 18 and pin 19 that is, XTAL1 and XTAL2 respectively. It creates a frequency used to keep track of time, to provide a stable clock signal for digital integrated circuits.

(H) Opto-isolator: Also known as an opto-coupler is a device containing an infrared LED and a matching phototransistor, mounted close together within a light-excluding package.

(I) Bridge rectifier: It is made up of four diodes and it is used in converting the 12V AC to 12V DC.

(J) Voltage regulator: The specification of the voltage regulator is the 7805, whose function is to maintain the voltage level to 5V in the power supply unit.

3.2. Working Operation

The electric meter is used for energy measurement. It is a single phase meter interfaced to a microcontroller via ADC (Analog Digital Converter). The ADC is used because the signal coming from the meter is analog whereas that needed by the microcontroller is a digital signal; thus, the ADC helps to achieve this signal conversion. Also, both the load and meter are connected to the ADC. The 220V from the mains which is the meter is converted to a 5V dc for use in the microcontroller using an opto-coupler (also known as an optical isolator, which is a component that transfers electrical signals between two isolated circuits by using light and it also prevents high voltage from affecting the system receiving the signal).
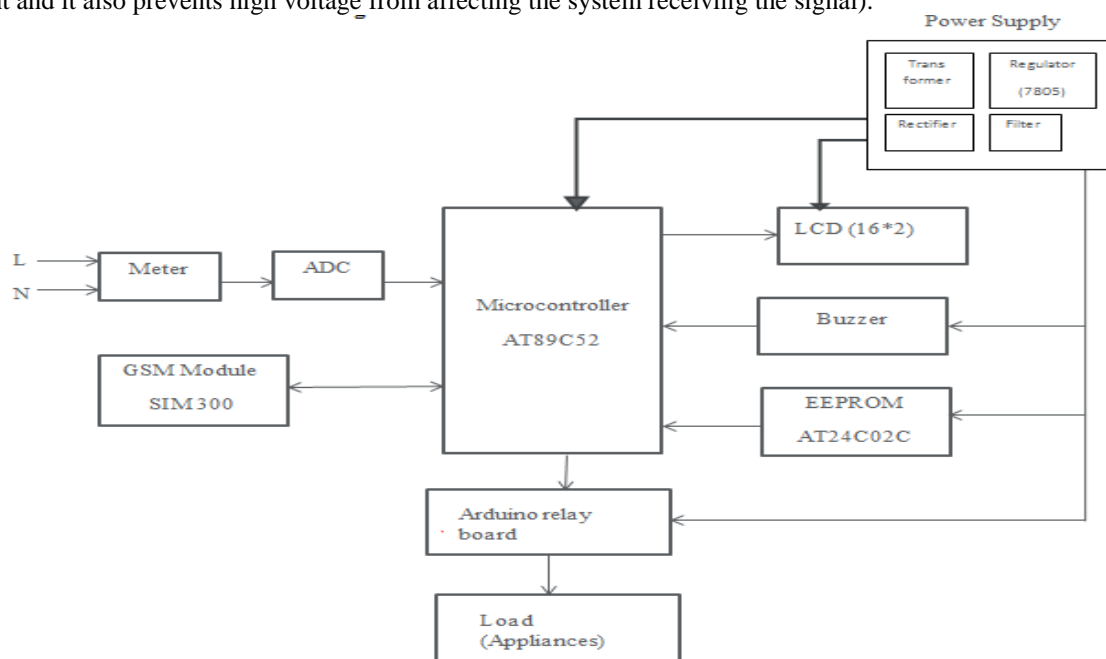

Figure 2:   General block diagram

The purpose of the microcontroller is to send display data to the LCD and control the various functions of the meter. The microcontroller also continually checks for balance stored in the EEPROM, and if balance in credit is low, it sends a message to the consumer through the GSM module. Depending on the result, the microcontroller will activate the buzzer if the credit is low and the controller triggers the relay if the credit goes very low. An EEPROM is used to store various calibration parameters of the meter such as the recharge made and also stores the meter's data during a power-down. The GSM module provides the wireless connection and SMS-based facility for the design. Lastly, Power connection and disconnection is implemented using a relay which is a switching device, it is also used to activate the load. The more the load added, the faster the recharge that is used up.

The coding emphasizes the fact that it reduces human labour but increases he efficiency in calculation
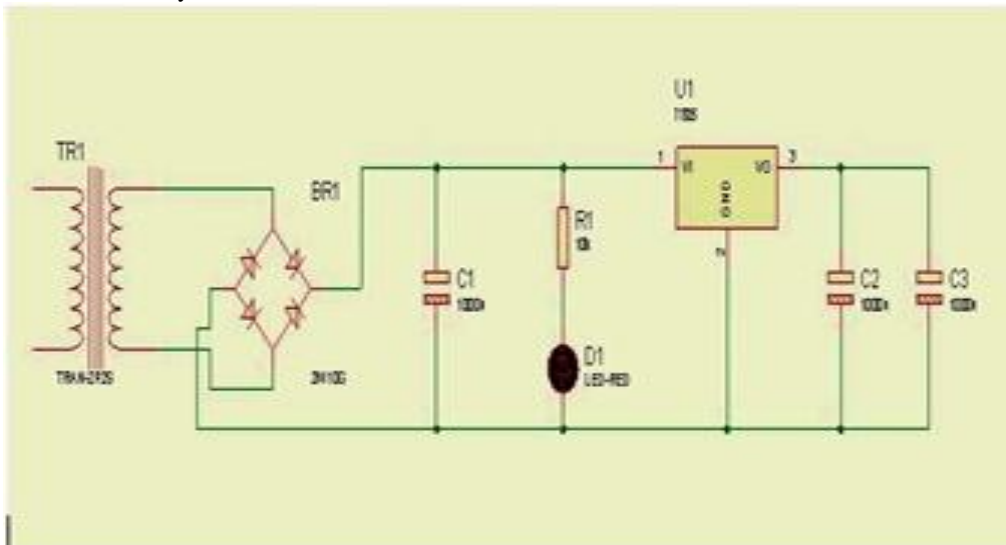
of bills used for electricity.

Figure 3: The power supply unit showing the components embedded in it

*Circuit connection***:** Transformer with a voltage rating of 12V is used, 7805 regulator, LED, rectifier, capacitors and resistor. The 230V, 50Hz ac signal is fed to the primary of the transformer as input and the secondary of the transformer is fed for DC output to the bridge rectifier. The regulator is fed from the output of the diode and the resistor through the capacitor for input purpose. The output of the regulator is then fed to the other capacitor which filters ripple.
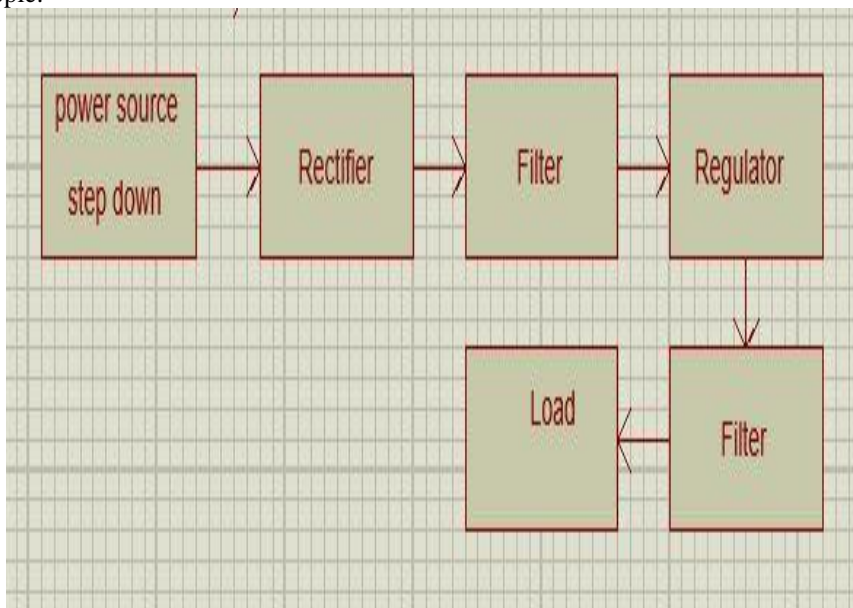
Figure 4: Block diagram of the power supply unit

*Circuit Explanation***:** The power supply configuration consists of the transformer having a voltage rating of 12V DC, which is the power source. It is responsible for stepping down this voltage to about 5V used in the microcontroller. The transformer is thus interconnected to the bridge rectifier circuit which converts the AC input power into DC output power. During the positive half-cycle of supply, two series connected pair diodes of the four diodes conducts that is, it allows the flow of current while the other two do not. During the negative half-cycle the two diodes which did not conduct initially, conducts in this cycle whereas the other two do not conduct here.

This rectifier is suited for high voltage application because the peak inverse voltage during the period

of non-conduction is equal to the peak voltage. The capacitor performs the duty of filtering ripples that is, disturbances and it blocks DC current/voltage. The light emitting diode (LED) blinks at a faster rate if the load consumption increases while it blinks at a slower rate at less load consumption thus, it is used for physical detection. Moreover, the 7805 voltage regulator maintains the voltage level of the circuit at a rating of 5V to prevent burning of the circuit during high voltage and damage during the occurrence of an open circuit.
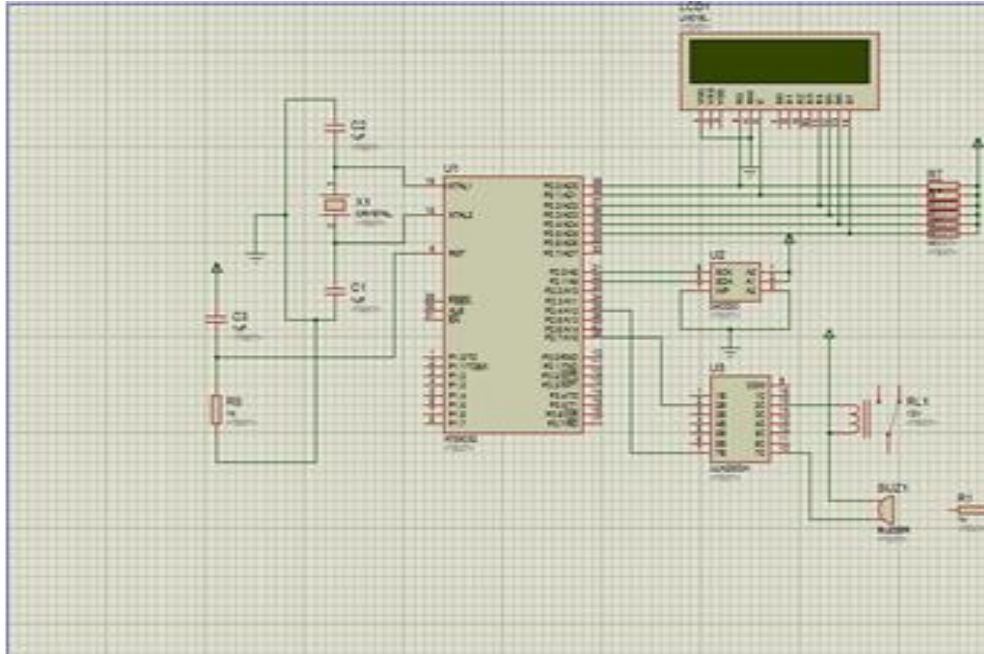
Figure 5: Design schematic diagram

3.3. Mathematical Model of the System

The instantaneous power loss, $P_{loss}(t)$ in a transmission

(A) $P_{loss}(t) = P_{source}(t) - P_{load}(t)$ (1)

Where $P_{source}(t)$ is the instantaneous power that the source injects into the transmission line and $P_{load}(t)$ is the instantaneous power consumed by the load at the other end of the transmission line.

Thus the energy loss, E_{loss}, is given by:

(B) $\qquad E_{loss} = \int ab P_{loss}(t) \, dt$

(2)

Where a and b are respectively the starting point and ending point of the time interval being evaluated. It must be noted that a fairly accurate description of $P_{loss}(t)$ as a function of time

(C). Total energy losses = Energy supplied – Bills paid

Total losses = NTL + Tl   (3)

Where NTL = Non-Technical Losses

TL = Technical Losses

(D). Computation Load meters

X = a+b+c   (4)

Where X = Sum of load meters

a, b, c are 3 different load meters

(E). Residential Meter = Sum of Load meter*illegal Load

Y=X*d   (5)

Where Y = Residential ISM d = illegal loads which are d1 and d2

d1 is the illegal load within the Residential ISM and d2 is that outside the Residential ISM.

3.4. Programming Language and Simulation Software Utilized

The Programming languages used:
 (A) Assembly language which is the hex code
(B) .M-IDE (Microcontroller Integrated Development Environment) used for the code compilation
The implementation flowcharts are as shown in Figures 6 and 7. People always tamper their meter, when the total unit loaded into the meter is exhausted, the algorithm shown in Figure 6 would apply. The steps involved in actualizing this are:
Number of load meter as a, b and c
2. Calculate a, b and c as sum of Load meter given as X
3. Illegal load = 1.01 and above but not less than 1 (d1 and d2)
4. No illegal load d1 and d2 = 1
5. Calculate X*d1 or d2 or X*d1 and d2 as Y
6. Equate Z = X
7. Verify if Z < Y
    If Yes, display illegal load detected and send SMS alert to utility company
    If No, return to number 2 or loop number 2
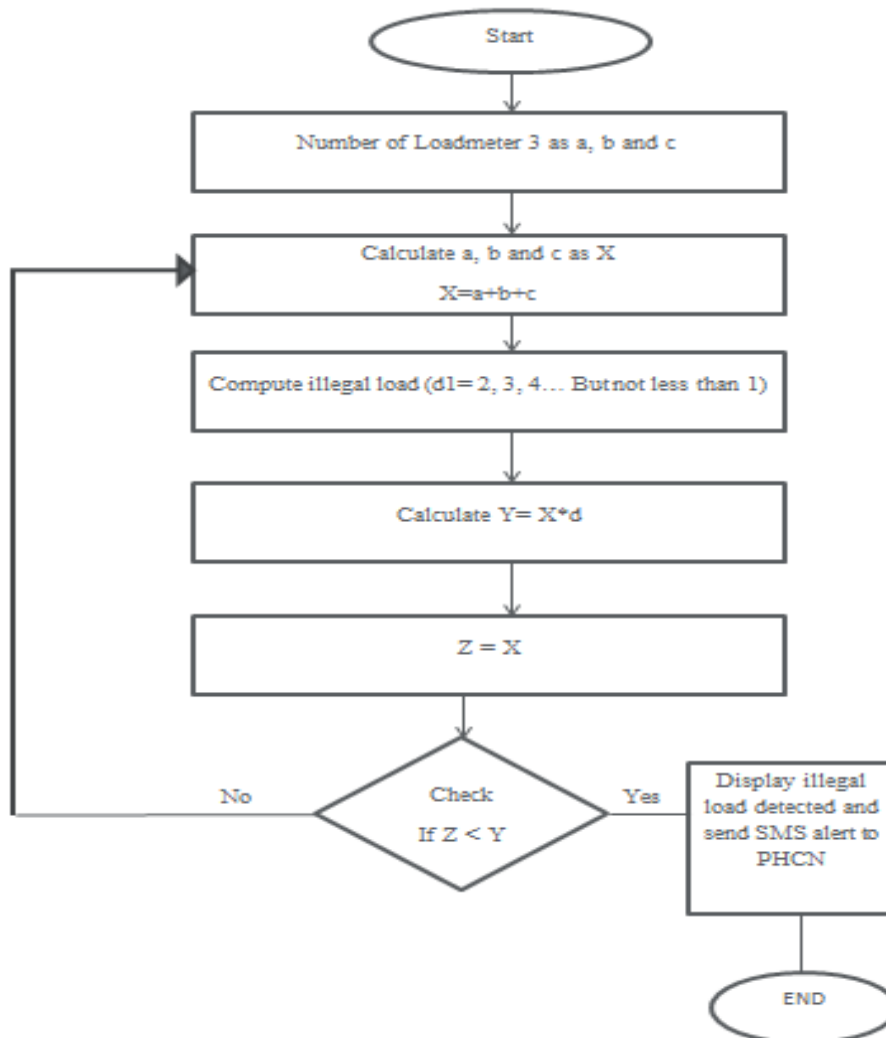8. End

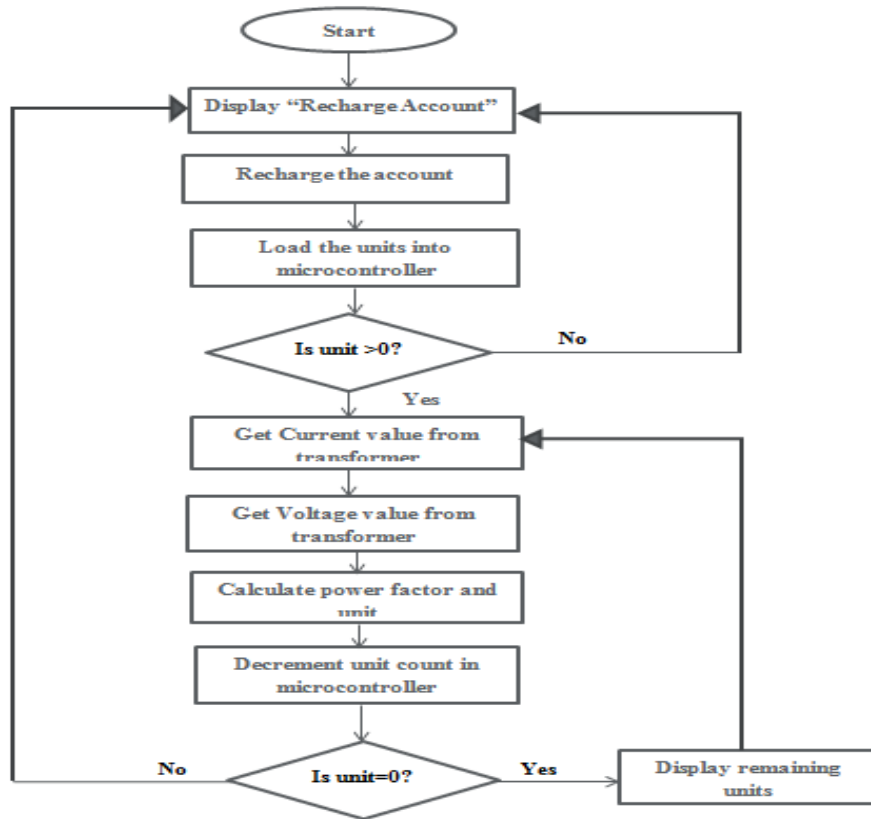Figure 6: Flow chart for the integrated fingerprint attendance

Figure 7: Flow chart for account recharge

Residential ISM: Its function is similar to that of the main ISM except that it is a concentrator for smaller coverage region. It is recommended to be installed inside the house as shown in Fig. 8
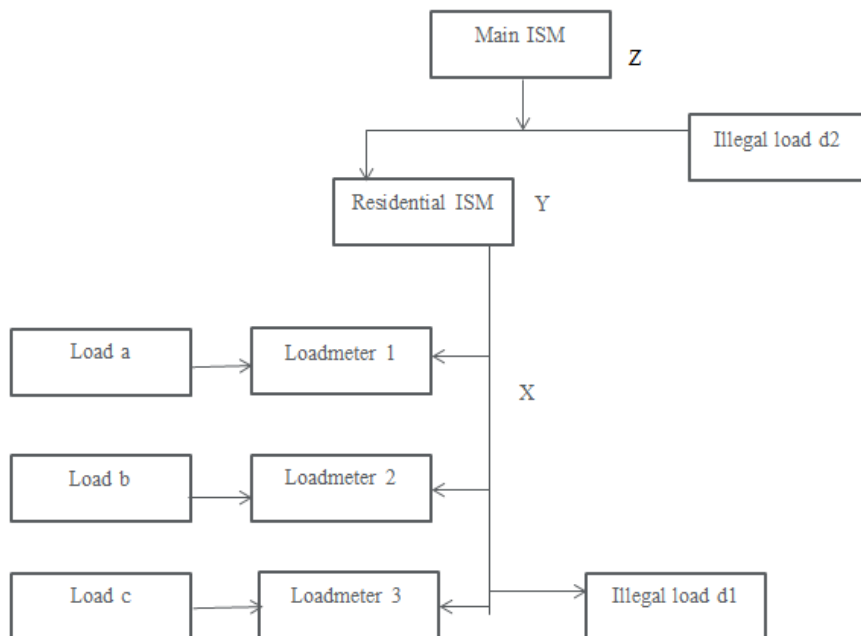

Figure 8: Metered consumption detection method showing illegal load tampering
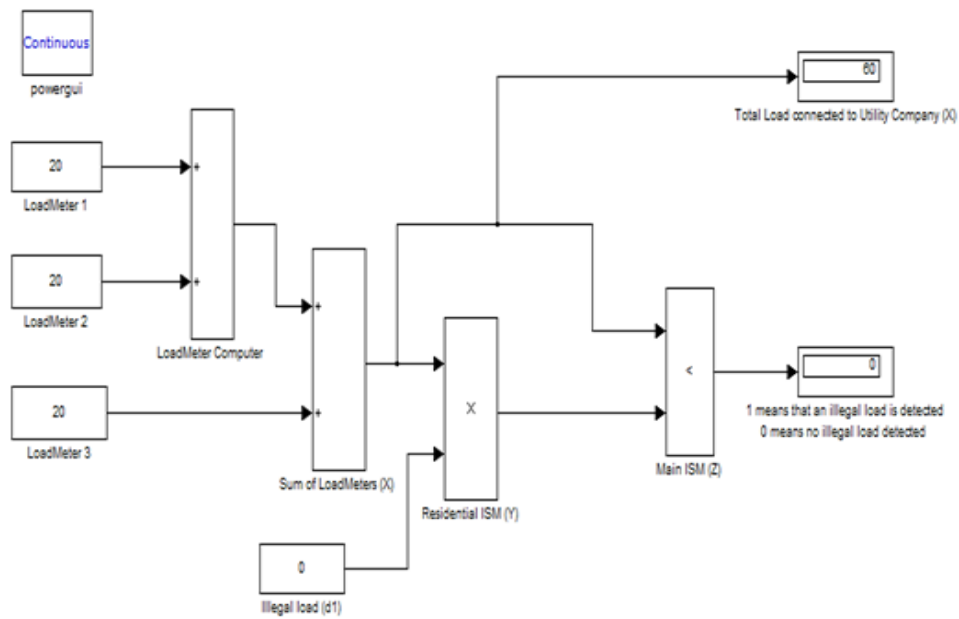
Figure 9: Simulink simulation of the anti-theft metering system.

Load Meter: It's an Intelligent Prepaid Energy Meter (iPEM) which measures the energy consumed by the load connected to it. This measurement is called the metered energy.
Load: This is the true load (metered load) connected to the Load meter. Load a, load b and load c as seen in Fig
Illegal Load: This is the unmetered load. This load enjoys energy consumption from the power utility through bypass (power theft). From Fig.8, Load d1 and load d2 are illegal loads. The illegal connection or bypass is done before the power utility meters. Fig. 8 shows the implementation steps involved detection of illegal loads connected to the meter, while Fig. 9 is resulting Matlab/Simulink model of the power theft metering system with the display and the algorithm and the block diagram is demonstrated using assumed values and the results is shown.

IV. RESULTS AND DISCUSSION

The types of simulation that are performed include:
➤ Varying the loads connected to the Residential ISM.
➤ Varying the illegal load connected within the Residential ISM.
➤ Varying the illegal loads connected within and outside the Residential ISM.
➤ Varying both the loads connected to the Residential ISM and also the illegal loads connected within and outside the branch ISM.

Table I: Simulation of load meters and illegal loads with ISM(s)

Loadmeter a	Loadmeter b	Loadmeter c	Illegal load within Residential ISM d1	Illegal load outside Residential ISM d2	Sum of Loadmeter X	Residential meter ISM (X*d1*d2) = Y	Main ISM
20	20	20	1	1	60	60*1	60
20	20	20	2	1	60	60*2=120	60
20	20	20	1.5	1	60	60*1.5=90	60
20	20	20	1.25	1	60	60*1.25=75	60
20	20	20	1	1	60	60*1*1=60	60
15	5	10	1	1	30	30*1*1=30	30
15	5	10	1	1.05	30	30*1*1.05	30
25	20	15	1.05	1.75	60	30*1.05*1.75	60
20	20	20	1	2	60	60*2 = 120	60

From Table I, the results of the number of simulations conducted, it can be observed that varying the loads read by the load meters does not affect the Residential ISM reading or the main ISM reading of the loads connected to the utility company. As long as no illegal loads are detected by the Residential ISM or the Main ISM located at the transformer for better performance and monitoring, the GSM module will not alert the utility company for a site investigation. Immediately, an illegal load is connected to the utility system either within the Residential ISM jurisdiction, the illegal load is instantly detected no matter how small the illegal load is.

V. CONCLUSION

The design, simulation and construction of a GSM-based prepaid meter has been achieved. It x-rayed various forms of electricity theft which include unaccountability of servicemen, irregularities of billing leading to a reduction of funds by the utility companies has also been achieved as this work prevents one on one contact between the end user and the workers.

With remote monitoring of the meter reading and sending SMS whenever there is abnormal readings in the customer electricity meter, the developed system may e able to help Utilities reduce the incidences of household electricity theft.

Automation of the customer billing system has been achieved as the meter keeps track of the consumers load on a timely basis. This design, therefore, removes the manual reading of meters with its attached consequences of time consuming system and bill manipulation which reduces remove generation by utilities while adding higher bills to the consumer.

The work also revolves around the automatic disconnection and connection when the recharge is low or high respectively and extra cost due to reconnection is removed.

 Further improvement will be needed in including miniaturized monitoring cameras in the customer meter which will monitor physical activities around the meter in each household to check other illegal acts that were not covered in this work.

REFERENCES

[1]   Devidas, A. R and Ramesh, M. V, "Wireless Smart Grid Design for Monitoring and Optimizing Electric Transmission in India", 2010 Fourth International Conference on Sensor Technologies and Applications (SENSOR COMM), pp. 637-640, 2010.
[2]   Shoeb S. Sheikh, et'l, "Design and Implementation of Wireless Automatic Meter Reading System", International Journal of Engineering, Science and Technology, Vol. 3, No. 3, pp. 2329-2334, March 2011.
[3]   Amit Jain and MohnishBagree, "A Prepaid Meter using Mobile Communication", International Journal of Engineering, Science and Technology, Vol. 3, No. 3, pp. 160-166, April 2011.
[4]   Koay .B. S., et'l, " Design and Implementation of a Bluetooth Energy Meter", proceedings of the Joint 4th International Conference on Information, Communication and Signal Processing and the 4th Pacific Rim Conference on Multimedia Vol. 3, pp. 1474-1477, 2003.
[5]   Hong. L and Ning. L, "Design and Implementation of Remote Intelligent Management System for City Energy Resources based on Wireless Network", Study of Computer Application pp. 237-239, 2004.
[6]   Malik S. H, Aihab. K, and Erum .S, "SMS Based Wireless Home Appliance Control System (HACS) for Automating Appliances and Security", Issue in informing Science and Information Technology, pp. 887-894, 2009.
[7]   Maheswari .C and Jejanthi. R, "Implementation of Energy Management Structure for Street-Lighting System", A Journal of Modern Applied Science, pp. 6-10, 2009.
[8]   Sayema. S, Faeq. A, Mohd.H, "Electricity theft- A Major Issue in Power industry", Nov 2012, (www.slide.net/.../ Electricity theft/) Dan Suriyamongkol, "Non-technical losses in Electrical Power Systems". Retrieved 26/06/2014.
[10]   F. I. Anyasi, B. O. Omijeh, and G. I. Ighalo, "SMS-Based Recharge Protocol for Prepaid Energy Billing System", International Journal of Engineering Innovation & Research, Vol. 1, pp. 553-558, 2012.
[11]   Z. A. Khan, S. M Raza, N. Jaavaid, A. Mahmood, U. Qasim, M. Anas, "Minimizing Electricity Theft using Smart Meters in AMI", Aug 2012.
 [12]   T. B. Smith, "Electricity theft: a comparative analysis," Elsevier Journal Energy Policy, Vol. 32, No. 18, pp. 2067-2076, Dec. 2004.
[13]   S.S.S.R. Depuru, L. Wang, V. Devabhaktuni, and N. Gudi, "Measures and Setbacks for Controlling Electricity Theft," in proceedings of North American Power Symposium, pp. 1-8, Sept. 2010.
[14]   Z. Wang, D. Nikovski, A. Esenther, H. Sun, K. Sugiura, T. Musa, K. Tsuru, "Smart Meter Data Analysis for Power Theft Detection", July 2013.
[15]   K. Jubi and J. Mareena, "Prepaid Energy Meter with GSM Technology", American International Journal of Research in Science, Technology, Engineering & Mathematics, Vol.3, No. 2, pp. 195-198, August 2013.
[16]   N. Mehmood, Z. A. Ali, A. A. Sidiqui, M. Asif and S. Wasi, "Electronic Meter Reader and Data Base Management System", IEEE, 2011
[17]   T. Chandler, "The technology development of automatic metering and monitoring systems", in IEEE International Power Engineering Conference, December 2005

Research Paper   Open Access

The Role of Citizen Participant in Urban Management (Case Study: Aligudarz City)

Abdolhamid Malek Mahmudi, Hamid reza Saremi

Department of Architectural and urban planning, Boroujerd branch, Islamic Azad University, Boroujerd, Iran
Assistance Professor Department of Art and Architecture, Tarbiyat Modares University, Tehran, Iran

Abstract: *Today, in our times, human participation has been considered as a key to develop communities. And new urban planning, instead of theoretical and cognitive issues, are more likely leading to practical planning, implementations and participations. the intention of this survey is, recognizing the methods and procedures of participation planning in order to use the most of people's participation ability to develop the urban areas, And also have a check at the rate of citizen's partnership and their role in the development of Aliguodarz city.*
This research is applied and the research method is "descriptive – analytical". The method of data collected is field and questionnaire. In order to was used from libraries resource, organizations internet and papers. Finding show, there is oriented relation between sexual and participant. Also, there is oriented relation between citizen participant and economic and social condition
Key word: *Citizen participant, urban management, Aligoudarz*

I.   Introduction

Studying the evolution of human societies, the development and improvement are obtained when human cooperate and participate during their life with each other. Participation is a set of attitudes, procedures and behaviors that make people to discuss and investigate the facts and conditions of their lives, so that they can plan what to do and they can find the results and evaluate them. (Chambers and Blackburn, 1996; p, 1) so one of the participatory methods is citizen partnership in development. The city is at last belongs to all the citizens and wardens so that planners cannot act and decide instead of them. (Moledan, 2002, p, 128) In this matter, it is necessary that power be distributed in urban public fields so that citizens can be directly engaged in city matters and find their roles as active citizens and feel more responsible in the aspect of urban problems. When citizens are involved in urban issues of whole city as a backbone, and they develop a sense of responsibility and making decisions, therefore it would be much easier for the wardens of the city to solve the urban problems. (Journal of Council, 2000)

A neighborhood is also a social pyramid that makes the pillars of a bigger pyramid which is the city and it also contains other social elements of the city. Neighborhood is a social context and it includes a public discipline. A part of this public discipline is public duty and the other part of it, is insured by an efficient city governor. Overall, the feeling of belonging to a particular place increases one's feeling of responsibility towards preserving and retaining the social discipline of the neighborhood. And because of this, city governors have less problems towards this matter. (Mashhadizadeh Dehaghani, 1999).

Among industrial countries, France is one the successful countries in the discussion of participation subject. Statesmen of France (Prime Minister and Mayor) have carried a program entitled "neighborhood community development". The innovation of this program is the close cooperation between government and urban agencies and role of citizen in the process of city development. (Athari, 2002).

The subject of citizen participation in urban areas in third world countries such as Iran, due to low appropriate cooperation in both legal and social parts, still considers as a new phenomenon that has not been properly in right theoretical or practical position. It is essential to search for the forms of the participation in order to have more attention to sustainable development in urban areas.(Yavar,2001). Participatory planning was introduced in 1940s by using people's opinion about the urban municipal comprehensive over Europe. And 1960s may be considers as the most important decade in formation of philosophical and theoretical issues involved in urban planning and participation. (Moradi,2001).

Azadi (2001) has come to results such as the importance of widespread public participation in planning, equipping, managing, implementing, maintenance and comprehensive public management assessing in his thesis named "The role of participation in integrated management and sustainable development".

And also Eyvazi Abdullahi (2005) have reached to this conclusions that there is a straight and positive relation among membership in organizations, more communicating with information resource incentives, council's view of training and advancement planning, council's technical knowledge in sustainable development and the severity of natural resources damage and environmental degradation in his thesis entitled " Analysis of public organization participations in extension plannings toward permanent development". Hodseni (2006) indicates in his master's thesis which named" urban structural-spatial improvement in urban permanent development(sample case Jolfa neighborhood)", that creation of ethnic social networks as communities and urban groups and creating the necessary context for communication among residents can solve urban problems and improve environmental situation for residents, as an effective feedback.((masomii, 2011).

Since the most important gauge for a sustainable city, is creating mental and spiritual relaxation and providing citizen's needs, Therefore, in urban planning, planners should pay attention to ecological limitations, economical issues, social, life quality, cultural issues, moralities, gregariousness, social profit and loss, citizen political development and etc. And with today's emphasis on importance of public participation as a key strategy for sustainable development which occurs at any scale, it will be clear that the urban development can play a sustainable role. (Khaksari, 2006).

II. Theoretical framework

2.1. Urban management

There is no general principle for urban management concept and the main meaning of this term is very confusing. Stern believes that, urban management doesn't have a specific definition and content (Stern, 1993). According to the tastes, perception of people and also political-social demands of different eras had different meanings. We can still see these differences in meaning and concept in the recent era. The World Bank defines urban management as a quasi-commercial activity for governments. In other words, urban management means, managing urban affairs and high performance in order to use the World Bank loans. Urban management is sometimes considered as a tool for implementing the urban policies, which means urban managing science. *Van Dijk* defines urban management as an effort for coordinating and integrating the public and private actions for overcoming problems that urban residents encounter, and creating more competitive, fairer and more stable cities. *Van clink* and *Bramesta* also defined modern urban management as the process of implementing, coordinating and assessing the integrated strategies with city's authorities' help, by considering the private section objectives and citizen's benefit, in a political framework that in higher levels of government, is being edited for approaching the sustainable economic development potential (Van Dijk,2006).

2.2. Participation

Citizen participation is one of the core values of democracy. Democratization means an increase in citizen participation in public affairs (Don-yun, 2003). In fact, Citizen participation plays a critical role in building healthy communities by creating more empowered constituencies who can leverage greater and more equal access to available resources (Pennie G, 2009).

In urban management, participation has two meanings, the first meaning of participation concept, can be considered cooperation between private sectors and municipality. In this kind of cooperation, the private sector which acts according to the market rules, in order to get economical profits and by receiving service cost that presents, cooperates with municipality and, hence, in performing duties, helps the municipality. Municipality monitors the activity of this section and giving part of duties to the private section does not mean that the municipality is not responsible toward the quality of the presenting services. The second concept of the participation emerges in the cooperation of community sector with municipality. This sector has other names such as social sector or private non-for-profit sector (mozayyeni, 1997).

2.3. Participation approach in Urban Management

In the recent two decades, many organizations and institutes that intervene urban management and planning at global levels, have emphasized on promoting the participation view for encouraging a kind of management and planning approach "Bottom-up" and enabling community in order to monitor development actions and had considered to make decision in solving urban problems based on local communities to fulfill the necessary conditions for citizen's welfare. From 1990, urban development approach, has experienced an important revolution in its paradigm; learning from previous experiences and "top-down" conventional view, would give a pattern that lies on the approach different from the past, and that is "down to up" approach; shift from a prescriptive view to the participative one based on government-oriented solutions for problem solving

methods with emphasis on civic society is one of the features of new development pattern, which has fundamental emphasis on the role of people, local communities and civic society (Haji pour, 2006).

According to the capacity and power of citizens, the urban management should be on the basis of the principles that in fact create the fundament of this structure. These principles can be listed as follows:

 Principles of urban civility and citizens' education
 Principles of continuous poll from citizens
 Principles of codified rules for informing and guiding citizens
 Principles of gaining trust of public and private sector
 Principles of verifying and revising the actions which have been done (Mozayyeni, 2000).

III. Research method

This research is applied and the research method is "descriptive – analytical". The method of data collected is field and questionnaire. In order to was used from libraries resource, organizations internet and papers (eshraqi, 2001:45). So the research hypothesis is:

- There is oriented relation between sexual and participant.
- There is oriented relation between citizen participant and economic and social condition
-

IV. Studied area

Aligoudarz is a city in and capital of Aligudarz County, Lorestan Province, Iran. At the 2006 census, its population was 78,690, in 18,115 families. Aligudarz is located 503 km from Tehran and situated in a region which is a mixture of plain and foothill, thus enjoying a mountainous mild climate. Oshtorankuh Mountain range and Aligudarz River are situated here. The origins of the city are unknown. The city of Aligudarz was once called Al-e Goodarz (meaning sons or tribe of Goodarz, a mythical Iranian hero from the Persian national epic Shahnameh).In the past, the monastery of this city was a religious training center for the Kizilbash and darvishes.
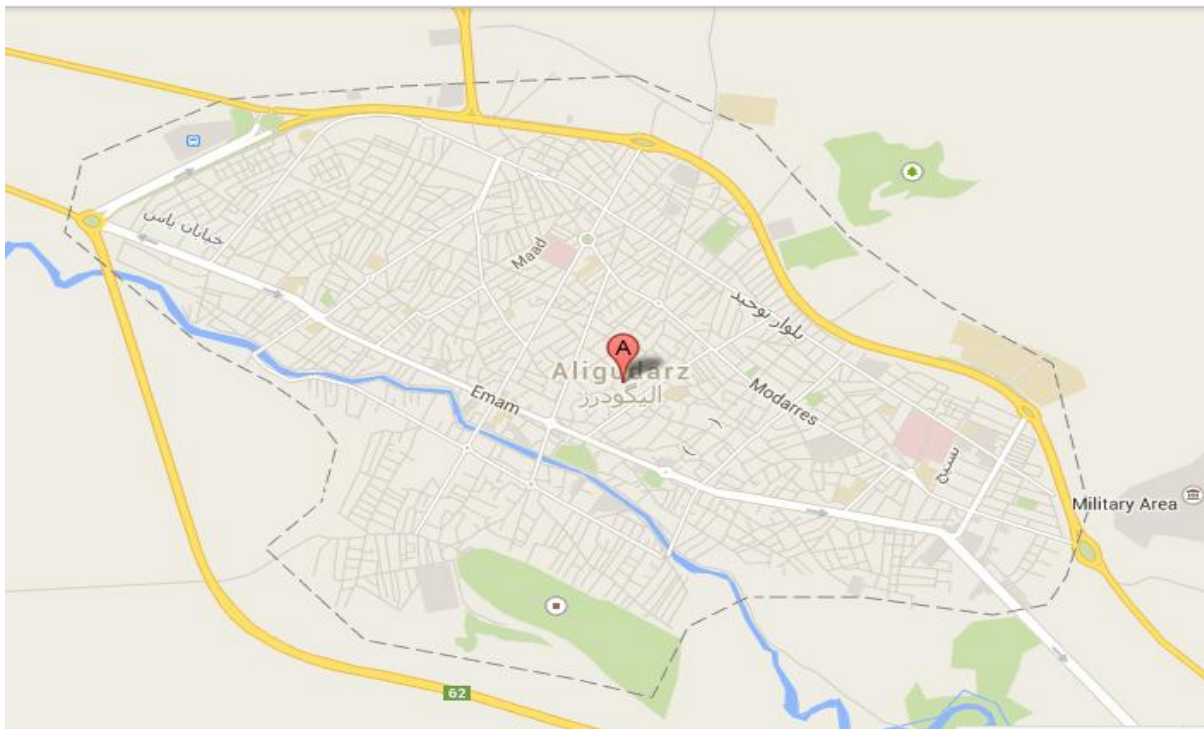
Figure 1: Aligoudarz city

V. Findings

This section was divided two sections. Descriptive findings and analytical findings. So in continue explain them.

5.1. Descriptive findings

In order to descriptive statistical society, indicators were defined in questionnaire. Thus was used from descriptive statistical. Therefore the graphs show relation between studied indicators. Indicators are, sexual, economic (income) condition, satisfaction of local governance function
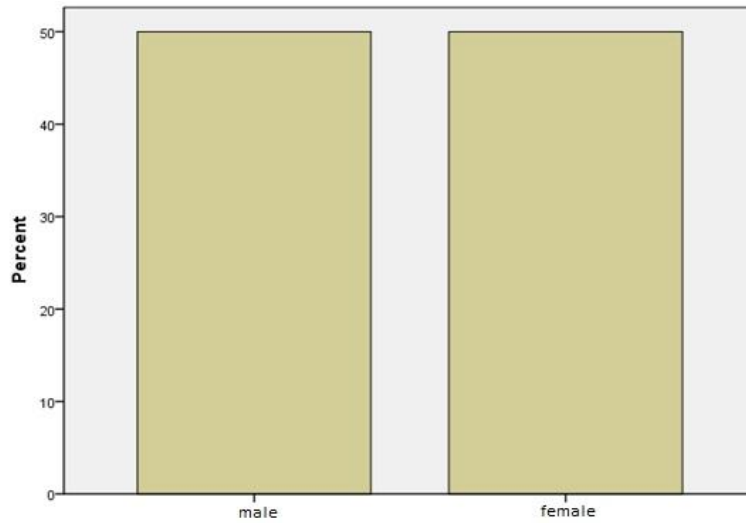
Figure 2: sexual condition
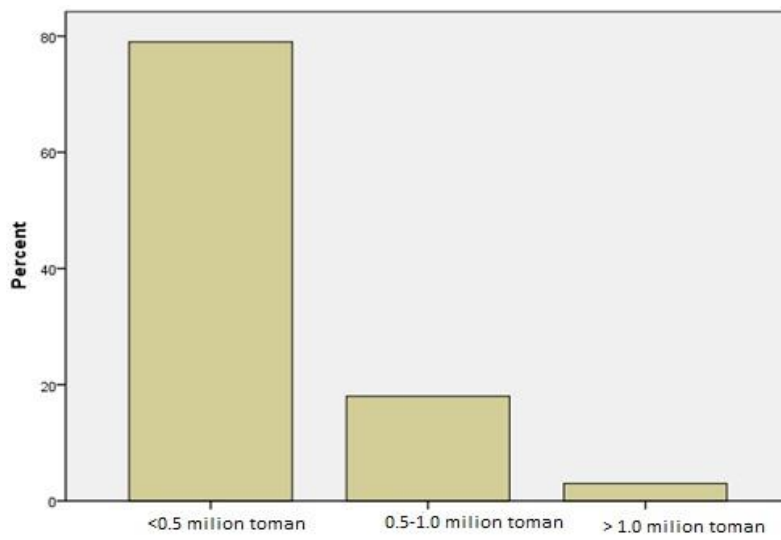
Figure 3: income condition
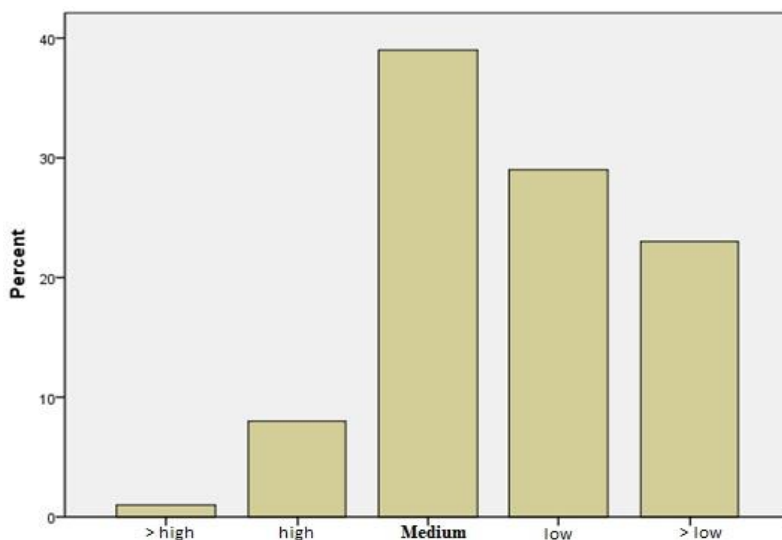
Figure 3: satisfaction of local governance function

5.2. Analytical data

In order to detecting relation between indicators should be used analytic statistic. So, we use from Pearson's coefficient of contingency method. Mentioned method show contingency between indicators . The amount is between -1 to 1. Thus, is studied relation between defined indicators.

	Cases					
	Valid		Missing		Total	
	N	Percent	N	Percent	N	Percent
The relation between participate and income	100	100.0%	0	.0%	100	100.0%

Pearson's coefficient of contingency

		Value	Approx. Sig.
Nominal by Nominal	Contingency Coefficient	.107	.562
N of Valid Cases		100	

	Cases					
	Valid		Missing		Total	
	N	Percent	N	Percent	N	Percent
Sexual & participate	100	100.0%	0	.0%	100	100.0%

Pearson's coefficient of contingency

		Value	Approx. Sig.
Nominal by Nominal	Contingency Coefficient	.025	.806
N of Valid Cases		100	

According above table there is oriented relation between indicators. Also, the amount is positive. They are 0.8 and 0.5. So the hypothesis is true.

VI. Conclusion

City councils establishment in Iran is an important step moving from a centralized system to a decentralized planning system and urban management based on citizen's participation. Concurrent with city council establishment, neighborhoods council associations also were established in order to citizens are in contact with their representatives directly.

According to this study, we have come to this result that the rate of citizen participation of Aligoudarz city is pretty good. Thus citizens feel responsible for their neighborhood and are trying to keep it. Also they want the security of their neighborhood and are interested in decision making and participating in plans which are made for the neighborhood's development. According to this survey the long living term has not had a big effect on participation. One of its reasons can be, being un familiar with urbanization culture, uneven distribution in some neighborhoods, new buildings and lack of appropriate services. And in the participation subject, we have come to this result that most of the citizens are likely tend to participate.

And this shows that participating for citizens is somehow a crystallization matter. On the other hand, the officials of the city did not provide much opportunity for them. Some researchers have been working in this field, including Majla, he came to this conclusion in his survey about participation that citizen participation rate have an outstanding effect on planning, city development and improvement and urban management. (Taghva, 2011, p, 305) In the participation aspect, the positive respondents results shows that most citizens believe that income increase does not affect sustainable development individually, but increasing the citizen's social and economical database simultaneously in training, income and employment will be affective. On the other hand, the hypothesis is true. There is oriented relation between indicators.

References

[1] Arjmand Nia, Asghar: Non-Governmental Organizations, Organized Participation Strategy. In: Journal of Urban Management, No. 5, Tehran, 2001.
[2] Congress of Non-Governmental Organizations and future challenges: Special Issue 2, Iran, 2001.
[3] Document of Darakeh Locality Identification, Darakeh Locality Counselling, 2007.

[4]   Don-yun, Chen. Tong-yi, Huang and Naiyi Hsaio: The Management of Citizen Participation in Taiwan: A Case Study of Taipei City Government's Citizen Complaints System. In: International Journal of Public Adminstration, Vol. 26, No. 5, 2003.

[5]   Hajipur, Khalil: Neighborhood based Planning, an efficient approach on creating sustainable Urban Management. In: Journal of Fine Arts Magazine, No. 26, Tehran, 2006.

[6]   Hekmat Nia, Hassan and Moussavi, Mirnajaf: Historical analysis of Citizen Participation in governance of cities of Iran. In: Journal of Geographical Research, No. 80, pp. 121-136, Tehran, 2004.

[7]   Khalilkhah, B: Deficiencies of Services in Tehran. In: thesis of M.S., Human geography of Rural and Urban, Professor Dr. Mozafar Sarafi, Shahid Beheshti University, 1998

[8]   Lee, Y.-J: Subjective quality of life measurement in Taipei. In: Building and Environment, Vol. 43(7), 2008.

[9]   Mozayyeni, Manouchehr: Municipal, Councils and Urban Management in Iran. In: Journal of Urban Management, No. 2, Tehran,2000.

[10]   Mozayyeni, Manouchehr: Urban and Rural Management in Iran. In: National Organization of Land and Housing, pp. 121-136, Tehran, 1997.

[11]   Pennie G. Foster-Fishman, Steven J. Pierce and Laurie A. Van Egeren: Who Participates and Why: Building a Process Model of Citizen Participation. In: Health Educ Behav, 2009.

[12]   R. Epley, Donald & Menon, Mohan: A Method of Assembling Cross-sectional Indicators into a Community Quality of Life. In: Social Indicators Research, Vol.88, 2008.

[13]   Rezvani, M.R. and others: Development and Assessment of Urban Quality of Life indicators. In: Journal of Urban and regional Studies and Research, first year, No. 2, Tehran, 2009. Stren, R: Urban Management in Development Assistance. In: Cities, Vol. 10, No. 2, 1993.

[14]   Van Dijk, M. Pieter: Managing cities in developing countries: The theory and practice of urban management. In: Edward Elgar publishing, 2006.

Research Paper   Open Access

A Concept of Input-Output oriented Super-efficiency in Decision Making Units.

Dr.S.Chandrababu[1], Dr.S.Hariprasad[2]

[1,]Lecturer in Statists, N.P.S Govt College, Chittoor
[2,]Assistant Professor in Statistics, P.V.K.N Govt College, Chittoor,
[3,]Corresponding Author: Dr.S.Chandrababu

ABSTRACT : *In data envelopment analysis the input and output decision making units plays a major role to evaluate the efficiency and its super-efficiency. In this paper, super-efficiency can be assessed through graphically with simple notations. The area pointed on the feasibility of decision making units when i) Extremely efficient, ii) Efficient, but not extremely efficient, iii) Weakly efficient and iv) Inefficient.*

KEY WORDS: *Super efficiency, Data Envelopment Analysis, Decision Making Units, Input and output Super efficiency.*
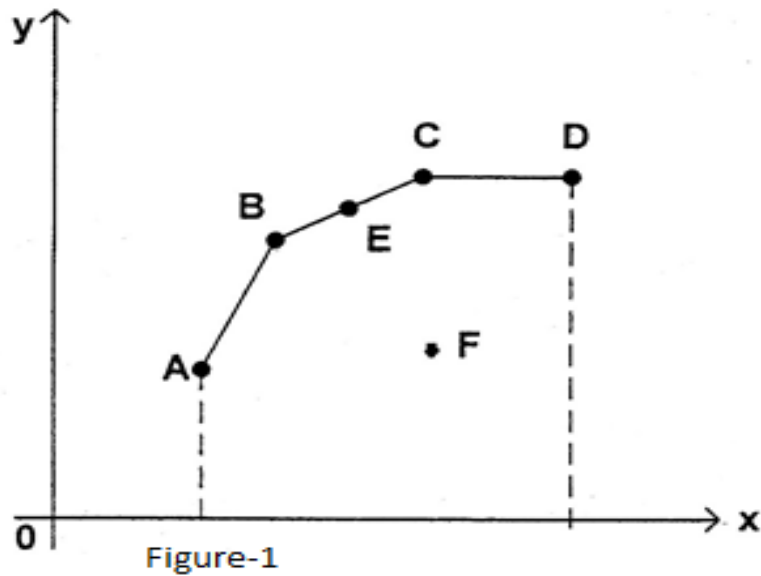
I. INTRODUCTION

The data envelopment analysis as formulated by BCC gives input and output targets to the decision making units. These targets are pro rata. For an inefficient DMU inputs are decreased and outputs are increased pro rata. Pro rata input targets reveal input losses and output targets yield output losses of a decision making unit whose efficiency is under evaluation. A major deficiency of DEA is the DMU_0 under evaluation chooses multiplier weights most advantageous to it. To get out of this problem the multi-objective DEA problems have to be solved. In this approach we minimize the maximum deviation or sum of all the deviations. This approach identifies fewer numbers of DMUs as efficient. The efficiencies are evaluated exposing all the DMUs to the same light.

II. SUPER EFFICIENCY

When efficiency problem is solved for all the DMUs in competition, it is possible that more than one DMU arises with 100% efficiency score. If further analysis is to be performed to rank the efficient units one may solve super-efficient problem for extremely efficient units. In fact efficient DMUs are three types, extremely efficient, efficient but not extremely efficient and weekly efficient. To find super efficiency of extremely efficient DMU, its input and output vectors are removed from the reference technology. Consequently, the production possibility set shrinks which allows DMUs to become super-efficient attaining super efficiency score that exceeds unity. There is no need that a super efficiency problem to be feasible when RTS are variable. If an input based super – efficiency problem is infeasible then the corresponding output based super-efficiency problem is feasible. Similarly, if an output based super –efficiency problem is infeasible then the corresponding input based super-efficiency problem is feasible.However, for CRS production possibility set, both the super efficiency problems are always feasible.

The concept of 'Super-efficiency' arises if (i) the Decision Making Unit (DMU) is extremely efficient and (ii) the DMU under evaluation is removed from the reference set.

Figure-1

In figure - 1 we find six DMUs A, B, C, D, E and F. The DMUs A, B, C and D are extremely efficient. These DMUs determine the frontier production function. DMU E is efficient but not extremely efficient since, its output, input pair is determined as a convex combination input, output pairs of DMUs B and DMU C. DMU F is inefficient. All the DMUs employ one input and produce one output.

The production possibility set is enveloped by a piecewise linear frontier constituted by the line segments AB, BC and CD. If T stands for graph (production possibility set) of the technology, then it takes the from

$$T = \left\{ (x,y) \sum_{j=1}^{n} \theta_j x_j \le x, \sum_{j=1}^{n} \theta_j y_j \le y, \theta_j \ge 0 \sum_{j=1}^{n} \theta_j = 1 \right\}$$

Where $x \in R_+^m$, $y \in R_+^s$ x_j and y_j are respectively the input and output vectors of DMU_j.

To estimate input technical efficiency of DMU_0 we solve the following linear programming problem.

$$\lambda_0^* = Min \quad \lambda_0$$

Subject to

$$\sum_{j=1}^{n} \theta_j x_{ij} \le \lambda_0 x_{i0}, \qquad i = 1, 2, \dots\dots \dots, m$$

$$\sum_{j=1}^{n} \theta_j y_{ij} \ge y_{r0} \qquad\qquad r = 1, 2, \dots\dots \dots, s \qquad\qquad \dots\dots\dots\dots[1]$$

$$\sum_{j=1}^{n} \theta_j = 1 \qquad , \qquad \theta_j \ge 0$$

There arise four cases

[1] DMU_0 is extremely efficient
[2] DMU_0 is efficient, but not extremely efficient
[3] DMU_0 is weakly efficient
[4]   DMUs is inefficient

If a DMU is extremely efficient we obtain, $\lambda_0^* = 1$, $\theta_j^* = 0$, $\forall$ $j \neq 0$, $\theta_0^* = 1$

$$s_i^{-*} = s_r^{+*} = 0, \quad \forall \ i \wedge r$$

If DMU_0 is weakly efficient the optimal solution is of the form

$$\lambda_0^* = 1 , \ \theta_j^* = 0 , \ \forall j \neq 0 , \ \theta_0^* = 1$$

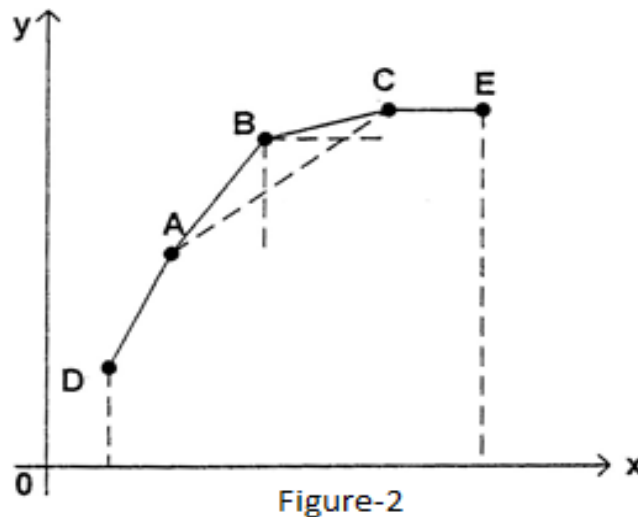$$s_i^{-*} \neq 0 \ \text{For some 'i' and / or} \ s_r^{+*} \neq 0 \text{ , for some 'r'}$$

If the DMU under evaluation is inefficient then we have the following optimal solution:

$$\lambda_0^* < 1 , \theta_0^* = 0 , \sum_{j \neq 0} \theta_j^* = 1 \text{ , some input and / or output slacks are non-zero.}$$

If an extremely efficient DMU is removed from the references set we obtain.

$$\left(\sum_{j \neq o} \theta_j \ x_{ij} , \sum_{j \neq o} \theta_j \ y_{rj} \right), \qquad i = 1, \ 2, ... \ ..., \ m \ \text{ And } r = 1, \ 2 .... \ .., \ s$$

Consequently the production possibility set shrinks.

Figure-2

The frontier production function is determined by the decision making units A, B, C, D and E. DMU B is extremely efficient[1].

If DMU B is removed from the reference set the production possibility set is found to be enveloped by the line segments DA, AC and CE. Consequently, the resultant production possibility set is a subset of the original production possibility set.

---

[1] A DMU is said to be extremely efficient if its input and output vectors cannot be expressed as a convex combination of the input, output vectors of two or more than two points of the production possibility set, frontier.

The output oriented technical efficiency of DMU_0 can be computed by solving the following linear programming problem.

$$\gamma_0 = \text{Max} \quad \gamma_0$$

Subject to

$$\sum_{j=1}^{n} \theta_j \, x_{ij} \leq x_{i0}, \qquad i = 1, 2, \dots\dots\dots \dots, \ m$$

$$\sum_{j=1}^{n} \theta_j \, y_{nj} \leq \gamma_0 \, y_{r0}, \qquad r = 1, 2, \dots\dots\dots \dots, \ s \qquad \dots\dots\dots\dots \qquad [\,2\,]$$

$$\sum_{j=1}^{n} \theta_j = 1 \qquad\qquad \theta_j = 0$$

If DMU_0 is extremely efficient, we must have the optimal solution as follows.

$$\gamma_0^* = 1 \ , \ \theta_0^* = 1 \ , \ \theta_j^* = 0 \ , \ \forall \ \ j \neq 0$$

$$s_i^{-*} = s_r^{+*} = 0$$

Super efficiency refers to extremely efficient DMUs, since if an efficient DMU that is not extremely efficient or weakly efficient or an inefficient DMU is removed from the reference set the production possibility set remains to be the same.

Input super efficiency:

DMU B below is extremely efficient and it is removed from the reference set. The following input super – efficiency problem is solved for

DMU B = DMU_0.

Figure-3
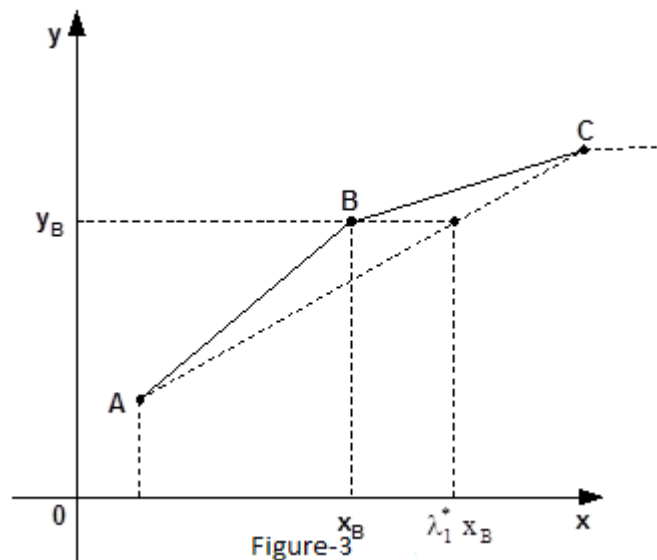
$$\lambda_1^* = \text{Min} \quad \lambda$$

Subject to

$$\sum_{j \neq 0}^{n} \theta_j \, x_{ij} \leq \lambda_1 \, x_{i0}, \qquad i = 1, 2, \ldots\ldots\ldots \ldots, \quad m$$

$$\sum_{j \neq 0}^{n} \theta_j \, y_{rj} \geq y_{r0},$$

$$\sum_{j \neq 0}^{n} \theta_j = 1 \qquad , \quad \theta_j \geq 0, \, \forall j$$

$\ldots\ldots\ldots\ldots\ldots$[3]

The super – efficiency score of DMU_0 is λ_1^*. It can be seen that $\lambda_1^* > 1$. DMU_0 is said to be input super-efficient, because to produce the output vector of DMU_0, the remaining DMUs or a convex combination of them need to utilize more inputs than the DMU under evaluation viz., DMU_0. The input saving of the super-efficient DMU is $\left(\lambda_1^* - 1\right) x_0$.

Thus, larger is λ_1^* above unity greater is the super-efficiency of the DMU.

Output Super Efficiency

Figure-4
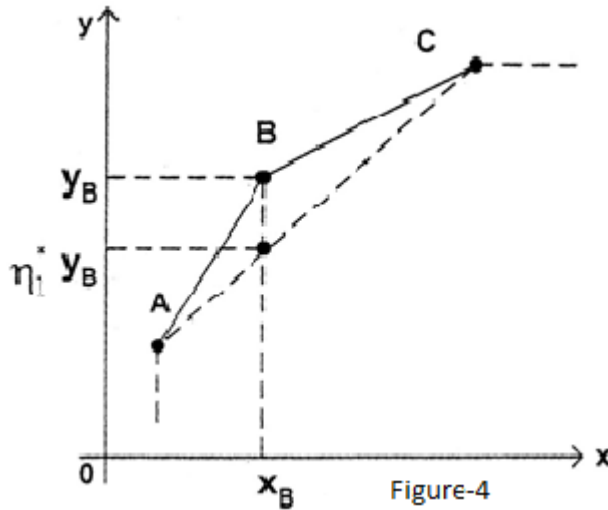
Consider the following output super –efficiency problem

$$\gamma_1^* = \text{Max} \quad \gamma_1$$

Subject to

$$\sum_{j \neq 0} \theta_j \, x_{ij} \leq x_{i0}, \qquad i = 1, 2, ... \; ......, \; m$$

$$\sum_{j \neq 0}^{n} \theta_j \, y_{rj} \leq \gamma_1 \, y_{r0}, \qquad r = 1, 2, ... \; ......, \; s \qquad \Bigg\} \qquad ....[4]$$

$$\sum_{j \neq 0}^{n} \theta_j = 1, \qquad \theta_j \geq 0, \; \forall j \neq 0$$

The super-efficiency score of $DMU_0 = DMU\ B$ in the above diagram is $\gamma_1^* < 1$. With the inputs of DMU_0 the other DMUs or a convex combination of them shall be able to produce lesser output than what DMU_0 actually produces. The output super-efficient DMU enjoys output gains. The output gain of output super-efficient DMU is $\left(1 - \gamma_1^*\right) y_0$.

DMU B which is both input and output super-efficient has its constraints feasible in input and output orientations.

A study of super-efficiency problem has at least three applications

[1]   If an input oriented or output oriented DEA problem is solved, it is likely that there exists more than one technical efficient DMU. In such a situation these efficient DMUs have to be ranked. If all super-efficiency problems are feasible, the extremely efficient DMUs can be ranked according to their super-efficiency. Larger super-efficiency implies better the DMU is ranked.

[2]   An input oriented super efficiency problem can be solved to estimate input gains of an extreme efficient DMU. An output oriented super-efficiency problem may be solved to estimate output gains of extreme point DMU.

[3]   In sensitivity analysis of an extreme efficient DMU, the super-efficient Data Envelopment Analysis (DEA) is used.

III.   CONCLUSION:

Characterized the input and output oriented targets in decision making analysis. The concept of 'Super-efficiency' is evaluated if (i) the Decision Making Unit (DMU) is extremely efficient and (ii) the DMU under evaluation is removed from the reference set.

BIBLIOGRAPHY:

[1]   **Bankar, R.D., Charnes, A., Cooper, W.W. (1984):-** "Some models for the estimation of technical and scale inefficiency in Data Envelopment Analysis", Management Science, 30, 1078-1092.

[2]   **Banker, R.D. and Morey, R. (1986):-** "Efficiency Analysis for exogenously fixed inputs and outputs in operations research", 34, 89-98.

[3]   **Banker, R.D., and Thrall, R.M. (1992):-** "Estimation of Returns to Scale using Data Envelopment Analysis", European Journal of Operations Research, 62, pp.74-84.

[4]   **Charnes A., Cooper, W.W. and Rhodes, E. (1978):-** "Measuring the efficiency of decision making units", European Journal of Operations Research, No.2: 429-444.

[5]   **Sciford and Zhu (1999):-** "Infeasibility of Super Efficiency DEA models", Infor 33, pp. 174-187.

[6]   **Subramanyam, G., Swamy, S.B., (1994):-** "Production Efficiency Difference between Large and Small Banks", Artha Vijnana, September, Vol. 36, No. 3, pp. 183-193.

[7]   **Yue, Piyu, (1992):-** " Data envelopment analysis and commercial bank performance: A primer with applications to Missouri banks", Federal Reserve Bank of St. Louis Economic Review 74(1), pp. 31-45.

[8]   **Zenios, Christiana V., Stavros, A., Zenios, Kostas Agathocleous and Andreas C. Soteriou, (1999):-** "Benchmarks of the efficiency of bank branches", Interfaces 29(3), pp. 37-51.A. and Revanker, N.B., (1969), "Generalized production functions, Review of Economic Studies, 36, 241-250.

Structure and Surface Characterization of Nanostructured Tio$_2$ Coatings Deposited Via HVOF Thermal Spray Processes

[1,]Maryamossadat Bozorgtabar , [2,]Mohammadreza Jafarpour
[a] *Department of Materials Engineering, Majlesi Branch, Islamic Azad University, Isfahan, Iran.*
[b] *Mobarakeh Steel Company, Isfahan, Iran*

ABSTRACT : *Titanium dioxide coatings were deposited by high velocity oxy-fuel spraying (HVOF) with the use of agglomerated P25/20 nano-powder and different spraying parameters (e.g. fuel/flow ratio) to determine their influence on the microstructure, crystalline structure and surface feature of the coatings. The microstructure of as-sprayed TiO$_2$ coatings was characterized by scanning electron microscope (SEM), transmission electron microscope (TEM) and X-ray diffraction (XRD). Surface features were investigated by Fourier transform infrared (FT-IR) and X-ray photoelectron spectroscopy (XPS). The results showed that the fuel and oxygen flow ratio have an important influence on the microstructure, anatase content, surface chemical state and surface feature of the TiO$_2$ coatings.*

KEY WORDS*: Nano materials; Coatings; Microstructure; TiO$_2$; Thermal Spray; XPS.*

I.   INTRODUCTION

Titanium dioxide (TiO$_2$), since the first report of the Honda–Fujishima effect, has received great attention in a range of scientific and industrial fields, such as light-induced water splitting, dye-sensitized solar cell and self-cleaning surfaces [1, 2]. Due to its unique electronic, photo-electronic and catalytic properties Photo-degradation of an organic contaminant becomes one of the most important applications of TiO$_2$, which is a fast-growing research area in recent years [3, 4]. In order to increase TiO$_2$ application activity, many methods are put forward, such as selecting TiO$_2$ nano-crystalline particles [5, 6]. So far, a vast amount of energy and effort has already been devoted to this subject by researchers. Now it seems to be the right time to find more practical ways to use the technology on an industrial scale. Crystal structure and surface characteristics of TiO$_2$ play an important role in its many applications, and this article addresses their importance in the expanded use of TiO$_2$. Among the two TiO$_2$ crystalline phases, anatase and rutile that can contribute to the photo-catalysis, it is generally assumed that the anatase, the metastable phase which by thermal treatment irreversibly turns into rutile, allows a higher-photo-catalytic degradation of the pollutants. However, some anatase powders containing small quantities of rutile present a better efficiency than those of pure anatase [7]. For example, titanium dioxide can be used in powder form (slurry) or immobilized in a thin film or coating form obtained by different deposition techniques (thermal spray, sol-gel, dip-coating, and physical or chemical vapor deposition, etc.) [8, 9].

Among coating procedures, thermal spray is characterized as a flexible and efficient process which has been widely used to deposit both metallic and non-metallic coatings. The thermal spraying process has many advantages, including its low cost, formation of thicker coatings quickly, a wide selection of materials and a process that is much simpler than other coating processes [10]. Thus thermal spraying is considered to be the optimal method for producing TiO$_2$ coatings in most industrial applications [11]. During thermal spraying, powders are heated and accelerated and then projected on to a substrate, followed by flattening, rapid cooling and a solidification process, which results in a typical quenched microstructure. Thermal spray processing is a commercially relevant, proven technique for processing nano-structured coatings [12, 13]. Thermal spray techniques are effective because agglomerated nano-crystalline powders are melted, accelerated and impacted against a substrate, and quenched very rapidly in a single step. This rapid melting and solidification promotes the retention of the nano-crystalline phase and produces a uniform amorphous structure. Retention of the nano-crystalline structure leads to enhanced wear behavior, greater hardness, and sometimes a reduced coefficient of friction compared to conventional coatings [12, 13].

The investigation on TiO_2 coatings deposited through conventional flame spraying and plasma spraying showed that the coatings consisted mainly of the rutile phase with only a low fraction of anatase phase, despite the crystalline structure of the initial powders. The anatase content in the coatings was around 10 to 15% deposited with the spray powder at a well-melted condition regardless of the spray powders original crystalline structure [14, 15]. Toma et al. [16] have reported that the coating with 12.6% by volume anatase content could be deposited through a gas fuel high velocity oxy-fuel (HVOF) spray when TiO_2 powder in the anatase phase was used as feedstock. Yang et al. [17] have reported an anatase content of 35% by volume and 55% by volume was achieved in the gas fuel HVOF coating deposited with rutile and anatase powder. In this research, the coatings were deposited through a liquid fuel high velocity oxy-fuel spray with different fuel and oxygen flow ratio using TiO_2 nano-powders containing anatase and rutile as feedstock. The influence of the fuel and oxygen flow ratio on anatase content ratio, crystal size, morphology of the coating, surface chemical state and surface feature were investigated accordingly.

II.   MATERIALS AND EXPERIMENTAL ASSESSMENT

Materials: P25/20 TiO_2 nanopowders were used as the feedstock for coating deposition. The powder used in this research was a commercially agglomerated and granulated nano-powders with an average agglomerated size of 20 μm, containing both anatase and rutile phases. 5×50×50 mm stainless steel plate was employed as a substrate for the coating deposition. Prior to the spraying process, the substrate was blasted with silicon carbide grit in order to increase the adhesive strength of the coating to the substrate.

Coating Deposition : The Met Jet III High velocity oxy-fuel (HVOF) gun was used to spray coatings at a stand-off distance of 336 mm. Kerosene was used as a liquid fuel. The powder feed rate was fixed at 8 g/min and the powder was carried to the HVOF flame by N_2 at a flow rate of 4 l/min, through a nozzle diameter of 11 mm. During the spraying, the flow of fuel and oxygen was altered incrementally to control the heating condition of the spray powders and thus provide a measure of the heating effectiveness of the fuel/oxygen ratio. Table I summarized the spray condition of the coatings.

Characterization :

X-Ray Diffraction: X-rays diffraction (performed with a Philips PW3710 diffractometer) using Cu Ka radiation was employed to determine the anatase-to-rutile ratio in the feedstock powder and HVOF sprayed coatings. Scan step was 0.02°/sec with a step time of 0.5sec in the   20 –70° 2θ range. The volume percentage of anatase was determined according to the following relation [18]:

$$A = \frac{1}{1+1.265\frac{IR}{IA}} \times 100 \quad (1)$$

Where IA and IR are the X-ray intensities of the anatase (101) and the rutile (110) peaks, respectively. The crystallite size was evaluated from the X-ray diffraction patterns based on the Scherrer formula as shown in the following equation [18]:

$$t = \frac{0.9\lambda}{B\cos\theta} \quad (2)$$

With B = corrected peak width at half maximum intensity, λ = X-ray wavelength and   θ = Bragg diffraction angle.

Scanning and Transmission Electron Microscopy: The morphology of the feedstock powder and the microstructures of the coatings were examined using S360 Cambridge scanning electron microscope (SEM). TEM images were obtained using the LEO 912 transmission electron microscope that employed a tungsten electron gun in the voltage range of 120 kV with an optical point-to-point resolution of   1 nm. Samples were gently scraped from the substrate and examined by TEM.

FT-IR & X-Ray Photoelectron Spectroscopy : Infra-red spectra were recorded with a Fourier transform infra-red spectrometer (BRUKER, VECTOR33). Samples (gently scraped from the substrate) were carefully ground and diluted in non-absorbent KBr matrices (2-5 % by weight). All FT-IR spectra are shown in transmission units and obtained under atmospheric conditions. The chemical composition and valence state of the elements were carried out by X-ray photoelectron spectroscopy (VG Microtech, XR3E2) with an aluminum anode energy source at Ka = 1486.6 V. The pressure in the analysis chamber of the spectrometer was 10^{-9} mbar during acquisition. Binding energies were referenced to C1s (carbon contamination) at 285 eV.

III. RESULTS AND DISCUSSION

Coatings crystalline structure : The crystalline structure of the elaborated HVOF-coatings was studied by XRD analysis. Fig 1 shows the XRD patterns of feedstock powder and coatings. It appears that the passage of the nano-particles in the flame involves a modification of their chemical state compared to the initial nano-powders, and which depends on the condition of the HVOF processes. The Fe peak is due to the effect from the iron in the SS substrate. Fig 2 shows the anatase content ratio of coatings. The C1 and C2 coatings, (obtained by 120 and 160 ml/min fuel flow rate and 800 l/min oxygen flow rate), contain anatase phases, with a ratio of about 80% by volume and 78% by volume respectively, which is more than the original feedstock powder content of 75% by volume. In contrast, the C3 and C4 deposited coatings, (with 120 and 160 ml/min fuel flow rate and 600 l/min oxygen flow rate), the ratio of anatase reached 36% by volume and 60% by volume respectively. It is clear that different fuel and oxygen flow rates cause different anatase-to-rutile phase transformation. As the fuel flow rate into the gun increases whilst the oxygen flow rate remains constant, the anatase content decreases, which cause a more significant explosion, result in higher torch temperatures. This higher explosion causes the torch velocity to increase due to the constant nozzle diameter, so by increasing fuel flow ratio, both the temperature and torch velocity has increased [19]. Higher fuel flow rate has thus resulted in higher velocities and temperatures and has also affected the anatase-rutile transformation and the retained anatase in the coating. By increasing the fuel flow rate, the gas velocity at the exit of the nozzle changed very little compared to the change in the gas temperature, [20] which (a) created more semi-molten particles, and (b) caused a lower solidification rate of particle droplet on the substrate, which consequently increased the rutile phase content in the coating. It is reported that rather than a constant fuel-to-oxygen ratio, the heat and velocity produced in the gas stream changes as the fuel and oxygen flow rate is varied, so that the results of coating with 800 and 600 l/min oxygen flow rates are significantly different.

Average anatase and rutile crystallite size of C1 to C4 coatings are shown in Fig. 3. In the C1, C2, C3 and C4 coatings, the anatase crystallite size reached 20.7, 25.9, 20.7 and 25.9 respectively from 25.9 nm of feedstock powder, in other words no change in C2 & C4 coatings while the rutile crystallite size reached 17.3, 17.3, 52.1 and 34.6 nm respectively from 41.7 nm feedstock powders. It is clear that different fuel and oxygen flow rates causes different changes in the crystallite size, and different changes in anatase and rutile crystallite size. The rutile crystallite size changed more than the anatase crystallite size. It is believed that in the thermal spray process, the formation of rutile is due to the molten particle and its slower solidification rate, while the formation of anatase is due to the anatase remaining in the primary particles, but also due to the rapid solidification rate of the molten particle on the substrate [21].Thus by changing the degree of melting of the particles in flight and also their solidification rate by changing the fuel and oxygen flow rate, changes in the anatase and rutile crystallite size can be obtained. With the higher fuel flow rate, there is a higher jet stream temperature and a higher degree of melting, so that the rutile crystallite size that forms from the molten droplets is also changed.

Coatings morphology : The SEM images of the surface and cross section microstructure of the C3 and C4 coatings can be observed in Fig.4 and Fig.5. The microscopic analysis showed that the morphologies of the sprayed coatings depend on the different coating conditions. The TiO_2 deposits have low porosity and are characterized by a layered microstructure, which can be observed in most thermally sprayed deposits. The coatings are built-up by the semi-melted and melted nano-particles impacting on the substrate that flatten to form splats, which consecutively pile on top of the others. In the C3 and C4 coatings, the semi-melted particles increase with the increase in the fuel flow rate. In the HVOF process, the velocity of the torch and in-flight particles are too high (about 1200 m/sec) and the temperature of torch is too low (about 2400° C) respectively, since this high speed causes very little heat to flow to the in-flight particles, therefore the degree of melting of the particles becomes too low [19]. Consequently, more semi-molten (molten surface and non-molten cores) particles contain higher amounts of anatase than fully molten particles can contain. [22]. By increasing the fuel flow ratio, the heat induced to the particles is increased, which in turn causes the ratio of semi-molten particles to non molten particles on the substrate to be increased.Fig.6 presents the typical TEM morphologies of the sprayed C1 coating. The size of most grains in the C1 coating is less than 30 nm with the average grain size being about 20 nm, which coincides with the grain size in the as-sprayed coatings measured by XRD.

Result of FT-IR and XPS: The FT-IR spectra of the feedstock powder, C1 to C4 sprayed coatings are shown in Fig. 7. For powder and coatings, the peaks at 460, 620 and 910/cm in the range of 400–1000/cm are contributions from the anatase TiO_2 [23, 24], which are also consistent with the observation from the XRD. Also it is believed that the broad peaks at 3400 and 1638/cm correspond to the surface-adsorbed water and hydroxyl groups [23,24]. The decrease in the intensities of these peaks in the FT-IR spectra of the C4 and C3 with larger anatase/rutile crystalline size was noted. Probably this was due to the decrease of specific surface areas which

caused the reduction of the adsorbed water. XPS analysis was mainly studied to evaluate the valence state of the titanium and the evolution of hydroxyl group on the TiO_2 surface [24]. Fig. 8(a) and (b) provides XPS spectra of the C1 coating, its titanium Ti2p and oxygen O1s and the results for O1s and Ti2p peaks. Six peaks of Ti2p1/2, Ti2p3/2, O1s, N1s, Fe2p3 and C1s were seen for the C1 coating. C1s peak at 284.6eV were organic polluted carbon used for calibration. The Fe peak is due to the substrate. Spectral data are summarized in Table II. For the TiO_2 sprayed coatings, the Ti2p peaks were identified at 458.5 and 463.9eV for Ti2p3/2 and Ti2p1/2 respectively, corresponding to Ti^{4+}; no reduction in the valence state of titanium was observed in the coating. The O1s spectrum displayed peaks at 529.5eV associated with $Ti-O^{(1)}$ bonds in TiO_2 (see Fig. 9), and at 530.3eV that corresponded to the hydroxyl ($Ti-O^{(2)}H$), and at 532eV related to chemisorbed water ($Ti-O^{(3)}H2$) [25, 26] as can be observed in the XPS spectra in Fig. 8(b). From results on O1s spectra in Table II, the amount of hydroxyl groups and water on the surface of the C1 coating was calculated, the ratio O/Ti was near the stoichiometric limit in the coating. Moreover, hydroxyl groups have a beneficial role in the photo-catalytic applications. It appears that the degradation of the pollutant was realized by the intermediate hydroxyl radicals formed by the reaction of the photo-generated holes with the hydroxyl groups or water chemisorbed on the surface. Indeed, a higher hydroxylation of the surface seemed to enhance the photo-catalytic activity of the TiO_2 [24]. Thus, the C1 coating presented an all-favorable surface characteristic to favor an increasing photo-catalytic behavior.

IV. CONCLUSION

Titanium dioxide coatings were established by high velocity oxy-fuel spraying using kerosene fuel with Degussa P25/20 nano-powder as material feedstock. The microstructure, surface feature, crystal structure and surface chemical state of the samples were carefully analyzed, and from this analysis it clearly indicates that these features are strongly depended on the spray conditions. Phase composition changed from anatase in the powder to rutile in the as-sprayed coatings. A significant phase transformation from anatase to rutile occurred when the coatings were obtained by the higher fuel/flow ratio in the spray. The anatase phase was preserved in the coatings resulting from a lower fuel/flow ratio. Anatase and rutile crystallite size in the feedstock powder changed in the sprayed coatings. The change in the rutile crystallite size was greater than that of the anatase. The microstructure of the coatings was found to be dependent on fuel and oxygen flow ratios. In the higher fuel flow ratios, the melted zone is greater. It seems that the anatase content, anatase/rutile crystallite size and the microstructure are closely related to the flow rate of the fuel and oxygen. It is noted that the chemical composition of the coating is TiO_2, with correct stochiometry. The results showed that the surface of the coatings have adsorbed water and hydroxyl groups. It seems that the surface-adsorbed water and hydroxyl groups of coatings are dependent on the anatase/rutile crystallite size, since in the larger crystallite size they were reduced. It was found that the coating obtained under the lowest fuel/flow ratio with 800 l/min oxygen flow rate (C1), had the highest anatase content ratio (80%), the smallest crystallite size and showed the highest surface-water absorbed and hydroxyl groups that is important for its photo-catalytic function.

REFERENCES

[1]   Park IS, Choi SY, Ha JS .High-performance titanium dioxide photocatalyst on ordered mesoporous carbon support. Chem. Phys. Letters 2008; 456:198-201.

[2]   Demeestere K, Dewulf J, Witte BD, Beeldens A, Langenhove HV.Heterogeneous photocatalytic removal of toluene from air on building materials enriched with TiO_2. Building and Envi 2008; 43: 406-414.

[3]   Ma YS, Chang CN, Chiang YP, Sung HF, Chao AC. Photocatalytic degradation of lignin using Pt/TiO_2 as the catalyst. Chemosphere 2008; 71: 998-1004.

[4]   Yasomanee JP, Bandara J. Multi-electron storage of photoenergy using Cu_2O-TiO_2 thin film photocatalyst. Solar Energy Materials & Solar Cells 2008; 92:348-352.

[5]   Jensen H, Joensen KD, Jŕgensen JE, Pedersen JS, Sŕgaard Egg. Characterization of nanosized partly crystalline photocatalysts. J. Nanoparticle Research 2004;6:519-526.

[6]   Apátiga LM, Rubio E, Rivera E, Castaño VM. Surface morphology of nanostructured anatase thin films prepared by pulsed liquid injection MOCVD. Surf. Coat. Technol. 2006; 201: 4136-4138.

[7]   Iizuka Y, Kubo T, Nakahira A, Onodera D, Ozawa N, Yao T. Development of environmentally friendly photocatalyst with nano-size pore structure coated with thin Ti-oxide. Appl. Catalysis B: Envi. 2007; 76: 51–56.

[8]   Teoh WY, Amal R, Ma¨dler L, Pratsinis SE. Flame sprayed visible light-active $Fe-TiO_2$ for photomineralisation of oxalic acid. Catalysis Today 2007; 120:203-213.

[9]   Piera E, Ayllón JA, Doménech X, Peral J. TiO_2 deactivation during gas-phase photocatalytic oxidation of ethanol. Catalysis Today 2002; 76: 259-270.

[10]   Lima RS, Marple BR. Enhanced ductility in thermally sprayed titania coating synthesized using a nanostructured feedstock. Mater. Sci. Eng. A 2005; 395:269-280.

[11]   Berger-Kellera N, Bertrand G, Filiatre C, Meunierc C, Coddeta C. Microstructure of plasma-sprayed titania coatings deposited from spray dried Powder. Surf. Coat. Technol. 2003; 168: 281-290.

[12]   Ajayan PM, Schadler LS, Braun PV. Nanocomposite Science and Technology. Wiley; 2003.

[13]   Koch CC. Nanostructured Materials Processing, Properties and Potential Applications. New York; William Andrew Publishing Norwich: 2002.

[14]   Chwa SO, Klein D, Toma F L, Bertrand G, Liao H, Coddet C, Ohmori A. Microstructure and mechanical properties of plasma sprayed nanostructured TiO$_2$–Al composite coatings. Surf. Coat. Technol. 2005; 194:215- 224.

[15]   Kanazawa T, Ohmori A. Behavior of TiO$_2$ coating formation on PET plate by plasma spraying and evaluation of coating's photocatalytic activity. Surf. Coat. Technol. 2005; 197:45-50.

[16]   Toma FL, Bertrand G, Chwa SO, Klein D, Liao H, Meunier C, Coddet C. Microstructure and photocatalytic properties of nanostructured TiO$_2$ and TiO$_2$–Al coatings elaborated by HVOF spraying for the nitrogen oxides removal. Mater. Sci. Eng. A 2006; 417:56-62.

[17]   Yang G, Li C, Wang Y, Li C. Dominant microstructural feature over photocatalytic activity of high velocity oxy-fuel sprayed TiO$_2$ coating. Surf. Coat. Technol. 2007; 202: 63-68.

[18]   Spurr RA, Myers H. Quantitative Analysis of Anatase-Rutile Mixtures with an X-Ray Diffractometer. Anal. Chem. 1957; 29: 760-762.

[19]   Yanga GJ, Lia CJ, Hana F,Ohmori A. Microstructure and photocatalytic performance of high velocity oxy-fuel sprayed TiO$_2$ coatings. Thin Solid Films 2004; 466: 81- 85.

[20]   Li M, Christodes P D. Modeling and analysis of HVOF thermal spray process accounting for powder size distribution. Chem. Eng. Sci. 2003; 58: 849 - 857.

[21]   Yi Z, Wei W, Lee S, Jianhua G. Photocatalytic performance of plasma sprayed Pt-modified TiO$_2$ coatings under visible light irradiation. Catal. Commu. 2007; 8: 906-912.

[22]   Gaona M, Lima RS, Marple BR. Influence of particle temperature and velocity on the microstructure and mechanical behavior of high velocity oxy-fuel (HVOF)-sprayed nanostructured titania coatings. J. Mate. Processing Technol. 2008; 198: 426-435.

[23]   Xiaoa J, Penga T, Lia R, Penga Z, Yan C. Preparation, phase transformation and photocatalytic activities of cerium-doped mesoporous titania nanoparticles. J. Solid State Chem. 2006; 179:1161-1170.

[24]   Toma FL, Bertrand G, Begin S, Meunie C, Barres O, Klein D, Coddet C. Microstructure and environmental functionalities of TiO$_2$-supported photocatalysts obtained by suspension plasma spraying. Appl. Catal. B: Envi. 2006; 68:74-84.

[25]   Tai WP, Oh JHl Fabrication and humidity sensing properties of nanostructured TiO$_2$-SnO thin film. Sensores & Actuators B 2002; 85:152-157.

[26]   Backman U, Auvinen A, Jokiniemi JK. Deposition of nanostructured titania films by particle-assisted MOCVD. Surf. Coat. Technol.2005; 192: 81-87.
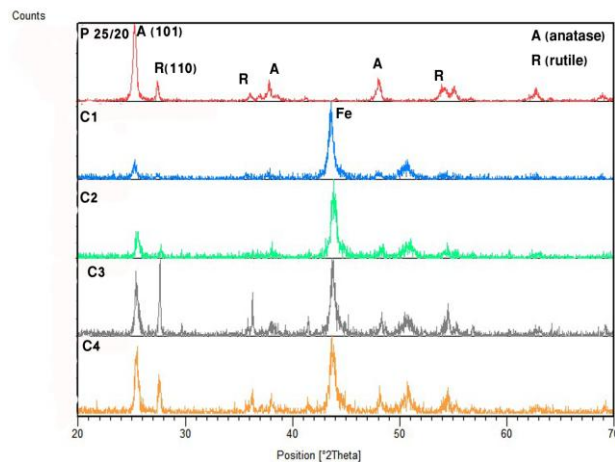
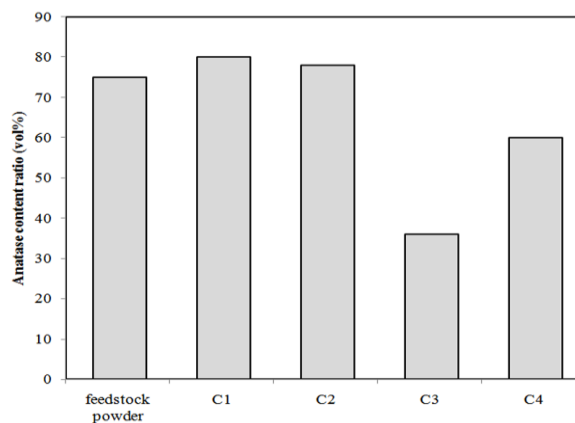Figure.1. XRD patterns of feedstock powder and TiO$_2$ sprayed coatings at different process parameters.

Figure.2. Anatase content ratio of TiO$_2$ sprayed coatings at different process parameters.
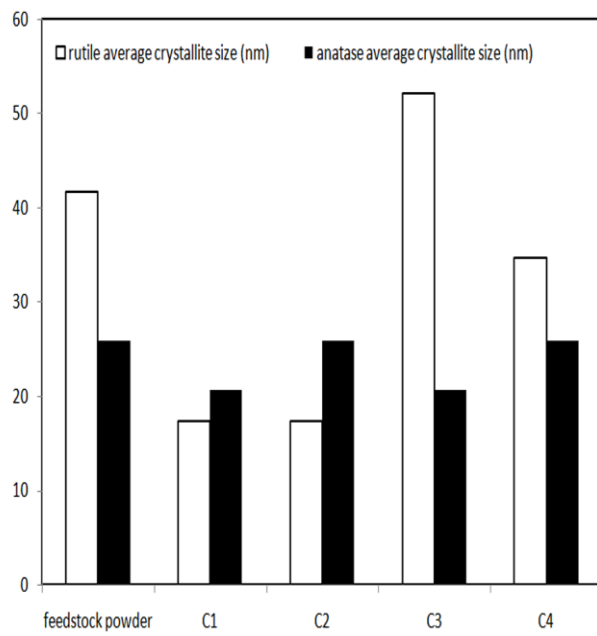
Figure.3. Rutile/anatase crystallite size of TiO_2 sprayed coatings at different process parameters.

Figure.4. SEM images of (a) surface and (b) cross section of C3 Coating (Fuel flow rate: 160 ml/min, Oxygen flow rate: 600 l/min).
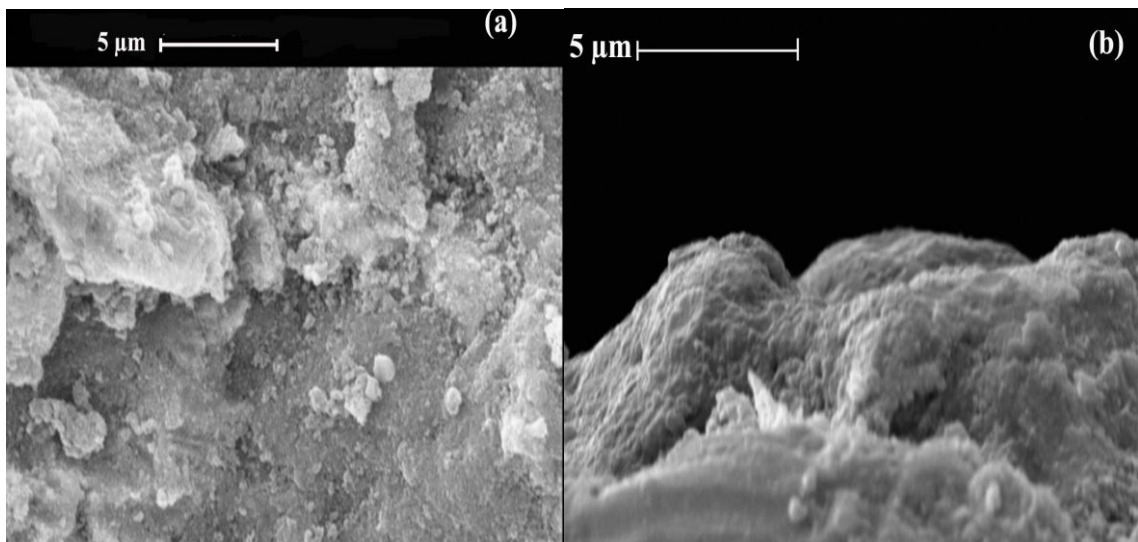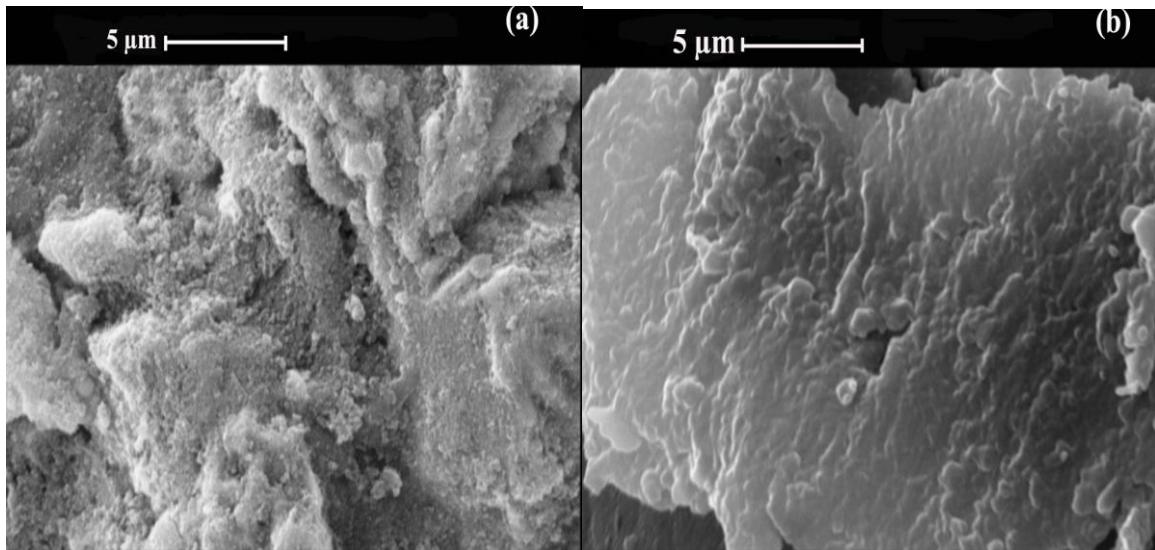
Figure.5. SEM images of (a) surface and (b) cross section of C4 Coating (Fuel flow rate: 120 ml/min, Oxygen flow rate: 600 l/min).
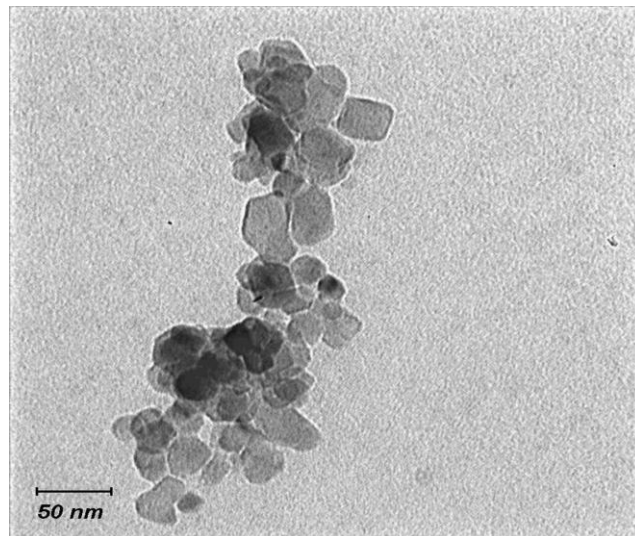
Figure.6. TEM image of C1 coating (Fuel flow rate: 120 ml/min, Oxygen flow rate: 800 l/min).
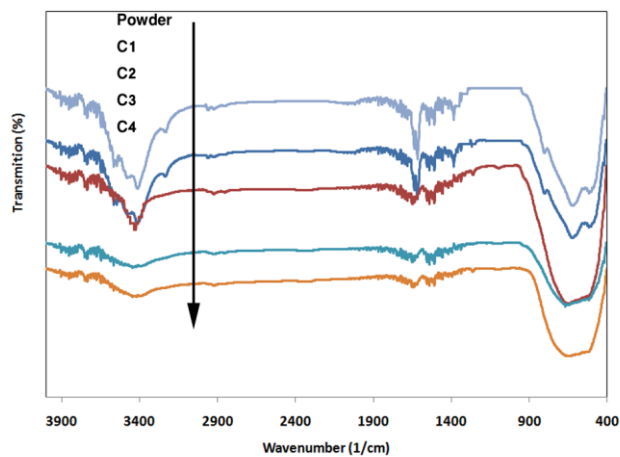
Figure7. FT-IR patterns of feedstock powder and TiO_2 sprayed coatings at different process parameters.
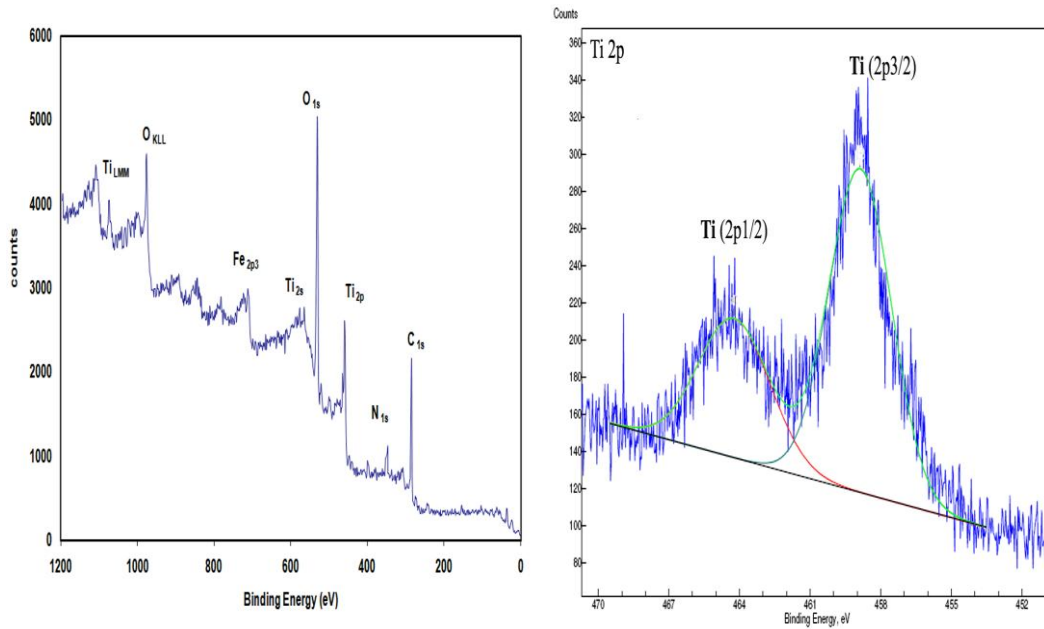
Figure.8. (a) XPS spectra of C1 coating, (b)Ti2p and O1s XPS spectra of C1 coating (Fuel flow rate:120 ml/min, Oxygen flow rate:800 l/min).
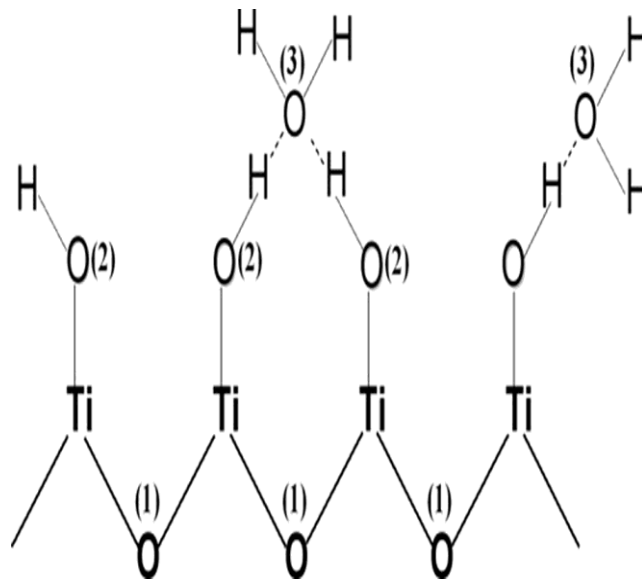
Figure.9. Schematic representation of the hydrated titanium dioxide surface.

Table I. Thermal spray parameters of TiO$_2$ coatings.

Samples	Fuel flow rate(ml/min)	Oxygen flow rate (l/min)
C1	120	800
C2	160	800
C3	160	600
C4	120	600

Table II. Binding energy values and oxygen species content for C1 sprayed coating (Fuel flow rate: 120 ml/min, Oxygen flow rate: 800 l/min).

C1 coating	Ti2p		O1s			$O^{(1)}/Ti \pm 0.2$
	Ti2p3/2	Ti2p1/2	Ti–$O^{(1)}$	Ti–$O^{(2)}$H	Ti–$O^{(3)}$H2	
Binding energy (eV)	458.5	464	529.5	530.8	532	2
Oxygen content (%) ($\pm$5)			71.1	18.5	10.4	

Research Paper   Open Access

Experimental Evaluation of Aerodynamics Characteristics of a Baseline Airfoil

[1,] Md. Rasedul Islam, [2,] Md. Amzad Hossain, [3,] Md. Nizam Uddin and [4,]Mohammad Mashud

[1,2,3,4,]*Department of Mechanical Engineering, Khulna University of Engineering & Technology (KUET), Bangladesh*

ABSTRACT : *A wind tunnel test of baseline airfoil NACA 0015 model was conducted in the Wind tunnel wall test section of the Department of Mechanical Engineering at KUET, Bangladesh . The primary goal of the test was to measure airfoil aerodynamic characteristics over a wide range of Angle of Attack (AOA) mainly from Zero degree to 20 degree AOA and with a wind tunnel fixed free stream velocity of 12m/s and at Re = 1.89×10^{5}. The pressure distribution in both upper and lower camber surface was calculated with the help of digital pressure manometer. After analysis the value of C_l and C_d was found around 1.3 and 0.31 respectively.*

KEYWORDS: *Base line airfoil NACA 0015, Wind tunnel test, Aerodynamic Characteristics, AOA, Reynolds Number*

I. INTRODUCTION

The cross-sectional shape obtained by the intersection of the wing with the perpendicular plane is called an airfoil. The camber, the shape of the mean camber line, and to a lesser extent, the thickness distribution of the airfoil essentially controls the lift and moment characteristics of the airfoil [1]. Symmetric airfoils are used in many applications including aircraft vertical stabilizers, submarine fins, rotary and some fixed wings [2][3]. Here in this paper the chosen airfoil was tested to find the reliability of aerodynamics characteristics and to understand the nature of difficulties arises in a newly setup wind tunnel [4][5]. This evaluation of aerodynamic properties is measured and recorded so that future research work on active flow separation control especially by CFJ method will be convenient and comparable to each other but it's not our concern now [6]. The Chosen Aerofoil NACA 0015 model has chord length of 30 cm and span of 50 cm and pressure were measured at 31 point along chord length in each camber surface by digital pressure manometer with a free stream of velocity 12m/s. Once getting pressure distribution, all other propertied like Coefficient of pressure C_p, lift Coefficient C_l, Drag coefficient C_d, Drag Polar, C_l/C_d were also calculated.

II. MODEL CONSTRUCTION AND METHODOLOGY

Designing NACA 0015 model by using surface profile equations.

For NACA 0015, Chord of the airfoil, c= 0.3 m

Maximum wing thickness, t= last two digit × % c=15×$\frac{1}{100}$×0.3 =0.04

Maximum camber, m= first digit × % c = $0 \times \frac{1}{100} \times 0 = 0$

Distance from leading edge to maximum wing thickness, p= second digit×10% c

$$= 0 \times \frac{10}{100} \times 0.3 \quad = 0$$

Maximum wing thickness, $y_t = t \times (1.4845\sqrt{x} - 0.6300\,x - 1.7580\,x^2 + 1.4215\,x^3 - 0.5075\,x^4)$

The mean chamber line,

$$y_c = \frac{m}{p^2}(2px - x^2) \quad \text{For } 0 < x < p$$

And, $\frac{dy_c}{dx} = \frac{2m}{p^2}(p - m)$

$$y_c = \frac{m}{(1-p)^2} [1 - 2p + 2px - x^2] \quad \text{For } p \leq x \leq c$$

$$\text{And, } \frac{dy_c}{dx} = \frac{2m}{(1-p)^2} (p - x)$$

Now, coding a C-program including above equation and the upper and lower surface equation and after compiling this program, a set of data were measured for the desired airfoil [7]. Plotting these data on any data plotting software gives the profile like below:

Fig.1: NACA 0015 airfoil profile   Fig.2: 3D Model view of Airfoil NACA 0015

After the construction, model were placed on an open loop Aerolab wind tunnel having test section geometry of 1m x 1m and has an operating speed from 0-40 m/s (0-145 miles per hour). This is made possible by a 10-horse power motor that drives a fan. After applying free stream velocity of 12 m/s, the value of pressure and hence the value of C_p also calculated at different AOA. AOA has changed manually by a clamp hooked assembly passing through the test wall section having a proper calibration of angle [8]. Following is the schematic view of total setup:
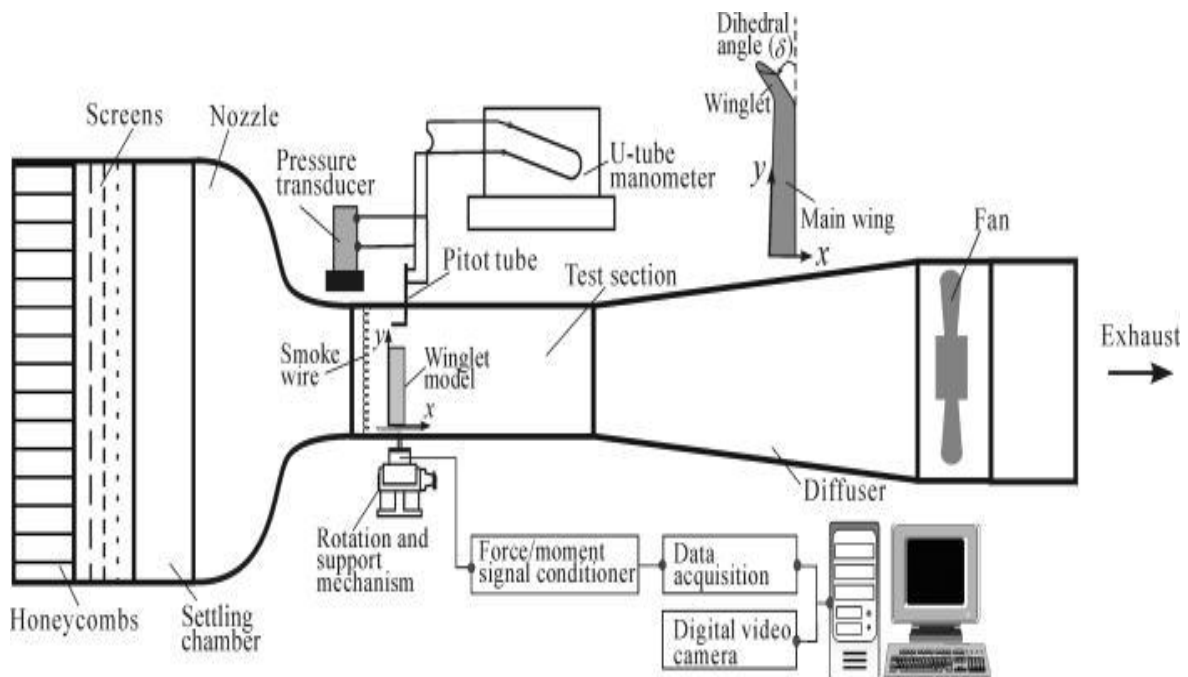
Fig.3: Schematic view of wind tunnel setup where test was conducted.

III.   Figures and Tables

At AOA = 05 deg., 12 deg., 20 deg; the following value of C_p was witnessed.
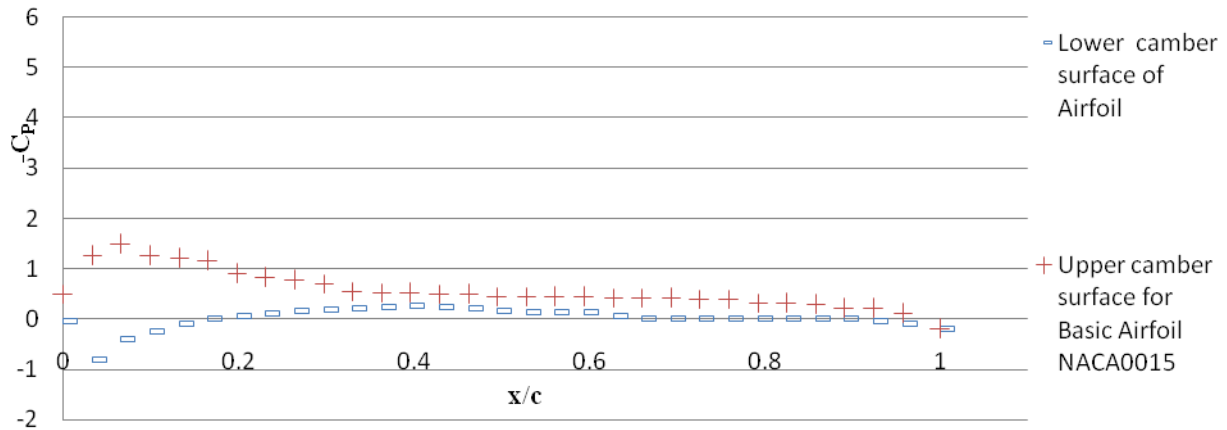
Fig.4: -C_p vs. x/c at AoA= 05 deg.

From Fig.4 we can see that the stagnation point is indeed on the underside of the wing very near the front at $\frac{x}{c} = 0.01$. There are no flat areas of C_p which indicates that there is no boundary layer separation. The pressure distribution shows a smooth variation in both upper camber surface and lower camber surface. The maximum value of -C_p in Baseline Airfoil are 1.5 and 0.25 at upper camber surface and lower camber surface respectively.
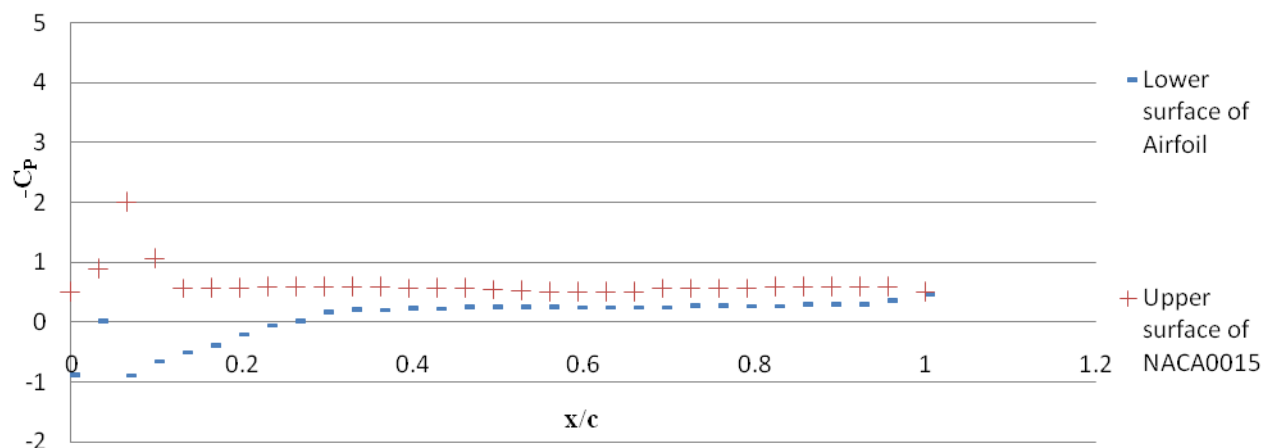
Fig.5: -C_p vs. x/c at AoA= 12 deg.

From Fig.5 we can see that the stagnation point is indeed on the underside of the wing very near the front at $\frac{x}{c} = 0.022$. There are no flat areas of C_p which indicates that there is no boundary layer separation. The maximum value of -C_p in Baseline Airfoil are 2.0 and 0.20 at upper camber surface and lower camber surface

respectively. Since the value of pressure coefficient is increased this indicates that with further increase in AOA, the pressure in upper camber surface will be detached from the wall hence will offer boundary layer separation.
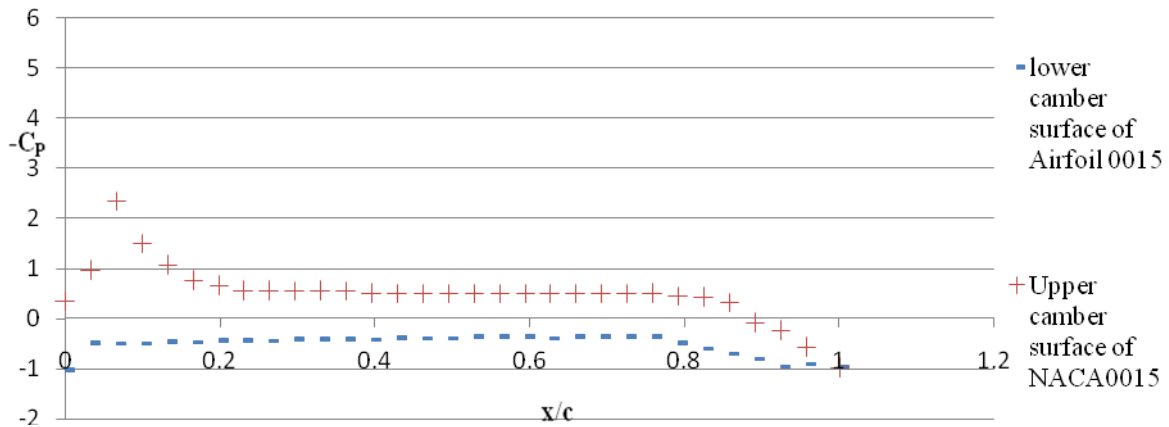
Fig.6: $-C_p$ vs. x/c at AoA= 20 deg.

From Fig.6 it seems that the value of Cp is smooth but at this stage boundary layer separation is occurred and the value of drag coefficient is increased with a plunged in lift coefficient.

The following table shows the value of C_l, C_d and C_l/C_d at different Angle of Attack (AOA) :

Angle of Attack(AOA)	C_l	C_d	C_l/C_d
0	0.01	0.01	1
5	0.6	0.02	30
10	1.3	0.08	16.25
12	1	0.105	9.52
20	0.9	0.25	3.6
25	0.85	0.31	2.74

Table 1: values of C_l, C_d and C_l/C_d at different Angle of Attack (AOA) of an airfoil NACA 0015.

The profile of C_l Vs. AOA is given below:
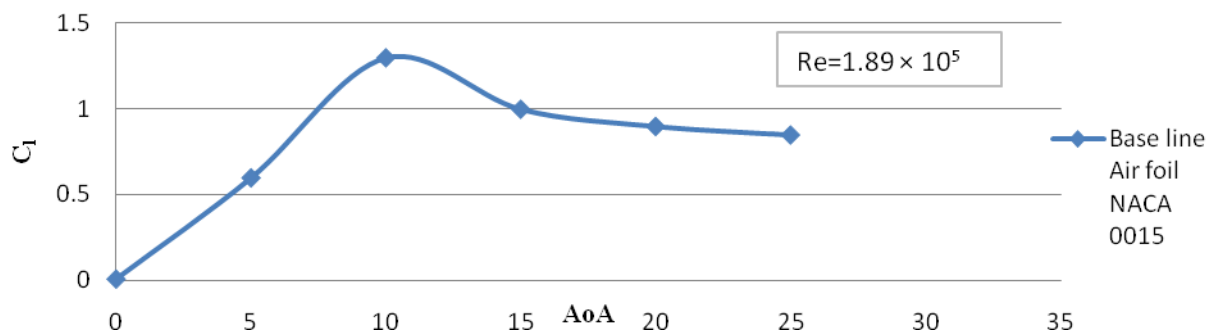
Fig.7: C_l Vs. AOA

From Fig.7 It is clear that $C_{l)max}$ = 1.3 at AOA = 10 deg.

The profile of C_d Vs. AOA is given below:
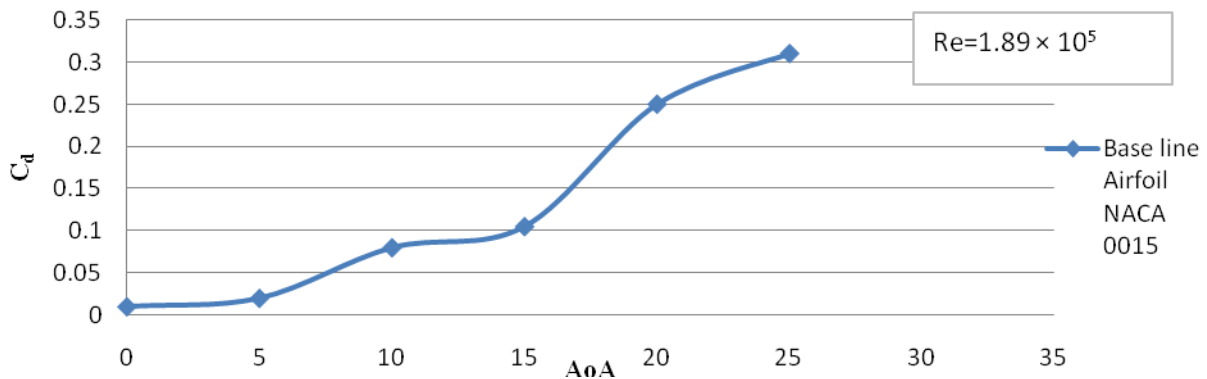
Fig.8: C_d vs. AOA

From Fig.8 It is clear that the value of C_d is increased as the AOA is increased.

The profile of C_l/C_d vs. AOA is given below:
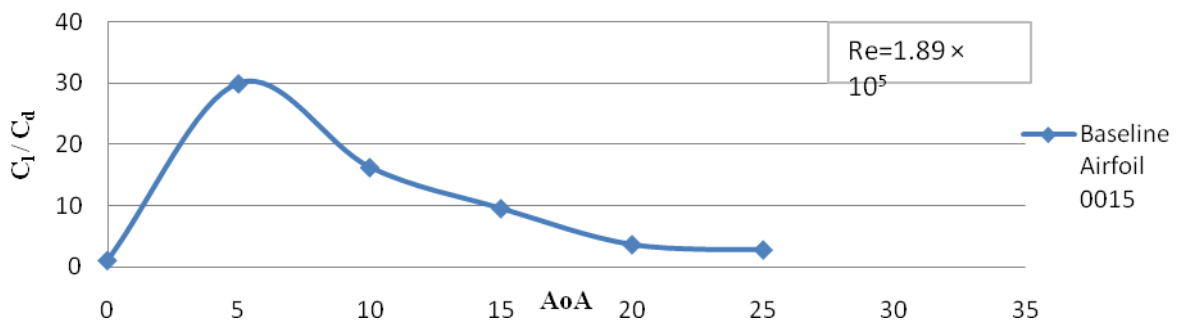
Fig.9: C_l/C_d vs. AOA

From Fig.9 It is clear that the maximum value of C_l/C_d is 30 and is gradually decreased as the value of AOA is increased.

The smoke flow visualization technique is used to observe the flow separation at different AOA. After 12 degree Angle of Attack the snap short of flow visualization is given below:

Fig 10: snap short of smoke flow visualization after 12 degree AOA.

IV. CONCLUSION

The NACA 0015 airfoil was analyzed for the lift, drag and moment coefficients as planned. From this subsonic wind tunnel test of an Airfoil NACA 0015 it is found that the boundary layer separation is occurred in between 15-20degree AOA and the maximum value of C_l is 1.3 at AOA = 10 deg. and $C_{d)\ max} = 0.31$ at AOA = 25 deg. And this value of C_d is increased gradually with the increase in AOA. The optimum AOA of this NACA 0015 Airfoil is found to be around 12 deg. It is clear from this paper that boundary layer separation is not controlled or delayed as well as aerodynamic characteristics in not easy to enhance with this type of conventional way. With some modification, techniques like Active flow separation should be applied in future work to enhance the aerodynamic characteristics.

V. Acknowledgements

REFERENCES

[1] W. L. I. Sellers, B. A. Singer, and L. D. Leavitt, "Aerodynamics for Revolutionary Air Vehicles." AIAA 2004-3785, June 2003.
[2] Haritonidis, J. H., "Wind Tunnels". Aerospace Engineering, The Ohio State University, Columbus, 2008.
[3] Miller, S. D., "Wind Tunnels". Aerospace Engineering, The Ohio State University, Columbus, 2008.
[4] Haritonidis, J. H., "Lift, Drag and Moment of a NACA 0015 Airfoil". Aerospace Engineering, The Ohio State University, Columbus, 2008.
[5] Gilat, Amos, and Vish Subramaniam. Numerical Methods for Engineers and Scientists: An Introduction with Applications Using MATLAB. Hobeken, NJ: John Wiley & Sons, Inc., 2008.
[6] Anderson, John D., Jr. Fundamentals of Aerodynamics. Fourth Edition. Boston: McGraw-Hill, 2007.
[7] A.Jameson,L.Martinelli,and N. A.Pierce. Optimum aerodynamic design using the Navier –Stokes equation. Theorical and Computational Fluid Dynamics, 10: 213–237, 1998.
[8] A.Seifert,A.Darabi,and I. Wygnanski. Delay of airfoil stall by periodic excitation. AIAA Journal, 33(4):691–707, July 1996.

| Research Paper | Open Access |

Production and Comparartive Study of Pellets from Maize Cobs and Groundnut Shell as Fuels for Domestic Use.

[1]Kyauta E. E., [1]Adisa A.B., [1]Abdulkadir L.N. and [2]Balogun S.,
[1]*Mechanical Engineering Department, Abubakar Tafawa Balewa University, Bauchi.*
[2]*Mechanical Engineering Technology Department. Federal Polytechnic, Bauchi*

ABSTRACT : *The economic development of any nation is unavoidably a prerequisite of the amount of energy available for its consumption. The need to develop alternative energy sources for fossil fuel is clear due to its scarcity, persistent increase in price and non renewability. The development of energy from biomass is one area among the various energy alternatives that has considerable promise and is receiving attention. This paper handles the production and comparative study of solid fuels from agricultural waste (i.e. maize cobs and groundnut shell) that can serve as alternative energy sources for domestic use, using the densification process. The material were grounded and sieved to particle sizes of 0.425mm and below and was compressed into pellets of 12.5mm diameter and 13mm length at a minimum pressure of 275 bars. The characteristics of the pellets determined were moisture content, ash content, combustion rate and calorific value. The result showed that groundnut shell pellets attained a higher temperature than maize cobs. The temperatures attained by 100g of each type of fuel were 756^0C and 600^0C for ground nut and maize cob pellets respectively. The result of the net calorific value test for maize cob was found to be 13.8MJ/kg while that of groundnut shell pellets was 13.9MJ/kg. These results showed that the pellets are capable of generating heat that is sufficient for domestic use if appropriate appliances are used.*

KEYWORDS: *solid fuels, agricultural waste, groundnut shell pellet, maize cobs pellet, combustion rate, calorific value.*

I.   INTRODUCTION

A fuel is a collection of elements, which will readily combine with oxygen (combustion) and release thermal energy continuously in sufficient quantity for practical use. When a fuel is burnt chemical changes take place, which are all accompanied by the release of energy in the form of heat and light [1]. The patterns of consumption of these fuels have varied over the years as relative prices have also changed. For example oil has changed from being one of the cheapest forms of fuel to being almost the most expensive [2].Since increased energy consumption is an unavoidable prerequisite of future economic development, the need to develop alternative energy sources is clear.

The development of energy from Biomass is one area among the various energy alternatives that has considerable promise and is receiving attention. Biomass is a non- conventional and renewable energy obtainable mainly from organic matter and plants residue. In Nigeria for instance, energy supply is mainly through the conventional fuels (oil, natural gas and coal) but due to scarcity and increase in fuel prices most people in the rural and urban areas are always forced to use wood [3].According to a survey report of Sokoto Energy Research Center (SERC: [4] fuel wood was found to be a predominant energy source in the household with about 70-80% households depending on it as their cooking fuel in both remote villages and towns. A wide variety of techniques are available to utilize biomass resources, but the most efficient have been to burn them directly for heat. But this approach has a limitation because demand for energy is often remote from biomass production area. Hence to reduce transportation problem and to increase the versatility of biomass energy, it is often desirable to convert biomass to a variety of more convenient fuel forms. The crop residues that are commonly used as sources of energy includes rice husks, sugar cane fiber, groundnut shells, maize cobs, coconut husks and palm oil fiber etc. The use of biomass as alternative sources of energy is attractive because it addresses both problems of waste disposal and fuel wood shortages. The extraction of useful energy from biomass could bring very significant social and economic benefits to both rural and urban areas.

Pellet fuels are clean and easy to handle and this makes them particularly suitable for domestic use. They can be used in specifically designed stoves. Using pellet fuels reduces dependence on finite fossil fuels like oil or gas and does not contribute to the green house effects, which causes global warming. The physical and chemical composition of groundnut shell and maize cobs is shown in Table 1.

Table 1: *Physical and Chemical Composition of Groundnut shells and Maize cobs*

Properties	Units	Groundnut shell	Maize(corn) Cob
Carbon	%	14.99	19.73
Hydrogen	%	16.42	15.56
Nitrogen	%	1.21	0.38
Oxygen	%	63.62	54.98
Sulfur	%	3.00	4.48
Moisture content	%	8.76	42.98
Ash content	%	0.76	4.85
Gross Calorific Value	MJ/kg	17428	19480
Net Calorific Value	MJ/kg	13785	16028

Source: [5]

Some of the methods adopted for conversions of biomass are: anaerobic digestion; direct combustion; pyrolisis; gasification; fermentation and densification technology. These methods function to process biomass conveniently into solid, liquid and gaseous fuels. The efficiency of the conversion process determines how much of the actual energy can be practically utilized. Densification as employed in this research is the process of compaction of biomass at a very high pressure using a die or mould to produce solid fuels (e.g. pellet, cubes, log and briquette) that can be easily stored transported and burned more efficiently. This process improves the calorific value of the fuel and also reduces the cost of transporting the residue [6]. Densification of biomass under high pressure brings about mechanical inter locking and increased adhesion between the particles, forming intermolecular bonds in the contact area. The binding mechanism under high pressure can be divided into adhesion and cohesion forces, attractive forces between solid particles and interlocking bonds [7].

Pelletizing is the process of producing pellets by compaction of Biomass at a very high pressure. These products have significantly smaller volumes than the original biomass and thus have a larger Volumetric Energy Density (VED) making them a more compact source of energy, easier to transport and store than natural biomass [13].

II.   MATERIALS AND METHODS

Materials collection : The groundnut shells were obtained in Yelwa-Kagadama whereas the maize cobs were collected at Federal Polytechnic Bauchi in Gwallameji, all in Bauchi Local Government area of Bauchi state.

Materials preparation : The groundnut shells and the maize cobs were pounded to reduce the sizeof the samples. It was later grounded into powder in a grinding mill. The powdered materials were sieved into different particle sizes ranging of 425µm and below.   The weights of samples retained on each screen were expressed as a percent of the total weight. The percent passing is the cumulative amount retained subtracted from 100 [9]. Plate A and B showed the sieved samples.
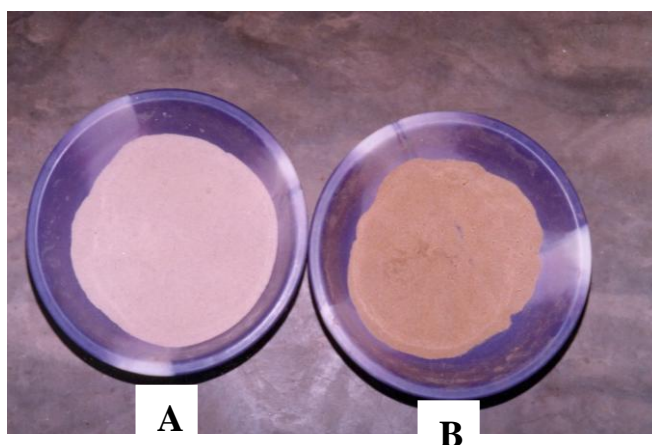
(A) Maize Cobs (B) Ground Groundnut Shell

Mould design : A metallic mould was designed to withstand compaction pressure and to enable uniformity of size, ensure easy flow and high efficiency of pellets. A metallic mould will permit repetition and can be efficiently used for mass production [10]. Mild steel was considered for the mould material due to its lower cost, availability and machinability.

Experimental Method :

Determination of moisture content: The samples were weighed and dried in an oven for four hours at $105^{\circ}C$ and then weighed again. The moisture content was determined on the wet basis using the equation below [10].

$$m_c = \frac{(m_2 - m_1) - (m_3 - m_1)}{(m_2 - m_1)} \times 100$$

Where

m_c =*moisture content*
m_1 = *wt of empty container*
m_2 = *wt of container + sample before drying*
m_3 = *wt of container + sample after drying.*

Determination of ash content: The samples were weighed and burnt in a furnace at $350^{0}C$ and left overnight in the furnace. The ash content was then determined on the dry basis as follows [12].

$$A_c = \frac{(m_a - m_1)}{(m_2 - m_1)} \times 100$$

Where A_c = Ash content
m_2 = wt of sample + container
m_a = wt of container + Ash.
m_1 = wt of container

Determination of calorific value: Samples calorific values were determined using a bomb calorimeter at the metallurgical Research and Development center Jos

**Determination of Combustion Rate:** 50g and 100g of the groundnut shell and maize cob pellet samples were each weighed in sample containers and burnt. The combustion was initiated by the addition of a little kerosene. The temperature of the burning samples was taken at intervals until it completely burnt. This test was conducted in a form of open fire under indoor conditions.

Fig. 1. Determination of Combustion Rate.

Water Boiling Test: 50g and 100g of pellets were used to boil two litres of water, the temperature and time taken for the water to boil was measured.

Rate of deterioration of pellets : This was achieved by storing the pellets at room temperature with a temperature range of between 29^oC to 33^oC, relative humidity between 80% - 90% for a period of six months.
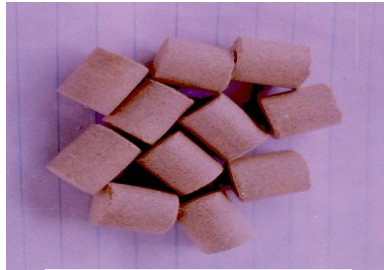
Groundnut shell pellet   **Maize cob pellet**

III.   RESULTS AND DISCUSSION

Nature of Pellets: Each of the groundnut shell pellets weighed approximately 2.3g while maize cobs pellets weighed 1.9g. The pellets can completely dissolve when it comes in contact with water as such it should be stored in polythene bags or in a dry place. The groundnut shell is seen to be a better material for pellet fuel than maize cobs. The sulfur and nitrogen content of the fuel varied between 1 - 3% (Table 2). This value falls below 5% hence will not cause problem to the environment. [11], this percentage is low and has also been shown to be harmless to humans by Pellet manufacturers [12].

Moisture Content : The moisture content was calculated on wet basis and the result of the test carried out are as shown in Table 2. The values of the test showed that the moisture content was within the pellet fuel quality and standard of between 5 – 10% as recommended by the Pellet Fuel Institute [13].

Ash Content : This result is as shown in Table 2, with a highest value of 17.9% for maize cobs and 10.2% for groundnut shells. These values are higher than that of wood pellets as reported by [14]. However, it shows that about 70 – 80% of the fuel can be burnt completely and will likely produce a substantial heat that is needed for domestic use.

Calorific Value : The results of this test is as shown in Table 2. A little difference in the energy content of the maize cob pellets and groundnut shell pellets was observed. This can be attributed to the constituents of the fuel and moisture content which were 13.06% and 11.48% for groundnut shell and maize cobs respectively. These calorific values are lower when compared to 16.7MJ/kg and 19.3MJ/kg for groundnut shell and maize cob respectively [16]. The moisture contents were found to be 3-10% for groundnut shells and 4.5% for maize cobs. These results obtained (maize cobs 13.8MJ/kg and groundnut shell 13.9MJ/kg) still showed a high energy content that can meet domestic needs such as cooking, water boiling and space heating.

Combustion Rate Test : It was observed that the pellets maintained their shape even in the ash form. Two set of tests were conducted (for 100g and 50g) and the results were then compared.

Figure 1 shows the combustion rate of 50g groundnut shell and maize cobs pellets respectively. The groundnut shell pellets attained a temperature of about 750 ^oC in less than 30 minutes and sustained a temperature above 100 ^oC for a period of about 40 minutes while maize cobs pellets attained a maximum temperature of 600^oC in less than 20 minutes and sustained a temperature of 100^oC for 50 minutes.
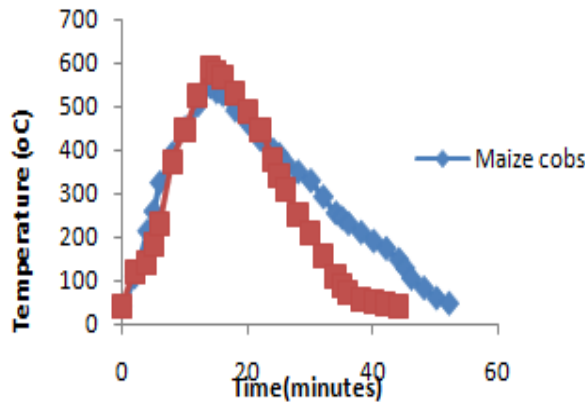
Fig 2: Combustion rates of 50g groundnut shell and maize cob pellets
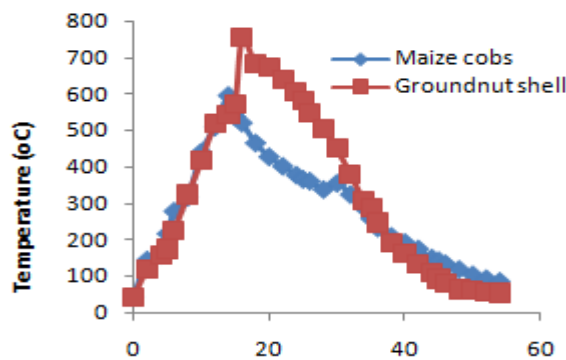
Fig 2: Combustion rates of 100g groundnut shell and maize cob pellets

Figure 3 shows the results for 100g of groundnut shell

Figure.2 shows the results of groundnut shells and maize cob pellets respectively. In these cases the groundnut shell generated a temperature of about 600 ^{o}C in less than 20 minutes which gradually reduces to about 100 ^{o}C after 35 minutes while maize cob pellets generated a temperature of 575 ^{o}C. This dropped gradually to about 100 ^{o}C in 40 minutes, and then settled at a room temperature of 45 ^{o}C. Figures 1 and 2 compare the combustion rates for 50g and 100g for groundnut shell and maize cob pellets. It can be seen that the groundnut shell pellets gave a higher temperature than the maize cob pellets.

Water Boiling Test : In the water boiling test, three different quantities of pellet fuel samples (50g and 100g) were used to raise the temperature of two liters of water. The recorded times are as shown in Table 3. This shows that as the quantity of fuel increases the amount of heat generated also increases and the shorter the time to bring the water to boil..The ground nut shell also show a higher energy value than maize cobs.

Table 2: Characteristics of Pellets Samples

Properties	Pellets Sample	%
Moisture content	Groundnut shell	5.8
	Maize cobs	3.6
Ash content	Groundnut shell	10.2
	Maize cobs	17.9
Gross Calorific value	Groundnut shell	15.31
	Maize cobs	15.55
Net Calorific Value	Groundnut shell	13.9
	Maize cobs	13.8
Nitrogen	Groundnut shell	1.66
	Maize cobs	2.21
	Groundnut shell	1.41
Sulphur	Maize cobs	2.23

Table 3: Water Boiling Test of Pellets

Sample	Time (min)	Temperature (^{0}C)
50g Groundnut shell Pellets	20	73
50g maize Cob Pellets	20	60
100g Groundnut shell pellets.	30	92
100g Maize cob Pellets.	30	84

IV.   CONCLUSION

A renewable energy source was developed by converting groundnut shell and maize cobs into solid pellet fuel without a binder. In addition to providing a source of energy this also contributes to the efforts of restoring environmental quality. The cost of disposing unwanted materials left over after processing groundnut and maize will be substantially reduced. A metallic mould was used to enable uniformity of size, ensure easy flow and high efficiency of pellets. The mould also permits repetition for mass production. Mild steel was considered for the mould material due to its lower cost, availability and machinability. The pellets have light weight (1- 2 g), fairly strong and can withstand compressive force of at least 800N, so they can be easily transported. The pellet needs to be stored in a dry environment particularly that of the maize cobs because their strength drops with moisture increase. This is because the rate of moisture absorption is higher in maize cobs than groundnut shells which reduce the adhesion and cohesion forces. The sulfur and nitrogen content of the fuel varied between 1 - 3% this percentage is low and has also been shown to be harmless to humans. With flame temperatures above 600 ^{o}C, it can be employed in cooking, water boiling and room heating if appropriate pellet devices are used. With calorific value of above 13 MJ/kg pellets can be employed in small-scale industries for example (baking, food processing etc). The rate of deterioration of the maize cobs pellets is higher than that of the groundnut shell pellets which suggests that groundnut shell is a better material for pellet production.

Recommendations : It has been established that pellet fuel can be produced from groundnut shells and maize cobs without the use of a binder. Nevertheless, kinetic analysis of the flame, complete chemical analysis of the pellets, design of a pellet machine and pellet stove are some areas that further research work can be carried out.

REFERENCE

[1]   Bell A.E. (1970) Mechanical Engineering Science. Cassel London pp. 216.
[2]   Fraiser A.I. (1986) The Use of Wood as Industrial and Domestic Energy in Rural Areas of Britain and The Transfer of Wood Energy Technology Developing Countries. International Forest Science Constancy. United Kingdom Pp259- 260.
[3]   Garba B. and Atiku A. (1997) Thermal Studies of Some Tropical Tress Species and Their Performance in Improved Wood Burning Stoves. Nigerian Journal of Renewable Energy Vol.5 No 13.Pp 16-30.
[4]   Sambo A.S. (2001) Renewable Energy Technology for National
        Development Status Prospects and Policy Development. Journal of the Nigerian Society of Engineers Vlo.30 No 1.9923-30
[5]   Jekayinfa S.O and Omisakin O.S (2005).The Potentials of Some Agricultural Waste as Local Fuel Materials in Nigeria. CIGR Journal, Vol. VII.
[6]   British Biogen (2003) Internet Address: http:www.britishbiogen.Co.Uk/Bioenergy/pellets.html
[7]   Grover P.D. and Mishra S.K. (1996) Biomass Briquetting Technology and Practice. Food and Agriculture Organization of the United Nations, Bangkok. Regional Wood Energy Development Program (RWEDP).
[8]   Nicholas P.C. and Tyler G.H. (1984) Handbook of Chemical Engineering Calculations.Mc. GrawwHill Book Company, pp 145.
[9]   9. Kumar D. and Jan S.K. and Barware B (1983) Material Science and Manufacturing Processes Viicas Publishing home. N York, Delhi pp. 205.
[10]   Kyari M.S. (2000) Production of Solid Fuel Briquettes from Corn cobs. Unpublished M.Sc. Abubakar Tafawa Balewa University pp. 23.
[11]   Jekayinfa S.O and Omisakin O.S (2005).The Potentials of Some Agricultural Waste as Local Fuel Materials in Nigeria. CIGR Journal, Vol. VII.
[12]   British Colombia Pellet Fuel Manufactures Association (no date) Internet Address http://www.pellets.org/about.html
[13]   Pellet Fuel Institute (2004) Internet Address http://www.pellets.heat.org/fuel/html.
[14]   Austrian Center for Renewable Energy (ACRE). No date Internet Address. http://acre.murdoch.edu,au/refiles/biomass/text.html
[15]   Obenbeger I. and Thek G. (2002) Physical Characterization and Chemical Composition of Densified Biomass Fuel With Regard to their Combustion Behavior. Proceedings of 1st World Conference on Pellets. Stockholm Sweden.
[16]   Food and Agricultural Organization FAO (2000) Environmental and Natural Working paper. The energy and Agricultural Nexus. Rome.

Enhancement of Aerodynamic Properties of an Airfoil by Co Flow Jet (CFJ) Flow

[1,]Md. Amzad Hossain , [2,]Md. Nizam Uddin , [3,]Md. Rasedul Islam and
[4,]Mohammad Mashud

[1,2,3,4,]*Department of Mechanical Engineering, Khulna University of Engineering & Technology (KUET),
Bangladesh*

ABSTRACT : *A wind tunnel test of baseline airfoil NACA 0015 and CFJ0015-065-065 model was conducted in the Wind tunnel wall test section of the Department of Mechanical Engineering at KUET, Bangladesh. The primary goal of the test was to investigate and compare the airfoil aerodynamic characteristics over a wide range of Angle of Attack (AOA) and with a wind tunnel free stream velocity of 12m/s , $Re = 1.89 \times 10^5$, $C_\mu = 0.07$ at $M = 0.030$ kg/s. The CFJ increases $C_{L\ max}$ by 82.5% and decreases Drag by 16.5% at Stall AOA when compared to the baseline air foil. The main goal is to proof that Flow separation is controlled and delayed with the use of CFJ Technique over an Airfoil.*

KEYWORDS- *wind tunnel test, Base line airfoil NACA 0015 and CFJ0015-065-065, Aerodynamic Characteristics, AOA, Reynolds Number, Flow separation control.*

I.   INTRODUCTION

Flow control is playing a more and more important role to improve aircraft aerodynamic Performance [1][2]. To enhance lift and suppress separation, various flow control techniques have been used including rotating cylinder at leading and trailing edge[3][4][2], circulation control using tangential blowing at leading edge and trailing edge[5][6] [7][8][9][10], multi-element airfoils[11][12],pulsed jet separation control[13][14][15], etc. The different flow control methods have their different features. This thesis paper applies the new flow control technique of the co-flow jet cascade to high lift airfoil since both experience severe adverse pressure gradient at high loading. Unlike the conventional circulation control airfoils, for which the jets are mostly implemented at leading and trailing edge, the co-flow jet (CFJ) airfoil is implemented on the majority area of the suction surface of the airfoil. The co-flow jet airfoil is to open a long slot on the airfoil suction surface from near leading edge to near trailing edge. A high energy jet is then injected near the leading edge tangentially and the same amount of mass flow is sucked away near the trailing edge. The turbulent shear layer between the main flow and the jet causes a strong turbulence diffusion and mixing, which enhance the lateral transport of energy and allow the main flow to overcome the severe adverse pressure gradient and stay attached at high angle of attack (AOA)[16][17][18]. An active Flow separation control technique such as CFJ technique has several advantages over conventional flow control techniques. Here The main objectives of this thesis paper is to investigate the performance of airfoil characteristics by co-flow jet (CFJ) flow control technique in order to reduce the Drag coefficient, increase the Lift coefficient, and control the Flow separation over air foil geometry.

II.   MODEL DESIGN AND MODEL CONSTRUCTION

Model overview:

Co-flow jet airfoil (CFJ) geometry is slightly different from the conventional airfoil. Firstly baseline airfoil NACA 0015 has the as usual conventional nomenclature which shown in Fig.1.But The co-flow jet airfoils are defined using the following convention: CFJ4dig-INJ-SUC, where 4dig is the same as NACA4 digit convention, INJ is replaced by the percentage of the injection slot size to the chord length and SUC is replaced by the percentage of the suction slot size to the chord length. For example, the CFJ0015-065-065 airfoil has an injection slot height of 6.5% of the chord and a suction slot height of 6.5 % of the chord. The suction surface shape is a downward translation of the portion of the original suction surface between the injection and suction

slot. The injection and suction slot are located at 6.72% and 88.72% of the chord from the leading edge [19]. The slot faces are normal to the suction surface to make the jet tangential to the main flow. The cambered airfoil and CFJ0015-065-065 airfoil are tested in the wind tunnel tests.

Base line Airfoil NACA 0015 model design and Construction:
         Designing NACA 0015 model by using surface profile equations.
     For NACA 0015, Chord of the airfoil, c= 0.3 m

Maximum wing thickness, t= last two digit $\times$ % c=15$\times\frac{1}{100}\times$0.3 =0.04

Maximum camber, m= first digit $\times$ % c = $0 \times \frac{1}{100} \times 0 = 0$

Distance from leading edge to maximum wing thickness, p= second digit$\times$10% c

$$= 0 \times \frac{10}{100} \times 0.3 \quad = 0$$

Maximum   wing   thickness,

$y_t = t \times (1.4845 \sqrt{x} - 0.6300\, x - 1.7580\, x^2 + 1.4215\, x^3 - 0.5075\, x^4)$

The mean chamber line,

$y_c = \frac{m}{p^2} (2px - x^2)$ For 0 < x < p

And, $\frac{dy_c}{dx} = \frac{2m}{p^2} (p - m)$

$y_c = \frac{m}{(1-p)^2} [1 - 2p + 2px - x^2]$ For p $\leq$ x $\leq$ c

And, $\frac{dy_c}{dx} = \frac{2m}{(1-p)^2} (p - x)$

Now, coding a C-program including above equation and the upper and lower surface equation and after compiling this program, a set of data were measured for the desired airfoil [7]. Plotting these data on any data plotting software gives the profile like below:

Fig.1: Airfoil nomenclature   Fig.2: NACA 0015 airfoil profile   Fig.3: 3D Model view of Airfoil NACA 0015
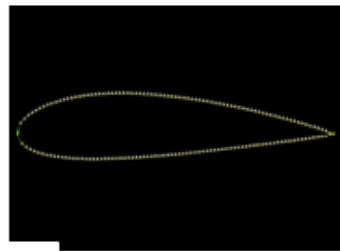
CFJ Airfoil design and Construction:

     The selected CFJ for performance investigation is CFJ 0015-065-065. That means it has suction and injection slot of length 6.5% of chord. The distance of the slot from the leading edge of the airfoil is taken as 6.72% of chord for injection slot and 88.62% of chord for suction slot. The profile of CFJ is simple obtained from the conventional equations for NACA 4 digit airfoil as discussed earlier with some simple modification in the equation of upper and lower surface. This modification is given below.

The equation of upper surface:

For x $\leq$ 0.0672 and x $\geq$ 0.8872 $x_u = x - y_t(x) \sin\theta$
                            And, $y_u = y_c + y_t(x) \cos\theta$
For 0.0672 $\leq$ x $\leq$ 0.8872 $x_u = x - y_t(x) \sin\theta$
                   And, $y_u = y_c + y_t(x) \cos\theta - 0.0065$

Others equations are remain same. The C-program for generate data for CFJ is attached last. The obtained CFJ 0015-065-065 airfoil profile is given below.
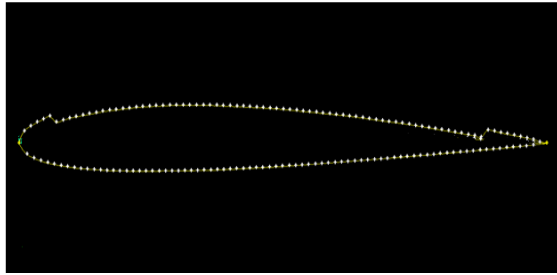
Fig. 4: CFJ 0015-065-065 airfoil.
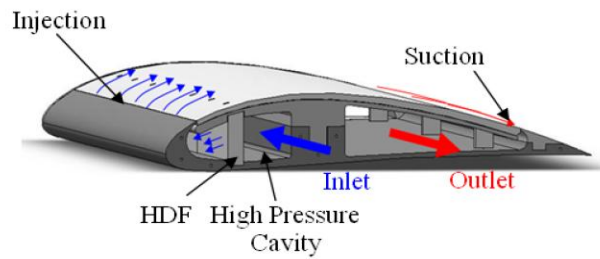
Fig.5: 3-D cross section of CFJ airfoil

III. EXPERIMENTAL SETUP AND PROCEDURE

This schematic diagram shows the overall setup of wind tunnel in Aerodynamics lab of Mechanical Engineering Department at KUET, Bangladesh.

Experimental Setup:
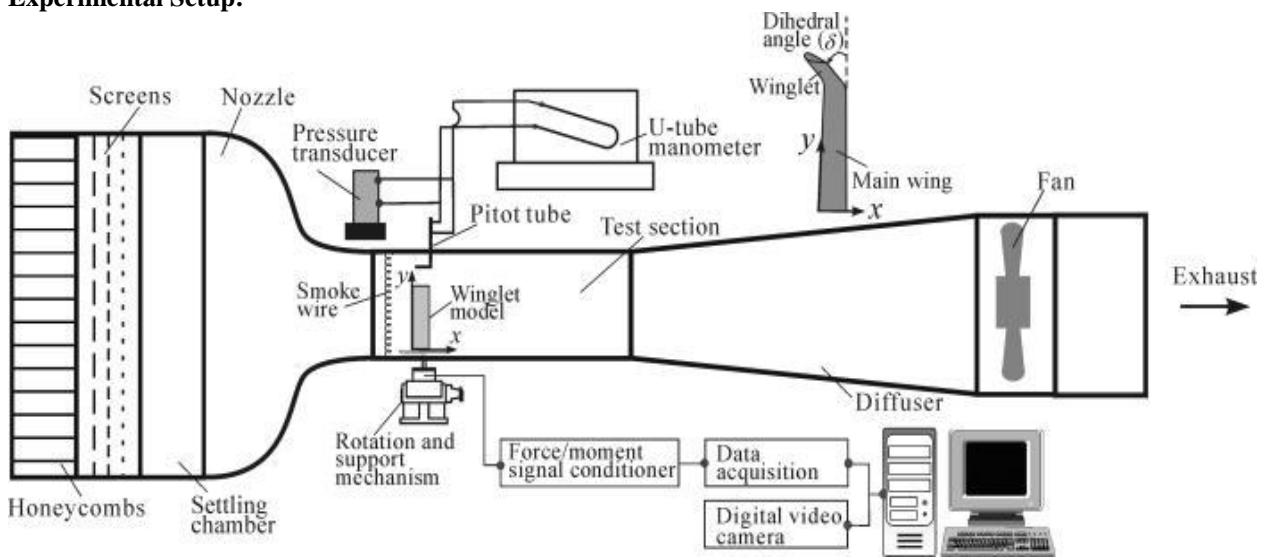
Figure 6: Schematic view of experimental setup

An Aerolab wind tunnel having tested section geometry of 1m x 1m and has an operating speed from 0-40 m/s (0-145 miles per hour). This is made possible by a 10-horse power motor that drives a fan. The applied free stream velocity is 12 m/s.

Constructed CFJ0015-065-065 Aerofoil

Snapshot of CFJ aerofoil placed under wind tunnel test

CFJ aerofoil connected with high pressure compressor line

Snapshot of high pressure compressor and low pressure vacuum pump

Fig.7: Photograph of experimental setup during the wind tunnel test.

Working procedure:

| Turn on vacuum pump and begin pulling vacuum (Pressure is controlled by wheel valve and measured by Flow meter) | → | Start compressor (Pressure is controlled by wheel valve and measured by Flow meter) | → | Connect different probes and Turn on all instrument |

| Start air injection Dial in suction mass flow rate | ← | Turn on wind tunnel (turn on all electric circuit) | ← | Set zero degree angle of attack (Clamp is used to hold the airfoil and indexing is used to set the AoA) |

| Only continue after the suction mass flow rate is desirable Start air suction and sampling | → | Measuring the pressure by manometer on different equally spaced slot in both upper camber (Here pressures in lower camber are remain constant since there is no change in lower | → | Different Airfoil characteristics are calculated after having pressure distribution. Plotting different figure. (Here V_{jet} is calculated by Pitot tube and M= 0.03 kg/s were kept constant) |

| Repeat the same procedure to justify the fluctuation of uncertainty and identify the correct data. | ← | Measuring the pressure and different Airfoil characteristics | ← | Rotate airfoil to desired angle of attack |

IV.   FIGURES AND TABLES

After calculating the total pressure and temperature in injection slot, the value of Mach number were measured. Once the Mach number is found then the values of Injection velocity is calculated for different AoA and its reach to 24 m/s at M= 0.03 kg/s and it shows a steady trend over 20 to 30 deg AoA.
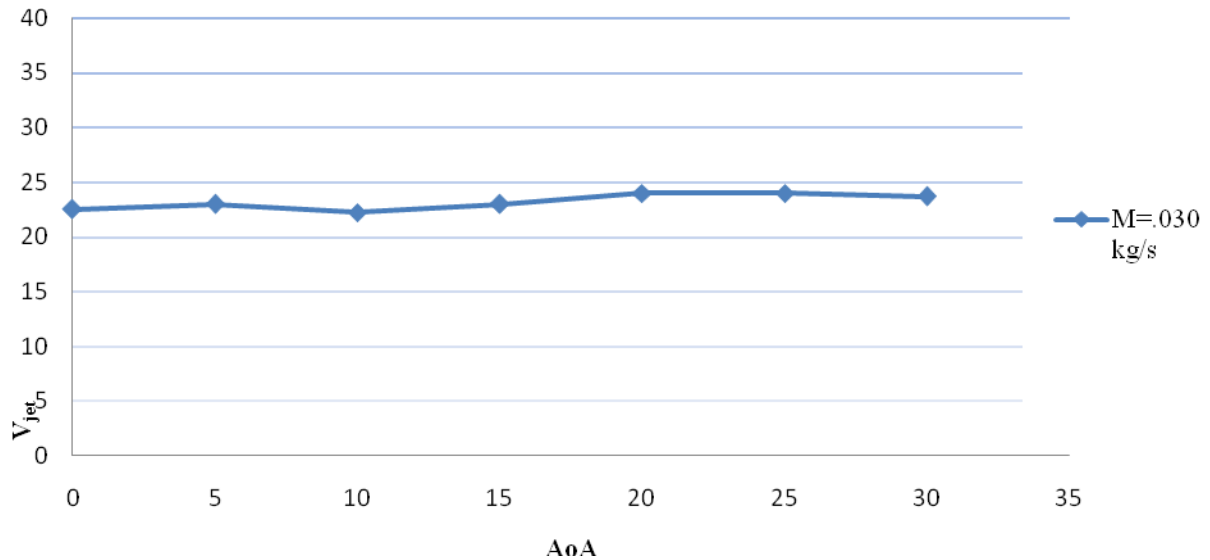
Fig. 08: Graphical Representation of Injection Velocity with AOA at M= 0.30 kg/s.

The value Jet Momentum Coefficient is calculated with the help of V_{jet} , mass flow rate, free stream velocity and Density. The value of C_μ is 0.07 at stall AoA at M = 0.030 kg/s.
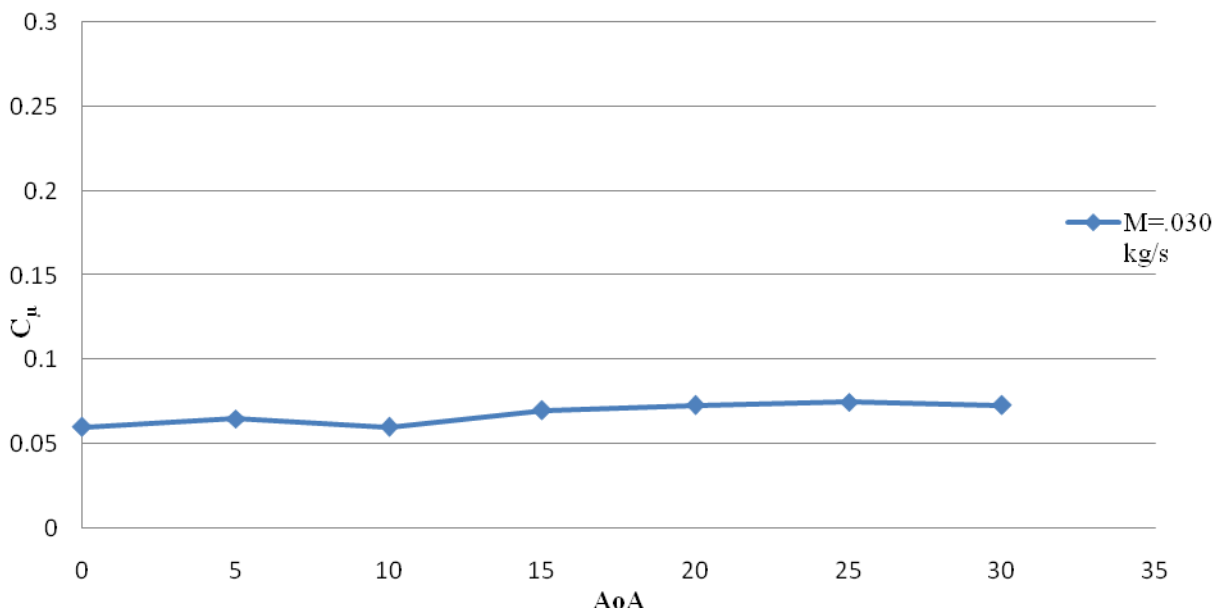
Fig. 09: Graphical Representation of C_μ with AoA at M = 0.30 kg/s

The measured value of $-C_p$ from pressure distribution along the upper camber and lower camber on both Airfoil with respect to different chord length position at different AoA are given below:
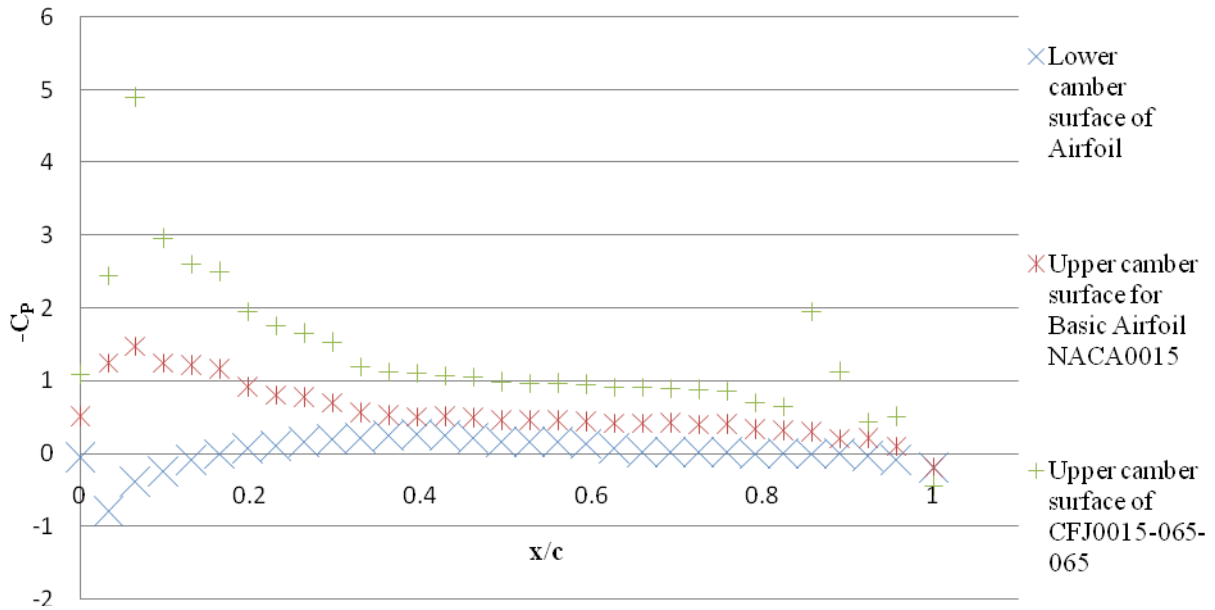
Fig. 10: Graphical Representation of -C_p with x/c at AoA= 05deg.
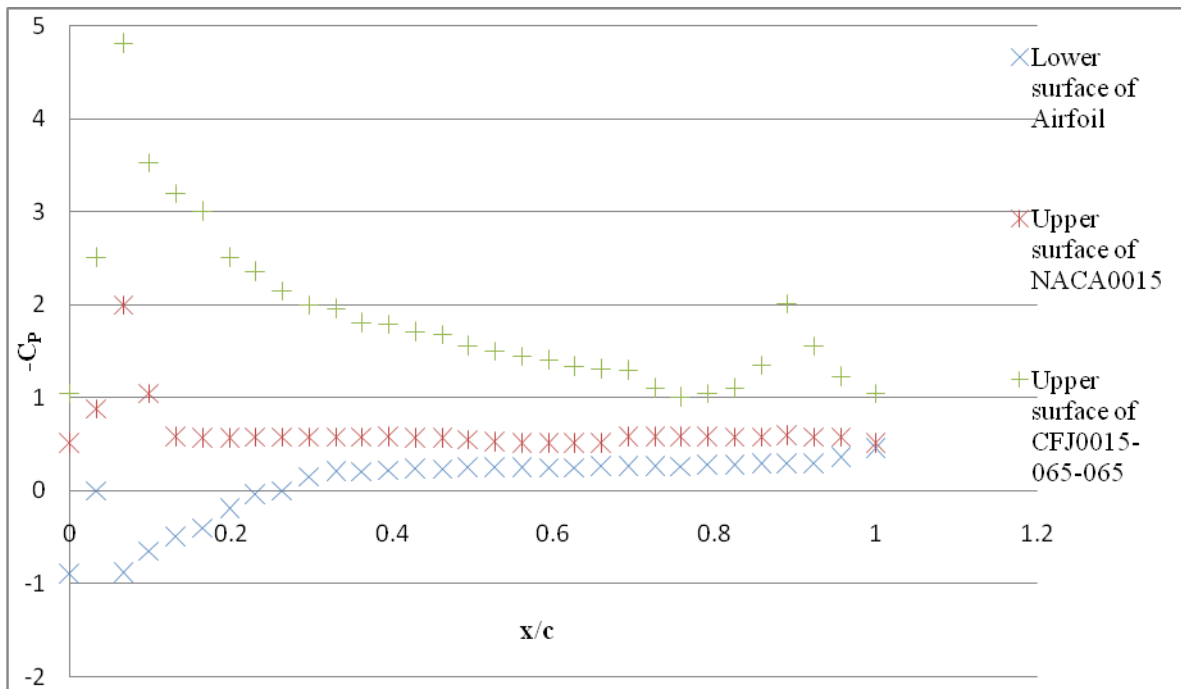
Fig. 11: Graphical Representation of -C_p with x/c at AoA= 12deg.

It was seen that at AOA = 05,12 deg the CFJ0015-065-065 aerofoil shows the steady ,smooth attached boundary layer over aerofoil geometry since the value of −Cp is quiet smooth. But for Baseline Aerofoil NACA 0015 it is also seen that at AOA = 12deg, the stall is occurred and Flow separation is start here and after that lift is reduced gradually and drag is increased bit by bit.
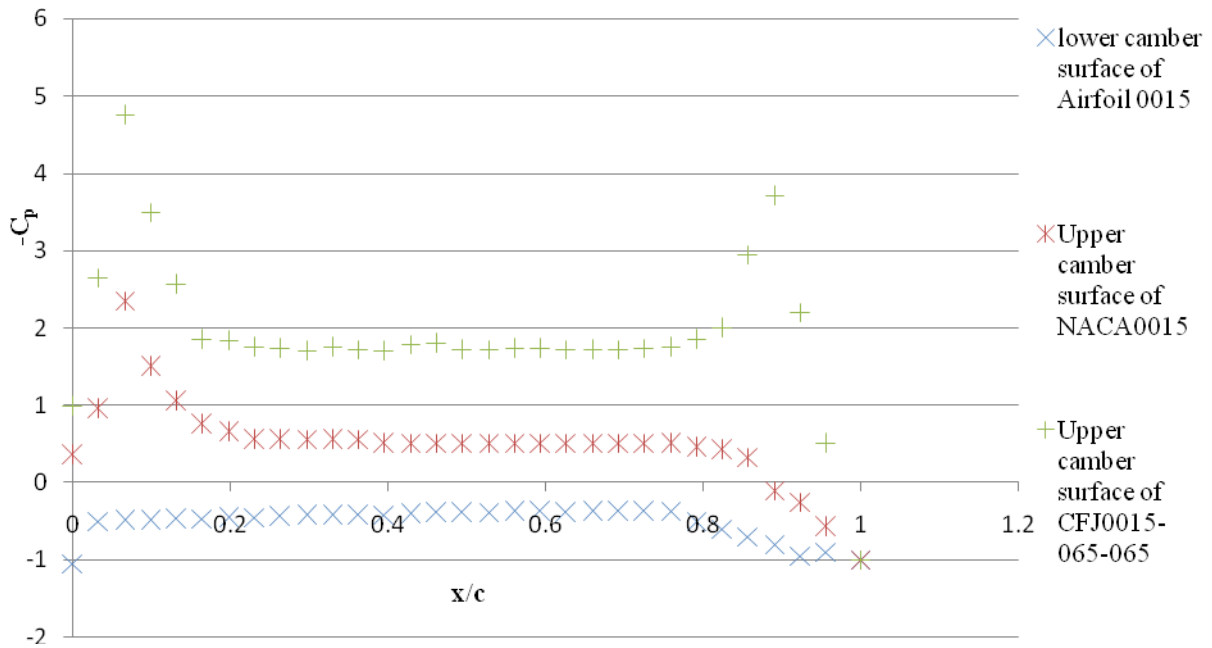
Fig. 12: Graphical Representation of -C_p with x/c at AoA= 20deg.

It was seen that at AOA =20 deg. The value of –Cp is shows some abrupt changes especially in suction slot of CFJ aerofoil i.e. 20 deg. is the stall margin for CFJ0015-065-065 and after that flow is detached from upper camber surface. But in CFJ aerofoil flow is delayed to separate until 20 deg. AOA where it was starts at 12 deg AOA in case of baseline airfoil.

At C_μ =0.07, Re=1.89 $\times$ $10^5$the values of C_l for both Airfoil geometry with different AoA are given below:
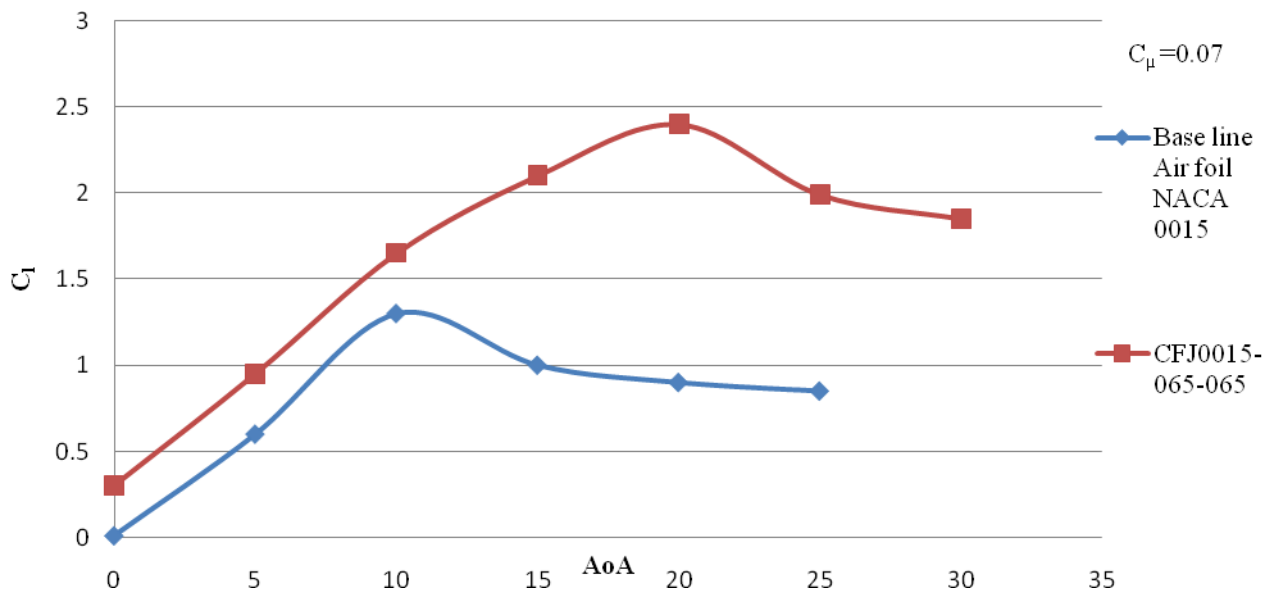
Fig. 13: Graphical Representation of Lift coefficient with angle of attack for both CFJ0015-065-065 and Baseline Airfoil at C_μ =0.07 and Re=1.89 $\times$ 10^5.
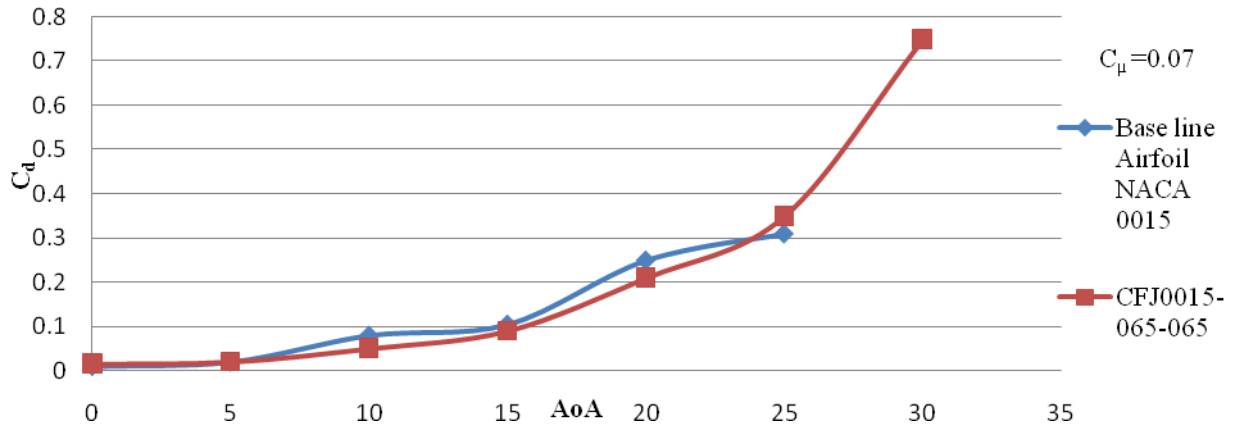
Fig. 14: Graphical Representation of Drag coefficient with angle of attack for both CFJ0015-065-065 and Baseline Airfoil at C_μ =0.07 and Re=1.89 × 10^5
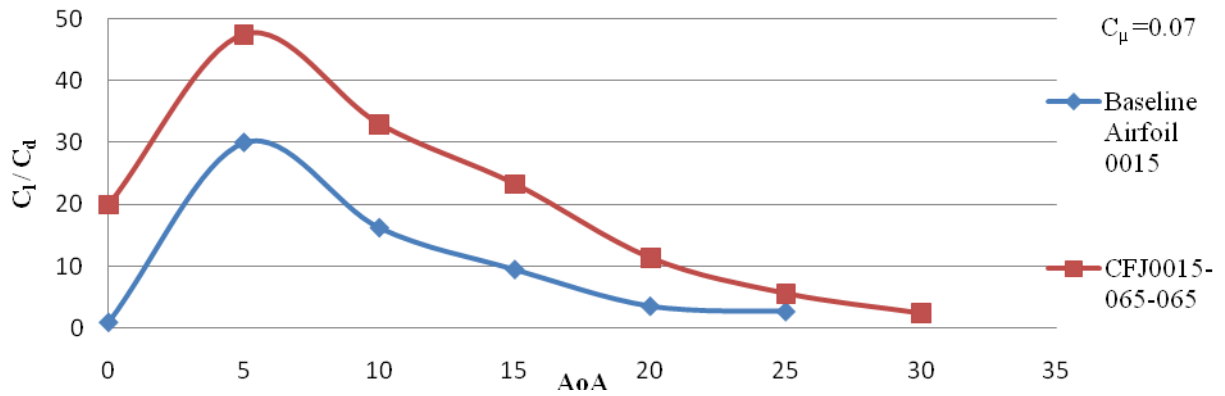
Fig.15: The change of C_l/ C_d with AoA for both CFJ0015-065-065.
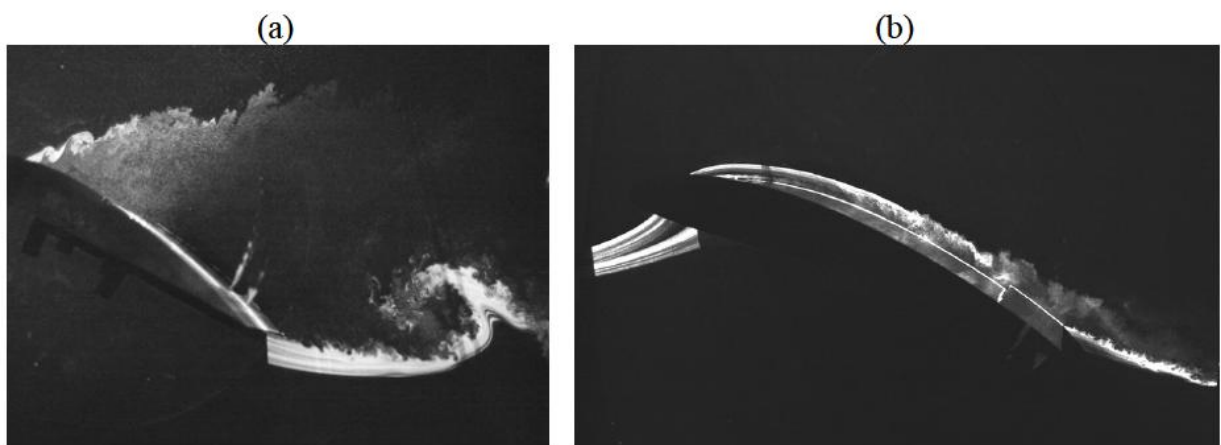
Fig.16: Smoke Flow Visualization for (a) Baseline airfoil NACA 0015 at AOA = 15 deg. and (b) CFJ0015-065-065 (C_μ =0.07) at AOA=20° deg.

V. CONCLUSION

The Following conclusion is drawn from this research paper:

Aerodynamics characteristics	CFJ0015-065-065	Baseline Airfoil NACA0015	Remarks : considering the effect of using CFJ technique over base line aerofoil
Free stream velocity	12 m/s	12 m/s	---
Mass Flow Rate	0.030 kg/s		---
Stall AoA	20 deg	12 deg	Stall angle improved
V_{jet}	24 m/s		---
C_{μ}	0.07		----
$C_{l\,max}$	2.45	1.35	C_l Improved
Lift Improvement Drag Reduction	82.5% 16.7% (compared with Baseline Airfoil)		Both characteristics is improved
$C_{d\,max}$	0.20 at Stall AoA	0.09 at Stall AoA	Considerably low
C_l/C_d Vs. AoA	47	30	Improved
Flow separation delay time	Improved since stall AOA is increased	As usual	Improved

VI. ACKNOWLEDGEMENTS

REFERENCES

[1]   M. Gad-el Hak, "Flow Control: The Future," Journal of Aircraft, vol. 38, pp. 402-418, 2001.
[2]   M. Gad-el Hak, Flow Control, Passive, Active, and Reactive Flow Management. Cambridge University Press, 2000.
[3]   V. Modi, M. Fernando, and T. Yokomizo, "Drag Reduction of Bluff Bodies Through Moving Surface Boundary Layer Control." AIAA Paper No. 90-0298, 1990.
[4]   D. Cichy, J. Harris, and J. MacKay, "Flight Tests of a Rotating Cylinder Flap on a North American Rockwell YOV-10A Aircraft." NASA CR-2135, 1972.
[5]   L. C. Bradley, "An Experimental Investigation of A Sting-Mounted Finite Circulation Control Wing." M.S. Thesis, Air Force Institute of Technology, 1995.
[6]   N. Wood, L. Robert, and Z. Celik, "Control of Asymmetric Vortical Flows over Delta Wings at High Angle of Attack," Journal of Aircraft, vol. 27, pp. 429-435, 1990.
[7]   N. Wood and L. Robert, "Control of Vortical Lift on Delta Wings by Tangential Leading-Edge Blowing," Journal of Aircraft, vol. 25, pp. 236-243, 1988.
[8]   N. Wood and J. Nielsen, "Circulation Control Airfoils-Past, Present, Future." AIAA Paper 85-0204, 1985.
[9]   R. J. Englar, L. A. Trobaugh, and R. Hemmersly, "STOL Potential of the Circulation Control Wing for High-Performance Aircraft," Journal of Aircraft, vol. 14, pp. 175-181, 1978.
[10]   R. J. Englar, "Circulation Control for High Lift and Drag Generation on STOL Aircraft," Journal of Aircraft, vol. 12, pp. 457{463, 1975.
[11]   A. Smith, "High-Lift Aerodynamics," Journal of Aircraft, vol. 12, pp. 501-530, 1975.
[12]   J. Lin, S. Robinson, R. McGhee, and W. Valarezo, "Separation Control on High Reynolds Number Multi-Element Airfoils." AIAA Paper 92-2636, 1992.
[13]   K. McManus and J. Magill, "Airfoil Performance Enhancement Using Pulsed Jet Separation Control." AIAA Paper 97-1971, 1997.

[14]   K. McManus and J. Magill, "Separation Control in Incompressible and Compressible Flows Using Pulsed Jets." AIAA Paper 96-1948, 1996.

[15]   H. Johari and K. McManus, "Visulation of Pulsed Vortex Generator Jets for Active Control of Boundary Layer Separation." AIAA Paper 97-2021, 1997.

[16]   G.-C. Zha, (team members: David Car, and W. Copenhaver), "Super Diffusion Cascades Using Co-Flow Jet Flow Control." National Research Council Summer Faculty Final Report, Aug.23, 2002.

[17]   D. Car, N. J. Kuprowicz, J. Estevadeordal, G.-C. Zha, and W. Copenhaver, "Stator Diffusion Enhancement Using A Re-circulating Co-flowing steady Jet." ASME GT-2004-53086, ASME TURBO EXPO 2004, June 14-17, 2004.

[18]   Y. Liu, L. N. Sankar, R. J. Englar, K. K. Ahuja, and R. Gaeta, "Computational Evaluation of the Steady and Pulsed Jet Effects on the Performance of a Circulation Control Wing Section." AIAA Paper 2004-0056, 42nd AIAA Aerospace Sciences Meeting and Exhibit, Reno, Nevada 5 - 8 Jan 2004.

[19]   Wells, Adam Joseph, "Experimental Investigation of an Airfoil with Co-Flow Jet (CFJ) Flow Control."UF 2005.

Research Paper   Open Access

Weighted Denoising With Multi-Spectral Decomposition for Image Compression

[1,]Tamboli S. S. [2,]Dr. V. R. Udupi
[1,]ADCET, Ashta
[2,] GIT, Belgaum

ABSTRACT: *A modified approach to image compression is proposed in this paper. The objective of image compression based on multi spectral representation is developed. The denoising process of image coding is improvised so as to achieve higher processing accuracy with high PSNR value. A multi wavelet coding with a modified weighted filtration approach is proposed. The simulation observation evaluates the proposed approach and the comparative analysis of the proposed approach presents the improvement in coding efficiency.*

KEYWORD: *Image compression, Multi spectral coding, preprocessing, and denoising.*

I.   INTRODUCTION

With the upcoming of new technologies the demand for new services and their usage is also increasing. New standards and architectures are coming up to achieve the objective of higher system performance. In various demanded services imaging applications are growing at a faster rate. For current demanded services new image coding approaches were proposed. These approaches are focused mainly to achieve better compression factor or higher accuracy. In the process of image coding the initial process is to remove the noise artifacts during the preprocessing operation. In Image coding inappropriate and coarse results may strongly deteriorate the relevance and the robustness of a computer vision application. The main challenge in noise removal is suppressing the corrupted information while preserving the integrity of fine image structures. Several and well-established techniques, such as median filtering are successfully used in gray scale imaging. Median filtering approach is particularly adapted for impulsive noise suppression. It has been shown that median filters present the advantage to remove noise without blurring edges since they are nonlinear operators of the class of rank filters and since their output is one of the original gray values [1] [2]. The extension of the concept of median filtering to color images is not trivial.

The main difficulty in defining a rank filter in color image is that there is no "natural" and unambiguous order in the data [3] [4]. During the last years, different methods were proposed to use median filters in color image processing [5] [6]. In vector filtering, the challenge is to detect and replace noisy pixels and preserve the relevant information. But it is recognized that in some image areas most of vector filters blur thin details and image edges [7] [8] even if many works such as Khriji and Gabbouj [9]. Generally impulse noise contaminates images during data acquisition by camera sensors and transmission in the communication channel. In [10] Chan and Nikolova proposed a two-phase algorithm. In the first phase of this algorithm, an adaptive median filter (AMF) is used to classify corrupted and uncorrupted pixels; in the second phase, specialized regularization method is applied to the noisy pixels to preserve the edges and noise suppression. The main drawback of this method is that the processing time is very high because it uses a very large window size of 39X39 in both phases to obtain the optimum output; in addition, more Complex circuitry is needed for their implementation. In [11] Srinivasan and Ebenezer proposed a sorting based algorithm in which the corrupted pixels are replaced by either the median pixel or neighborhood pixel in contrast to AMF and other existing algorithms that use only median values for replacement of corrupted pixels. At higher noise densities this algorithm does not preserve edge and fine details satisfactorily. In this paper a novel robust estimation based filter is proposed to remove fixed value impulse noise effectively.

The proposed filter removes low to high density fixed value impulse noise with edge and detail preservation upto a noise density of 90%. Recently, nonlinear estimation techniques are gaining popularity for the problem of image denoising. The well-known Wiener filter for minimum mean-square error (MMSE) estimation is designed under the assumption of wide-sense stationary signal and noise (a random process is said to be stationary when its statistical characteristics are spatially invariant) [12]. For most of the natural images, the stationary condition is not satisfied. In the past, many of the noise removing filters were designed with the stationary assumption. These filters remove noise but tend to blur edges and fine details. This algorithm fails to remove impulse noise in high frequency regions such as edges in the image. To overcome the above mentioned difficulties a nonlinear estimation technique for the problem of image denoising has been developed based on robust statistics. Robust statistics addresses the problem of estimation when the idealized assumptions about a system are occasionally violated. The contaminating noise in an image is considered as a violation of the assumption of spatial coherence of the image intensities and is treated as an outlier random variable [12]. In [13] Kashyap and Eom developed a robust parameter estimation algorithm for the image model that contains a mixture of Gaussian and impulsive noise. In [12] a robust estimation based filter is proposed to remove low to medium density Gaussian noise with detail preservation. Though the techniques were developed for filtration of Gaussian or impulsive noise they are been developed for gray level images and are not suitable for color images. These approaches work on the method of denoising based on the current pixel or on the relevance surrounding pixels to make a decision.

The adaptive filtration is an emerging solution to the dynamic noise processing. However in the process of dynamic filtration proper denoising value is required to eliminate the noise effect. In this paper a modified filtration approach for image denoising is presented. A denoised sample is then processed to achieve best representation achieving both compression improvement and coding efficiency. To achieve the objective JPEG 2000 coding standard were presented. The coding in such architecture is developed using wavelet transformation. However the spectral representation of such coding is limited and finer resolution information are neglected. This assumption reduces the coding accuracy. In this paper a multi-spectral decomposition for image compression is proposed. Wavelet-based coding [14, 15] provides substantial improvements in picture quality at higher compression ratios. For better performance in compression, filters used in wavelet transforms should have the property of orthogonality, symmetry, short support and higher approximation order. Due to implementation constraints scalar wavelets do not satisfy all these properties simultaneously. Multiwavelets [16, 17] which are wavelets generated by finite set of scaling functions, have several advantages in comparison to scalar wavelets. One of the advantages is that a multiwavelet can possess the orthogonality and symmetry simultaneously [15, 18, 19] while except for the 'Haar' (scalar wavelet) cannot have these two properties simultaneously. Thus Multiwavelets offer the possibility of superior performance and high degree of freedom for image processing applications, compared with scalar wavelets. Multiwavelets can achieve better level of performance than scalar wavelets with scalar wavelets with similar computational complexity. With these approaches in this work a new image coding approach integrating modified denoising and multi spectral representation is proposed. The remaining section of the work is presented in 6 sections, where section 2 outlines the image coding system and its modeling approach. The conventional image coding approach is presented in this section. The proposed image coding methodology is presented in section 3. Section 4 presents the simulation observation obtained for the proposed approach and a conclusion is presented in section 5.

II. IMAGE CODING SYSTEM

The JPEG-2000 image compression architecture is the fundamental architecture consisting an encoder and decoder unit. The function of the encoder is to create a set of symbols from the given input data which is transmitted through a channel and then feed to decoder where we can reconstruct the image. There is a possibility that the reconstructed output image can the replica of the input image or the reconstructed image is distorted image due to channel interference. Figure 3.1 shows convention block diagram of a compression system.
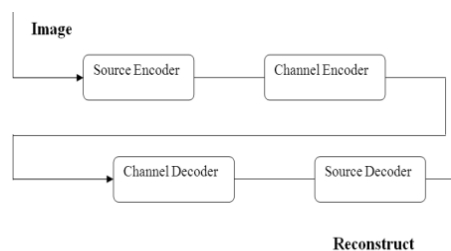

Figure 1: conventional Block Diagram of an Image compression system.

In the process of encoding the image is preprocessed for filtration and output is then processed using DWT. To perform the forward DWT the JPEG2000 system uses a one-dimensional (1-D) subband decomposition of a 1-D set of samples into low-pass and high-pass samples. Quantization refers to the process of approximating the continuous set of values in the image data with a finite (preferably small) set of values. After the data has been quantized into a finite set of values, it can be encoded using an Entropy Coder to give additional compression. An entropy coder encodes the given set of symbols with the minimum number of bits required to represent them using Huffman coding. The Huffman decoder block carries out decoding reading the unique code bits passed in place of the data bit. The dequantizer unit dequantizes the decoded data bits. Inverse transformation is the process of retriving back the image data from the obtained image values. The image data transformed and decomposed under encoding side is rearranged from higher level decomposition to lower level with the highest decomposed level been arranged at the top. There are several ways wavelet transforms can decompose a signal into various sub bands.The decomposition of the signal into different frequency bands is simply obtained by successive high pass and low pass filtering of the time domain signal. . First, the low pass filter is applied for each row of data, thereby getting the low frequency components of the row. But since the low pass filter is a half band filter, the output data contains frequencies only in the first half of the original frequency range. Now, the high pass filter is applied for the same row of data, and similarly the high pass components are separated.
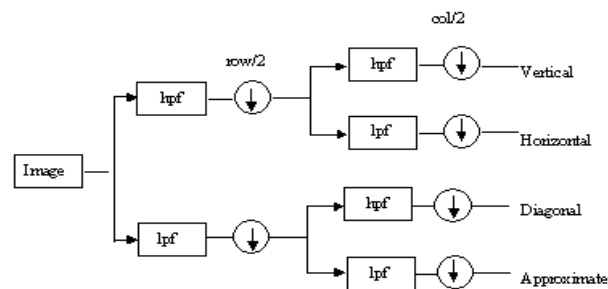
Figure 2 : Wavelet Decomposition of the image sample

To perform the forward DWT the JPEG2000 system uses a one-dimensional (1-D) subband decomposition of a 1-D set of samples into low-pass and high-pass samples. Low-pass samples represent a down-sampled, low-resolution version of the original set and High-pass samples represent a down-sampled residual version of the original set. The Huffman code is found to be more optimal since it results in the shortest average codeword length among all encoding techniques that assign a unique binary codeword to each pattern. In addition, Huffman codes possess the prefix-free property, i.e., no codeword is the prefix of a longer codeword. The first step in the encoding process is to identify the unique patterns in the test set. A codeword is then developed for each unique pattern using the Huffman code construction method. The obtained Huffman tree is then used to construct code words for the patterns of a data set. These code words are assigned to the data bits for compression. The rate of compression achieved is considerably high compared to other encoding techniques due to its variable length property. Typical image coder generally consist of this encoding process, however this method require extensive training of non adaptive entropy codes and has to maintain a codebook for encoding and decoding. System following Huffman coding generally shares the codebook under transmission and reception. These parameters make the coding system non efficient. An enhance coding proposed by Shapiro [1] over come these excessive codebook maintenance.

The inverse fast wavelet transform can be computed iteratively using digital filters. The figure below shows the required synthesis or reconstruction filter bank, which reverses the process of the analysis or decomposition filter bank of the forward process. At each iteration, four scale j approximation and detail sub images are up sampled and convolved with two one dimensional filters-one operating on the sub images columns and the other on its rows. Addition of the results yields the scale j +1 approximation, and the process is repeated until the original image is reconstructed. The filters used in the convolutions are a function of the wavelets employed in the forward transform.

Figure 3: reconstruction unit for IDWT

The simplest of smoothing algorithms is the Mean Filter. Mean filtering is a simple, intuitive and easy to implement method of smoothing images, i.e. reducing the amount of intensity variation between one pixel and the next. It is often used to reduce noise in an image. The idea of mean filtering is simply to replace each pixel value in an image with the mean (`average') value of its neighbors, includ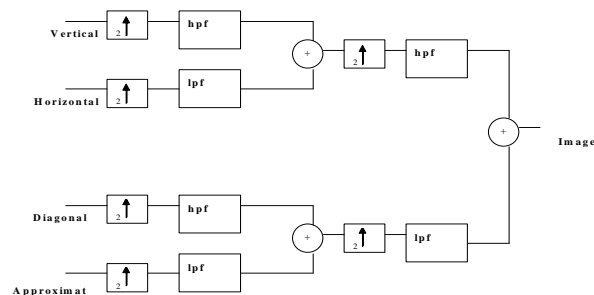ing itself. This has the effect of eliminating pixel values, which are unrepresentative of their surroundings. The mean value is defined by,

$$M n F (x_i) = \frac{1}{N} \sum_{i=1}^{N} x_i$$

Where, N – number of pixels

x_i – corresponding pixel value,

i= 1….. N

The mean filtration technique is observed to be lower in maintaining edges within the images. To improve this limitation a median filtration technique is developed. The median filter is a non-linear digital filtering technique, often used to remove noise from images or other signals. Median filtering is a common step in image processing. It is particularly useful to reduce speckle noise and salt and pepper noise. Its edge-preserving nature makes it useful in cases where edge blurring is undesirable. The idea is to calculate the median of neighbouring pixels' values. This can be done by repeating these steps for each pixel in the image. a) Store the neighbouring pixels in an array. The neighbouring pixels can be chosen by any kind of shape, for example a box or a cross. The array is called the window, and it should be odd sized.
b) Sort the window in numerical order
c) Pick the median from the window as the pixels value.
The process of this filtration is limited to the surrounding pixel only. This limitation of noise suppression and a finer representation is presented in the following section.

III. WEIGHTED MULTI-SPECTRAL (WMS) CODING

In a Spatial Median Filter the vectors are ranked by some criteria and the top ranking point is used to replace the center point. No consideration is made to determine if that center point is original data or not. The unfortunate drawback of these filters is the smoothing that occurs uniformly across the image. Across areas where there is no noise, original image data is removed unnecessarily. In the proposed weighted filtration approach, after the spatial depths between each point within the mask are computed, an attempt is made to use this information to first decide if the mask's center point is an uncorrupted point. If the determination is made that a point is not corrupted, then the point will not be changed.
The proposed modified filtration works as explained below,
[1]. Calculate the spatial depth of every point within the mask selected.
[2]. Sort these spatial depths in descending order.
[3]. The point with the largest spatial depth represents the Spatial Median of the set. In cases where noise is determined to exist, this representative point is used to replace the point currently located under the center of the mask.
[4]. The point with the smallest spatial depth will be considered the least similar point of the set.
[5]. By ranking these spatial depths in the set in descending order, a spatial order statistic of depth levels is created.
[6]. The largest depth measures, which represent the collection of uncorrupted points, are pushed to the front of the ordered set.
[7]. The smallest depth measures, representing points with the largest spatial difference among others in the mask and possibly the most corrupted points, and they are pushed to the end of the list.
This prevents the smoothing by looking for the position of the center point in the spatial order statistic list.

For a given parameter ζ (where $1 \le \zeta \le$ masksize), which represents the estimated number of original points under a mask of points. As stated earlier, points with high spatial depths are at the beginning of the list. Pixels with low spatial depths appear at the end.

  If center point 'c' $\le \zeta$ then current pixel MSF (ζ, x_i) = r_c

elsif center point 'c' $> \zeta$ then current pixel MSF (ζ, x_i) = r_1

else if c =1 then, pixel canot be modified.

If the position of the center mask point appears within the first ζ bins of the spatial order statistic list, then the center point is not the best representative point of the mask, and it is still original data and should not be replaced.

Two things should be noted about the use of ζ in this approach. When ζ is 1, this is the equivalent to the conventional Median Filter. When ζ is equal to the size of the mask, the center point will always fall within the first ζ bins of the spatial order statistic and every point is determined to be original. This is the equivalent of performing no filtering at all, since all of the points are left unchanged. The algorithm to detect the least noisy point depends on a number of conditions. First, the uncorrupted points should outnumber, or be more similar, to the corrupted points. If two or more similar corrupted points happen in close proximity, then the algorithm will interpret the occurrence as original data and maintain the corrupted portions. While ζ is an estimation of the average number of uncorrupted points under a mask of points, the experimental testing made no attempt to measure the impulse noise composition of an image prior to executing the filter.

These filter outputs are then processed for multi spectral operation.

The conventional wavelet transform is a type of signal transform that is commonly used in image compression. A newer alternative to wavelet transform is the multiwavelet transform. Multiwavelets are very similar to wavelets but have some important differences. In particular, whereas wavelets have an associated scaling function $\Phi(t)$ and wavelet function $\Psi(t)$, multiwavelets have two or more scaling and wavelet functions. For notational convenience, the set of scaling functions can be written using the vector notation $\Phi(t) = [\Phi_1(t), \Phi_2(t)..., \Phi_r(t)]^T$, where $\Phi(t)$ is called the multiscaling function. Likewise, the multiwavelet function is defined from the set of wavelet functions as $\Psi(t) = [\Psi_1(t), \Psi_2(t)..., \Psi_r(t)]^T$ Called a scalar wavelet, or simply wavelet where r = 1, $\Psi(t)$. While in principle 'r' can be arbitrarily large, the multiwavelets studied to date are primarily for r = 2. The multiwavelet two-scale equations resemble those for scalar wavelets defined by;

$$\phi(t) = \sqrt{2} \sum_{k=-\infty}^{\infty} H_k \phi(2t - k)$$

$$\psi(t) = \sqrt{2} \sum_{k=-\infty}^{\infty} G_k \phi(2t - k)$$

However, {H_k} and {G_k} are matrix filters, i.e., H_k and G_k are "r x r" matrices for each integer k. The matrix elements in these filters provide more degrees of freedom than a traditional scalar wavelet. These extra degrees of freedom can be used to incorporate useful properties into the multiwavelet filters, such as orthogonality, symmetry, and high order of approximation. The key idea is to figure out how to make the best use of these extra degrees of freedom.
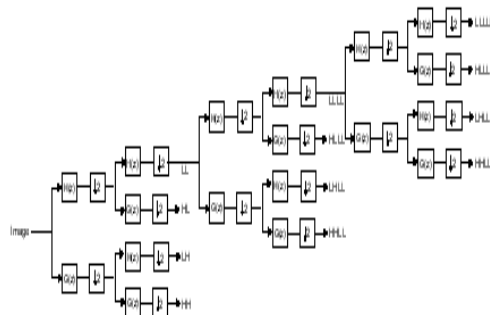
Figure4 : Pyramidal decomposition of multi spectral decomposition

For the processing of MRI image using multiwavelet, the typical approach is to process each of the rows in order, and process each column of the result. Nonseparable methods work in both image dimensions at the same time. While non-separable methods can offer benefits over separable methods, such as savings in computation.

They are generally more difficult to implement. Computing Discrete Multi-wavelet Transform, scalar wavelet transform can be written as follows:

$$
\begin{pmatrix}
H_o & H_1 & H_2 & H_3 & 0 & 0 \\
G_o & G_1 & G_2 & G_3 & 0 & 0 \\
0 & 0 & H_0 & H_1 & H_2 & H_3 \\
0 & 0 & G_0 & G_1 & G_2 & G_3
\end{pmatrix} \quad (1)
$$

Figure 5: Filter coefficient for the Multi spectral decomposition

Where H_i and Gi are low and high pass filter impulse responses, are 2-by-2 matrices which can be written asfollows:

$$
\begin{pmatrix}
H_o & H_o & H_1 & H_1 & \ldots & \ldots & \ldots & \ldots & \ldots \\
H_o & H_o & H_1 & H_1 & \ldots & \ldots & \ldots & \ldots & \ldots \\
G_o & G_o & G_1 & G_1 & \ldots & \ldots & \ldots & \ldots & \ldots \\
G_o & G_o & G_1 & G_1 & \ldots & \ldots & \ldots & \ldots & \ldots \\
0 & 0 & 0 & 0 & H_o & H_o & H_1 & H_1 & \ldots \\
0 & 0 & 0 & 0 & H_o & H_o & H_1 & H_1 & \ldots \\
0 & 0 & 0 & 0 & G_o & G_o & G_1 & G_1 & \ldots \\
0 & 0 & 0 & 0 & G_o & G_o & G_1 & G_1 & \ldots
\end{pmatrix}
$$

Figure 6: Filtration process in Multi spectral coding

By examining the transform matrices of the scalar wavelet and multi-wavelets, it is observed that in multi-wavelets transform domain there are first and second low-pass coefficients followed by first and second high pass filter coefficients rather than one lowpass coefficient followed by one high pass coefficient. Therefore, if we separate these four coefficients, there are four sub bands in the transform domain. Since multi-wavelet decompositions produce two low-pass sub bands and two high pass sub bands in each dimension, the organization and statistics of multiwavelet sub band differ from the scalar wavelet case.
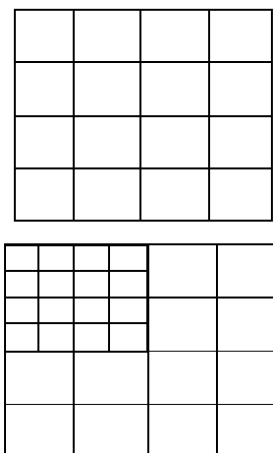
Figure7 : Conventional iteration of multiwavelet decomposition.

During a single level of decomposition using a scalar wavelet transform, the 2- D image data is replaced by four blocks corresponding to the sub bands representing either low pass or high pass in both dimensions. These sub bands are illustrated in Fig. 6. The sub band labels indicate how the sub band data were generated. For example, the data in sub band LH was obtained from high pass filtering of the rows and then low pass filtering of the columns.

The multi-wavelets used here have two channels, so there will be two sets of scaling coefficients and two sets of wavelet coefficients. Since multiple iteration over the low pass data is desired, the scaling coefficients for the two channels are stored together. Likewise, the wavelet coefficients for the two channels are also stored together. The multi-wavelet decomposition sub bands are shown in Fig.7. For multi-wavelets the L and H have subscripts denoting the channel to which the data corresponds. For example, the sub band labeled L_1H_2 corresponds to data from the second channel high pass filter in the horizontal direction and the first channel low pass filter in the vertical direction. This shows how a single level of decomposition is done. In practice, there is more than one decomposition performed on the processing image. Successive iterations are performed on the low pass coefficients from the pervious stage to further reduce the number of low pass coefficients. Since the low pass coefficients contain most of the original signal energy, this iteration process yields better energy compaction. After a certain number of iterations, the benefits gained in energy compaction becomes rather negligible compared to the extra computational effort. Usually five levels of decomposition are used. A single level of decomposition with a symmetric-antisymmetric multi-wavelet is roughly equivalent to two levels of wavelet decomposition. Thus a 3–level multiwavelet decomposition effectively corresponds to 6-level scalar wavelet decomposition. The scalar wavelet transform gives a single quarter-sized sub band from the original larger sub band. The multi-level decomposition is performed in the same way. The multi-wavelet decomposition iterates on the low pass coefficients from the pervious decomposition. In the case of the scalar wavelets, the low pass quarter image is a single sub band. But when the multi-wavelet transform is used, the quarter image of low pass coefficients is actually a 2 x 2 block of sub bands (the LL_j sub bands in Fig. 6. Due to the nature of the preprocessing and symmetric extension method, data in these different sub bands becomes intermixed during iteration of the multiwavelet transform. The intermixing of the multiwavelet low pass sub bands leads to suboptimal results. Consider the multi-wavelets transform coefficients resulting from single-level decomposition. It can be readily observed that the 2 x 2 "low pass" block (upper left corner) actually contains one low pass sub band and three band pass sub bands. The L_1L_1 sub band resembles a smaller version of the original image, which is a typical characteristic of a true low pass sub band. In contrast, the L_1L_2, L_2L_1, and L_2L_2 sub bands seem to process characteristics more like those of high sub bands. Also only L_1L_1 sub band contains coefficients with a large DC value and a relatively uniform distribution. The L_1, L_1, H_1 and H_2 sub bands, measured along the vertical direction.

IV. SIMULATION RESULT

This section represents the performance evaluation of the proposed approach. For the evaluation of the proposed system different images were tested as shown below. To test the accuracy of the developed approach, a color image with mean distortion is applied. To estimate the quality of a reconstructed image, the Root-Mean-Squared Error between the original and the reconstructed image is computed. The Root-Mean-Squared Error (RMSE) for an original image I and reconstructed image R defined by,

$$RMSE(I,R) = \sqrt{\frac{1}{I_w \times I_h} \sum_{i=0}^{Iw} \sum_{j=0}^{Ih} \left\| I(i,j) - R(i,j) \right\|^2}$$

To test the operation performance for developed system the PSNR for the system is evaluated under different medium distortion level. The coding robustness is evaluated over the level of distortion introduced at different level bit coding. To evaluate the process.

Original Image   Noised Image

(a)   (b)

Mean filtered   Median Filtered

(b)   (d)

weighted filter

(e)
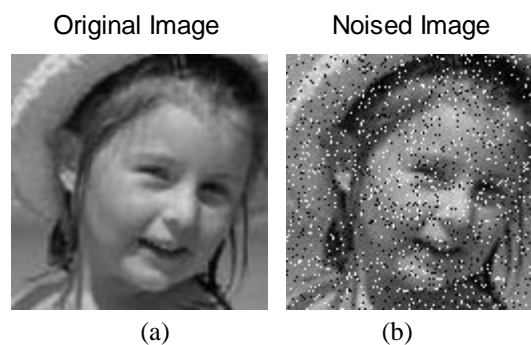
Figure 8: (a) Original sample, (b) Noised sample attacked with salt & pepper Noise at ρ =0.4, (c) filtered output after performing denoising using mean filtration, (d) Filtered output after performing median filtration, (e) Obtained result after filtration with proposed weighted filtration

The observation illustrates that the obtained visualization of the filtered result using weighted filtration is comparatively more accurate than the conventional filtration approach.
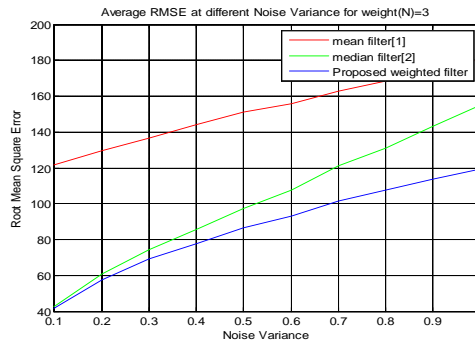
Figure 9: Average RMSE observation over variant Noise variance

Figure illustrates the obtained comparative analysis of the proposed weighted filtration approach over the conventional filtration technique. It is observed that the RMSE value for the proposed approach is decreased to about 40 units as comparative to the conventional approach.

weighted-Filtered at N=2

weighted-Filtered at N=3

(a)   (b)
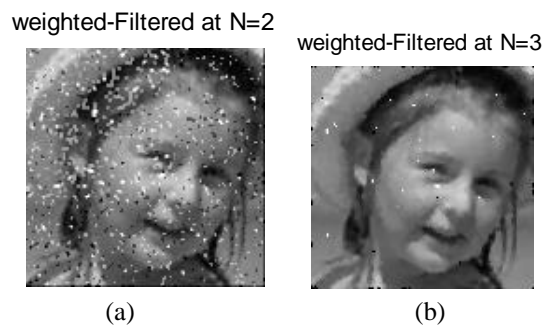
weighted-Filtered at N=4

(c)

Figure 10: (a) filtered output using weighted filtration at N=2, (b) filtered output using weighted filtration at N=3, (c) filtered output using weighted filtration at N=4

It is observed that the obtained filtration is improved with the block size increment. At N=4 the obtained filtration is comparatively accurate.
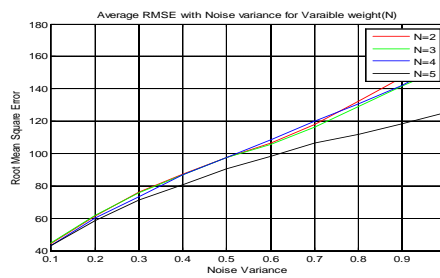
Figure 11: comparative average RMSE with the variation in noise level.

Figure shows the obtained comparative analysis after performing a block size variation. It could be observed that the RMSE value get minimized with the increase in the block size; at N=5 the obtained observation is minimum, hence an optimal N=5 value is chosen for the coding. A Similar observation is carried out over different samples and a comparative result for the developed method is as summarized in table 1.

Table 1: Observation for the obtained RMSE at different Noise variation

Noise Variance	Mean filter [1]	Median Filter [2]	Proposed weighted filter
0.1	125.5	67.23	43.5
0.2	123.5	67.1	43.11
0.3	121.4	66.4	42.23
0.4	120.1	65.7	41.71
0.5	119.2	65.4	41.4
0.6	117.9	64.32	40.3
0.7	116.2	62.8	39.6
0.8	114.5	61.44	38.3
0.9	113.3	60.7	37.2
1.0	110.3	60.33	36.1

The obtained observation illustrates an improvement of about 40 units in the obtained RMSE observation.
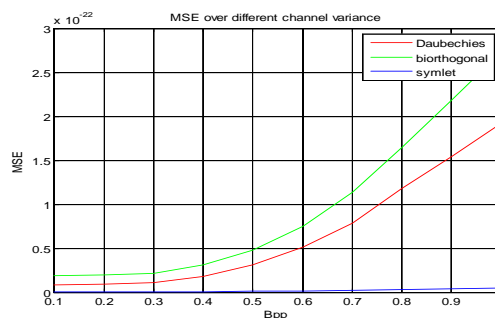
Figure 12: comparative analysis of different wavelet transformations at variable bpp.

Figure illustrates the comparatively analysis of multiple wavelet feasibility for developed method. It is observed that with the usage of symlet transformation the obtained MSE is lower.
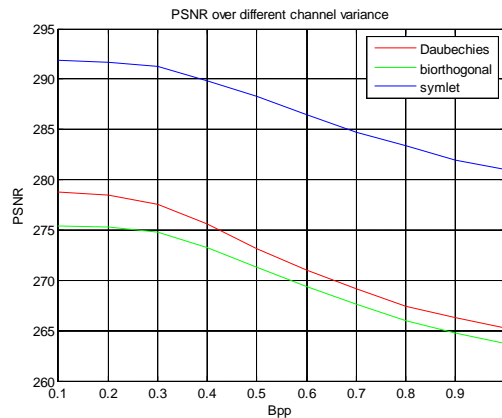
Figure 13: PSNR for different Bpp

The obtained PSNR value for different Bpp is developed. It is seen that higher bpp symlet transformation results in higher PSNR than the other transformation technique.
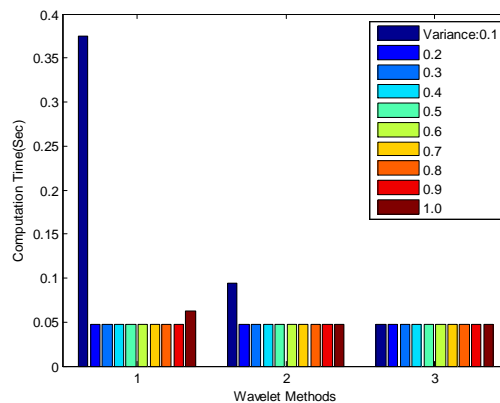
Figure 14: The computational time for the developed approach at different variance level

It is observed that the developed approach takes more time is computation due to higher noise value, whereas this time is reduced using symlet transformation.
A similar observation is carried out for other samples and the obtained observation is as shown,

(a) (b)

Mean filtered   Median Filtered

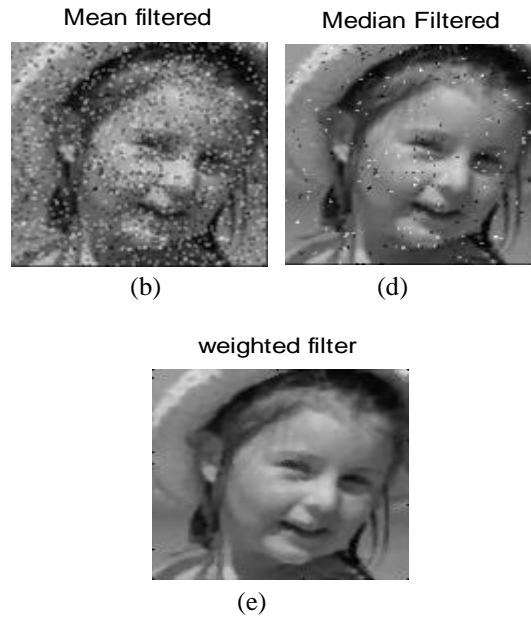(c)   (d)

weighted filter

(e)
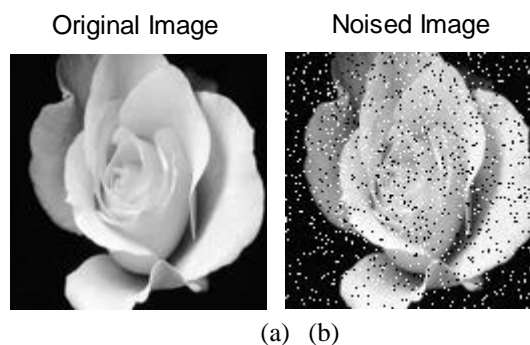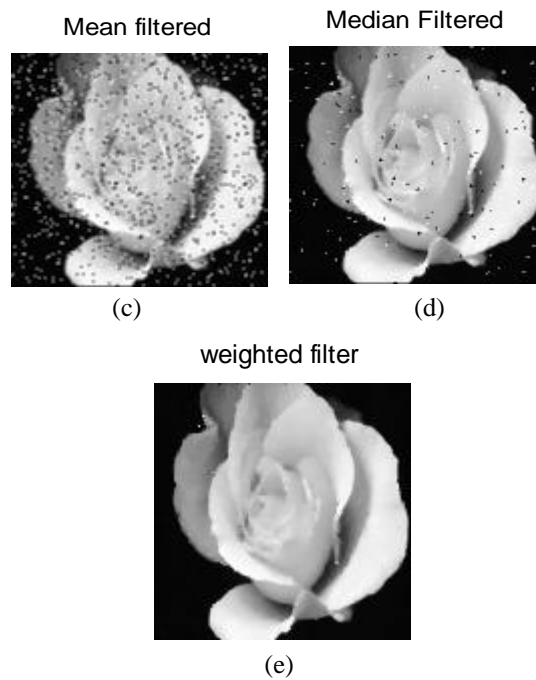
Figure 15: (a) Original Rose sample, (b) Noised sample attacked with salt & pepper Noise at ρ =0.4, (c) filtered output after performing denoising using mean filtration, (d) Filtered output after performing median filtration, (e) Obtained result after filtration with proposed weighted filtration
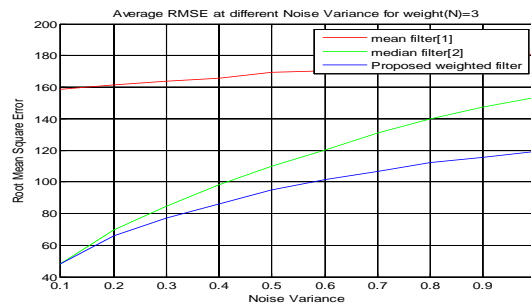
Figure 16: Average RMSE observation over variant Noise variance for the rose sample

weighted-Filtered at N=2   weighted-Filtered at N=3

(a)   (b)

weighted-Filtered at N=4

(c)
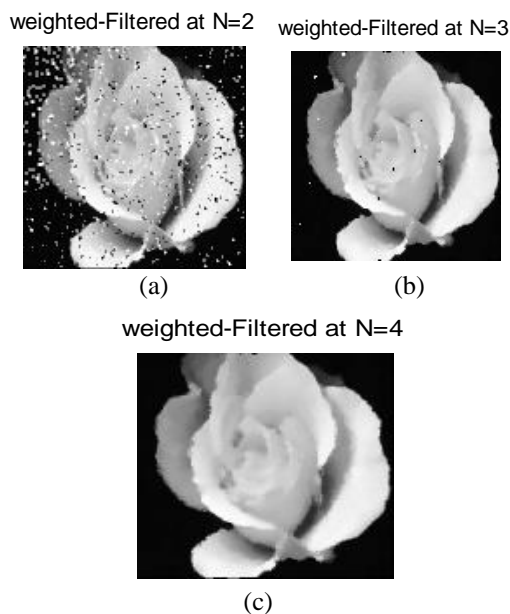
Figure 17: (a) filtered output using weighted filtration at N=2, (b) filtered output using weighted filtration at N=3, (c) filtered output using weighted filtration at N=4
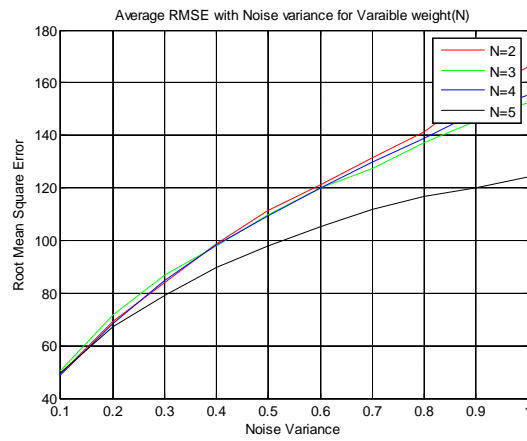
Figure 18: comparative average RMSE with the variation in noise level.
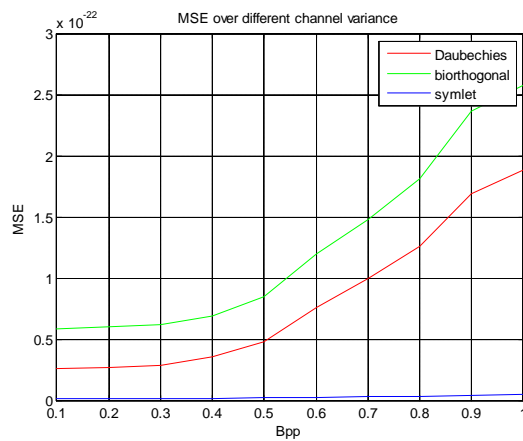
Figure 19: comparative analysis of different wavelet transformations at variable bpp
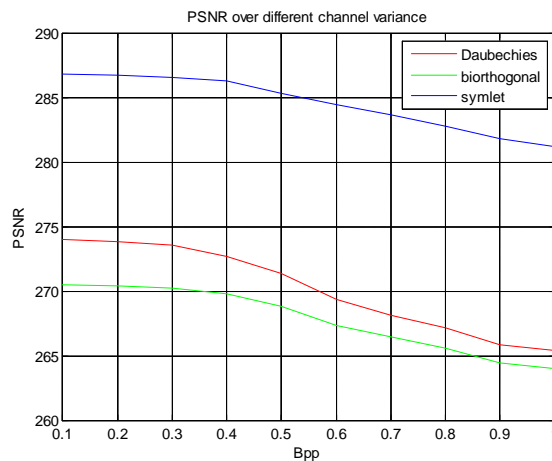
Figure 20: PSNR for different Bpp
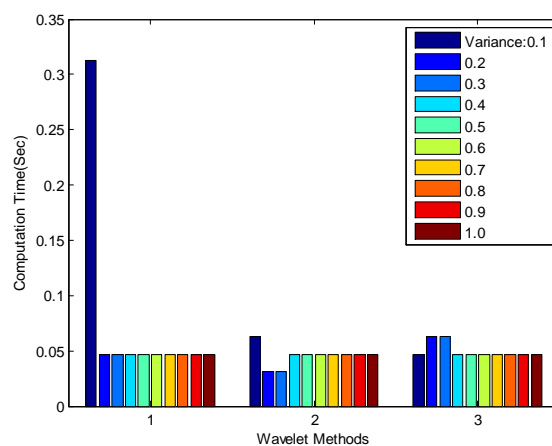
Figure 21: The computational time for the developed approach at different variance level

V. CONCLUSION

The image coding system proposed performance generally depends on weight value offered. Very-low-frequency content (ordinary images)usuallygives better performancefor images withscalarwavelet. However multiwavelets appear to excel at preserving high frequency content. In particular, multiwavelets capture the sharp edges and geometric patterns better that occur in images. With the incorporation of the proposed new coding approach of weighted multispectral coding an improvement of PSNR is achieved. This development leads to a new proposal in image coding architecture.

REFERENCES

[1]   R. Hodgson, D. Bailey, M. Naylor, A. Ng, and S. McCNeil, "Properties, implementations and applications of rank filters," Image Vision Comput., vol. 3, pp. 3–14, 1985.

[2]   M. Cree, "Observations on adaptive vector filters for noise reduction in color images", IEEE Signal Processing Letters, vol. 11(2), pp. 140–143, February 2004.

[3]   P. Lambert and L. Macaire, "Filtering and segmentation : the specificity of color images", in Proc. Conference on Color in Graphics and Image Processing, Saint-Etienne, France, September 2000, pp. 57–64.

[4]   I. Pitas and P. Tsakalides, "Multivariate ordering in color image filtering," IEEE Transactions on Circuits and Systems for Video Technology, vol. 1, pp. 247–259, 1991.

[5]   R. Lukac, B. Smolka, K. Plataniotis, and A. Venetsanopoulos, "Selection weighted vector directionnal filters," Computer Vision and Image Understanding, vol. 94, pp. 140–167, 2004.

[6]   M. Vardavoulia, I. Andreadis, and P. Tsalides, "A new median filter for colour image processing," Pattern Recognition Letters, vol. 22, pp. 675–689, 2001.

[7]   A. Koschan and M. Abidi, "A comparison of median filter techniques for noise removal in color images," in Proc. 7th german workshop on color image processing, vol. 34, No. 15, Germany, November 2001, pp. 69–79.

[8]   R. Lukac, "Adaptive vector median filtering," Pattern Recognition Letters, vol. 24, pp. 1889– 1899, 2002.

[9]   L. Khriji and M. Gabbouj, "Vector medianrational hybrid filters for multichannel image processing," IEEE Signal Proceesing Letters, vol. 6, No 7, pp. 186–190, 1999.

[10].   Raymond H. Chan, Chung-Wa Ho, and Mila Nikolova, "Salt-and-Pepper Noise Removal by Median-Type Noise Detectors and Detail-Preserving Regularization", IEEE Trans. Image Processing, vol. 14, no. 10, October 2005

[11].   K. S. Srinivasan and D. Ebenezer, "New Fast and Efficient Decision-Based Algorithm for Removal of High-Density Impulse Noises", IEEE signal processing letters, vol. 14, no. 3, march 2007.

[12].   Rabie, "Robust Estimation Approach for Blind Denoising", IEEE Trans. Image Processing, vol.14, no.11, pp.1755-1765, Nov 2005.

[13].   R. Kashyap and K. Eom, "Robust image modeling techniques with an image restoration application", IEEE Trans. Acoust.Speech, Signal Process., vol. ASSP-36, no. 8, pp. 1313-325, Aug. 1988.

[14]   Soman K. and Ramachandran K., Insight into Wavelets from Theory to Practice, Prentice Hall India, 2002.

[15]   Strela V., Heller P., Strang G., Topiwala P., and Heil Ch., "The Application of Multiwavelet Filter Banks to Image Processing," IEEE Transactions on Image Processing, vol. 8, no. 4, pp. 548-563, April 1999.

[16]   Martin M., "Applications of Multiwavelets to Image Compression," PhD Thesis, Deptartment of Electrical Engineering, Virginia Polytechnic Institute & State University, June 1999.

[17]   Martin M. and Bell A., "New Image Compression Techniques using Multiwavelets and Multiwavelet Packets," IEEE Transactions on Image Processing, vol. 10, no. 4, pp. 500-510,April 2001.

[18]   Vetterli M. and Strang G., "Time-varying Filter Banks and Multiwavelets," in the 6th IEEE Digital Signal Processing (DSP) Workshop, Yosemite, pp. 223-226, 1994.

[19]   Kim W. and Chung H., "On Preconditioning Multiwavelet System for Image Compression," International Journal of Wavelet Multiresolution and Information Processing, vol. 1, no. 1, pp. 51-74, 2003.

Switching Of Security Lighting System Using Gsm

Bakare, B. I [1,] Odeyemi, F. M[2]

[1,2](*Department of Electrical/Computer Engineering*
Rivers State University of Science and Technology, Port Harcourt, Nigeria)

ABSTRACT: .*This paper shows how ATMEGA168 microcontroller can be used to remotely control security lighting via Short Message Service (SMS) from a Global System for Mobile Communication (GSM) phone anywhere outside the home. A Mobile phone is configured to transmit SMS signal to a home-based GSM modem. The GSM Modem then sends the received SMS to a ATMEGA168 microcontroller. The Microcontroller accesses the received SMS and Changes the State of the appliances if the received signal aggresses with a pre - set code. When this is done, the microcontroller then sends signal to the GSM modem which in turn send back a reply to the mobile phone via SMS. The system utilizes a LCD display with resolution of 96*64 using PCD8544 Driver/Controller to display the ON/OFF state of the lighting device.*

KEYWORDS : *GSM, LCD, microcontroller, modem, SMS*

I.   INTRODUCTION

Mobile devices, such as mobile phones, are becoming multipurpose devices. Imagine being able to control all the electrical appliances in a house from virtually any place in the world, GSM home automation may seem like an idea of the future; however there are many possibilities of using it currently [1], The technology works by allowing communication between a receiver in the house and a mobile phone elsewhere. That receiver can then be signaled to "On" or "Off" appliances in the house based on command from the mobile phone. Through the use of micro-controller, any electrical or electronic device such as lighting a bulb can be controlled from a distance.[2] This paper presents a system that allows the user to control lighting systems remotely using mobile phones. It provides remote control via Short Messages Services (SMS) using Global System for Mobile Communication (GSM) technology. This system is related to past study which uses personal computer (PC) that contains the software components through which the lights and appliances are controlled and home security is monitored. This paper developed a system that uses a microcontroller instead of PC and hence the system size is reduced

.   The most common problem that home owners encountered in relation to lighting system is due to some negligence like leaving the lights ON in error resulting to greater power consumption. This wasted power directly affects the home owner electrical bills. Another problem is that of the busy home owners who will arrive home late at night; they may want to switch on their security lights from a distance in order to protect their house against robbery and crimes.[3].The mobile phone is configured to send SMS of the ON/OFF state of the appliance to a modem (a particular mobile phone line). The owner can control the system through his mobile phone by sending Attention (AT) commands to the Modem line and in turn, to the microcontroller. The system can also provide password security against operator misuse/abuse.

II. MATERIALS AND METHODS

The figure below shows the block diagram of the design
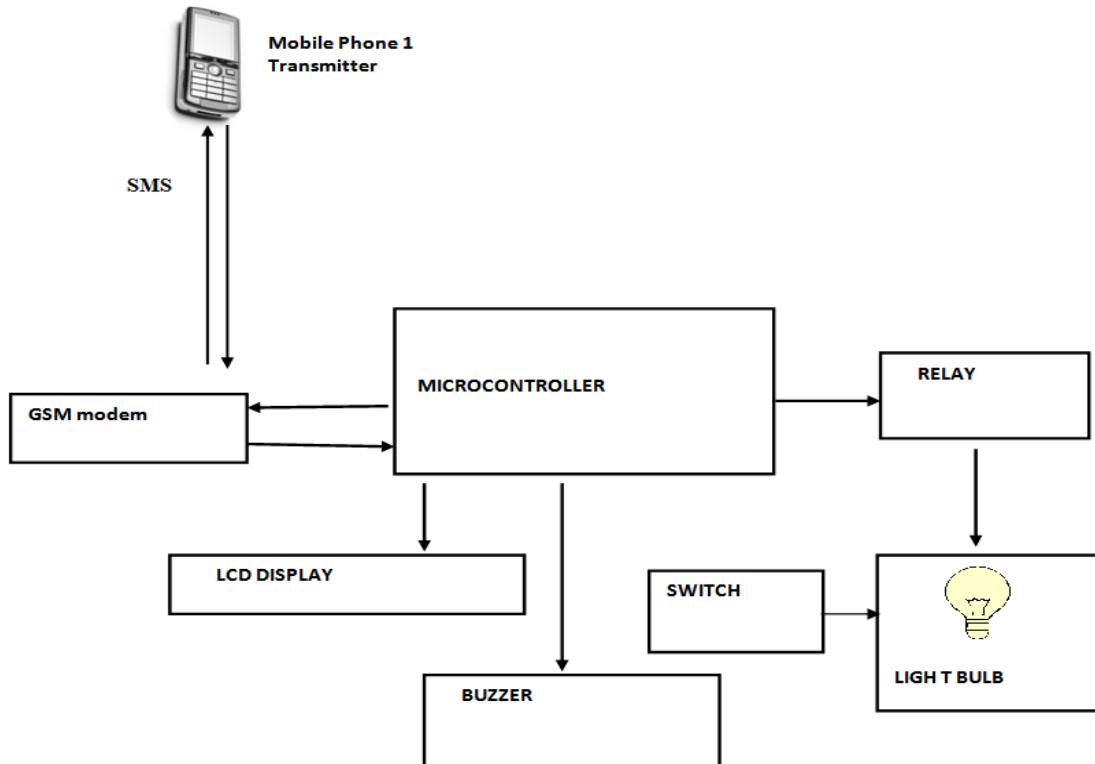
Figure 1: Block diagram of design

Principle of operation : The system is made up of two parts, namely; the transmitting part and receiving part. The transmitting part consists of a normal GSM phone which transmits signal via SMS. The receiving part consists of a microcontroller chip, a GSM modem, a buzzer, buttons and the appliance to be controlled .When the GSM phone transmits signal via SMS, the GSM modem receives it and sends it to the microcontroller. The microcontroller accesses the SMS and changes the state of the appliances if the signal is an appropriate code. When this is done, the microcontroller sends signal to the GSM modem to send back reply to the GSM phone via SMS. The switches are the alternative means of changing the state of the appliances. If the home owner is close to the transmitting end, he/she can use the Switch buttons to change the state of the appliances.The buzzer is for notification: to notify when there is a change of state. So whether one uses the switches or the GSM phone, a sound will be produced to notify a change of state. The display is a Liquid Crystal Display (LCD) which displays the signal processing results. For the security aspect, if one presses any of the switches, the GSM modem will send a signal via SMS to the GSM phone, notifying that there is a change of state in a particular appliance. Another security aspect is that if the cable of any of the appliances is cut, the GSM modem will also send a signal via SMS to the GSM phone notifying that a particular cable has been removed.

III. HARDWARE DESIGN ANALYSIS

The Buzzer Driver : The Buzzer requires a current of 30mAmps for proper operation as instructed by the datasheet.[4] The configuration is shown below.
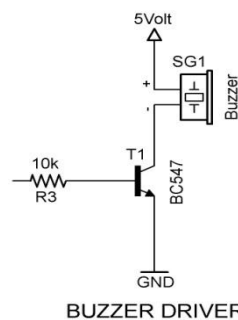
Figure 2: Buzzer driver.

The given transistor parameters are
Transistor (npn BC547)
Forward beta (β) = 290,

I_{CMAX} = 100mA,

Transistor's renowned equations

$$I_E = I_C + I_B \qquad (1)$$

$$I_C = \beta I_B \qquad (2)$$

From circuit analysis I_C = 30mA

$$30\ mA = 290 * I_B$$

$$I_B = \frac{30 * 10^{-3}}{290}$$

$$I_B = 0.000103448$$

$$I_B \cong 103.45\ \mu A$$

From the base emitter loop,

$$V_B - I_B R_B - V_{BE} = 0 \qquad (3)$$

$$I_B R_B = V_B - V_{BE}$$

$$R_B = \frac{V_B - V_{BE}}{I_B}$$

$$R_B = \frac{5 - 0.7}{103.45 * 10^{-6}}$$

$$R_B = 45432.5761$$

$$R_B \cong 45\ K\Omega$$

$$R_B \cong 43\ K\Omega$$

Using a smaller value of resistor that will yield a wider range of base current without endangering the transistor is ok but not exceeding the current limit of the base which is 500uAmps for 5mAmps of collector current and higher for higher values of the collector as well.

$$\therefore R_B \cong 10\ K\Omega$$

3.2 The Relay Driver

The current requirement of the coil of the relay is 30mAmps. The figure below depicts a typical connection of a relay driver.
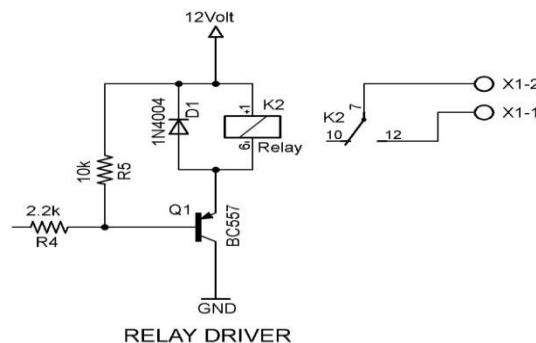
Figure 3: Relay driver

Considering a visual indication of the relay state, an LED was then included giving rise to the figure below.

RELAY DRIVER WITH INDICATOR
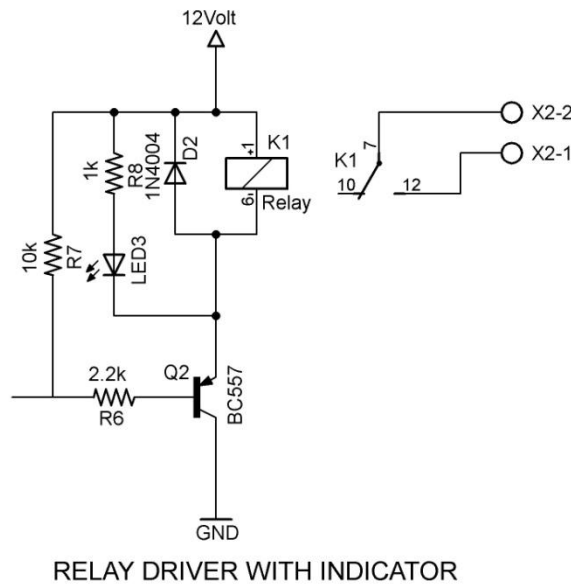
Figure 4: Relay driver with indicator

The component's parameters are
LED current: 10mAmps.
Relay coil current: 30mAmps
Transistor (npn BC557)
Forward beta (β) = 290,

I_{CMAX} = 100mA,
From circuit analysis I_C = 40mA

$$40 \ mA \ = \ 290 \ * \ I_B$$

$$I_B \ = \ \frac{40 \ * \ 10^{-3}}{290}$$

$$I_B \ = \ 0.000137931$$

$$I_B \ \cong \ 137.931 \ \mu A$$

From the emitter base loop,
The equivalent resistor of 1k(LED bias resistor) and 400(coil resistance) ohm is 285ohm and the loop equation is

$$V_{cc} \ - \ I_B R_{EQ} \ - \ V_{BE} \ - \ I_B R_B \ = \ 0 \qquad\qquad (4)$$

$$I_B R_B \ = \ V_{CC} \ - \ V_{BE} \ - \ I_B R_{EQ}$$

$$R_B \ = \ \frac{V_{CC} \ - \ V_{BE} \ - \ I_B R_{EQ}}{I_B}$$

$$R_B \ = \ \frac{12 \ - \ 0.7 \ - \ 138 \ * 10^{-6} \ * \ 285}{138 \ * 10^{-6}}$$

$$R_B \ = \ 81599.058$$

$$R_B \ \cong \ 82 \ K\Omega$$

The LCD Display : The display is used solely to display of project title and the indication of the status of the peripherals (lighting points), typical indications are:-
North light: ON
South light: OFF
West light: ON
East light: ON
Fluorescent: ON
        The title section is SMS CONTROLLED LIGHTING. The display supports 3.3volt for communication but tolerate 5volts for its logic io(input output) pins. The vdd must be a 3.3volt so two diodes(1N4148) is used to drop the voltage to a tolerable level of (5-2(0.7))= 3.6volts.

3.4 Power Supply
3.4.1 Transformer Design
The calculated load demand of the entire circuit is approximately 400mA; hence a transformer that is about 1000mA and above can be used for the circuit. Using a transformer with secondary voltage of 18V and current of 1000mA.
i.e. V_{ac} =18V
        I_{ac} = 1000mA
There are two quantities of interest with respect to the transformer design and their equations are

$$V_{AC} = \frac{V_{DC}}{1.41} \tag{5}$$

$$I_{AC} = \frac{I_{DC}}{0.62} \tag{6}$$

But

$$V_{DC} = Specified\ DC\ voltage + 2V_D \tag{7}$$

From equation (5)

$$V_{dC} = 1.41 * V_{AC}$$

$$V_{dC} = 1.41 * 18\ V$$

$$= 25.38\ V$$

From equation (6)

$$I_{dC} = 0.62 * I_{AC}$$

$$I_{dC} = 0.62 * 1000\ mA$$

$$= 0.62\ A$$

From equation (3.3)
        $V_{DC} = Specified\ DC\ voltage + 2V_D$
        Specified voltage = V_{DC} - $2V_D$
        Where V_D = 0.7volts

$$= (25.38 - 2(0.7))\ volts$$

$$= 23.98\ volts$$

3.4.2. Capacitor Design**:**
For the filter capacitor

$$C = \frac{I_{DC}}{(V_R * 100)} \tag{8}$$

$$V_W = 1.4 * V_{DC} \tag{9}$$

Where
        C   = Capacitance of the capacitor

V_R = ripple voltage

V_W = working voltage of capacitor

But

$$V_R = 0.48 * V_{DC} \tag{10}$$

$$= 0.48 \times 23.98 = 11.51V$$

From equation (7)

$$C = \frac{0.62}{(11.51 * 100)}$$

$$C = 538.7\mu F$$

$$V_W = 1.4 * V_{DC}$$

$$= 1.4 \times 23.98 = 33.57V$$

Hence a capacitor of 560µF, 50V and above can be used.
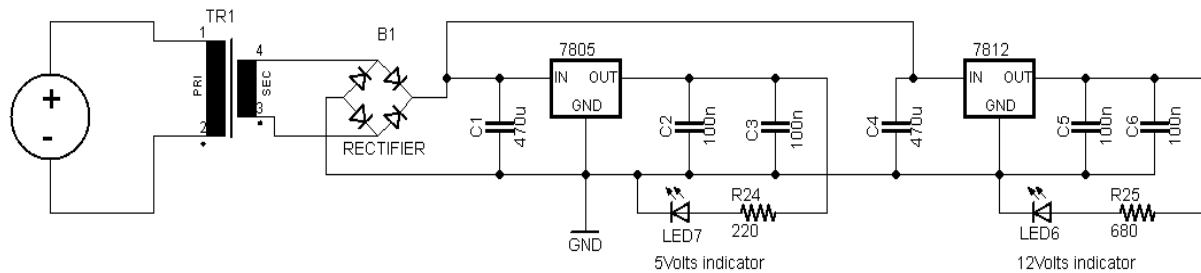
Figure 5: Power Supply Unit

From the circuit analysis, the load current is less than 500mA, so the parameters for design are V_m = 18v, … 500mA.

The voltage across the fitter capacitor

$$V_{r(peak)} = \sqrt{3} \, V_{r(RMS)} \tag{11}$$

$$= \sqrt{3} \frac{(2.4 I_{DC})}{C}$$

$$= \sqrt{3} \frac{(2.4)(500)}{560}$$

$$= \frac{2078.460969}{560}$$

$$V_{r(Peak)} = 3.712 \, V$$

$$V_{dc} = V_m - V_{r(peak)} \tag{12}$$

$$V_{dc} = (18 - 3.712) \, volts$$

$$V_{dc} = 14.28 \, volts$$

Since the voltage is greater than the minimum required voltage of the IC regulators, which are 7 volts and 12 volts respectively, the ICs can provide a reliable regulated voltage to the given load. Also, because the current required can be supplied by a bridge rectifier, a bridge rectifier IC chip was used and the output capacitor used for smoothing.

The Power indicator LED : The Power indicator LEDs used for this work are the conventional 5millimeter LED, though different colours are used its just for the purpose of differentiating 5volt rail from the 12volt rail. From datasheet, reference books and research materials, the current requirements of most common light emitting diodes (LEDs) are between 5mA to 20mA to give an appropriate radiation without endangering the LEDs.[4]
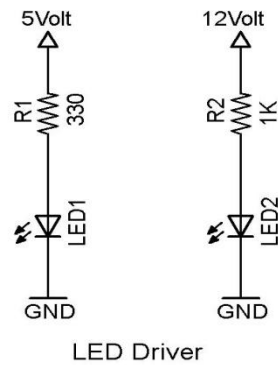
Figure 6: LED biasing

Given that,
Id = 10mA, (required current through LED)
Vd = 1.5volts, (voltage drop across LED)
Using KVL for a closed loop for LED1,

$$V_{CC\,1} - I_D R_1 - V_D = 0 \tag{13}$$

$$I_D R_1 = V_{CC\,1} - V_D$$

$$R_1 = \left(\frac{V_{CC\,1} - V_D}{I_D} \right)$$

$$R_1 = \left(\frac{5 - 1.5}{10 * 10^{-3}} \right)$$

$$R_1 = 350\ \Omega$$

$$R_1 \cong 330\ \Omega$$

Using KVL for a closed loop for LED2,

$$V_{CC\,2} - I_D R_2 - V_D = 0 \tag{14}$$

$$I_D R_2 = V_{CC\,2} - V_D$$

$$R_2 = \left(\frac{V_{CC\,2} - V_D}{I_D} \right)$$

$$R_2 = \left(\frac{12 - 1.5}{10 * 10^{-3}} \right)$$

$$R_2 = 1050\ \Omega$$

$$R_2 \cong 1000\ \Omega$$

3.6 The GSM Battery charging interface
        In order for the GSM phone to maintain its normal operation its required of it to have a steady supply of 5V luckily it has a battery in it but our paramount concern is charging it at regular interval,[5] this is achieved with the figure below.
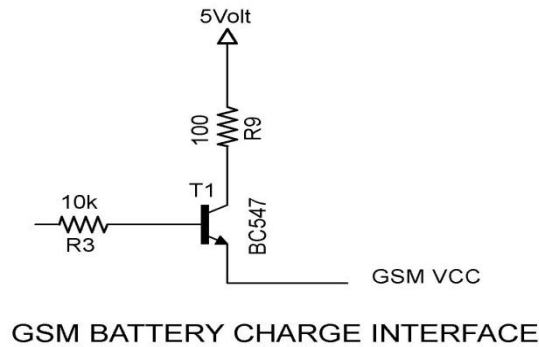
Figure 7: GSM Battery Charging Interface

From circuit analysis $I_C = 50mA$

$$50 \ mA \ = \ 290 \ * \ I_B$$

$$I_B \ = \ \frac{50 \ * 10^{-3}}{290}$$

$$I_B \ = \ 0.000172414$$

$$I_B \ \cong 172.414 \ \mu A$$

From the collector emitter loop,

$$V_{CC} \ - \ I_C R_C \ = \ 0$$

$$I_C R_C \ = \ V_{CC}$$

$$R_C \ = \ \frac{V_{CC}}{I_C}$$

$$R_C \ = \ \frac{5}{50 \ * 10^{-3}}$$

$$R_C \ = 100 \ \Omega$$

From the base emitter loop,

$$V_B \ - \ I_B R_B \ - \ V_{BE} \ = \ 0 \tag{15}$$

$$I_B R_B \ = \ V_B \ - \ V_{BE}$$

$$R_B \ = \ \frac{V_B \ - \ V_{BE}}{I_B}$$

$$R_B \ = \ \frac{5 - 0.7}{172.414 \ * 10^{-6}}$$

$$R_B \ = 24939.97$$

$$R_B \ \cong 22 \ K\Omega$$

The base resistor also maintains its available value which is 10K

3.7 The GSM interface

The GSM interface is solely for proper connection from the Mobile phone to the microcontroller because the GSM interface requires a 3.3V for its transmit and receive pins whereas the microcontroller provides 5v hence this interface circuit enables the 5v from the microcontroller to be converted to 3.3v before sending to the GSM pins for proper communication. The circuits below illustrate the spelt out principle.
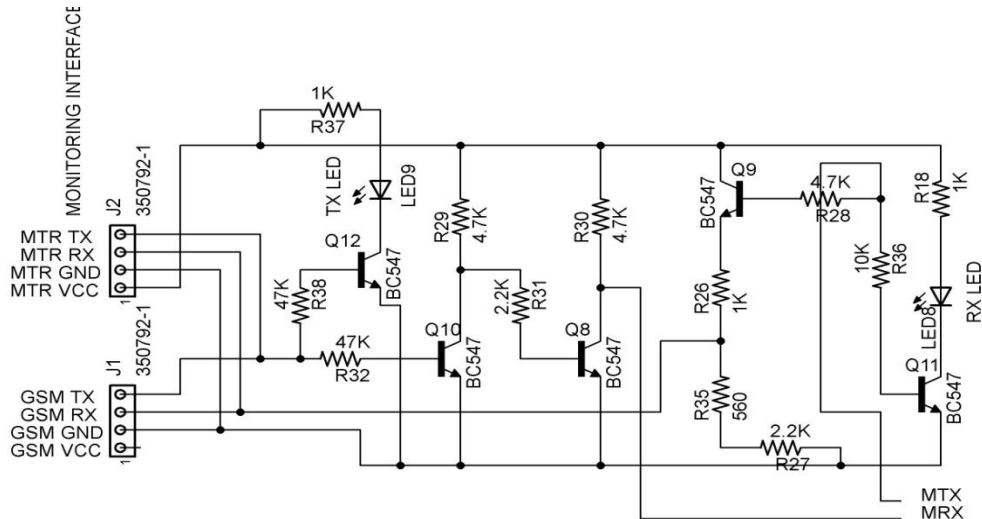
Figure.8: GSM Communication Interface

Switches : These five buttons are use to switch the five lighting point in question which are North light, South light, East light, West light and the fluorescent to the desirable states which is either ON or OFF, though the main function of these is purely toggling of state.

A typical switch or button connection used in a digital application is shown the figure below.
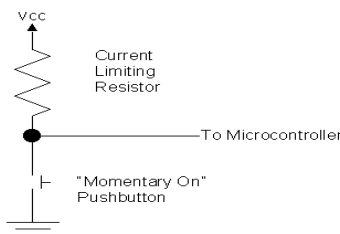
Figure 9 button press configuration

"Bouncing" is the term used to describe what happens when the switch is closed or opened. Instead of a single, square edge as you may expect, a switch change consists of many short spikes, this as a result of the button's contacts "bouncing" during the transition. [6]This is shown in the diagram below:
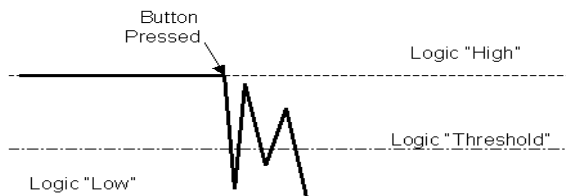
Figure10: illustration of button de-bouncing

Multiple Switch with ADC pin/Comparator : The ADC peripheral of the microcontroller can be used to detect one or more switch closings by using a few resistors. As shown in figure below
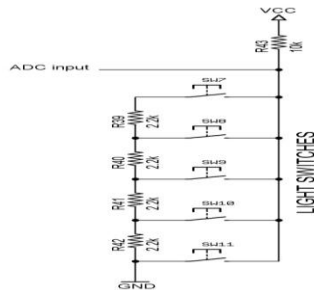
Figure11: Multiple button with ADC configuration

From the figure above any button pressed registers a different level of voltage to the ADC pin.

The complete circuit diagram is shown below with its individual parts included.

SMS CONTROLLED LIGHTING
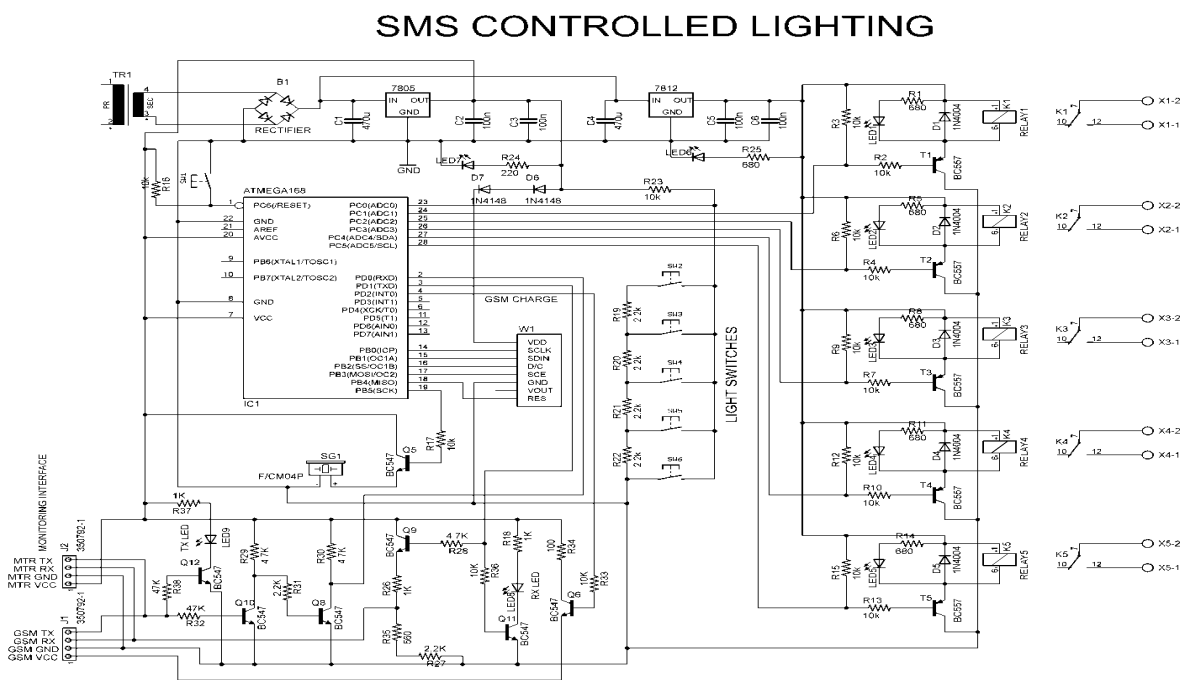
Figure 12: complete schematic diagram of SMS controlled lighting

IV SOFTWARE DEVELOPMENT

4.1Microcontroller Operations : This paper uses software for the microcontroller and the computer system. These programs were written using embedded C language, AT command and visual basic 6.0. Software development involves a series of steps which are necessary for the development of reliable and maintainable software. It is of great importance because hardware design cannot be of use in a microprocessor based system without dependable software. A. The flow chart is shown fig. 11 below.
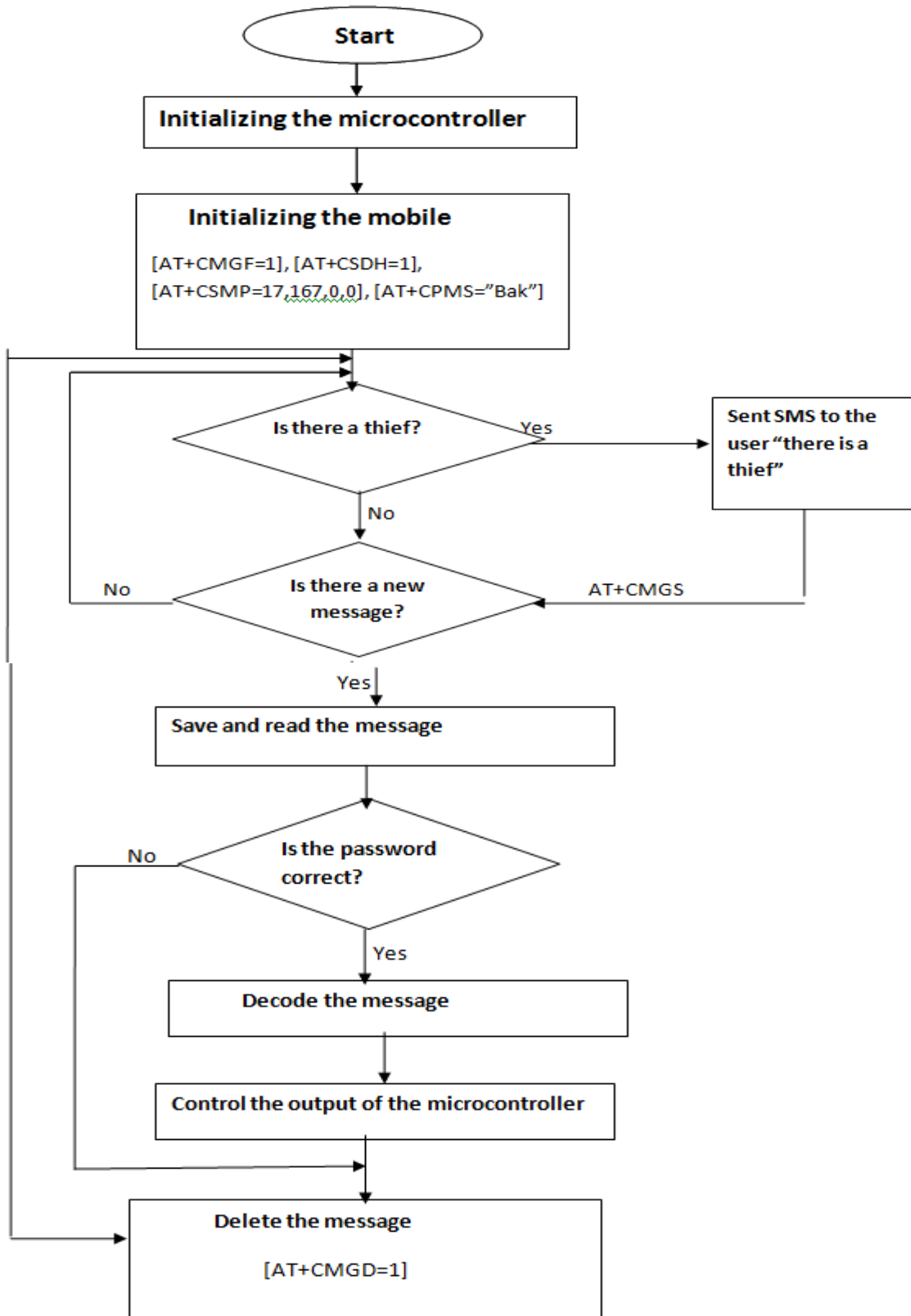
Figure11: Software programming flow chart

GSM phone and AT commands : The communication between the GSM module and the microcontroller is achieve through AT(Attention) commands with a serial communication protocol of UART(universal Asynchronous Receiver and Transmitter), with frame format parameters of 9600Baud rate, 8bit data, 1 start bit, 1 stop bit and no parity bit below are some command definitions to the GSM module are shown below.

4.2.1Command Definition

AT+CSCA: Set the SMS center address. Mobile-originated messages are transmitted through this service center.

AT+CMGS: Send short message to the SMS center

AT+CMGR: Read one message from the SIM card storage

AT+CMGD: Delete a message from the SIM card storage

AT+CMGF: Select format for incoming and outgoing messages: zero for PDU mode, one for Text mode

*AT+CSMP***:**   Set additional parameters for Text mode messages

All commands to the microcontroller is done with SMS, these messages have a format of COMMAND.SUBCOMMAND.PERIPHERAL#PIN

The command in this case is switch.

The subcommand is either ON, OFF or TOGGLE.

The peripheral is either of the five lighting points.

The pin is a four digit numeral personal identification number (pin).

So the typical format will be,

Switch.on.north light#0123

V. CONCLUSION

The Switching of Security Lighting System using GSM was discussed and the aim of the work which is the design and implementation of a GSM based Security Lighting system Controller has been completed. This system would make it easier for man to Control Security Lighting system from a distance. For places where GSM coverage is not available, there is need for the installation of GSM base transceiver stations, since the system operation is largely dependent on availability of efficient communication (network) coverage.

REFERENCES

[1] Friedhelm Hillebrand, "GSM and UMTS: The Creation of Global Mobile Communication", John Wiley, 2002

[2] C.O. Ohaneme, K.A. Akpado, E.N. Ifeagwu and C.O. Ezeagwu ,Implementation and Analysis of a GSM-Based Security System with Emergency Control, International Journal of Electronics Communication and Computer Engineering ,Vol. 5, Issue 1, 2014 pp 134 - 141

[3] The History of Text Messaging. Available:http://www.vxcl.org.htm/

[4] CD4017B Data Sheet (1999). [Online] Available: http://www.datasheetsdir.com/cd4017+download

[5] Delgado, A. R., Picking, R., & Grout, V. Remote-controlled home automation systems with different network technologies.Proceedings of the 6th International Network Conference (INC 2006), University of Plymouth, 11-14 July 2006, pp. 357-366. Retrieved from http://www.newi.ac.uk/groutv/papers/p5.pdf

[6] Boylestad, R. L. and Nashelsky, L. Electronic Devices and Circuit Theory, 7th Edition, Prentice-Hall Publications, Inc., New Jersey, 1999

[7] Neamen, D. A. Electronic Circuit Analysis and Design, 2nd Edition, McGraw-Hill, Inc., New York., 2001

| Research Paper | Open Access |

Recycling of Scrapped Mating Rings of Mechanical Face Seals

Oshuoha,I.C[1].,Tuleun,L.T[2],Oseni,M.I[3]

[1,2,3]*(Department of Mechanical Engineering, University of Agriculture, Makurdi, Nigeria)*

ABSTRACT : *Mechanical face seal is an auxiliary part of the equipment for process plant. They are expensive components, butthe mechanical face seals hardly functions for 1,000hours in operation before failure. As there is no use for the scrapped mating ring and absence of recycling companies especially in the less developed countries of the world, disposal of scrapped mechanical face seals is a serious problem. These seals are non-biodegradable. The success of this work will not only provide employment opportunities for people, production of cheaper machine (single point turning) tools for machine shops and a cleaner environment but, would also provide a relatively new area for researchers to work on.*

KEYWORDS : *auxiliary, disposal, environment, failure, scrapped*

I. INTRODUCTION

Mechanical face seals are mechanical components of equipment used for preventing leakages automatically in pipes and piping systems. Mechanical face seals are extensively used in centrifugal systems such as refineries, chemical and other industries where flow of fluids are required. The mechanical face seals, contains mating ring which is made of cemented carbides. Cemented carbides are classified into tungsten carbides and titanium-tungsten carbides [4].Manufacturing technology and machining processes mark a major distinction between Engineers and Scientists of developed countries and those of the less developed countries. In the case of the former, the manufacturing technology and machining processes have been fully explored and adequate attention given while in the latter there is little or no attention given to these processes. The technicians and technologists from less developed countries perform their duties adopting trial and error methods. This has led to backwardness because many materials, energy, time and money are expended on trials. The high rate of growth in manufacturing processes can only be achieved through improved manufacturing processes, methods and tooling not by trial and error [2]. It is worthy of note that technological advancement is aimed at lowering production cost, achieving higher quantity and better quality products. This goal can only be attained through optimal utilization of both human and material resources.

A lot of these non-leakage devices are used in the refinery and other piping systems. Large users agree in attributing a large proportion of process plant maintenance cost to mechanical seal failures [5]. The mechanical face seals are used for sealing products such as sour water, slop oil, liquefied petroleum gas, straight run kerosene, dehydrate gas oil, automotive gas oil, reformate gasoline, oil furfural mix and waste heat boiler [7].Mechanical face seal is a device that creates a non-leaking union between two machines or making a joint fluid-tight. The sealing occurs between surfaces, which moves relative to one another and involves the sealing of an annular relative motion. Mechanical face seals have extensive applications in places where centrifugal systems are required numerous power plant equipment applications, especially on pumps of different sizes and pressure ratings. Though, they are expected and are capable of rendering long-term service, mechanical face seals often times exhibit unsatisfactory performance by failing unexpectedly, resulting in a short life span. This reduces plant reliability and performance, which leads to expensive down-times and outages. The hardware are those components needed for installation on pumps and to ensure high process performance and reliability. The mechanical face seal is made up of: mating ring, rotating face, springs, secondary seal, tertiary seal, snap ring, disc plate and retainer.

II. MATERIALS AND METHODS

Tungsten carbide areexpensive. On the account of high cost, low strength and the difficulties of preparation of tungsten carbide, brazing a tip or block of the carbide to a carbon-steel shank produces carbide-

cutting tools. The most suitable metal for the shank is steel of about 0.5% carbon, in order to minimize the injurious effects of vibration and chatter on the brittle tip, the shank should be of generous cross-sectional proportion. To accommodate the tip a step or cavity is machined. Care being necessary to ensure that all surfaces are flat so that the tip is everywhere supported against pressure introduced when cutting. Failure to do this might result in bending stresses being introduced on the tip in service and its subsequent cracking. For securing the tip, brazing is usually employed [1]. Tungsten carbide is very hard, although by nature quite brittle, but nevertheless usable for some applications, such as dies and turning/cutting tools. Brazing is generally used when a tougher, stronger joint is required, provided that the work will be neither melted nor otherwise damaged by the higher temperatures involved in melting the brazing solder. Most ferrous and non-ferrous alloys of sufficiently high melting point can be brazed [3].The scrapped mating ring of mechanical face seal was obtained from the Kaduna Refinery and Petrochemical Company Limited, Kaduna. The mating ring was broken and the locally produced turning tools were produced at Jeo Best Welding Enterprise, Agbor. The machining of the various work pieces and the measurement of the tool vibrations were done at J & B Construction Company, Umunede. The chemical analysis of the mating ring and the measurement of the surface finish was performed at Delta Steel Company, Limited

III.   MATERIALS FOR PHYSICAL TESTS
The materials used include hand lens, liquid dye penetrant, and magnets.

Materials for production of the turning tools
The following materials were used for the production of the turning tools;
a.   mating ring;
b.   vice (heavy metal plate);
c.   maundy hammer;
d.   used synthetic cement (baggco) bag;
e.   metal plate;
f.   shanks of 0.5% carbon steel;
g.   brazing powder;
h.   oxy-acetylene welding device;
i.   grinding wheel/stone;
j.   lapping stone, pliers; and
k.   bevel and bevel protractor.
Both the locally produced and the standard tungsten carbide tools' were grinded to positive rake angle of $8°$ The physical and chemical properties of the scrapped mating ring is compared with that of standard tungsten carbide tools.

IV.   MATERIALS FOR CHEMICAL ANALYSIS
The material used for the chemical analysis of the mating ring is the digital spectrometer – GNR F20 metal analyzer.

Physical Tests
Visual Inspection : The first test performed on the scrapped mating ring was the visual inspection test. The naked eyes, hand lens and the liquid dye penetrant were employed. The defects could not be detected with the naked eyes, though it was observed that the mating ring had fine grain particles. The hand lens was used, this confirmed that the scrapped mating ring has a fine grain size, but revealed the presence of defects. The liquid dye penetrant used was bright red, while the developer was white. This made the defects easier for the naked eyes to view.

Magnetic Test : The scrapped mating ring was tested for magnetic properties using magnets of different types. Destructive Testing The destructive tests performed on samples of the mating ring, were hardness and impact test. This determined the resistance to shock loading and brittleness of the scrapped mating ring as described by Mohammed [6].

Production of turning tools : The scrapped mating ring is shown in plate 1. A synthetic used cement (baggco) bag was used to parcel the scrapped mating ring and placed on a heavy metal plate. It was then hit with the maundy hammer. This resulted in the shattering of the mating ring. Pieces of the mating ring were brazed onto shanks of 0.5% carbon of dimension 100mm by 20mm by 20mm, as a support for their cutting tips and edges.

The seating of the pieces of the mating ring are filled with the brazing powder/material, then the brazing was carried out using the oxy-acetylene gas welding

flame and aclamp. The grinding of the tools was performed on a tool cutter grinder to ensurecorrect cutting tool geometry. The tool was clamped on single point cutting tool attachment and asilicon carbide grinding stone fixed to the machine spindle. The tools produced were set andground, thereafter they were polished on a lapping stone to give a smooth surface finish. Plate 2shows the broken pieces of the scrapped mating ring. While plate 3 shows the samples ofproduced turning tools.

Plate 1: Scrapped Mating Ring

Plate 2 : Broken Pieces of Scrapped Mating Ring

Plate 3 : Samples of Produced Turning Tools

Chemical analysis : Chemical analysis was performed using a digital spectrometer - GNR F20 metal-analyzer. The digital spectrometer. A piece of the mating ring was placed on the spectrometer and sparked in an argon filled inlet, the rays were transmitted into a vacuum containing a spherical mirror which collimated the divergent light rays. The collimated light was diffracted by a plane grating and the resulting spectrum which was a measure of the different wavelengths of the constituent elements of the material, was analysed in an interfaced computer. The result produced:

a.   chemical composition; and
b.   percentage composition of the scrapped mating ring.

V.   RESULTS

Physical Tests
Visual Inspection : This revealed that the mating ring possessed some defects and that it has fine grainsize.

Magnetic Test : The pieces of mating ring were observed to possess magnetic properties as they weremagnetized by various magnets.

Hardness Test : Hardness testing results as shown in Table 1.

Chemical Analysis
Qualitative Analysis : The result of the qualitative analysis, showed that the mating ring is made up of : tungsten, carbon and cobalt, as shown in Table 1.

Quantitative Analysis : Table 1, gives the percentage composition of the mating ring and compared with that ofa standard tungsten carbide tool.

Machining/Turning Test Results : The various single point turning tools were used to machine carbon steel on the lathe machine,produced at a positive rake angle of 8° under the condition :At a speed of 180m/min , a feed of0.10mm/rev and varying the depth of cut from 0.1mm,0.2, …. 0.5mm.

TABLE 1 : CHEMO-PHYSICAL TEST ANALYSIS

Cutting Tool	Chemical Composition (%)	Grain size	Hardness HRA
Standard Tungsten Carbide	W = 87.7 Co = 10 C = 2.3	fine	91.1
Scrapped Mating Ring	W = 85 Co = 12 C = 3	fine	89.5

TABLE 2: RESULTS OF MACHINING CARBON STEEL WITH LOCALLY PRODUCED TOOLS.

Depth of Cut (mm)	Surface vibration Finish (/Um)	Freq (c/s)	Cutting Force (kgf)	Cutting Speed (m/min)
0.1	1.23	1.50	2.41	180
0.2	1.31	1.65	4.82	180
0.3	1.35	1.86	7.23	180
0.4	1.44	2.05	9.64	180
0.5	1.52	2.25	12.05	180

VI.   CONCLUSION

The hardness and chemical composition of the scrapped mating ring is very close to that of the standard tungsten carbide turning tool, which accounts for their closeness in chemo-physical properties.The machining results, shows that the tool produced from scrapped mating ring of mechanical face seal is comparatively suitable for use as single point turning tools in machine tools' workshop.

The following are recommendations :

(i) recycling of mechanical face seals for the production of turning tools should be

encouraged; and

(ii) further research in this area is desirable.

REFERENCES

[1]   Chapman W.A. J, (1979).Workshop Technology and Practice, 4th edition part 3, Pp189 – 191.
[2]   Ghosh A. and Mallik A.K, (1987). Manufacturing Science, (Engineering Science), Elllis Horwood series, New York, John Wiley & Sons Inc .Pp 30-36.
[3]   Higgins R.A, (1987).Engineering Metallurgy(Applied Physical Metallurgy), 6th edition,London, Edward Arnold Ltd. Pp632-7.
[4]   Kempster, M.H.A, (1975). Materials For Engineers, Hodder and Stoughton, London.Pp 213-219.
[5]   Leebeck A.O, (1991).Principle and Design of Mechanical Face Seal, New York,John Wiley & Sons Inc. Pp1-24.
[6]   Mohammed H.A, (2005). Developing an alternative use for scrapped kaduna refinery andpetrochemicals Kaduna, mating ring of mechanical face seals. PG researchthesis.Department of Mechanical Engineering, University Of AgricultureMakurdi, Nigeria. 105pp
[7.]   Nigerian National Petroleum Corporation, (1979). K.R Project, volume iv -7 mechanicalcatalogue for process unit (pumps and drivers).

Research Paper | Open Access

Improved RSA cryptosystem based on the study of number theory and public key cryptosystems

Israt Jahan, Mohammad Asif, Liton Jude Rozario
Department of Computer Science & Engineering, Jahangirnagar University, Savar, Dhaka, Bangladesh
Department of Computer Science & Engineering, Jahangirnagar University, Savar, Dhaka, Bangladesh
Department of Computer Science & Engineering, Jahangirnagar University, Savar, Dhaka, Bangladesh

ABSTRACT: *Security is required to transmit confidential information over the network. Security is also demanding in wide range of applications. Cryptographic algorithms play a vital role in providing the data security against malicious attacks. RSA algorithm is extensively used in the popular implementations of Public Key Infrastructures. In asymmetric key cryptography, also called Public Key cryptography, two different keys (which form a key pair) are used. One key is used for encryption and only the other corresponding key must be used for decryption. No other key can decrypt the message – not even the original (i.e. the first) key used for encryption. In this* paper*, we have proposed an* improved approach *of RSA algorithm using two public key pairs and using some mathematical logic rather than sending* one public key d *ire*ctly.*Because if an attacker has* an *opportunity of getting the* public key componet *they can find* private *key value by brute force search.*
General Terms: Cryptography, network security

KEYWORDS: IRSA, RSA, security, cryptography

I.   INTRODUCTION

Number theory may be one of the "purest" branches of mathematics, but it has turned out to be one of the most useful when it comes to computer security. Sensitive data exchanged between a user and a Web site needs to be encrypted to prevent it from being disclosed to or modified by unauthorized parties. The encryption must be done in such a way that decryption is only possible with knowledge of a secret decryption key. The decryption key should only be known by authorized parties.

In traditional cryptography, such as was available prior to the 1970s, the encryption and decryption operations are performed with the same key. This means that the party encrypting the data and the party decrypting it need to share the same decryption key. Establishing a shared key between the parties is an interesting challenge. If two parties already share a secret key, they could easily distribute new keys to each other by encrypting them with prior keys. But if they don't already share a secret key, how do they establish the first one? This challenge is relevant to the protection of sensitive data on the Web and many other applications like it. This line of thinking – in pre-Web terminology – prompted two Stanford University researchers, Whitfield Diffie and Martin Hellman, to write a landmark paper, "New Directions in Cryptography" in 1976 [6]. The paper suggested that perhaps encryption and decryption could be done with a pair of different keys rather than with the same key. The decryption key would still have to be kept secret, but the encryption key could be made public without compromising the security of the decryption key. This concept was called public-key cryptography because of the fact that the encryption key could be made known to anyone.

The full public-key method would come a year later as an application of another famous problem, integer factorization[11].

II.   RSA CRYPTOSYSTEM

The Rivest-Shamir-Adleman (RSA) cryptosystem is one of the best known public key cryptosystems for key exchange or digital signatures or encryption of blocks of data. RSA uses a variable size encryption block and a variable size key. The key-pair is derived from a very large number, n, that is the product of two prime numbers chosen according to special rules; these primes may be 100 or more digits in length each, yielding an n

with roughly twice as many digits as the prime factors.

The public key information includes n and a derivative of one of the factors of n; an attacker cannot determine the prime factors of n (and, therefore, the private key) from this information alone and that is what makes the RSA algorithm so secure.

2.1 RSA Key Generation Algorithm:

1. Generate two large random primes, p and q, of approximately equal size such that their product n = pq is of the required bit length, e.g. 1024 bits.
2. Compute n = pq and (φ) phi = (p-1)(q-1).
3. Choose an integer e, 1 < e < phi, such that gcd(e, phi) = 1.
4. Compute the secret exponent d, 1 < d < phi, such that ed ≡ 1 (mod phi).
5. The public key is (n, e) and the private key is (n, d). Keep all the values d, p, q and phi secret.

- ☐ n is known as the modulus.
- ☐ e is known as the public exponent or encryption exponent or just the exponent.
- ☐ d is known as the secret exponent or decryption exponent.

2.2 Encryption Algorithm

Sender A does the following:-
1. Obtains the recipient B's public key (n, e).
2. Represents the plaintext message as a positive integer m
3. Computes the cipher text $c = m^e \bmod n$.
4. Sends the cipher text c to B.

2.3 Decryption Algorithm

Recipient B does the following:-
1. Uses his private key (n, d) to compute $m = c^d \bmod n$.
2. Extracts the plaintext from the message representative m.

III.   NUMBER THEORY BEHIND RSA:

III.1 Prime Generation and Integer Factorization

Two basic facts and one conjecture in number theory prepare the way for today's RSA public-key cryptosystem.

FACT 1. **Prime generation is easy:** It's easy to find a random prime number of a given size.

This is a result of two other points: Prime numbers of any size are very common, and it's easy to test whether a number is a prime – even a large prime.
According to the Prime Number Theorem, the expected number of candidates to test will be on the order of ln x (the natural logarithm of x) where x is a typical number of the intended size.
"Large" in the cryptographic context typically means 512 bits (155 decimal digits) or more.

FACT 2. **Multiplication is easy:** Given p and q, it's easy to find their product, n = pq.

There are many efficient ways to multiply two large numbers.

CONJECTURE 3. **Factoring is hard:** Given such an n, it appears to be quite hard to recover the prime factors p and q.

Despite hundreds of years of study of the problem, finding the factors of a large number still takes a long time in general. The fastest current methods are much faster than the simple approach of trying all possible factors one at a time. (Such a method would take on the order of n steps.) However, they are still expensive. For instance, it has been estimated recently that recovering the prime factors of a 1024-bit number would take a year on a machine costing US $10 million. A 2048-bit number would require several billion times more work. [11]

III.2 Modular Exponentiation and Roots

Given this background, n will hereafter denote the product of two large, randomly generated primes. Let m and c be integers between 0 and n-1, and let e be an odd integer between 3 and n-1 that is relatively prime

to p-1 and q-1, meaning the following equation has to be satisfied:

gcd(e,(p-1).(q-1))=1

The encryption and decryption operations in the RSA public-key cryptosystem are based on two more facts and one more conjecture:

FACT 4.**Modular exponentiation is easy:** Given n, m, and e, it's easy to compute c = m^e mod n.

The value m^e mod n is formally the result of multiplying e copies of m, dividing by n, and keeping the remainder. This may seem to be an expensive computation, involving e-1 multiplications by m with increasingly large intermediate results, followed by a division by n. However, two optimizations make the operation easy:

     1. Multiplying by an appropriate sequence of previous intermediate values, rather than only by m, can reduce the number of multiplications to no more than twice the size of e in binary.

     2. Dividing and taking the remainder after each multiplication keeps the intermediate results the same size as n [2].

FACT 5. **Modular root extraction – the reverse of modular exponentiation – is easy given the prime factors:** Given n, e, c, and the prime factors p and q, it's easy to recover the value m such that c = m^e mod n.

The value m can be recovered from c by a modular exponentiation operation with another odd integer d between 3 and n-1. In particular, for this d, the following holds for all m:

m = (m^e)^d mod n .

This integer d is easy to compute given e, p, and q.

CONJECTURE 6. **Modular root extraction is otherwise hard:** Given only n, e, and c, but not the prime factors, it appears to be quite hard to recover the value m.

We will want to compute d from e, p and q , where d is the multiplicative inverse of d. It means

    e.d=1(mod Ø(n))

IV.   PROPOSED IRSA(IMPROVED RSA)ALGORITHM

     RSA is a block cipher in which the plaintext and cipher text are integers between 0 and *n*- 1 for some *n*. Encryption and decryption are of the following form, for some plaintext block M and cipher text block C:

C = *M$^{y/x}$*mod *n*

M = *C^d*mod *n* = (*M$^{y/x}$*)^{d}mod *n.*

Both sender and receiver must know the values of *n, y and x* only the receiver knows the value of *d.*

IV.1   Process of Encryption and Decryption:

This is a public key encryption algorithm with a public key of *KU = {y,n},{x}* and a private key of *KR = {d,n}.* For this algorithm to be satisfactory for public-key encryption, the following requirements must be met:

1. It is possible to find values of *y, x, d, n* such that (*M$^{y/x}$*) ^{d}= M mod *n* for all M<*n.*

2. It is relatively easy to calculate *M$^{y/x}$* and *C^d* for all values of M <*n.*

3. y is a multiple of x and e (which the public key in the normal RSA algorithm)
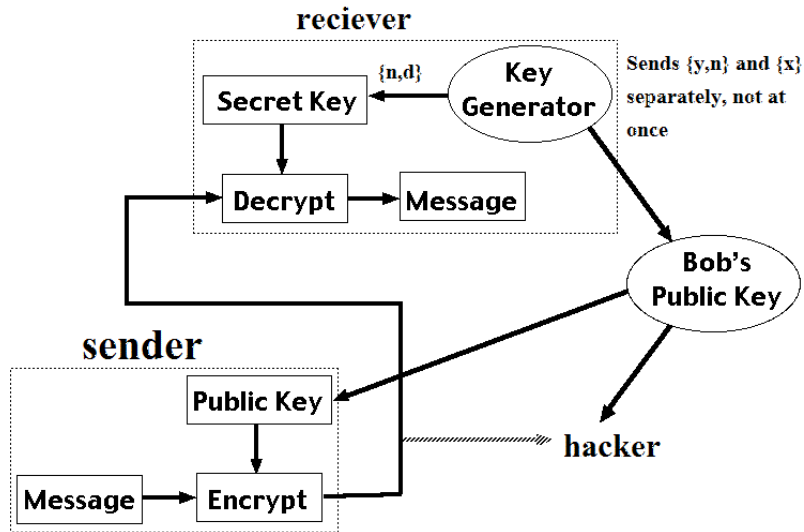
figure1 : process of IRSA algorithm

IV.2   Computational Steps:

• Begin by selecting two prime numbers, *p* and *q,* and calculating their product *n,* which is the modulus for encryption and decryption.

• Next, we need the quantity φ*(n) re*ferred to as the Euler totient of *n,* which is the number of positive integers less than *n* and relatively prime to *n.*

• Then select an integer *e* that is relatively prime to φ*(n) (i.*e., the greatest common divisor of *e* and φ*(n)* is 1).

• Select two numbers x and y such that y=xe

• Using this numbers formulate two public key {y,n},{x}

• Finally, calculate *d* as the multiplicative inverse of *e (which is public key in normal RSA),* modulo φ*(n).*

• Suppose that user A has published its public key and that user B wishes to send the message *M* to A.

• Then B calculates $C = M^{y/x}$(mod *n)* and transmits C.

V.   EXPERIMENTAL RESULTS

 In order to justify the performance we used different modulus length(256 bits, 512 bits,1024 bits) and the block sizes (128 bits,256 bits,512 bits,1024 bits). The two following table shows the experimental results of RSA and IRSA respectively.

TABLE 1: Table of experimental result on RSA

bitlength(n)	blocksize in bits	key generation(x) MS	Encryption time(y) MS	Decryption time(z) MS	Total time t=x+y+z MS
256	128	50	59	360	469
512	256	175	88	909	1172
1024	512	600	123	2710	3433

TABLE 2: Table of experimental result on IRSA

bit length(n)	blocksize in bits	key generation(x) MS	Encryption time(y) MS	Decryption time(z) MS	Total time t=x+y+z MS
256	128	63	67	368	498
512	256	187	97	918	1202
1024	512	612	133	2728	3473

The key genaration time comparison of RSA and IRSA is below
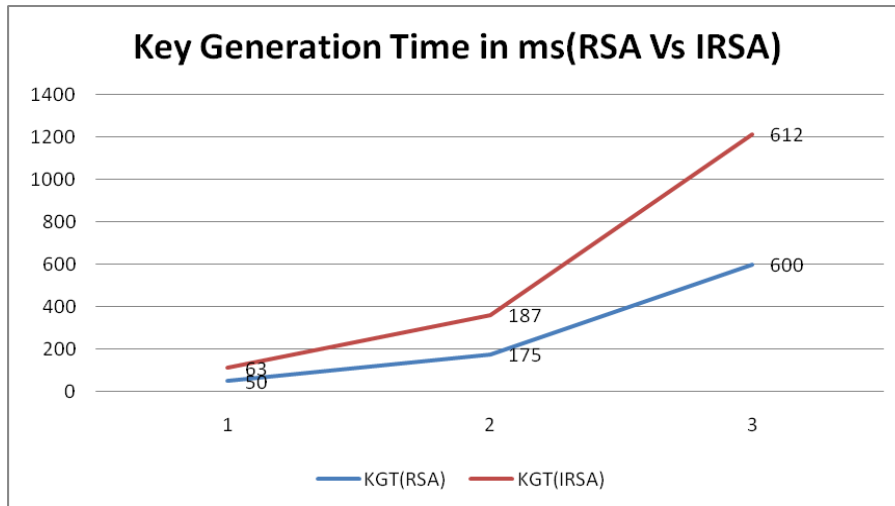
figure 2: Key generation time comparison of RSA and IRSA in ms

From the above figure it is clear that the key generation time in IRSA is greater than RSA key generation time as IRSA requires additional x and y to be generated.
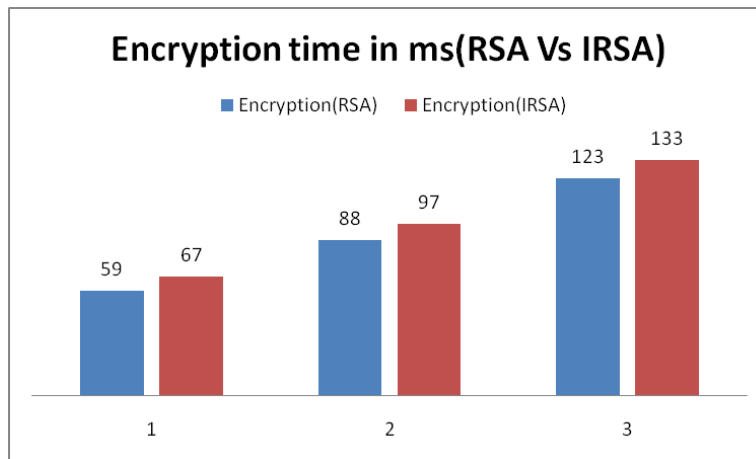
figure 3: Encryption time of RSA and IRSA

The above figure shows the encryption time of RSA and IRSA. As it is seen from the figure that IRSA takes more time than RSA to encrypt(in mili second),but the difference is very few.

The following figure shows the decryption time of RSA and IRSA and it is also of similar behaviour like figure 5.2, that is decryption time of IRSA is more than RSA.
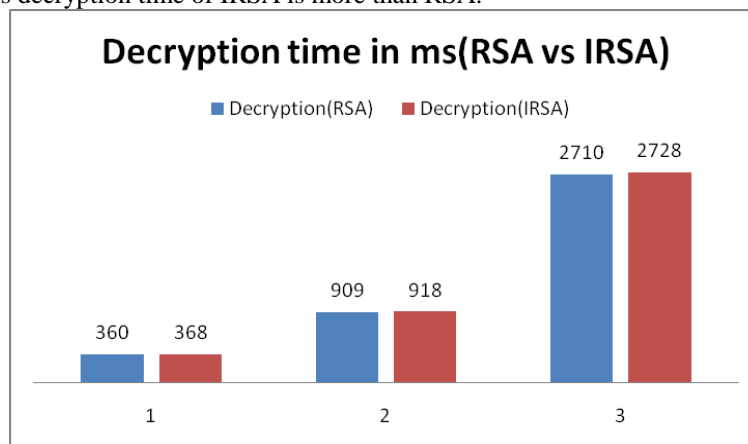
figure 4: Decryption time of RSA and IRSA

The total time comparison(including key generation,encryption and decryption)of RSA and IRSA is below:
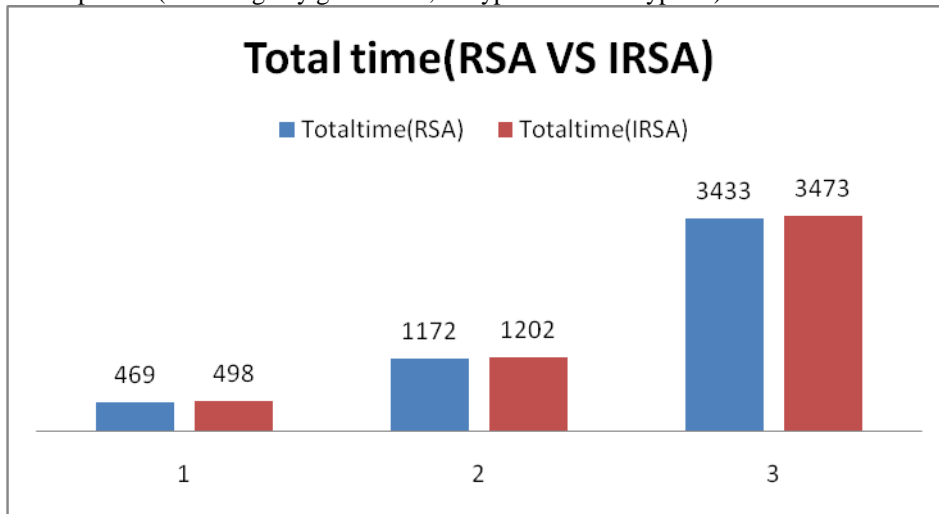
figure 5: Total time comparison of RSA and IRSA in ms (key generation+encryption+decryption)
The overall comparison between RSA and IRSA can be better seen from the following pi chart.
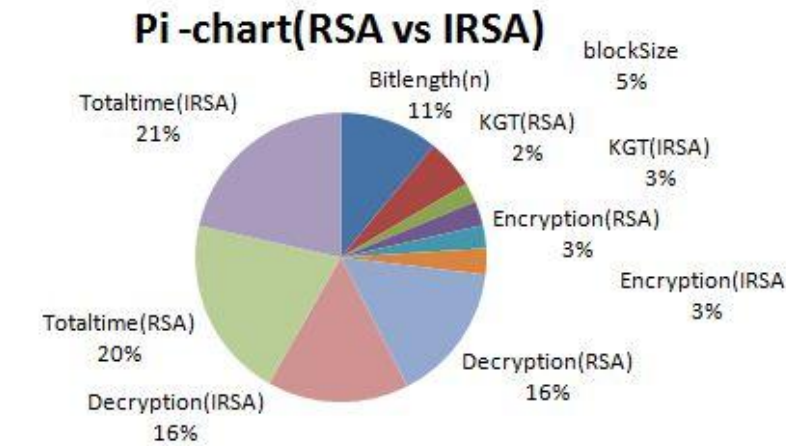
figure 6: pi-chart of overall comparison between RSA and IRSA

The table below shows the comparison between RSA and IRSA

TABLE 3: Table of comparison between RSA and IRSA

RSA	IRSA
Use only one public key	Use two public key
Less communication overload	High communication overload
More vulnerable to brute force attack	Less vulnerable to brute force attack
Less secure	More secure
The Public key is sent once	The Public key is sent separately twice

VI.   CONCLUSION

This research is a study of number theory and pulic key cryptosystems and based on this improving the RSA cryptosystem that is more reliable to brute force attack.RSA cryptosystem produces one public key to encrypt the message. Though it is hard to find out the factors of n and get p and q, two large prime numbers, therefore brute force attack is more difficult in our proposed algorithm as the encryption keys are sent separtely, not at once. The proposed RSA is used for system that needs high security but with less speed.

REFERENCES

[1] Shilpa M Pund, Chitra G Desai. Implemantation of RSA using Mersenne Prime. International Journal of Networking & Parallel Computing. Volume 1, Issue 3, Dec 2012-Jan 2013.

[2] S. Sharma, J.S. Yadav, P. Sharma. Modified RSA Public Key Cryptosystem Using Short Range Natural Number Algorithm. International Journal of Advanced Research in Computer Science and Software Engineering, volume 2, Issue 8, August 2012

[3] P.Saveetha,S. Arumugam, Study on improvement in RSA algorithm and its implementation.Volume 3, Issue 6,7,8 ,2012.

[4] P.S.Yadav, P. Sharma, Dr. K. P. Yadav, Implementation of RSA algorithm using Elliptic Curve algorithm for security and performance enhancement, International Journal of Scientific & Technology Research, Volume 1, Issue 4, May 2012.

[5] D. Pugila, H. Chitrala, S. Lunawat, P.M. Durai Raj Vincent, An Efficient Encryption Algorithm Based On Public Key Cryptography. International Journal of Engineering and Technology, Volume 5 No 3,Jun-2013.

[6] Burt Kaliski, "The Mathematics of the RSA Public-key Cryptosystem RSA Laboratory.

[7] Fatema Chowdhury, Munibur Rahman Chowdhury, "Essentials of Number Theory",Pi Publications,Dhaka Bangladesh.2005

[8] B.A. Forouzan, Cryptography & Network Security, Tata Mcgraw Hill publishing company limited, 2010.

[9] T.H. Cormen, C.E. Leiserson, R.L. Rivest, C. Stein, "Introduction to Algorithm", 2nd edition, MIT press,2002.

[10] A.S. Tanenbaum, "Computer Networks", 4th edition, Prentice Hall of India, 2007-2008.

[11] B.R. Ambedkar, S.S. Bedi, A New Factorization Method to Factorize RSA Public Key Encryption, International Journal of Computer Science Issues, Vol. 8, Issue 6, No 1, November 2011.

Research Paper   Open Access

Comparative Analysis of Cell Phone Sound insulation and Its Effects on Ear System

Nwafor I .G[1] and Bakare B. I[2]

[1, 2] (*Department of Electrical/Computer Engineering, Rivers State University of Science and Technology, Port Harcourt, Nigeria*)

ABSTRACT: *The sound intensity levels emitted from five different cell phones;(SAMSUNG A100, NEC 616V, NOKIA 1100, MOTOROLA 3Vi and SONY ERICSSON K750) were measured in Port Harcourt, Nigeria and the result was analyzed to ascertain if their various sound levels fall within the permitted range of personal sound exposure levels recommended by both International and Nigeria noise regulatory bodies. The result of the study shows that to lessen the risk of hearing problems from cell phones, it is advisable to switch ears usage regularly, use an earpiece which will eliminate the risk of electromagnetic waves from the cell phones and the use of speaker phones. This paper seeks to show why it is necessary to use cell phone sound insulation to reduce the effects of noise on the ear systems. The constant exposure to sound from cell phones can over time cause damage to the hearing abilities of the cell phone users. Hence, adequate cell phone sound insulation is needed to reduce the effects of loud sound intensity levels to the ear system.*

KEYWORDS: *Cell Phone, Damping, Electromagnetic waves, Insulation, sound intensity*

I.   INTRODUCTION

For years, there have been worries that cell phones can cause anything from cancer to brain tumors due to their strong vibrations. This situation became worrisome due to the increase in the number of young children carrying cell phones, using them for almost everything from gossip sessions to listening to music with the built-in MP3 players. The cell phone operator packages such as: MTN's Xtracool service in Nigeria encourages subscribers to make calls free of charge for six hours at a stretch. Also the new trend of merging the music walkman features with the cell phone will ensure most people spend more time with either the loudspeaker or earpieces of the cell phones in close proximity to their ears. The long term cell phone use particularly on one ear can cause inner ear damage [1]

The sound intensity levels emitted from five different cell phones;(SAMSUNG A100, NEC 616V, NOKIA 1100, MOTOROLA 3Vi and SONY ERICSSON K750) were measured in Rivers State university of Sciences and Technology (RSUST),. Port Harcourt, Nigeria using Eagle-Y 139A model, IEC 651 type II and NEDA 1604 IEC 6F22 sound level meter. The aim of the research is to critically analyze the sound level of the cell phones at the different measuring points within RSUST with a view to determining the sound insulation of the cell phone understudied and it effect on ear system.

Sound is subjective to humans; to some humans' high level of sound is noise while to some humans very high level of sound is pleasurable. The study conducted by the American Academy of Otolaryngology-Head, neck and surgery Foundation in Washington, D.C. which compared the hearing of hundred cell phone users and the fifty people who have never used cell phones show that there was significant different of hearing abnormalities between those who regularly use the cell phones and those who did not use the cell phones. Also, those who use the cell phones for more than sixty minutes a day for over four years had hearing losses at high frequencies.[2]. It was also observed that listening to sound at 85dB or higher over many years can cause some hearing loss [1]. It is for these reasons that the concept of sound insulation for cell phones is considered as an important step to reducing the potential risk of ear damage caused by constant exposure to cell phone sounds

II.   SOUND INSULATION

Sound insulation can be defined as a means of reducing the intensity level of sound with respect to a specified source and reception. Sound insulation affects sound in two different ways such as: sound reduction

and sound absorption. Sound reduction simply blocks the passage of sound waves through the use of distance and intervening objects in the path while Sound absorption operates by transforming the sound waves into heat energy which involves suppression of echoes, reverberation, resonance and reflection. The moisture level in a medium can also reflect sound waves thereby reducing and distorting the sound travelling through it and this makes moisture an important factor in sound insulation.

The prevention of transmission of sound and a reduction of sound energy transmitted into an air space can be achieved using different basic approaches such as: the use of distance, by damping, by method of room within a room and by noise cancellation

2.1   The use of distance

The energy density of sound waves decreases as they spread out, so that increasing the distance between the receiver and source results in a progressively lowering intensity of sound at the receiver. In a normal three dimensional setting, the intensity of sound waves will be attenuated according to the inverse square law of the distance from the source. By using an object to absorb sound, part of the sound energy is used to vibrate the mass of the intervening object, rather than being transmitted [3]

2.2   Damping

Damping is the process by which sonic vibrations are converted into heat over time and distance. It is achieved in several ways. One way is to add a layer of material such as lead or neoprene which is both heavy and soft. These can be used as a sound deadening layer in such areas as wall, floor and ceiling construction in sound studios where levels of air borne and mechanically produced sound are targeted for reduction or virtual elimination.

Making a sound wave transfer through different layers of material with different densities assists in noise damping. Open-celled foam is a good sound damper; the sound waves are forced to travel through multiple foam cell air pockets and their cell walls as sound travels through the foam medium. Styrofoam (XPS) and expanded polystyrene foam (EPS), commonly used for thermal insulation, are significant conductors of sound. Polystyrene's use as a sound damper should be avoided except in applications where moisture resistance and buoyancy is necessary.

2.3 A Room Within A Room (RWAR)

This is one method of isolating sound and stopping it from transmitting to the outside world where it may be undesirable. Most vibration and sound transfer from a room to the outside occurs through mechanical means. The vibration passes directly through the brick, woodwork and other solid structural elements. When it meets with an efficient sound board such as a wall, ceiling, floor or window, the vibration is amplified and heard in the second space. A mechanical transmission is much faster, more efficient and may be more readily amplified than an airborne transmission of the same initial strength.

The use of acoustic foams and other absorbent means are useless against this transmitted vibration. The user is required to beak the connection between the room that contains the noise source and the outside world. This is called acoustic de-coupling. Ideal de-coupling involves eliminating vibration transfer in both solid materials and in the air, so air-flow into the room is often controlled. This has safety implications, for example proper ventilation is assured and gas heaters cannot be used inside de-coupled space.[4]

2.4   Noise Cancellation

Noise cancellation generators for active noise control are relatively modern innovation. A microphone is used to pick up the sound that is then analyzed by a computer; then, sound waves with opposite polarity (not in phase) are output through a speaker, causing destructive interference and cancelling much of the noise [5]

III   Materials and Methods

The cell phones are used as sources of sound when measurements are taken both in the anechoic chamber and in the lecture theatre. The instruments and accessories used for the data collection include.

- Eagle-Y 139A model, IEC 651 type II and NEDA 1604 IEC 6F22 sound level meter:
- A measuring tape
- Five different cell phones (Samsung A100, NEC 616v, Motorola 3vi, Nokia 1100 and Sony Ericsson K700)

3.1   Presentation of Data

Measuring tape was used to measure the distances between each cell phone and the sound level meter during each data collection. The sound level meter measures the sound pressure levels emitted from the various cell phones in both the anechoic chamber and the lecture theatre. When the cell phone is ringing the sound level

of the ringing cell phone is recorded by the sound level meter. The measurements in the lecture theatre was taken when the room was empty to avoid sound interference when the theatre is full with people

TABLE 1:   OUTSIDE RSUST ANECHOIC CHAMBER (LECTURE ROOM)
MEASUREMENTS

	SAMSUNG	NEC 616V	NOKIA 1100	MOTOROLA 3VI4	SONY ERISSON K750	AVERAGE
INPUT SOUND (SOURCE OF SOUND)	72	72	72	72	72	72dBA
OUTSIDE SOUND (SOUND MEASURED INSIDE THE LECTURE ROOM)	70	70.5	70	70.5	70	70.5dBA

TABLE 2:   INSIDE RSUST ANECHOIC CHAMBER MEASUREMENTS

	SAMSUNG	NEC 616V	NOKIA 1100	MOTOROLA 3VI4	SONY ERISSON K750	AVERAGE
OUTSIDE SOUND (SOUND MEASURED INSIDE ANECHOIC CHAMBER)	65	68	64	66	64	65dBA
INPUT SOUND (SOURCE OF SOUND)	72	72	72	72	72	72dBA

3.2   Data Analysis and Discussion

From the values obtained from tables 1 and 2 as shown in data presented above, it is necessary to verify the Inverse Square Law as pertaining to sound intensity level which states that a drop of 6.02dB is a factor of doubling the distance of the sound.

To verify the Inverse Square Law for a sound source in an ideal environment void of sound interference.

For example:
A sound source of 60 dB is measured at 10m; if the distance were doubled to 20m, the sound level expected will be;

$I_1 = 60dB$ at $r_1 = 10m$

doubling $r_1 = 10 \times 2 = 20m = r_2$

From the formula for decibel difference, which states $\Delta D = 2 \log(r_1/r_2)$

$$\Delta D = I_2 - I_1 = 20 \log(r_1/r_2)$$
$$\Delta D = I_2 - I_1 = 20 \log(10/20)$$
$$\Delta D = I_2 - I_1 = 20 \log(0.5)$$
$$\Delta D = I_2 - I_1 = -6.02 \, dB \qquad\qquad (1)$$

Equation (1) therefore proves the law that the decibel difference anytime the distance, r_1 is doubled $= 6.02 \, dB$. That means the sound intensity decrease by $6.02 \, dB$, anytime the distance measured is doubled.

This law for each cell phone intensity value when the distance r, is doubled is shown below.

3.2.1   *SAMSUNG A100*

From data in table 1 in result paragraph

At $r_1 =$ initial distance $= 0.3 \, m$

$I_1 =$ initial intensity $= 69.84 \, dB$

Doubling $r_1 = 0.3 \times 2 = 0.6 \, m = r_2$

At $r_1 = 0.06 \, m$

$I_2 =$ initial at $r_2 = 63.84 \, dB$

From the inverse square law, $I_2 - I_1$ should be approximately equal to 6.02 dB
Therefore,
$$I_1 - I_2 = 69.84 - 63.84 = 6.00 \text{ dB} \tag{2}$$

The obtained value in equation (2) is very close to the expected value of 6.02 dB so it can be concluded that the inverse square law is verified for this phone.

3.2.2   NEC 616 V
From data in table 1 in result paragraph
At r_1 = initial distance = 0.3 m
I_1 = initial intensity = 89.84 dB
Doubling r_1 = 0.3 x 2 = 0.6 m = r_2
At r_1 = 0.06 m
I_2 = initial at r_2 = 83.84 dB

From the inverse square law, $I_2 - I_1$ should be approximately equal to 6.02 dB
Therefore,
$$I_1 - I_2 = 69.84 = 6.00 \text{ dB} \tag{3}$$

The obtained value in equation (3) is very close to the expected value of 6.02 dB so it can also concluded that the Inverse Square Law is verified for this phone.

3.3.3   NOKIA 1100
From data in table 1 in result paragraph
At r_1 = initial distance = 0.3 m
I_1 = initial intensity = 87.84 dB
Doubling r_1 = 0.3 x 2 = 0.6 m = r_2
At r_1 = 0.06 m
I_2 = initial at r_2 = 79.84 dB

From the Inverse Square Law, $I_2 - I_1$ should be approximately equal to 6.02 dB
Therefore,
$$I_1 - I_2 = 87.84 - 79.84 = 8.00 \text{ dB} \tag{4}$$

The obtained value, although 2 dB more than the expected value of 6.02 dB is still acceptable if it is taken, into consideration the imperfect conditions of the Anechoic Chamber used for measurement. So we can also conclude that the Inverse Square Law is verified for this phone.

3.3.4   MOTOROLA 3VI
From data in table 1 in result paragraph
At r_1 = initial distance = 0.3 m
I_1 = initial intensity = 87.84 dB
Doubling r_1 = 0.3 x 2 = 0.6 m = r_2
At r_1 = 0.06 m
I_2 = initial at r_2 = 79.84 dB

From the Inverse Square Law, $I_2 - I_1$ should be approximately equal to 6.02 dB
Therefore,
$$I_1 - I_2 = 87.84 - 79.84 = 8.00 \text{ dB} \tag{5}$$

The obtained difference is similar to that achieved for the Nokia 1100 and for the same reason stated for Nokia 1100, it can also conclude that the Inverse Square Law has once more been verified for the Motorola 3Vi phone.

3.3.5   SONY ERICSSON K750

From data in table 1 in result paragraph

At r_1 = initial distance = 0.3 m

I_1 = initial intensity = 83.84 dB

Doubling r_1 = 0.3 x 2 = 0.6 m = r_2

At r_1 = 0.06 m

I_2 = initial at r_2 = 77.84 dB

From the Inverse Square Law, $I_2 - I_1$ should be approximately equal to 6.02 dB

Therefore,

$I_1 I_2$ = 83.84 − 77.84 = 6.00 dB   (6)

The obtained value in equation (6) is very close to the expected value of 6.02 dB so it can also be concluded that Sony Ericsson K750 obeys the Inverse Square Law.

 The tables below confirm that when the distance is doubled the sound intensity level is 6. 00dB for all the cell phones showed below and that confirms the inverse law of sound intensity level

<center>TABLE 3: SAMSUNG</center>

INITIAL DISTANCE (r_1)	INITIAL INTENSITY (I_1)	DOUBLING DIATNACE (r_2)	INITIAL (I_2)	$I_2 - I_1$
0.3M	69.84dB	0.3x2=0.6m	63.84dB	63.84 − 69.84dm = 6.00dB

<center>TABLE 4: NEC 616V</center>

INITIAL DISTANCE (r_1)	INITIAL INTENSITY (I_1)	DOUBLING DIATNACE (r_2)	INITIAL (I_2)	$I_2 - I_1$
0.3M	89.84dB	0.3x2=0.6m	83.84dB	83.84 − 89.84dm = 6.00dB

<center>TABLE 5: NOKIA 1100</center>

INITIAL DISTANCE (r_1)	INITIAL INTENSITY (I_1)	DOUBLING DIATNACE (r_2)	INITIAL (I_2)	$I_2 - I_1$
0.3M	87.84dB	0.3x2=0.6m	79.84dB	87.84 − 79.84dm = 8.00dB

<center>TABLE 6: MOTOROLA 3VI4</center>

INITIAL DISTANCE (r_1)	INITIAL INTENSITY (I_1)	DOUBLING DIATNACE (r_2)	INITIAL (I_2)	$I_2 - I_1$
0.3M	87.84dB	0.3x2=0.6m	79.84dB	79.84 − 87.84dm = 8.00dB

<center>TABLE 7: SONY ERISSON K750</center>

INITIAL DISTANCE (r_1)	INITIAL INTENSITY (I_1)	DOUBLING DIATNACE (r_2)	INITIAL (I_2)	$I_2 - I_1$
0.3M	83.84dB	0.3x2=0.6m	77.84dB	77.84 − 83.84dm = 6.00dB

 It has been established that measurements of the sound pressure levels of the five selected cell phones are done with sound level meter (Eagle-Y 139A model, IEC 651 type II and NEDA 1604 IEC 6F22) and from the data in tables 1 and 2, the SamsungA100 recorded the lowest sound pressure levels, out of the five selected cell phones, which shows that it has the most efficient sound insulation compared to other cell phones. While the highest sound pressure levels were recorded from the NEC 616v phone which shows that its sound insulation was the least efficient in comparison with the other five selected cell phones.

3.4 Sound Exposure Levels

Sound (Noise) exposure levels recommended by both International and Nigeria noise regulatory bodies are shown in figure 8 and figure 9 below. In Nigeria noise level standard was set by the Federal Environmental Protection Agency (FEPA), now known as federal Ministry of Environment for the protection of Nigerians Against the effect of noise as well as the environment while Intentional Noise Exposure Limit as presented by the United Kingdom(U.K) is used as the International benchmark

TABLE 8: STANDARD NOISE EXPOSURE LIMIT IN NIGERIA

Duration per day (hours)	Permissible Exposure limit dB(A)
16	85
12	87
8	90
6	92
4	95
3	97
2	100
1.5	102
1	105
0.5	110
0.25	115

TABLE 9: INTENTIONAL NOISE EXPOSURE LIMIT (UNITED KINGDOM CRITERIA)

Duration per day (hours)	Permissible Exposure limit dB(A)
8HRS	90
4HRS	93
2HRS	96
1HR	99
30 MINS	102
15 MINS	105
8 MINS	108
4 MINS	111
2 MINS	114
1MIN	117
30 SEC	120

IV.   CONCLUSION

The paper shows the relevance and various methods of cell phone sound insulation. It can be seen from the values of the sound pressure levels obtained from the measurements that cell phones do emit quite a good dose of sound power which although comparable to the sound emitted during normal human conversation, is more damaging due to the close proximity of the loud speaker to the human ear. The work also shows that despite the sound insulation levels of the cell phones, the cell phone users are constantly exposed to ear damage. It is important that the cell phone users be aware of the dangers posed by constant exposure to fairly loud sound generated by cell phones so as to avoid cases of ear damage despite the degree of sound insulation of the cell phones

REFERENCES

[1].   British Government Research Foundation*, Defeating Deafness*, Gray's Inn Rd. London WCLx8BEE.,2002, Pp330 -332.
[2]   Bosan, A, Zaidi.S.H and Nobel T, *The problem of noise* Pakistan Journal of Otolaryngology , vol. 11. ,1995, Pp 128-131
[3]   Forrest, M.R. and Coles, R.R.A. *Problems of Communication and Ear Protection in the Royal Marines*. J. Royal Navel Medical, Vol. 81, 1970, pp. 226-230
[4]   Krypter, K. D, *Exposure to Steady-State Noise and impairment of Hearing,* J. Acoustic Society AM Vol. 35,1963,. pp 1515
[5]   Abolo, N.W. *,Research on Sound Intensity Measurement in an Anechoic Chamber and comparing the results with a non-treated lecture theatre in R.S.U.S.T Environment*,B.sc Project, Rivers States University of Science and Technology,Port Harcourt, 2003.

Research Paper   Open Access

An Evaluation of Skilled Labour shortage in selected construction firms in Edo state, Nigeria

Oseghale, B.O.; Dr Abiola-Falemu, J.O.; Oseghale G.E

Maintenance Department Regional Center for Aerospace Survey Along Road 1, Obafemi Awolowo University, Ile-Ife Osun State, Nigeria.
Federal University of Technology Akure, Nigeria.
Department of Building Obafemi Awolowo University, Ile- Ife Osun State, Nigeria.

ABSTRACT: *The study investigated skilled labour requirement in the construction industry of Edo State. The study aimed at assessing the current state of the construction industry's skilled workforce, causes and prevalence of skilled labour shortage and the effect of skilled labour shortage in construction project delivery. The method employed for collection of data includes distribution of structured questionnaires. The data collected were analyzed using Frequency tables, percentages, mean response analysis, relative importance index and cross tabulation. The research identified the most severe factors responsible for labour shortage to include; no clear carrier path, high mobility of construction workers and low wages. The study found that construction firms are not sending their skilled workforce for training, and that the skilled workers are unwilling to recommend the profession to their children. The research revealed that the construction firms were paying extra money for labour, and Schedule delay in their construction programmes as a result of skilled labour shortage. The study found aging workforce in the construction trades sampled, and that the entrance of young people into the construction trades was very low.*

KEY WORDS: *Skilled Labour, Shortage, Construction Industry, Construction Firms*

I.   INTRODUCTION

The construction industry occupies a focal position in a nation's economy. It is an essential contribution to the process of development [1].The construction industry is a global industry known for its generation of jobs at different skill and professional levels. In terms of value of its output, its global market is reported to be around $1.5 Trillion as of today [2]. The construction industry contributes about 5 percent to the Gross Domestic product GDP [3] in Nigeria. The author in [4] affirmed that it contributes about 50% percent of Nigerian government expenditure. It therefore shows that the construction industry is crucial in National development.

Modern construction is a complex, highly organized process. Not only is it a science and a commercial business, but it is a creative art. For the newest recruit to the mature craftsman of many years' experience, it is a rewarding, often tough and demanding discipline. Every person employed within the construction process makes a direct contribution not only to the community in general but also to the nation at large [5].In world labour market, construction workers are said to be over 100 million, constituting 6-7 % of the world labour force [2]. In the construction industry employment is characterised by relatively high rates of attrition among subcontractors as well as waged workers, and this is manifested in periodic labour shortages [6; 7; 8; 9].
The findings of the Chartered Institute of Building survey (CIOB) [10] indicate that a shortage of Skills Labour continues to be a challenge for the construction industry. The CIOB [10] predicted that this issue is likely to worsen as the demand for construction increases.

The CIOB research findings indicate that people possessing crafts/trades and senior/middle Management skills are highly sought after. From time to time employers in a number of countries refer to the difficulties they have in recruiting labour of the requisite quality, even on occasion when the labour market is relatively slack. Yet academic work on this issue is relatively sparse and in particular little is known of the consequences of such situations. Despite the perceived importance of skill shortages in Nigeria, the literature addressing these issues is limited.

According to the Institute of Management and Administration cited in [11] the skilled craft shortage is not a shortage of workers rather it is a shortage of adequately trained skilled and productive workers available for certain jobs. With the construction industry requiring some of the most highly skilled workforce to do some of the most dangerous jobs, replacement and recruitment proves to be difficult. Reasons that have been given for the skilled labour shortage include lack of training, an aging workforce, poor image of the workers, and an industry that does not appeal to many youth [12;13;14; 15; 11].

The authors in [16] opined that skill shortages are a complex labour market Phenomenon, and are related to business performance. They went further to state that Skill shortages are often portrayed as a major problem for the economies of many countries. Yet, there is surprisingly little evidence about their prevalence, causes and consequences in the Nigerian construction industry. Although there are no statistics to show whether, there is shortage of skilled craftsmen in the Nigerian construction industry, expert and other stakeholders in the industry believe that there is shortage of skilled trades in the industry. This research is conducted in response to concerns from stakeholder about the perceived shortage of skilled Workers and the impact that this shortage may be having on the industry ability to meet the growing residential and commercial demand for construction. This study therefore assesses the state of the Nigerian construction industry with respect to skill labour shortage, the prevalence, causes and effects on building project delivery. The trades selected for this study were Bricklaying, Carpentry, painting and Plumbing. This trades were selected because of their level of dominance in building construction works.

II.   LITERATURE REVIEW

Research work of [15] revealed a number of factors which have combined to influence the construction skill shortfall, some of these include; The introduction of new tec hnologies which have reconstituted the skill required [17;12, 18].The growth in self-employment and the use of labour only sub-contractors which have reduced the commitment and investment in training within the industry [19;20;21;22] self-employed craftmen in turn are not able to handle their qualification improvement issues and there is a direct correlation between the fall of trainee members and the numbers of self-employed [23;24; 25; 13;14;26).

The poor image of the industry which unfavourably affects the popularity as a career choice [12;13;14]. The image is low among workers themselves as the majority of construction crafts workers of various ages and experience would never recommend their trade to their children [26].

High mobility of construction workers as the result of unattractive image, unsafe work place, irregularity of the workload, lack of respect and opportunities for training.

The dissatisfaction with labour organization especially the unstable workload as the reason of the release by received workers. [27;28;29].

The site safety and quality of work always the least and last to be attended to as they are always the conflicting goals running in different directions to earning and speed (18-20).

Globalization has added also negative ethnic characterization of cultural differences of multi-lingual construction teams. [30;31;32;33].

The combination of these factors has led to a labour market reliant upon a casual workforce, incorporating high levels of self-employment, low levels of training investment and hence, low quality skills. [13;34;35].

III.   RESEARCH METHODOLOGY

The research examined the state of the Nigerian construction industry, its workforce, determined the prevalence of skilled labour shortage, assessed the causes of skilled labour shortage and the effects of skilled labour shortage on building project delivery.

The research involved gathering and collection of primary data. This involved responses to a personal interview with the aid of a structured questionnaire. Two (2) forms of questionnaires were designed and distributed. The first was designed to obtain information from managers in the construction industry, having construction projects in Edo state; the second one was designed to obtained information from skilled workers in the various trades to know their perceptions on key issues facing the construction industry. The construction trades selected for this study were Bricklaying, Carpentering, Plumbing and Painting. The choice of these trades was as a result of their level of dominance in the building industry. The distribution of these questionnaires was conducted to cut across the various sections or senatorial districts in Edo state. There are three senatorial districts in Edo state which includes: Edo south, Edo central and Edo north senatorial districts. A systematic random sampling technique was used in selecting the building contractors that were sampled in these senatorial districts, but the choice of each contracting firm was a function of the total number of such firms operating in that area. Construction trades were also sampled in these senatorial districts.

SAMPLE FRAME AND SAMPLE SIZE

The sample frame for this study were construction firms registered with Edo State Government, University of Benin, Edo State University, Auchi Polytechnic and others having project with local government. A total of 200 firms were identified and used as the sampling frame. 30 % of the sample frame was used as the sample size for this study making a total of 60 firms for questionnaire type A. The first questionnaire was directed to the managers and supervisors of construction firms, (Questionnaire type A) while the second type of questionnaire was administered to the tradesmen (Questionnaire type B)

METHOD OF DATA ANALYSIS.

In the analysis of the data collected for this research work, various methods of analytical/statistical techniques used were cross tabulation, percentage, frequency distribution, mean response analysis, and relative importance index.

DATA ANALYSIS AND DISCUSSION OF RESULTS
(QUESTIONNAIRE TYPE A)
Educational and professional qualifications of respondents

Table 1: Academic and Professional Qualification of Respondents

Description	Frequency	Percent
GCE/SSCEOL	7	19.4
B.Sc		
FTC	3	8.3
HND	1	2.8
MNIOB	14	38.9
MNIQS	2	5.6
M.Sc	1	2.8
Total	8	22.2
	36	100.0

Table 1 above represents the Academic and Professional qualifications of the respondents. This show that the respondent possess the required qualification in the industry to be able to contribute their quota effectively in this study.

Table 2: Profession of Respondents in the Construction industry

Description	Frequency	Percent
Estate surveyors	1	2.8
Architecture	4	11.1
Building	14	38.9
Civil Engineering	6	16.7
Quantity Surveying	6	16.7
Others	5	13.9
Total	36	100.0

Table 2 shows the various professions of respondents sampled. This shows that the respondents cut across the various professional who possess the require knowledge about the subject under survey to contribute their quota.

Table 3: Respondents Working Experience

Description	Frequency	Percent
<2yrs	1	2.8
2-4yrs	10	27.8
5-7yrs	2	5.6
8-10yrs	4	11.1
over 10yrs	19	52.8
Total	36	100.0

Table 3 shows the number of years of respondents working experience in the study area. This shows that the respondent sampled have relevant experience in the industry to be able to respond all the questions asked.

Table 4: Nature of Business set-up

Nature of Business	Frequency	Percent
Sole proprietorship	11	30.6
Partnership	1	2.8
Limited liability company	10	27.8
Public liability company	14	38.9
Total	36	100.0

Table 4 shows the nature of Business set-up of the respondent sampled. The implication of this is that all the firms sampled cut across small, medium and large business enterprises.

Table 5: Category of Registration of the Company with Federal Ministry of workers and Housing

Category of Registration	Frequency	Percent
Category A	6	16.7
Category B	4	11.1
Category C	22	61.1
Category D	4	11.1
Total	36	100.0

Table 5 shows the category of registration of the firm sampled. 16.7% were registered in category A, 11.1% were registered in category B, while 61.1% were registered under category C and 11.1% were registered under category D. This show that all the firm sampled were registered under different categories, and that they execute jobs ranging from small scale to large scale.

Table 6: Nature of work undertaken

Nature of work undertaken	Frequency	Percent
Building works	16	44.4
Civil Engineering works	3	8.3
Both building and civil Engineering	17	47.2
Total	36	100.0

Table 6 shows the nature of work undertaken by the various firms sampled. 44.4% executed Building works, 8.3% undertook Civil Engineering works while 47.2% were involved in both Building and Civil Engineering works.

Table 7: Number of permanent Employees

Number of permanent employees	Frequency	Percent
< 30 employees	17	47.2
30 -100 employees	10	27.7
Over 100 employees	9	25.0
Total	36	100.0

Table 7 shows the number of permanent employees working in the construction companies sampled. 47.2% had less than 30 employees, while 27.7% had between 30-100 employees and 25.0% had above 100 employees in three companies as permanent staff.

Table 8: Method of Recruitment.

Method of recruitment	Frequency	Percent
Formal interview through head office only	9	25.0
Formal interview through regional office only	3	8.3
On site without formal interview	10	27.8
Combination of all of the above	14	38.9
Total	36	100.0

Table 8 shows the method of recruitment adopted in the firms sampled. This shows that the companies used different method of recruiting employees, depending on the one that is suitable to them.

Table 9: Skilled labour Shortage

Description	Frequency	Percent
Yes	26	80.6
No	7	19.4
Total	36	100.0

Table 9 shows whether there is skilled labour shortage in the construction industry in Nigeria. 80.6% of the respondent agreed that there is skilled labour shortage, while 19.4% were of the view that there is no skill labour shortage. The implication of this is that majority of the managers agreed that they were experiencing skilled labour shortage in the various trades in the construction industry.

Table 10: Skilled labour shortage in bricklaying

Description	Frequency	Percent
YES	24	66.7
NO	12	33.3
Total	36	100.0

Table 11: Skilled labour shortage in carpentry

Description	Frequency	Percent
YES	27	75.0
NO	9	25.0
Total	36	100.0

Table 12: Skilled labour shortage in plumbing

Description	Frequency	Percent
YES	20	55.6
NO	16	44.4
Total	36	100.0

Table 13: Skilled labour shortage in painting

Description	Frequency	Percent
YES	29	80.6
NO	7	19.4
Total	36	100.0

Tables 10, 11, 12, and 13 shows the skilled labour shortage in the four trades sampled in the construction industry. 66.7% experience skilled labour shortage in Bricklaying, 75% experience skilled labour shortage in carpentry while 55.6% experience skilled labour shortage in plumbing and 80.6% experienced skilled labour shortage in painting. This shows that mangers were experiencing skilled labour shortage in the four trades sampled.

Table 14: Rate of labour shortage in Bricklaying

Description	Frequency	Percent
very low	9	25.0
Low	16	44.4
High	T	19.5
very high	4	11.1
Total	36	100.0

Table 14 shows the rate of labour shortage in bricklaying. 25% of respondents agreed that the rate of labour

shortage were very low, 44.4% agreed that the rate of labour shortage were low, while 19.5% of respondents agreed that the rate were high, and 11.1% of the respondents agreed that the rate were very high. This shows that the rate of labour shortage in bricklaying have not reached an alarming rate.

Table 15: Rate of Labour shortage in Carpentry

Description	Frequency	Percent
very low	8	22.2
Low	17	47.2
High	6	16.7
very high	5	13.9
Total	36	100.0

Table 15 shows the rate of labour shortage in carpentry. 22.2% of respondents agreed that the rate of labour shortage were very low, 47.25 agreed that the rate were low, while 16.7% agreed that the rate were high and 13.9% agreed that the rate were very high.

Table 16: Rate of labour shortage in Plumbing

Description	Frequency	Percent
very low	6	16.7
Low	5	13.9
High	16	44.4
very high	9	25.0
Total	36	100.0

Table 16 shows the rate of labour shortage in plumbing. 16.7% of the respondents agreed that the rate of labour shortage in this trade were very low, 13.9% agreed that the rate were low while 44.4% agreed that the rate were high and 25.0% agreed that the rate were very high.

Table17: Rate of labour shortage in Painting

Description	Frequency	Percent
Very low	19	52.8
Low	9	25.0
High	7	19.4
very high	1	2.8
Total	36	100.0

Table 17 shows the rate of labour shortage in painting. 52.8% show that the rate were very low, 25% show that the rate were low, while 19.4% show that the rate were high and 2.8% show that the rate of shortage were very high. This shows that the rate of labour shortage in this trade is relatively low.

Table 18 : Relative Importance Index for the rate of skilled labour shortage

Question 15-17		RII	Rank
q15c	Rate of labour shortage in plumbing	0.67	1
q15b	Rate of labour shortage in carpentry	0.53	2
q15a	Rate of labour shortage in bricklaying	0.52	3
q15e	Rate of labour shortage in painting	0.34	4

RII was calculated for the rate of skilled labour shortage among the trades surveyed.
Table 18 shows the results of the relative importance index that were conducted the rate of skilled labour shortage in the five trades sampled (plumbing, carpentry, bricklaying and painting). The result shows that the rate of skilled labour shortage in plumbing was ranked number 1 followed by carpentry, bricklaying and painting respectively.

Table 19: Mean Response Analysis for causes of skilled labour shortage.

		MRA	Rank
q16i	No clear cut career path	2.83	1
q16d	High mobility of construction workers	2.69	2
q16h	Low wages	2.67	3
q16j	Diminishing craftsperson training programme	2.61	4
q16b	Growth of self employment	2.58	5
q16e	Dissatisfaction with labour organization	2.53	6
q16a	Introduction of new technologies	2.47	7
q16g	Ethnic characterization	2.44	8
q16f	Poor safety of construction work	2.31	9
q16c	Poor image of the industry	2.03	10

MRA –Mean Response Analysis

Table 19 shows the result of the mean response analysis that was conducted for the identified causes of skilled labour shortage in the construction industry. In the ranking No clear cut career path came first, followed by High mobility of construction workers, Low wages, Diminishing craftsperson training programme, Growth of self employment respectively while Poor image of the industry had the lowest ranking.

Questionnaire Type 2

Table 20: Type of trade/craft

Description	Frequency	Percent
Carpenters	23	25.8
Bricklayers	25	28.1
Plumbers	21	23.6
Painters	20	22.5
Total	89	100

Table 20 shows the types of trade that were surveyed for this study. Thirty questionnaires were printed and distributed for each trade of four (carpenters, bricklayers, painters and plumbers) making a total of one hundred and twenty (120) questionnaires. The percentage response rate is 74% which is adequate for the project work.

Table 21: Sex of the craft

Description	Frequency	Percent
Male	89	100.0

Table 21 show the sex of the respondents craft in the construction industry in the study area 100% were male, this shows that the craft in the study area were male dominated.

Table 22: Age of craft men

Description	Frequency	Percent
18-25yrs	4	4.5
26-33yrs	17	19.1
34-41yrs	26	29.2
42-49yrs	24	27.0
Above 50yrs	18	20.2
Total	89	100.0

Table 22 show the Age of craftmen surveyed. 4.5% were between 18-25 years old, 19.1% were between 26-33

years of Age, 29.2% were between 34-41 years of Age while 27% were between 42-49 years of Age and 20.20% were above 50 years. This shows that 76.4% of the craftmen have their Ages above 33 years. This shows that the rates of new entrance of young people into the construction trade were very low and it poses serious implication for the future of the construction industry in Nigeria in the area of skilled labour requirement.

Table 23: Place of Residence in Relations to site/office

Description	Frequency	Percent
Very far	24	27.0
Not too far	55	61.8
Close	10	11.2
Total	89	100.0

Table 23 shows the place of residents of the respondents in relation to their site offices. 27% of the respondents choose very far, 61.8% choose not too far and 11.2% close. The implication of this is that if the company does not have means of transportation for transporting the workers to site. It then means that workers were incurring more expenses in order to get to their various sites.

Table 24: Nature of Employment

Description	Frequency	Percent
Permanent staff	2	2.2
Daily paid	21	23.6
Contract staff	40	44.9
Sub contractor	26	29.2
Total	89	100.0

Table 24 shows the nature of employment of the skilled labour. Only 2.2% of the respondents were permanent staff of the construction company, 23.6% were engaged on daily paid, while 44.9% were contract staff and 29.2% were sub-contractors. The implication of this is that the construction firms were not employing skilled labour as permanent staffs of the construction firms.

Table 25: Employment Qualification ofCrafts men/trade

Description	Frequency	Percent
No response	1	1.1
Primary school plus apprenticeship	53	59.6
Modern school plus apprenticeship	5	5.6
Secondary school plus apprenticeship	18	20.2
Technical school graduate	12	13.5
Total	89	100.0

Table 25 shows employment qualification of crafts men/trades. 59.6% of the respondents holds primary school certificates plus apprenticeship, 5.6% of the respondents holds modern school certificates plus apprenticeship while 20.2% of the respondents holds senior secondary school certificates plus apprenticeship and 13.5% were technical school graduates. The implication of this is that a higher percentage has only primary school certificates and might not be able to take down instructions pass to them by the supervisor accurately.

Table 26: Level of Satisfaction of Employees on the amount of wages/salaries earns.

Description	Frequency	Percent
No response	2	2.2
Very good	13	14.6
Good	32	36.0
Fair	25	28.1
Poor	17	19.1
Total	89	100.0

Table 26 show the level of satisfaction of employees on the amount of wages earned. 14.6% of the respondents say the wages is very good, 36% of respondents say the wages were good, while 28.1% say the wages wee fair and 19.1% say the wages were poor. The implication of this is that a larger percentage is not satisfied with the wages earned.

Table 27: Skilled Labour Shortage

Description	Frequency	Percent
No response	4	4.5
Yes	59	66.3
No	26	29.2
Total	89	100.0

Table 27 shows the result of skilled labour shortage among the skilled labour force. When the respondents were asked whether there was skilled labour shortage in their trades, 66.3% of the respondent picked yes while the 29.2% pick no and 4.5% were not having any response.

Table 28: Regularity of Training for permanent staff of construction

Description	Frequency	Percent
No response	18	20.2
Regular	3	3.4
Not regular	7	7.9
Never on training	61	68.5
Total	89	100.0

Table 28 investigated the training of staff of construction firms. The respondents were asked on how regularity their firms send them of training. 20.2% of the respondents hard no response, 3.4% of the respondents say there were sent regularly for training, while 7.9% of respondents say the training were not regular, and 68.5% of the respondents say they were never sent on training.

Table 29: Reasons why Construction firms are not sending out workers for training

Description	Frequency	Percent
No response	24	27.0
Cost	48	53.9
Fear of leaving for another company	14	15.7
Others	3	3.4
Total	89	100.0

Table 29 shows the result of the reasons why construction firm were not training their workers. When the respondents were asked the reasons why the construction firms were not sending out workers for training 27% of the respondents had no response, 53.9% of the respondents say the reason were cost, while 15.6 say the reason were fear of leaving for another company.

Table 30: Recommendation of this trade or profession for respondents Children

Description	Frequency	Percent
No response	17	19.1
Yes	18	20.2
No	54	60.7
Total	89	100.0

Table 30 shows the result of the recommendation of trade or profession to respondents' children. When the respondents were asked whether they would recommend this trade or profession for respondent's children, 20.2% of the respondent's says, yes while 60.7% say no and 19.1% had no response. The implication of this is that craft men were not proud of their profession. When the respondents were asked the reasons why this trade

or profession cannot be recommend for respondent's children, 4.6% had no response, 18.0% says the reasons were Low wage, 16.9% say the reason were no clear cut carrier path, 3.4% says the reason were poor safety of construction work, while 43.8% say the reason were poor image attached to the trade and 3.4% of the respondents says the reason wee other different from the ones above.

Table 31: Type of trade/craft * Age (Crosstab)

Description		Age					Total
Type of trade/craft		18-25yrs	26-33yrs	34-41yrs	42-49yrs	above 50yrs	
Carpenters	Count	0	1	7	4	11	23
	% within Type of trade/craft	.0%	4.3%	30.4%	17.4%	47.8%	100.0%
	% within Age	.0%	5.9%	26.9%	16.7%	61.1%	25.8%
	% of Total	.0%	1.1%	7.9%	4.5%	12.4%	25.8%
Bricklayers	Count	4	6	8	4	3	25
	% within Type of trade/craft	16.0%	24.0%	32.0%	16.0%	12.0%	100.0%
	% within Age	100.0	35.3%	30.8%	16.7%	16.7%	28.1%
	% of Total	4.5%	6.7%	9.0%	4.5%	3.4%	28.1%
Plumbers	Count	0	7	0	10	4	21
	% within Type of trade/craft	.0%	33.3%	.0%	47.6%	19.0%	100.0%
	% within Age	.0%	41.2%	.0%	41.7%	22.2%	23.6%
	% of Total	.0%	7.9%	.0%	11.2%	4.5%	23.6%

	Description	Age					Total
		18-25yrs	26-33yrs	34-41yrs	42-49yrs	above 50yrs	
	% within Type of trade/craft	.0%	15.0%	55.0%	30.0%	.0%	100.0%
Type of trade/craft	% within Age	.0%	17.6%	42.3%	25.0%	.0%	22.5%
	% of Total	.0%	3.4%	12.4%	6.7%	.0%	22.5%
Count	4	17	26	24	18	89	
% within Type of trade/craft	4.5%	19.1%	29.2%	27.0%	20.2%	100.0%	
% within Age	100.0%	100%	100.%	100%	100.%	100.0%	
% of Total	4.5%	19.%	29.2%	27.%	20.2%	100.0%	

Table 31 shows the result of cross tab for type of trade/craft age, 0% of the carpenters have their ages between 18-25 years, 4.3% of the carpenters have the ages between 26-33 years, 30.4% of the carpenters have their Ages between 34-41yrs, while 17.4% of the carpenters have their Ages between 42-49 yrs, and 47.8% of the carpenters have their Ages above 50 yrs.
The implication of this is that there were no new entrance of young people into the carpentry profession and over 45% of the carpenters already have their Ages above 50 years and they are still climbing. This is a serious implication for the construction industry in Edo state Nigeria.

Types of trades
Bricklayers
16% of the Bricklayers have their Ages between 18-25 yrs, 24% of the Bricklayers have their Ages between 26-33yrs, 32% of the Bricklayer has their Ages between 34-41 yrs, while 16% of the Bricklayers have their Ages between 42-49 years and 12% of the Bricklayers have their Ages above 50 years. This shows that 60% of the Bricklayer has their Ages above 33yrs. The entrance of young people into this trade is low but compared to the trade of carpenters, the entrance is still better.

Plumbers

From the plumbers surveyed 0% of them have their Ages between 18-25yrs, and 34-41 yrs 33.3% have their Ages between 26-33 yrs, while 47.6% of the plumbers have the Ages between 42-49 yrs and 19% of the plumbers have their Ages above 50 years. This shows that about 66% of the plumbers have their Ages above 41 yrs. Old. This again shows that the entrance of young people into this trade is very low.

Painters

0% of the painters have their Ages between 18-25 years, and above 50 yrs. 15% of the painters have their Ages between 26-33 yrs, while 55% of the painters have their Ages between 34-41 years and 30% of painters have their Ages between 42-49 years. This shows that 85% of the painters have their Ages above 33 years. This show that there experience workers on the construction industry but the entrance of young people into this trade is very low.

Table 32: Relative Importance index for the effects of labour shortage

		RII	Rank
q17a	Paying extra money for labour	0.6875	1
q17c	Schedule delay caused by labour shortage	0.680556	2
q17b	Encountering cost overruns	0.659722	3

Table 32 shows the result of relative importance index that were conduct for the effects of skilled labour shortage in the construction industry. The result show that paying extra money for labour was ranked no 1 followed by schedule delay caused by labour shortage (No 2) and encouraging cost overruns was ranked number 3.

IV.   CONCLUSION

In the assessment of skilled labour requirements in the construction industry in Edo State, Nigeria, 80% of the managers surveyed agreed that they were experiencing construction skilled labour shortage in the four trades sampled. (i.e Bricklaying, carpentry, painting and plumbing). 75% of carpenters, 56% of Bricklayer, 76% of plumbers and 65% of painters surveyed affirmed that there were skilled labour shortages in their various trades. The research found that the most severe factors responsible for the skilled labour shortage were; No clear carrier path, High mobility of construction workers, Low wages, Diminishing craftsperson Training programmes.

The research revealed the effects of skilled labour shortage to include; (1) paying extra money for labour (2) Schedule delay caused by labour shortage and (3) cost overruns. The findings reveals aging workforce in the construction trades sampled, as over 65% of the carpenters were above forty two (42) years old, 60% of the Bricklayer were above 33 year old, about 65 of the plumber were above 42years and 85% of the painters were above 42years. The research found that the entrance of young people of between 18 -25years into the construction trades sampled were very low.

REFERENCES

[1]   Oseghale, G.E & Ata, O. (2008). Reasons for delay in building projects: the case study of edo state Nigeria. The professional builder.*Journal of the Nigerian institute of building*, 81-88.
[2]   The Ambekar Institute for Labor Studies, Mumbai.Capacity Building for the Promotion of Labour Rights for Vulnerable Groups of Workers.Study Report 'Naka' Workers (Construction Industry), TheAmbekar Institute for Labor Studies, Mumbai.
[3]   Olaloku, F.A. (1987).The Second-Tier Foreign Exchange Market (SFEM) and the construction industry in Nigeria.Options and challenges, construction in Nigeria, Lagos, *3*, 20-23.
[4]   Kazier, M.I. (1987).The development of indigenous contracting in Nigeria. *The Engineer*, Lagos, *9 (2)*, 41.
[5]   Ward, P.A. (1979)**.**Organization and procedures in the construction industry*. Great Britain. Macdonald and Evans Ltd.
[6]   Tucker, R., Bennett and Eickmann, K., (2001). *Pulp and paper projects feel impacts from skilled construction labour shortage.* Available from: http://findarticles.com/p/articles/mi ga3636/is 200109/ai n8981837 (Accessed 23 April 2009).
[7]   Chan, P., Clarke, L., and Dainty, A. (2011) The dynamics of migrant employment in construction:Can supply of skilled labour ever match demand? In: Ruhs M and Anderson B (eds)Who Needs Migrant Workers? Labour Shortages, Immigration, and Public Policy, Oxford: Oxford University Press, pp. 225–255.
[8]   Erlich, M., and Grabelsky, J.(2005). Standing at the crossroads: The building trades in the twenty-first century. Labor History 46(4): 421–445.
[9]   McGrath-Champ, S., Rosewarne, S., and Rittau, Y. (2011) From one skill shortage to the next: The Australian construction industry and geographies of a global labour market. Journal of Industrial Relations 53(4): 467–485.
[10]   Chartered Institute of Building, 2008.Skills Shortages in the UK Construction Industry, Chartered Institute of Building Survey.
[11]   Olsen, D., Tatum, M., and Defnall, C., (2012). How Industrial Contractorsare Handling Skilled Labor Shortages in the United States, *48th ASC Annual International Conference Proceedings.*
[12]   SLIM Report (2002). Craft and skilled trades SLIM learning theme report skills and learning intelligence module, 52.

[13] Dainty, A.R.J., Ison, S.G. & Root, D.S. (2004). Bridging the skill gap: *A regionally driven strategy for resolving the construction labour market crisis, Engineering, Construction and Architectural Management11(4)* 275-283.

[14] Tarnoki, P. (2002)**.** The real world of managing project: 'Soft-side'. 2nd SENET conference in project management,cavtat, Croatia,555-559.

[15] Lill, I. (2004).Evaluation of labour management strategies in construction TUT Press, Tallinn, 115.

[16] Healy, J., Mavromaras, K., Sloane, K. (2011). Adjusting to Skill Shortages: Complexity and Consequences, IZA DP No. 6097.

[17] Agapiou, A., Price, A.D.F. &Mccaffer, R. (1995). Planning future construction skill requirements understanding labour resource issues, *Construction Management and Economics 13(2)* 149-161.

[18] Wells, J. & Wall, D. (2003**).** The expansion of employment opportunities in the building construction sector in the content of structural adjustment: some evidence from Kenya and Tanzana. *Habitat international*,*27 (3)*,325-337.

[19] Chini, A.R., Brown, B.H. & Drummond, E.G. (1999). Causes of the construction Skilled labour shortage and proposed solutions. *ASC Proceeding of the 35ᵗʰ Annual conference. California Polytechnic State University, San luis Obispo, California, 187-196.*

[20] Druker, Jac, R. (2000).*National collective bargaining and employment flexibility in the European building and civil Engineering Industries ConstructionManagement and Economics (18)* 699-709.

[21] Haksever, A.M; Demir, I.H. & Omer, G. (2002).Assessing the benefits of longterm relationship between contractors and subcontractors in the UK.*International journal for construction marketing*. No. 3,pp. 63-91

[22] Janssen, J. (2000). The European construction industry and its competitiveness: a construct of the European commission,construction management and economics, *18*,711-720.

[23] Crowley, L.G., Lutz, J.D. & Burleson, R.C. (1997). Functional illiteracy in construction industry. *Journal of Construction Engineering and Management 123(2)* 162-170.

[24] Mackenzie, S., Kilpatrick, A.R. &Akintoye, A. (2000), UK construction skill shortage response strategies and analysis of industry perception construction management and economics,*18*,853-862.

[25] Sybenni, G. (1998)**.** A qualification traps in the German construction industry: changing the production model and the consequences for the training system in the German construction industry. Construction management and economics *16*,593-601.

[26] Liska, R.W. (2002). Attracting and retaining a skilled construction workforce. Construction innovation and global competitiveness: 10th international symposium RC press, *Cincinati*, 1270-1282

[27] Cahul, P. &Postel-vinay, F. (2002)**.** *Temporary jobs, employment protection and labour market performance, Labour Economics 9(1)* 63-91.

[28] Haas, C.T., Rodrigues, A.M., Glover, R. &Goodrum, P.M. (2002).Implementing a multi-skilled workforce, construction management and economics.*19* 633-641.

[29] Smithers , G.L & Walker D.H.T. (2000). The effect of workplace on motivation and demotivation of construction professionals, construction management and economics,*18*,833-841.

[30] Belic, S. (2002**)**. Reality and preconceptions about the style of management in construction: *2ⁿᵈ SENET Conference on Project Management*, Cavtat, 568-573

[31] Bust, P.D., Gibb, A.G.F., & Pink, S. (2007). Managing construction health and safety. Migrant workers and communication.*Safety Message, Safety Science, in press, corrected proof.*

[32] Jaselskis, E.J., Stong, K.C., Aveiga, F., Canales, A.E., Jahren, C. (2007).Successful multinational workforce intergration program to improve construction site performance,safety science, in press, corrected proof.

[33] Wilson, F.D. (2003).Ethnic niching and metropolitan labour market, social science research,*32 (3)*,429-466.

[34] Briscoe, G., Dainty, A.R.J & Millet, S.J. (2000).*The impact of the tax system on self employment in the British construction industry, international journal of manpower,21(8)* 596-613.

[35] Kashiwagi, T. & Tam, S. (2002).Solving the construction craftperson skill shortage problem through construction undergraduate and graduate education ASC 38th Annual Conference Virgina Polytechnic Institute and state University. Blacksburg,VA, 165-176.

Research Paper   Open Access

The differentiation between the turbulence and two-phase models to characterize a Diesel spray at high injection pressure

L. Souinida[1], M. Mouqallid[1] and L. Affad[2]
1(ENSAM-UMI Meknès, MOROCCO)
2 (FST Mohammedia, MOROCCO)

ABSTRACT: *The aim of this work is a study of the dynamics of the diesel spray in a combustion chamber of a Diesel engine of direct injection during the injection spray. To do it, the computer code Fluent (simulator of turbulent multiphase, multi-dimensional and unsteadies flows) is used to model the behavior of the spray in two dimensions. The spray evolution is simulated by using the Reynolds Averaged Navier-Stokes equations with a many models of closure of these equations, such as: Spalart Allmaras, k-ε, k-ω, k-k$_L$-ω, SAS, RSM. The two-phase flow is modeled by using the Volume of Fluid model and its coupling with Level-Set model, where the two phases behave as a pseudo-fluid with an indicator function determining the volume fraction of each phase. In this study, we demonstrate the evolution of the volume fraction field of the liquid and the averaged velocity field of the mixture, characterizing the behavior of the dynamic spray. Also, we drew the temporal evolution of the penetration length of our calculation (for all turbulence models cited above) with the experiment curve and that of computer code AVBP. Finally, we deduced the appropriate model of turbulence and two-phase flow for better characterizing the dynamic of the diesel spray.*

Keywords: *Diesel spray, CFD, RANS, Turbulence, VOF_Level-Set, Fluent.*

I. INTRODUCTION

Car manufacturers are facing increasingly severe regulations on pollutant emissions and fuel consumption. To respect these regulations, new combustion concepts in Internal Combustion Engine (ICE) have been developed. The Direct Injection (DI) diesel engine represents one of these concepts. Although it has shown a great potential, it still requires a comprehensive work to allow a better understanding. In fact, the efficiency of the combustion of the fuel and therefore the performance of a diesel engine depends on the quality of the fuel–air mixture. In conventional combustion systems, where the fuel is injected directly into air, it is necessary to provide adequate conditions for a good macrostructure of the mixture in the combustion chamber. This involves that the injected fuel must be uniformly distributed in the combustion chamber in the very short time interval available for the mixture formation. The fuel–air mixture process is strongly influenced by the spray behavior, which depends on several parameters. These parameters can be classified into two groups: parameters related to the diesel injection system (injection pressure, injection nozzle...) and others associated with the environment (ambient air density, ambient temperature...) where the spray is injected **[1-2]**.
During the recent years, Computational Fluid Dynamics has become one of the most important tools for both understanding and the considerable sensitivity of the model to small changes brought upon by numerical resolution, particularly in the area where onset of the transition occurs. The goal was the improvement of the diesel spray in the Internal Combustion Engine (ICE). The fuel injection process and the subsequent fuel–air mixing formation play a major role in the combustion and the pollutant emissions in the ICE. Even now, some of the processes involved in these phenomena, such as primary atomization and dense zone close to the nozzle, are not fully understood **[6–8]**.
The two-phase and turbulent nature of the diesel spray makes the study by DNS (Direct Numerical Simulation) or LES (Large Eddy Simulation) very heavy in computation time. Then, using the RANS (Reynolds Averaged Navier-Stokes) approach is privileged by Diesel motorists. The system of averaged equations the sense of Reynolds containing a nonlinear term characterizing the turbulence: the stress tensor of Reynolds. This term set a closure problem. To remedy this problem, one must resort to the turbulence modeling. Hence, several models

have been developed in literature. For example, the model of Spalart Allmaras, k-ε, k-ω, SAS, RSM and k-k$_L$-ω for several industrial applications of single-phase or multiphase flows at high Reynolds number. The aim of this paper is to see the applicability of these models to better characterize the behavior of the diesel spray.

In this study, we have chosen the Euler description and used the biphasic model VOF and its coupling with the Level-Set model, which is suitable for free-surface flow with a fixed mesh **[6-7]**. We will test both to decide which one better describes the two-phase nature of the diesel spray: is it the VOF model or the coupling "VOF_Level-Set".

The remaining of the presentation proceeds as follows. In Section II, we write the basic equations of interest. We present, in Section III, our numerical simulations. Results and discussion are pointed out in Section IV. We draw some concluding remarks in the last section.

II. BASIC EQUATIONS

The incompressible transient form of and the Reynolds Averaged Navier-Stokes equations with the assumptions of constant physical properties are described below in the following equations:

$$\frac{\partial U_i}{\partial x_i} = 0 \; ; \qquad (1)$$

$$\frac{DU_i}{Dt} = \frac{\partial}{\partial x_j}\left[\vartheta \frac{\partial U_i}{\partial x_j}\right] - \frac{1}{\rho}\frac{\partial P}{\partial x_i} - \frac{\partial \overline{u_i u_j}}{\partial x_j} + F_s ; \qquad (2)$$

$$\frac{\partial \rho E}{\partial t} + \frac{\partial \rho E U_j}{\partial x_j} = \frac{\partial U_i \tau_{ij}}{\partial x_j} - \frac{\partial q_j}{\partial x_j} . \qquad (3)$$

These equations express the mass conservation law, the quantity of movement and the total energy, respectively. There, U_i and u_i are the average and fluctuating velocity components in direction x_i, $\overline{u_i u_j}$ is the Reynolds stress tensor, P is the pressure, ϑ is the kinematic viscosity, ρ is the fluid density, F_s is the term of surface tension, E is the total energy, τ_{ij} is the strain rate tensor, and q_j is the heat flux. The term of Reynolds stress tensor causes a problem of closure. This is why we need turbulence models.

The inclusion of the turbulent fluctuation on the mean flow equations via the eddy viscosity is traduced by the following relation (Boussinesq hypothesis).

$$\overline{u_i u_j} = \frac{2}{3} k_{TOT}\delta_{ij} - \vartheta_{TOT}\left(\frac{\partial U_i}{\partial x_j} + \frac{\partial U_j}{\partial x_i}\right) \qquad (4)$$

This term in equation (2) is modeled by many turbulence models in this study, such as: spalart allmaras **[8]**, $k - \varepsilon$ **[9-11]**, $k - \omega$ **[12-13]**, SAS **[14]**, RSM **[15-17]** and $k - k_L - \omega$ **[18]** models.

The relationship between the ambient pressure and air ambient density is:

$$P = \frac{\rho RT}{M} \qquad (5)$$

Here, R is the constant of ideal gas, T the absolute temperature of the ambient air, and M the molar mass of the ambient air.

Finally, to describe the multi-phase flow character, used was made the VOF model and its coupling with the Level-Set model. To monitor the interface in its movement, we need the indicator function of each phase: The volume fraction α_k is advected by the local averaged velocity field, according to the following equation of the classical advection:

$$\frac{\partial \alpha_k}{\partial t} + U.\nabla \alpha_k = 0 \qquad (6)$$

If we consider only the problem of two phases, it is sufficient to calculate once the scope of this α_k function to identify each phase of the two phases in the whole space: For example, we calculate α_1 (volume fraction of fluid 1) field, then we determine α_2 (volume fraction of fluid 2) by: $\alpha_1 + \alpha_2 = 1$.

III. NUMERICAL SIMULATION

The tools used in this work are Gambit and Fluent. The former is a geometry and mesh generator and the latter is a numerical solver in the finite volume.

The injection conditions correspond to those of some experiment made by **Verhoeven et al. [19]**. The temporal profile of the velocity is imposed at the input (figure 1) **[20]**, deducted from the mass flow measurement made in Ref. **[19]**. To validate the model used in this study, we assumed that the direction of the exit velocity is normal and the turbulent intensity at the spray exit is 1%. The density of the liquid is $\rho_l = 780\ kg.m^{-3}$, its absolute temperature is $T = 360\ K$ and the diameter of injection is $d = 0.2\ mm$.
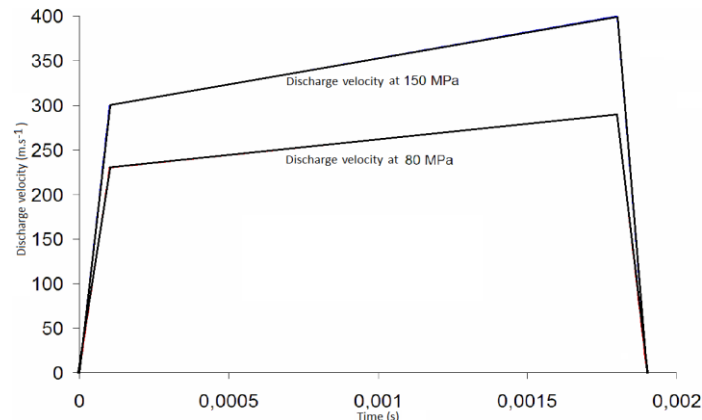
Figure 1: Injection velocity profile deducted by **Beau [20]**,
from the injection rate profile measured **[19]**.

To study the effect of turbulence models on the behavior of the spray, we fixed everything about the other calculation conditions (two-phase model, numeric schemes, injection and ambient conditions, mesh...) and by computing for each model. We deduced the model that will better describe the diesel spray by comparing the calculation results with those of the literature.

After choosing the appropriate turbulence model, we study the behavior of the spray for both models of the two-phase flow: the Volume of Fluid and its coupling with Level-Set.

IV. RESULTS AND DISCUSSION

In this paragraph, we present the results obtained by using the above described models for simulating the development of the non-evaporating Diesel spray at high injection pressure. The macroscopic and microscopic parameters used for the characterization of the spray are the length penetration, the volume fraction field of the liquid and the field of the averaged velocity of the mixture.

First let's start by comparing between turbulence models for an injection pressure $P_i = 800\ bar$. Then, for the same pressure, we will analyze the effect of the two-phase model. Finally, after the choice of the appropriate models, we present the results for high injection pressure ($P_i = 1500\ bar$).
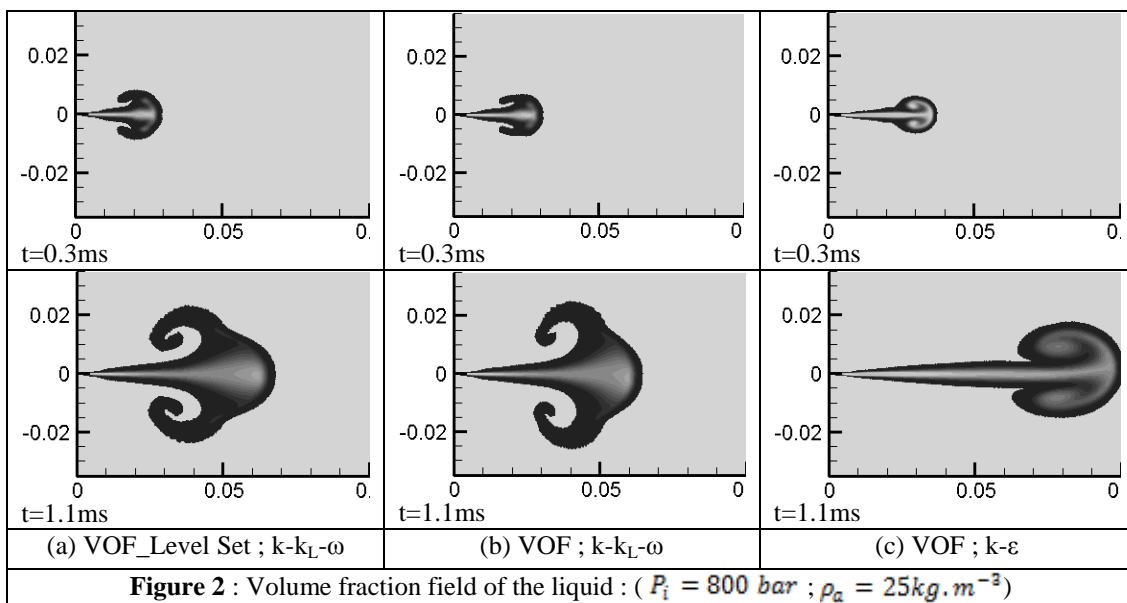
1. **The comparison between the turbulence and two-phase models**

We will do the comparison using the parameters that characterize the jet. These parameters are represented as follows:

The volume fraction field of the liquid

In figure 4, we visualized the volume fraction field of the liquid in two moments after injection (t=0.3ms; t=1.1ms) for three combinations of turbulence and two-phase models (a: VOF (Level Set) and k-k_L-ω, b: VOF and k-k_L-ω, c: VOF and k-ε).

The images of simulation show a symmetrical penetration of the jet into the gaseous environment. But, for the same moments after injection, the k-ε model gives greater penetration than the k-k_L-ω. We can note that the spray does not expands when using the k-ε model. For cons, we see very well the expansion of the jet using k-k_L-ω. This means that the k-k_L-ω takes into account the aerodynamic effects blocking longitudinally the jet to penetrate and expand radials.

| (a) VOF_Level Set ; k-k$_L$-ω | (b) VOF ; k-k$_L$-ω | (c) VOF ; k-ε |

Figure 2 : Volume fraction field of the liquid : ($P_i = 800 \ bar$; $\rho_a = 25 kg.m^{-3}$)

❖ **The penetration length of the spray**

The spray penetration is a very important factor for a direct injection diesel engine. The penetration is particularly important for the formation of the mixture "fuel-air", the shock with the wall and the shape of the combustion chamber. We chose this parameter to validate the result of numeric simulation of many models of turbulence and the two models describing the two-phase flow (cited above).

In figure 3, we drew the curve of temporal evolution of the penetration length of the spray after injection using these conditions ($P_i = 800 \ bar$; $\rho_a = 25 kg.m^{-3}$) for several turbulence models (k-ε ; SAS ; Spalart allmaras ; RSM ; k-k$_L$-ω) with the curve of the experiment [19] and of the curve of the filtered calculation [21].

The curves of figure 3 concerning the k-ε, the Spalart Allmaras and the SAS models show a linear penetration of the spray upon time after injection. Also, they highlight the concordance with that of the experiment between $t = 0ms$ and $= 0.2ms$: the phase of time after injection when the aerodynamics forces have low effect for the evolution of the spray. But, after $t = 0.2ms$, the curves move away of the curve of the experiment : the penetration remains fast, which means that the aerodynamics effects are negligible after that time. So, these turbulence models do not take into account the aerodynamic effects responsible of the blockage of spray after a time called "time to break up".

For the simulation curve using the k-k$_L$-ω model, it accords with the experiment and the filtered calculation by Martinez, highlighting two stages of penetration. Before $t = 0.2ms$, there is a rapid penetration and after this time, the penetration becomes slow. So, this model describes correctly the evolution of the penetration of spray taking into account the aerodynamics effect of the ambient milieu.

About the RSM model, the corresponding curve is very far than other simulation and experience curves.

After the analysis of different turbulence models, used to close the system of the averaged equations in the sense of Reynolds (to study the dynamic behavior of the diesel spray at the level of the temporal evolution of the penetration length), we can deduce that the k-k$_L$-ω is the model that can be valid in this case study.
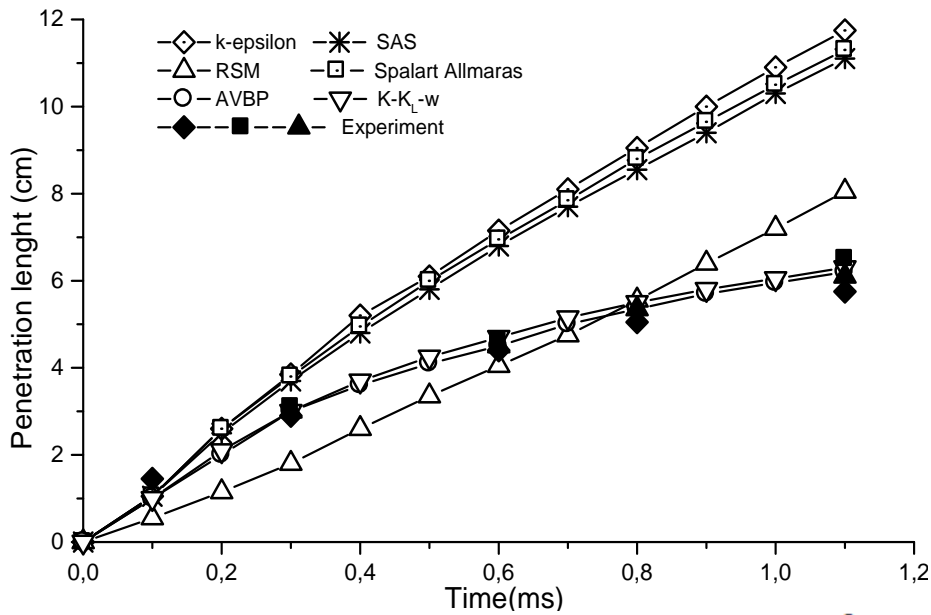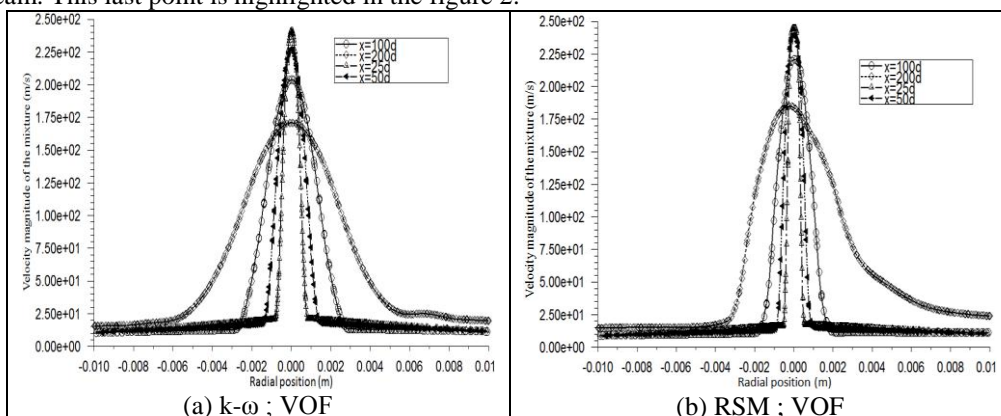
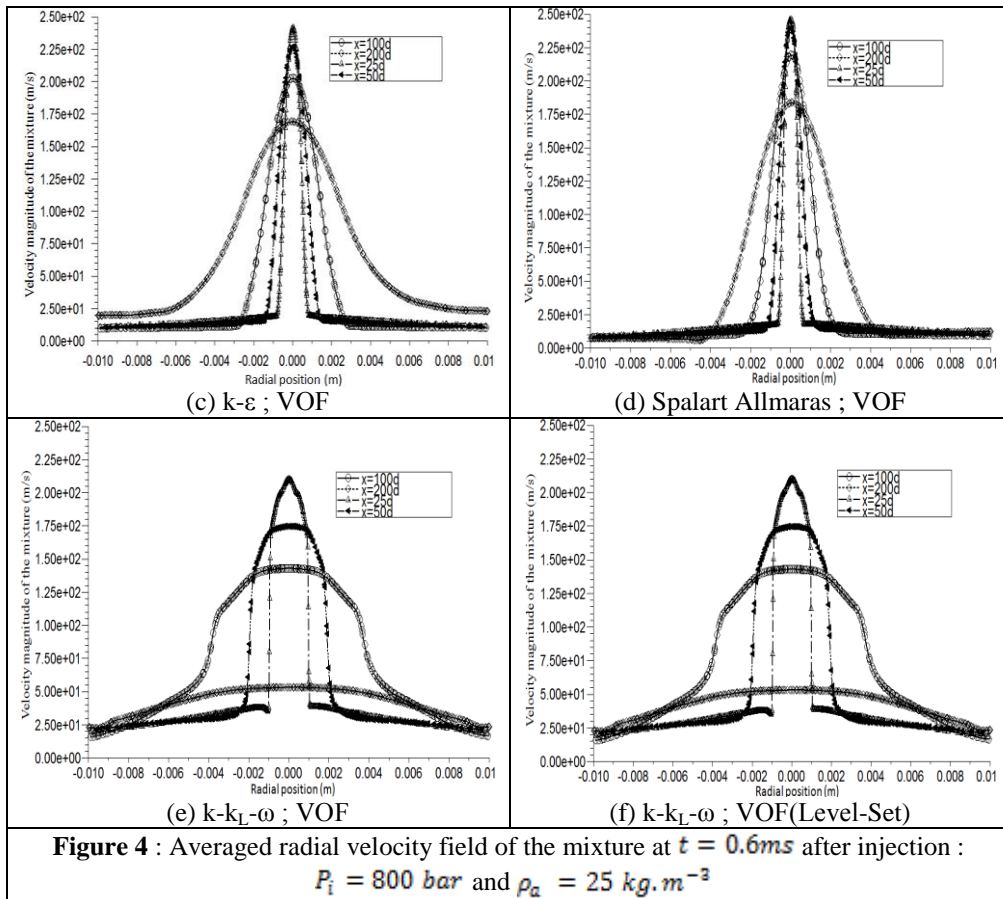**Figure 3**: Penetration length upon time: ($P_i = 800bar$, $\rho_a = 25kg.m^{-3}$)

❖ **The averaged velocity field of the mixture**

In the figure 3, we plotted the curves of the radial evolution of the averaged velocity of the mixture at several axial positions from the exit spray ($x = 25d$; $x = 50d$; $x = 100d$; $x = 200d$) for many turbulence models ((a) : k-ω, (b) : RSM, (c) : k-ε , (d) : Spalart allmaras, (e) and (f) : k-k_L-ω), used with VOF model which modeling the two-phase flow. Except the case (figure 3(f)), we used the coupling "VOF_Level-Set".

We can note, for all the curves that the radial evolution of the averaged velocity of the mixture is symmetrical relative to the jet axis. Except for the curve that corresponds to the RSM model (b), where: when we advance downstream, we lose the symmetry (the curve for $x = 200d$).

One can also note on the curves corresponding to the models (k-ω, RSM, k-ε, Spalart Allmaras) that the velocity remains maximal and equal to the axial jet exit velocity ($t = 0.6ms$ after injection) which overestimates the length of the potential core (the length where the velocity remains constant on the jet axis). For cons, the curves corresponding to the model k-k_L-ω, the velocity starts to diminish close by the outlet of the jet and which becomes very low away (at $x = 200d$).

One can see on the curves which corresponding to the model k-k_L-ω that a very important radial evolution compared to other models, which provides information on the expansion of the jet advancing downstream. This last point is highlighted in the figure 2.

| (a) k-ω ; VOF | (b) RSM ; VOF |

Figure 4 : Averaged radial velocity field of the mixture at $t = 0.6ms$ after injection :
$P_i = 800\ bar$ and $\rho_a = 25\ kg.m^{-3}$

2.   The volume fraction field of the liquid at high injection pressure

After choosing the appropriate models to study the behavior of the dynamic spray: the k-k_L-ω for turbulence models and the coupling VOF_Level-Set model for two-phase flow, we did the study by using these models at high pressure injection. In figure 5, we visualized the volume fraction field of the liquid by using injection and ambient conditions ($P_i = 1500\ bar$, $\rho_a = 25\ kg.m^3$) that are the same conditions of the experiment **[19]**. The images of simulation are agree with the experiment result **[19]**.

Figure 5 : Volume fraction field of the liquid : ($P_i = 1500\ bar$; $\rho_a = 25 kg.m^{-3}$)
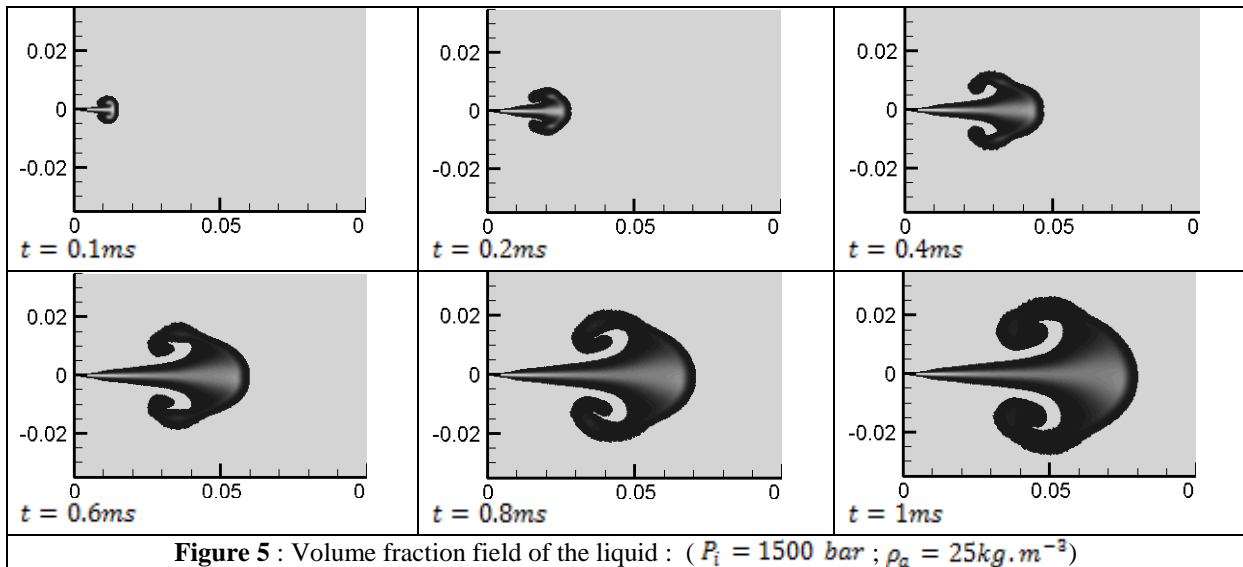
So, the k-k_L-w and the coupling "VOF_Level-Set" are the appropriate models for modeling the spray diesel at high injection pressure.

IV. CONCLUDING REMARKS

In this work, we studied the dynamic of the diesel spray in a combustion chamber of a Diesel engine of direct injection during the injection spray, at high injection pressure, in two dimensions. The penetration of a Diesel spray in a pressure chamber has been investigated numerically. The penetration length of the spray has been calculated at high pressure injection, with different turbulence models and two models of two-phase flow.

For the results, we visualized the evolution of the Diesel spray using the volume fraction field of the liquid and the longitudinal and radial evolution of the averaged velocity of the mixture. We drew the curves of the evolution of the penetration length of the spray. The comparison with the results of the experiment and the computation filtered gives an argument to prefer the k-k_L-ω model then the other models of turbulence for characterizing the behavior spray motion. Finally, we demonstrated the effect of two-phase models. We used the VOF models and its coupling with Level-Set, and we can remark a little difference on the conic form of the spray, which is clearly identified when we use the coupling VOF_Level-Set model.

REFERENCES

Journal Papers:

[2] A. Khalid, T. Yatsufusa, T. Miyamoto, J. Kawakami, and Y. Kidoguchi. "Analysis of Relation between Mixture Formation during Ignition Delay Period and Burning Process in Diesel Combustion". SAE Paper 2009 32 0018, pp.1 10, 2009.
[4] R. Lebas, G. Blokkeel, P. Beau, and F. Demoulin. "*Coupling vaporization model with the Eulerian–Lagrangian Spray Atomization (ELSA) model in diesel*". Engine conditions, SAE Technical Paper 2005-01-0213, 2005.
[6] C.W. Hirt and B. D. Nichols. "*Volume of Fluid Method for the Dynamics of Free Boundaries*". Journal of Computational Physics 39, 201-225 (1981).
[5] R. Lebas, T. Menard, P.A. Beau, A. Berlemont, and F.X. Demoulin. "*Numerical simulation of primary break-up and atomization: DNS and modelling study*". International Journal of Multiphase Flow 35 (3), 247–260.
[7] A.A. Oner, M.S. Akoz, M.S. Kirkgoz, and V. Gumus. "*Experimental Validation of Volume of Fluid Method for a Sluice Gate Flow*". Advances in Mechanical Engineering, Volume 2012 (2012), Article ID 461708, 10 pages.
[9] B. E. Launder and D. B. Spalding." *Lectures in Mathematical Models of Turbulence*". Academic Press, London, England. 1972.
[10] V. Yakhot and S. A. Orszag. "*Renormalization Group Analysis of Turbulence I Basic Theory*". Journal of Scientific Computing,. 1(1). 1–51. 1986.
 [11] T.-H. Shih, W. W. Liou, A. Shabbir, Z. Yang, and J. Zhu. "*A New - Eddy-Viscosity Model for High Reynolds Number Turbulent Flows - Model Development and Validation*". Computers Fluids. 24(3). 227–238. 1995.
[12] D. C. Wilcox. "*Turbulence Modeling for CFD*". DCW Industries, Inc. La Canada, California. 1998.
[13] F. R. Menter. "*Two-Equation Eddy-Viscosity Turbulence Models for Engineering Applications*". AIAA Journal. 32(8). 1598–1605. August 1994.
[14] F. Menter and Y. Egorov. "*The Scale-Adaptive Simulation Method for Unsteady Turbulent Flow Predictions. Part 1: Theory and Model Description*". Journal Flow Turbulence and Combustion. 85. 113–138. 2010.
[15] M. Gibson and B. E. Launder. "*Ground Effects on Pressure Fluctuations in the Atmospheric Boundary Layer*". J. Fluid Mechanic 86. 491–511. 1978.
[16] B. E. Launder. *Second-Moment Closure: Present... and Future*? Inter. J. Heat Fluid Flow. 10(4). 282–300. 1989.
[17] B. E. Launder, G. J. Reece, and W. Rodi. "*Progress in the Development of a Reynolds-Stress Turbulence Closure*". J. Fluid Mech. 68(3). 537–566. April 1975.
[18] D. Keith Walters and Davor Cokljat. "*A three-equation eddy-viscosity model for Reynolds-Averaged Navier-Stokes simulations of transitional flows*". Journal of Fluids Engineering. 130. December 2008.
[19] D.Verhoven, J. Vanhemelryck, and T. Baritaud (1998). "*Macroscopic and ignition characteristics of high-pressure sprays of single-component fuels*". SAE technical paper 981069.

Thesis:

 [1] J. Yon. "*Jet Diesel haute pression en champ proche et lointain : Etude par imagerie*". Doctorate Thesis, Rouan University, 2003.
[8] P. Spalart and S. Allmaras. "*A one-equation turbulence model for aerodynamic flows*". Technical Report AIAA-92-0439. American Institute of Aeronautics and Astronautics. 1992.
[20] P. Beau. "*Modeling atomization of a liquid jet-Application to Diesel sprays*". Doctorat Theses, University of Rouen (2006).
[21] L. Martinez. "*Simulation aux grandes échelles de l'injection de carburant liquide dans les moteurs à combustion interne*". Thèse soutenue Le 15 septembre 2009, Délivré par l'Institut National Polytechnique de Toulouse (INP Toulouse)

Books:

 [3] A.H. Lefebvre. Atomization and Sprays (Taylor and Francis 1989).

Research Paper   Open Access

Performance Analysis of LTE in Rich Multipath Environments Considering the Combined Effect of Different Download Scheduling Schemes and Transmission Modes

Anupama Tasneem, Md. Ariful Islam, Israt Jahan, Md. Jakaria Rahimi
Department of Electrical and Electronic Engineering, Ahsanullah University of Science & Technology, Bangladesh

ABSTRACT: - Long Term Evolution (LTE) is the new standard specified by Third Generation Partnership Project (3GPP) on the way towards the 4G mobile network. The LTE introduces enhance data link mechanisms to support successful implementation of new data services across the network. The incorporated scheduling mechanisms can significantly contribute to this goal. In this paper, we have compared the performance of Best Channel Quality Indicator (Best CQI) and Proportional Fair (PF) which are the two most popular scheduling algorithms used in LTE. The performance was compared in rich multipath environment using Transmit Diversity (TxD) and Open Loop Spatial Multiplexing (OLSM). In recent past similar comparison was carried out for rural environments [1]. In the rural environment the multipath effect was not significant. The results of simulation showed that both the Best CQI and PF perform fairly well for TxD in comparison with the OLSM technique. So here in this paper we have considered the urban environment which demonstrates significant effect due to multipath. The simulation results shows improvement in total throughput is not so significant using OLSM technique for the both the scheduling without much deterioration in the BLER. When the throughput is increased in OLSM, the BLER gets deteriorated drastically. Thus TxD is found to be working efficiently in rich multipath environments as it had been found previously for the rural environment.

KEYWORDS: -*Transmit Diversity, Spatial Multiplexing, Best CQI, Proportional Fair, Scheduling.*

I.   INTRODUCTION

The 3gpp LTE is designed to meet high speed data & voice support along with multimedia broadcast services. The scheduler in the Medium Access Control (MAC) layer of the eNodeB attempts to make appropriate apportionment of the resources with certain objectives like,

- Required Quality of Service (QoS) for applications.
- Optimized spectral efficiency ensuring high cell throughput under existing channel conditions.
- Fairness among User Equipment's (UEs) and applications.
- Limiting the impact of interference through special handling of cell edge users.
- Load balancing among cells.

There are six downlink channels. They are Physical Broadcast Channel (PBCH), Physical Control Format Indicator Channel (PFCICH), Physical Downlink Control Channel (PDCCH), Physical Hybrid-ARQ Indicator Channel (PHICH), Physical Downlink Shared Channel (PDSCH) and Physical Multicast Channel (PMCH). In this paper, the Physical Downlink Shared Channel (PDSCH) channel is taken into consideration. This channel can use various Multiple Input Multiple Output (MIMO) techniques, e.g. spatial multiplexing, transmit diversity and beam forming to improve the throughput and data rate. Under this channel, seven transmission modes are defined in Release 8. In this paper, the impact of transmission mode 2 and 3 is demonstrated which represent Transmit Diversity (TxD) and Open Loop Spatial Multiplexing (OLSM) respectively. For the apportionment of downlink resources, the following information is made available with the scheduler for consideration.

- Channel Quality Indicator (CQI) reports from UEs to estimate the channel quality.
- QoS description of the EPS bearers for each UE. This is available in the eNodeB from the downlink data flow.

The throughput of a UE may vary significantly with scheduling algorithm used, distance from eNodeB, multipath environment, multiple antenna techniques and UE speed. The effect of UE speed in the transmission mode performance is already discussed in [1]. The effect of scheduling algorithm, distance and transmission modes1 and 2 in throughput performance is considered through LTE system level simulations in [2].In this paper, we have focused mainly on the effect of TD and OLSM on Throughput and Block Error Rate (BLER) of LTE specially in rural environment. This report is organized as follows, in section 2 The Downlink Resource scheduling, LTE Transmission Modes are discussed in section 3, section 5 contains the simulation results, and finally conclusion in the section 6.

By analyzing these scheduling algorithms we will easily understand that, which method is useful and cost effective for the rural environment.

II.   DOWNLINK RESOURCE SCHEDULING

LTE uses Orthogonal Frequency-Division Multiple Access (OFDMA) for downlink transmission. In this case, a time-frequency resource grid is considered using sub-carriers in the frequency axis and symbols in the time axis. A resource element represents one sub-carrier and one symbol resource in the time-frequency resource grid.

Data is allocated to the UEs in terms of Resource Blocks (RB). In time, the length of a RB is one slot which is equal to 0.5 ms (millisecond). With 15 kHz sub-carrier spacing, the number of symbols in one slot is 6 and 7 for normal cyclic prefix and extended cyclic prefix respectively. In frequency, the length of a RB is 180 kHz. The number of sub-carriers in the 180 kHz span is 12 for 15 kHz sub-carrier spacing.

The eNodeB allocates different RBs to a particular UE in either localized or distributed way. The eNodeB uses DCI format 1, 1A, 1B, 1C, 1D, 2, 2A or 2B on PDCCH to convey the resource allocations on PDSCH for the downlink transmission [1]. The eNodeB uses one of the following three types of resource allocation for a particular UE [3].

- Resource Allocation Type 0
- Resource Allocation Type 1
- Resource Allocation Type 2

The scheduler at eNodeB attempts for appropriate apportionment of the resources among UEs. The Channel Dependent Scheduling can be made in both time and frequency domains. In this case, the scheduling adapts to channel variations and link adaptation is achieved. A user with better channel quality is given more resources as the user can make good use of these resources leading to higher cell throughput. The channel dependent scheduling allows transmitting at fading peaks. The Channel Dependent Scheduling (CDS) requires that sufficient information on uplink and downlink channel conditions is made available with the eNodeB. In order to perform Channel Dependent Scheduling (CDS) in frequency, the information about the radio channel needs to be frequency specific. The eNodeB can configure a more frequency specific information but it requires usage of more resources for this information. Also, the eNodeB can configure the availability of the information more frequently in time so that it can represent the variation of radio channel better but again at the cost of more resources for this information.

The UE reportsCQI which helps eNodeB estimate the downlink channel quality. The eNodeB can configure if the CQI report would correspond to the whole downlink bandwidth or a part of it which is called sub-band. CQI reporting for different sub-bands requires more uplink resources. The eNodeB can configure CQI reporting in the following ways [3].

- Wideband Reporting: The CQI reported corresponds to the whole downlink bandwidth
- eNodeB Configured Sub-Band Reporting
- UE Selected Sub-Band Reporting

The channel dependent scheduling leads to higher cell throughput and on the other hand, the scheduling should maintain some fairness among the users in their resource allocations. There is a tradeoff between fairness and cell throughput. The scheduler can exercise various methods as shown below in order to address this tradeoff.

- Best CQI: The CQI value can be expressed as a recommended transport-block size instead of expressing it as a received signal quality. It can be used for the scheduling. Best CQI scheduling algorithm uses these values as a reference for making decision of scheduling.
- Proportional Fair (PF): The scheduler can exercise Proportional Fair (PF) scheduling allocating more resources to a user with relatively better channel quality. This offers high cell throughput as well as fairness satisfactorily. Thus, Proportional Fair (PF) scheduling may be the best option.
- Scheduling for Delay-Limited Capacity:Some applications have very tight latency constraints and so, their QoS require certain guaranteed data rate independent of the fading states. This guaranteed data rate is called delay-limited capacity. The scheduler can allocate resources considering such special requirements.

III.   LTE TRANSMISSION MODES

PDSCH is configured with one of the following transmission modes according to Release 8 [4]. The choice of transmission mode may depend on the instantaneous radio channel conditions and the transmission mode may be adapted semi-statically.

- Transmission Mode 1: Using a single antenna at eNodeB
- Transmission Mode 2: Transmit Diversity
- Transmission Mode 3: SU-MIMO Spatial Multiplexing: Open-Loop
- Transmission Mode 4: SU-MIMO Spatial Multiplexing: Closed-Loop
- Transmission Mode 5: MU-MIMO Spatial Multiplexing
- Transmission Mode 6: Beam forming using Closed-Loop Rank-1 Precoding: It can also be seen as a special case of SU-MIMO Spatial Multiplexing.
- Transmission Mode 7:Beam forming using UE-Specific Reference Signals

The following sections briefly describe the transmission modes which are simulated for evaluation purpose.

3.1 Transmit Diversity (TxD)

In TxD Figure 1(a), Space Time Block Codes (STBC) are used to provide improvement against the channel deteriorating effects.Alamouti STBC is considered to be the simplest space-time block codes. It is well known that Alamouti codes [5] can achieve full diversity and full code rate simultaneously. But for MIMO Systems having more than two transmit antennas diversity and orthogonality can only be achieved at the cost of slower date rates. Therefore we cannot achieve high data rates beyond a certain value and powerful coding schemes are required to achieve higher data rates as the SNR (Signal to Noise Ratio) $\rightarrow \infty$ .Another issue with TxD is that it is single rank i.e. it does not support multi stream transmission [6].
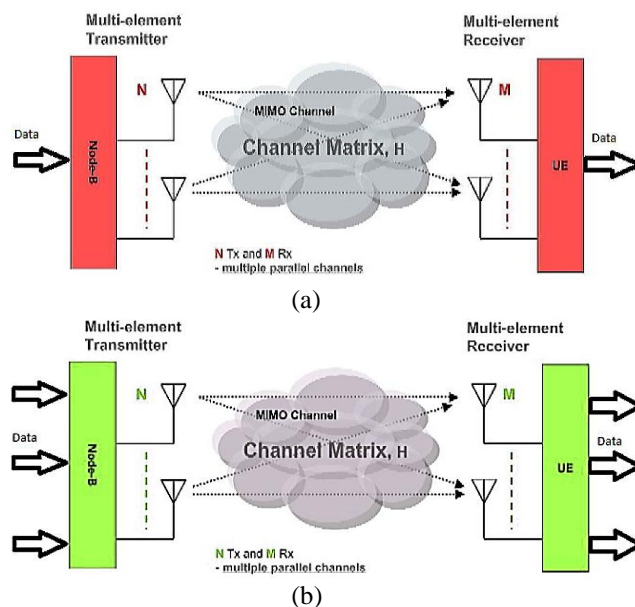

(a)

(b)

Figure1: (a) Block diagram of a MIMO transmission using Transmit Diversity, (b) Block diagram of a MIMO transmission using OLSM

3.2 Spatial Multiplexing(SM)

SM provides extra gain as compared to TxD [7].Independent data streams are transmitted from the NT transmit antennas in spatial multiplexing. There are two classes of spatial multiplexing, they are open and closed loop spatial multiplexing. OLSM is discussed in Figure 1(b). OLSM transmits the independent data streams without deploying any feedback algorithm. High data rate is achieved as compared to TxD as multiple independent streams are transmitted. This endorses high BLER. To compensate this BLER Closed Loop Spatial Multiplexing (CLSM) is used. In CLSM, essential amount of CSI is used as feedback which enables us to achieve high throughput with lower BLER. But the CLSM is not considered in this paper.

IV.   SIMULATION RESULTS

LTE system level simulator [8] was used with parameters shown in the table 1.5 UEs are placed randomly in one sector of a cell. Performance with Best CQIandProportional Fair scheduling has been observed

for five UEs at various distances from the eNodeB. The throughput has been determined for transmission modes 2 and 3 for rural propagation model.

Table 1:Simulation Parameters

Parameters	Assumptions
Transmission bandwidth	2.0GHz
Inter-site distance	5MHz
Thermal noise density	500m
Receiver noise figure	9dB
Simulation length	5000 TTI
UE speeds of interest	5km/hr
UEs position	5UEs/sector, located in target sector only.
Antenna	'TS 36.942'
Channel_model	PedB'
BS antenna gain	15 DBi [1]
Scheduler	Best CQI, Proportional Fair
Thermal noise density	-174dBm/Hz
TXmode	2,3
nTX x nRX antennas	2 x 2
eNodeB TX power	43dBm
Subcarrier averaging algorithm	EESM
Uplink delay	3TTIs
Macroscopic path loss model	'TS 36.942'

The simulation scenario can be seen as shown in the Figure 2.
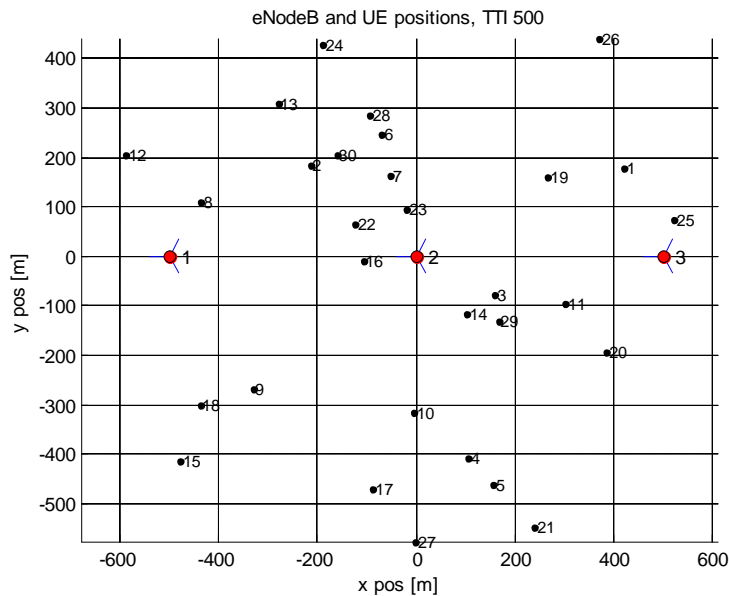
Figure2: The Initial Position of UEs with respect to the three eNodeBs.
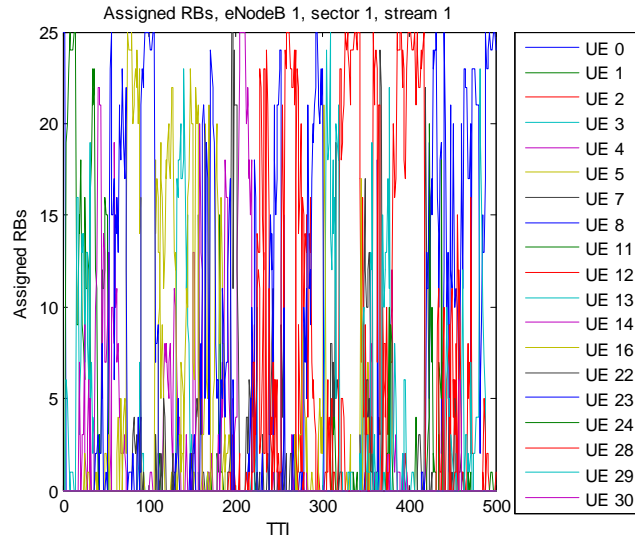
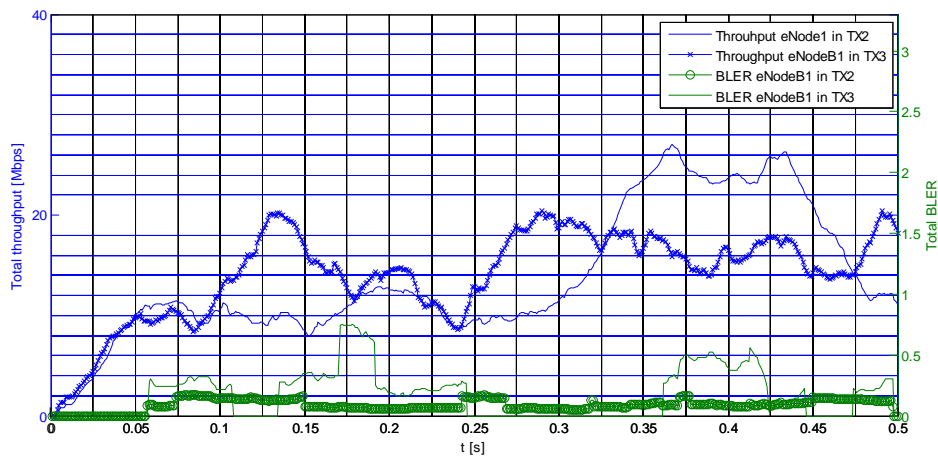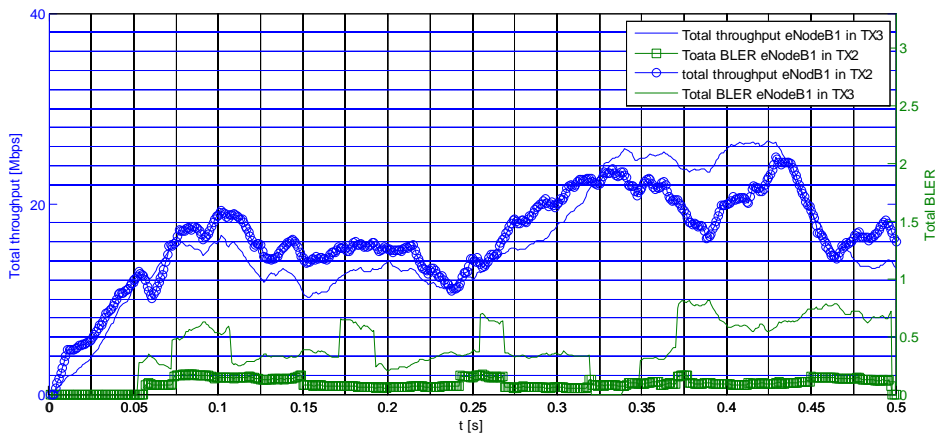Figure3: Assigned Resource Blocks (RBs) for eNodeB 1, sector 1, stream 1.

Figure4: Comparison of Total THROUGHPUT using PF in transmission mode 2 and 3(5MHz Bandwidth) along with corresponding BLER curves.

From the Figure 4 we can easily observe that, while using proportional fair scheduling, significant improvement in *instantaneous* throughput using transmission mode 3 is not consistent. Also no significant improvement is observed in *average* throughput. BLER performance is better in transmission mode 2.

Figure5: Comparison of Total THROUGHPUT using Best CQI in transmission mode 2 and 3(5MHz Bandwidth) along with corresponding BLER curves.

From the Figure 5 we can easily observe that, using Best CQI scheduling, no significant improvement is observed in both *instantaneous* and *average* throughput using transmission mode 3. BLER performance is much better in transmission mode 2.

V.   CONCLUSION

From the simulation results we get fairly good Throughput and BLER for both Best CQI and Proportional Fair schedulers in two different modes. But the analysis of the simulation graphs show that Proportional Fair scheduler has highest throughput values in transmission mode 2.At low BLER values Proportional Fair scheduler performed more efficiently than other scheduler algorithms. On the other way, the OLSM failed to show any significant improvement in Throughput. We also observed the Throughput and BLER of Round Robin, but did not get any expected results. If we want just high Throughput then the Best CQI schedulers will be a good choice for the system. But if high Throughput and lower BLER is a major consideration in the service requirement of the system then the Proportional Fair idea will be a better choice. It is also worth noting that the difference in the throughput results of the Best CQI and Empirical is not low and cannot be used to justify the argument for Proportional Fair as a better algorithm.

REFERENCES

[1] Md. Ariful Islam, Israt Jahan, Md. Reduan Hossain, Mahmudur Rahman, Abdullah-al-Mukit, Mr. Md. Jakaria Rahimi, "Performance Analysis of LTE in Rural Environments Considering the Combined Effect of Different Download Scheduling Schemes and Transmission Modes", Published-American Journal of Engineering Research (AJER) e-ISSN : 2320-0847 p-ISSN : 2320-0936 Volume-02, Issue-11, pp-293-299.(November, 2013).

[2] Mohammad T. Kawser, Abduhu. R. Hasin, Hasib M. A. B. Farid, Adil M. J. Sadik, Ibrahim K. Razu, Performance comparison between Round Robin and Proportional Fair scheduling: Methods for LTE, *Procedia Engineering,28-30 December 2011*, Dubai, UAE.

[3] 3GPP Technical Specification 36.213, 'Evolved Universal Terrestrial Radio Access (E-UTRA); Physical Layer Procedures', www.3gpp.org accessed in September 2013.

[4] Stefania Sesia, Issam Toufik and Matthew Baker, *LTE- the UMTS long term evolution: from theory to practice* (2009 John Wiley & Sons, Ltd. ISBN: 978-0-470-69716-0).

[5] "Switching between open and closed loop multi-stream transmission," Swedish Patent WO 2011/115 532 A1, 2011.

[6] J. Guan, X. Ye, and P. Tian, A robust scheme for transmit diversityand spatial multiplexing: Based on channel spatial correlation, *In International Conference on Multi-Media and Information Technology*, 2008.

[7] G. Wetzker, "Definition of spatial multiplexing gain," in Electronic Letters, 2005, accessed in August 2013.

[8] LTE System Level Simulator v1.0r295 by Institute Of communication and Radio Frequency Engineering, Vienna University of Technology, Vienna, accessed in November 2012.

Experimental Investigation on the Effects of Digester Size on Biogas Production from Cow Dung

Abdulkarim Nasir, Katsina C. Bala, Shuaibu N. Mohammed,
Abubakar Mohammed*, Isah Umar
Department of Mechanical Engineering, Federal University of Technology, Minna, Nigeria

ABSTRACT : *This paper presents the experimental investigation on the effect of digester size on biogas production. Experiments were carried out to produce biogas from different sizes of digester. 1.4 kg of cow dung was used to carry out the experiments. The temperature throughout the period of experimentation was within ambient temperature of 25^0C to 35^0C. It was observed that the pH values of the Digesters fluctuate between 5.4 and 7.6. This may be due to the activities of acid. Digesters A, B, C, D and E, with volumes of 250 ml, 500ml, 1000ml, 2000ml and 3000ml, produced a total biogas of 625 cm^3, 715cm^3, 1635cm^3, 2082cm^3 and 2154cm^3 respectively. Digester size is an important factor which has a direct effect on the quantity of gas produced. For the total biogas produced per litre of digester size, Digesters A, B, C, D and E, produces 2500 $cm^3 l^{-1}$, 1430 $cm^3 l^{-1}$, 1635 $cm^3 l^{-1}$, 1041 $cm^3 l^{-1}$ and 718 $cm^3 l^{-1}$ respectively.*

KEYWORDS : *Biogas, Cow dung, digester size, temperature, pH.*

I.   INTRODUCTION

Anaerobic digestion of animal waste on farms involves the breakdown of organic matter by bacteriological action to produce biogas and digested effluent (digestate). The pollution potential of digestate is lower, has fewer odours, contains fewer viable weed seeds, has fewer pathogens than the input slurry and is an excellent biofertiliser [1].The manorial value of the biomass is not diminished in this process, rather, it is enhanced. Biogas plant helps in obtaining both fuel and manure from the same quantity of biomass [2].Biogas is a clean and cheap fuel in the form of gas which contains mixture of gases: methane (50–75%); carbon dioxide (25–50%); nitrogen (0–10%); hydrogen (0–1%); hydrogen sulphide (0–1%); and oxygen (0–2%).The calorific value of biogas varies between 20-26 MJ/m^3 (5.6-7.2 kWh/m^3) depending on the methane content. In terms of heating oil, it is equivalent to approximately 0.5–0.7 litres oil/m^3 biogas. Biogas is thus an excellent source of renewable energy [1].

Anaerobic digestion requires a gastight tank with draw-off points for biogas in the headspace, a heating system to maintain optimum digester temperature (35^0C-40^0C), a method of loading inputs and unloading digestate. Mixing of digester contents is necessary to prevent settling of solids and crust formation, as well as to ensure an even temperature within the digester. Typically, mixing is carried out by mechanical stirrers or by biogas recirculation [1].During anaerobic digestion, various organic materials are degraded to biogas (methane, carbon dioxide and other traces of gases such as nitrogen, ammonia and hydrogen sulphide) [3]. The process is of great significance and also in many well-known habitats such as marched sediments and rumen. Methane fermentation has been known since long and methane formation in sediments was discovered in the 18th century, while anaerobic digestion has been used by man since the end of the 19th century [3].

The present and potential application of anaerobic digestion requires a detailed understanding of the process. Considerable research and development efforts are necessary on many aspects of the process varying from basic microbiology and biochemistry to engineering and economics. Knowledge on microbiology, biochemistry and anaerobic digestion control of methane production has increased considerably during the last decade but still far from sufficient-mainly due to the complexity of the process. The production of biogas happens only under strict anaerobic conditions.

The bacteria prefer to use oxygen to produce their energy intermediate because of the higher efficiency of the anaerobic process with oxygen as final electron acceptor in the breathing chain and electron transport phosphorylation. The fermentation is a reaction in which oxidation and reduction reactions are internally balanced, while some atoms of the energy source become more oxidized.

Biogas is used at all times and does not cause smoke in the kitchen which may affect the human lungs and also cause irritation of the eyes. Due to high methane thermal output (37 MJ/m^3); biogas cooks quicker and enhances village sanitation if latrines are attached to these biogas plants [4]. Most Agricultural, Industrial and Municipal wastes are used for the production of biogas and the final wastes are used as manures in the farm. It has been experimentally observed that the nitrogen, phosphorus and potassium content of the biomass were higher after anaerobic digestion [2]. This shows that digested animal or plant waste should be better manure than ordinary farm yard nature. This is because the waste material is in more finely divided state after digestion as the complex organic molecules like cellulose and semi celluloses would have been broken down. Digesters vary widely with regardto complexity and layout. No simple design can be considered as ideal, since many factors affect their arrangement and construction, and these needs to be considered for an optimum to be achieved for each particular set of circumstances and environmental conditions. There are however, some essential differences in digesters principles and for conveniences, digesters types have been loosely categorized into four sections; batch, continuous, high rate and others [5]. This order generally follows a pattern of ascending sophistication, the simpler designs usually falling into the description of a batch digester and the more complimented falls into the description of heated and stirred digester, two stage layout at the other of the spectrum. In this study, the effect of digester size will be investigated.

II. METHODS

2.1 Sample Collection and Preparation

Fresh cow dung samples used for the study were obtained in a large clean plastic container from a Cattle farm in Minna, Niger State, Nigeria. The samples were mixed with water at 40°C in a ratio of 1.4kg of the cow dung to 1 litre of water into slurry. The slurry was screened to remove unwanted materials before being introduced into the digester.

2.2 Physiochemical Parameters

Moisture Content

The moisture content of the cow dung was determined as follows: 2.0g of cow dung was weighed in a pre-weighed aluminium dried dish. The sample was then placed in an oven and dried to constant weight at 105^0C for 24 to 36 hrs. The weight of the aluminium dish, cow dung and dried cow dung were recorded and the moisture content of the sample was calculated using equation (1).

$$\% \ Moisture content = \frac{M_1 - M_2}{M_1 - M_0} \times 100 \qquad (1)$$

Where, M_0 is the weight of aluminum dish (g), M_1 is the weight of fresh sample and dish (g) and M_2 is the weight of dried sample and dish (g).

Ash Content

5.0 g of cow dung sample was weighed into a crucible previously ignited and weighed organic matter was charred by igniting the material on a hot plate in the fume cupboard. The crucible was placed in the muffle furnace and maintained at 600^0C for 6hrs. It was then cooled in a desiccator and weighed immediately. The recorded weights were used to calculate the ash content of the cow dung using equation (2).

$$\% \ Ash content = \frac{W_{a+c} - W_c}{W_s} \times 100 \qquad (2)$$

Where, W_s is the weight of cow dung (g), W_{a+c} is the weight of crucible and ash (g) and W_c is the weight of empty crucible (g).

Nitrogen Content

1.0 g of cow dung sample was introduced into the digestion flask. Kjedahl catalyst (5 selenium tablets) was added to the sample. 20 ml of concentrated acid was added to the sample and fixed to the digester until a clear solution was obtained. The cooked digest was transferred into 100ml volumetric flask and made up to mark with distilled water. 20 ml of 4% boric acid was pipetted into the conical flask. 5 drops of methyl red was added to the flask as indicator and latter diluted with 75ml of distilled water. 10ml of the digest was made

Alkaline with 20ml of 20% NaOH and distilled. The filtrate was then titrated against HCl normalcy of 0.1N. The percentage total Nitrogen was calculated using equation (3).

$$\% \, Total\, N_2 = \frac{(V_2 - V_1) \times N \times 0.014}{W_s} \times 100 \qquad \textbf{(3)}$$

Where, V_2 is the sample titre, V_1 is the Blank titre, W_s weight of cow dung and N is the Normality.

2.3 Digester Experimental Procedure

Digester sizes made of conical flask was used in carrying out the digestion operations. The different sizes of conical flask used were 250ml, 500ml, 1000ml, 2000ml and 3000ml and labelled Digester A, B, C, D and E respectively. The sample as prepared above was measured into the conical flask. Rubber stopper of various sizes were plugged into the mouth of the conical flasks with two openings: one for the gas and the other for placing thermometer on top of the stoppers. The gas outlet was connected to a water displacing section. From each of the digester A, **B,** C, D and **E** the following parameters were monitored: pH (hydrogen ion concentration), temperature and volume of gas produce (cm^3).The pH of the sample was monitored on a daily basis for 26 days using the pH meter after the initial standardization of the pH with buffer 4.0 and 7.0. The temperature of the digester was monitored twice daily (morning and afternoon) with a mercury in glass thermometer placed in the digester for 26 days. The volume of gas produced by each of the digester under investigation was monitored on a daily basis through the displacement of water in the measuring cylinder. The quantity of water displaced expressed in cm^3 is a direct effect of gas produced. The experiment was monitored over a period of 26 days.

III.   RESULTS AND DISCUSSION

The results of the experiments carried out to determine the effect of digester size on biogas production are presented in Figures 1 to 6 below.

3.1 Physiochemical Parameters

The physiochemical parameters, such as the percentage Moisture content, Ash content and Nitrogen of the fresh cow dung were calculated using equations (1) to (3) and shown in Figure 1. The values for the moisture content, Ash content and Nitrogen content were 75%, 3.8% and 2.5% respectively. The physiochemical parameters affect the quantity of biogas produce [6].
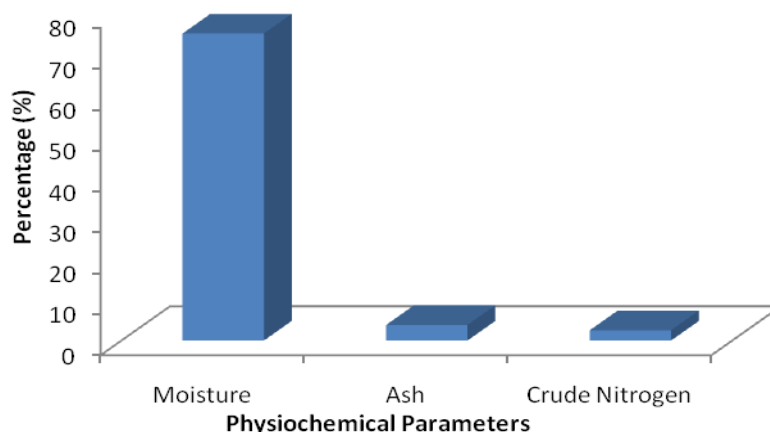

Figure 1. Physiochemical parameters of Cow dung

3.2 Temperature and pH of Digesters

Investigations reveal that in all the digesters under investigation, the pH value is a little neutrally within the first three days of operation (Figure 2), and then a fall from 6.0-6.8 was experienced. The fall might have been due to the activities of the acid forming bacteria involved in the digestion process for gas production. However, towards the end of the digestion process pH increased again to neutrality. This might have been due to the activities of the methanogenic bacteria, which were able to convert the product of acid forming bacteria to methane gas. This result is in agreement with the work of Fernando and Dangoggo (1986) and Maishanu et al. (1990)[7,8].

The effect of temperature reveals that throughout the period of experimentation it was within an ambient temperature of between 25^0C to 35^0C (Figure 3).This range of ambient temperature allows for proper digestion of the waste by the activities of microorganism within the digester and helps to enhance the smooth operations of the biogas digester. However, critical observation on the temperature effects reveals that lower amount of gas are produced in the morning until the temperature is increased above 30^0C.The effects of both the pH and temperature are initial factors that affect the level of Biogas.
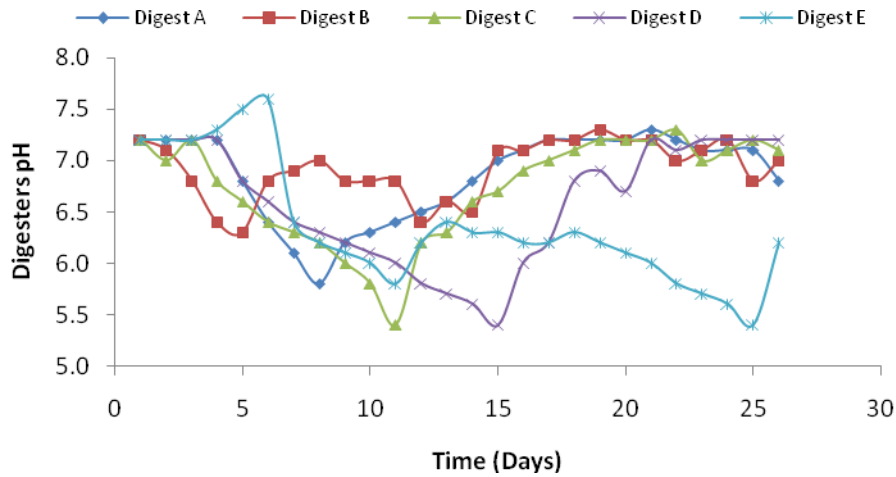
Figure 2. Changes in the pH of Digester materials during Digestion
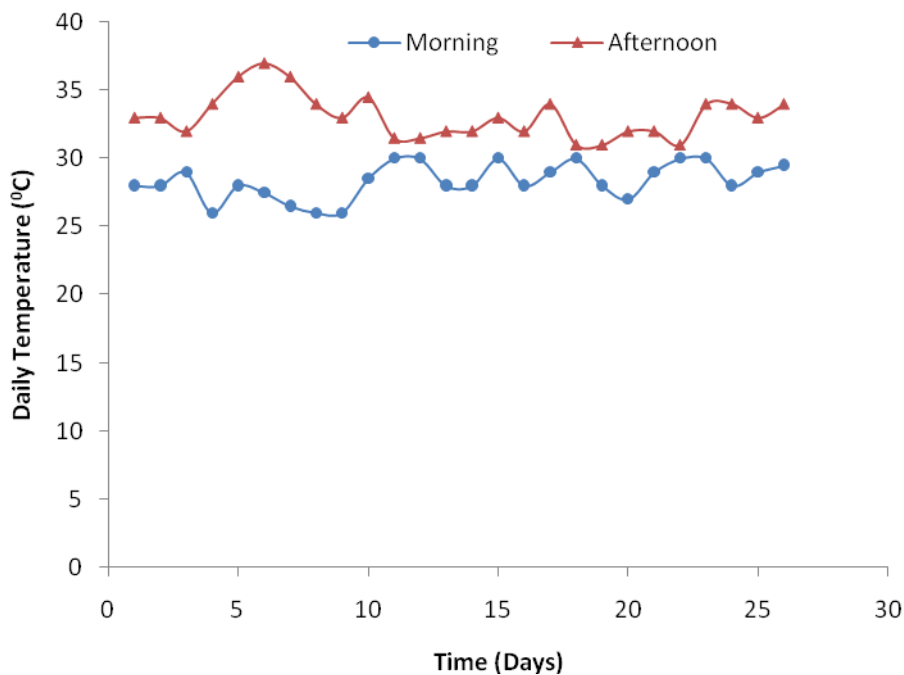
Figure 3. Daily Digester Temperature

3.3 Effect of Digester Size on Biogas Produced

Investigation revealed that in all digester sizes, during the first 6 days of operations, no gas was produced as shown in Figure 4. This might be as a result of the fact that the microorganism were in their formative stage for digestion process. However, from the 7th day, digesters C, D and E started producing some quantity of biogases (Figure 4). Thereafter gas produced was observed to increase with digester sizes. The peak for biogas production occurs between days 14 and 20 for Digesters D and E. While Digesters A and B maintained an average production of biogas. The maximum daily biogas production of 190 cm^3 occurred in Digester E on days 14 and 16. Digester A recorded the lowest biogas production of 5 cm^3 on day 25.

The effect of Digester sizes shows that Digester A with a volume of 250ml produced the least volume of 625cm^3 of biogas and Digester D and E, which has a volume of 2000 ml and 3000 ml, produced 2082 cm^3 and 2154cm^3 respectively as shown in Figure 5. The high volume of gas production in bigger digesters might be as a result of the fact that the materials were able to expose the greater surface area for rapid multiplications of the methaprogen for maximum utilization of the waste material for greater gas production.
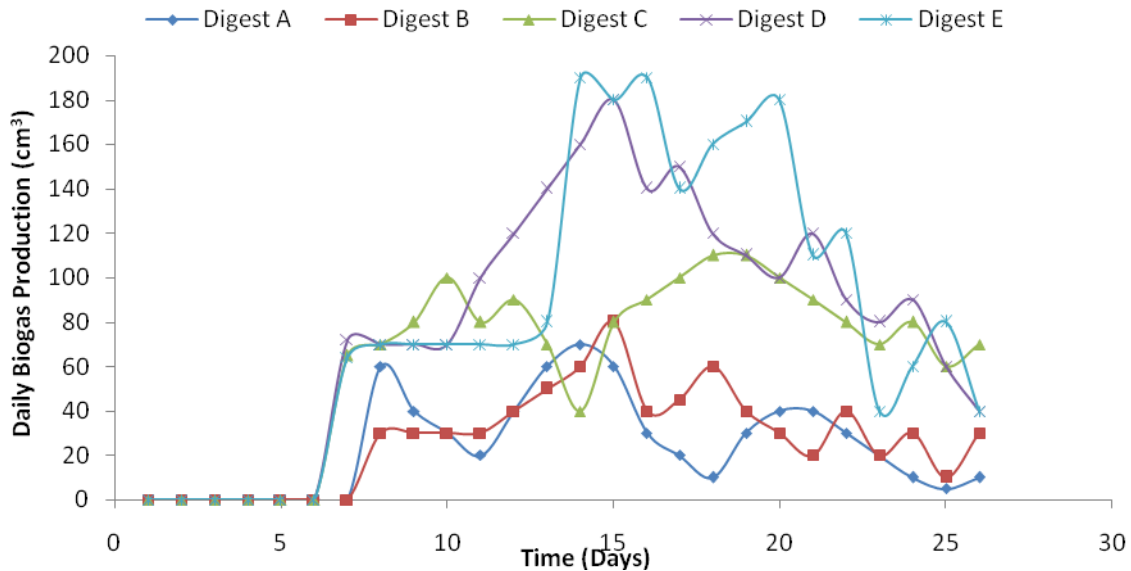
Figure 4. Daily Biogas Production
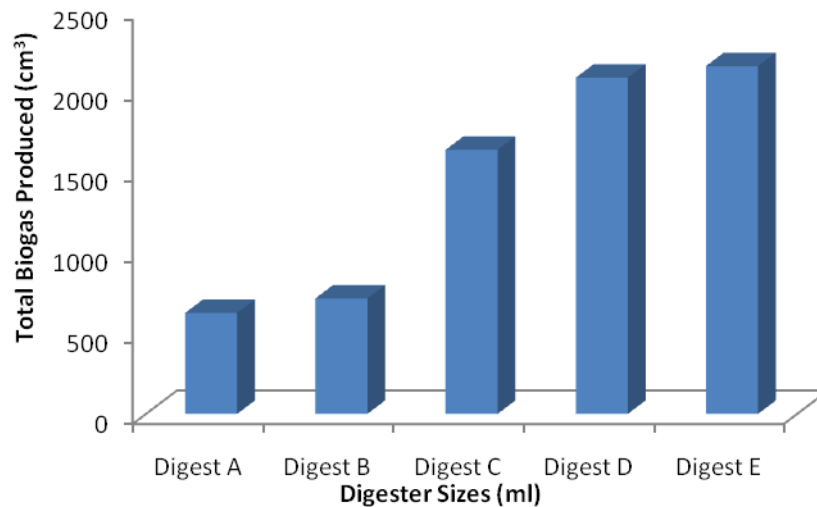
Figure 5: Total volume of gas produced by each digester

3.4 Optimal Biogas Production

Figure 6 shows the optimal biogas production for the digesters used. It can be seen that though the total volume of biogas produced increases with increase in digester sizes (Figure 5), the biogas produced per litre shows a different trend. The smallest Digester size of 250 ml produces the highest total biogas produced per litre of digester size of 2500 cm^{3}l^{-1}, while the largest digester size of 3000ml produces the smallest total biogas produced per litre of digester size of 718 cm^{3}l^{-1}. Digester C with a size of 1000 ml produces 1635 cm^{3}l^{-1}. The volume of total biogas produced per litre was higher for Digesters A and B, but lower for Digesters D and E. Digester C is the optimal digester size, above which the volume of total biogas produced per litre will fall below the total biogas produces (Figure 6). Depending on the cost of Digesters, if a higher total biogas production is required, Digester E should be used.
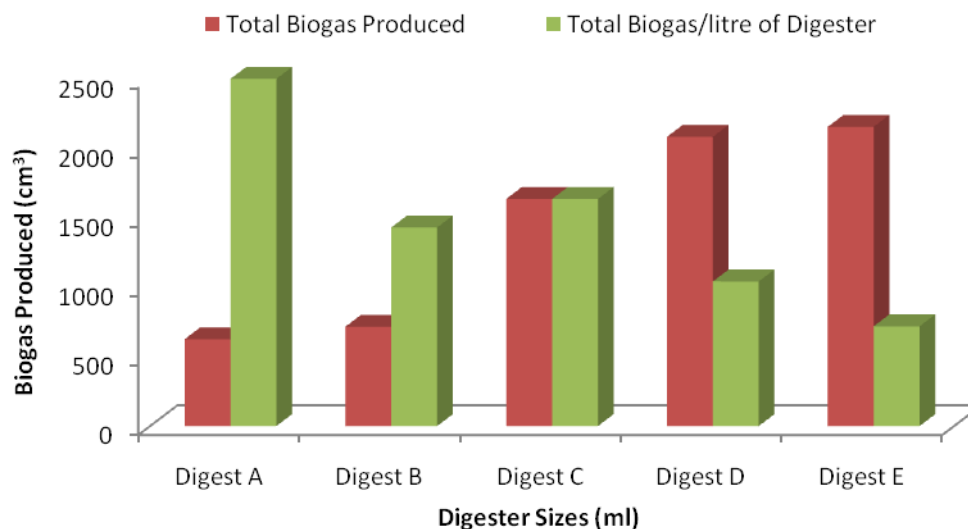
Figure 6.Biogas produced per litre of digester size

IV.   CONCLUSION

The experimental investigation of the effect of digester size on biogas production has been carried out. Experiments were carried out to produce biogas from different sizes of digester. 1.4 kg of cow dung was used to carry out the experiments. The temperature throughout the period of experimentation was within ambient temperature of 25 ^{0}C to 35 ^{0}C. It was observed that the pH values of the Digesters fluctuate between 5.4 and 7.6. This may be due to the activities of acid. Digesters A, B, C, D and E, with volumes of 250 ml, 500 ml, 1000 ml, 2000 ml and 3000 ml, produced a total biogas of 625 cm^3, 715 cm^3, 1635 cm^3, 2082 cm^3 and 2154 cm^3 respectively. Digester size is an important factor which has a direct effect on the quantity of gas produced. For the total biogas produced per litre of digester size, Digesters A, B, C, D and E, produces 2500 cm^{3}l^{-1}, 1430 cm^{3}l^{-1}, 1635 cm^{3}l^{-1}, 1041 cm^{3}l^{-1} and 718 cm^{3}l^{-1} respectively. Digester C is the optimal digester size, above which the volume of total biogas produced per litre will fall below the total biogas produces (Figure 6). Depending on the cost of Digesters, if a higher total biogas production is required, Digester E should be used.

REFERENCES

[1].   Peter Frost and Stephen Gilkinson, (2011). Interim Technical Report, 27 Months Performance Summary For Anaerobic Digestion Of Dairy Cow Slurry At AFBI Hillsborough.http://www.afbini.gov.uk/afbi-ad-hillsborough-27-months-june-11.pdf
[2].   Dioha, LJ. Gulma, M.A. and Nwagbo E.E. (1990). Isolations of Biogas products and effective utilization of biomass. Nigerian J, Solar Energy, Vol. 9 pp. 196-208.
[3].   Lawal A.K. (1997) `Biogas generation through ,anaerobic digestion of high pollution waste from industrial, domestic and other sources' A paper p resented at a 3 -day workshop on pollution control and challenges ahead held at the Akinrele Auditorium (FIIRO) between 6th -8th August 1997.
[4].   George A. M. (1992) `Biogas generation from piggery waste Seminar paper on Renewable Energy Sources.
[5].   Greo. J. R. (1976) Land disposal of waste' A necessary technology for environment management, National Solid Waste Management Association Technology. Ball 6, 10.
[6].   Rohjy, HabeebAjibola, Aduba, Joseph Junior, Manta, Ibrahim Haruna&Pamdaya, Yohanna, Development of Anaerobic Digester for the Production of Biogas using Poultry and Cattle Dung: A Case Study of Federal University of Technology Minna Cattle & Poultry Pen. International Journal of Life Sciences Vol.2. No.3. 2013. Pp. 139-149.
[7].   Fernando, C.E.0 and Dangoggo, S.M. (1996). As investigation of some parameters which affect the performance of biogas plants. Nigerian Journal Solar Energy 5:142 - 18.
[8].   Maishanu S. M. Musa U. and Sambo A.S. (1990). Biogas Technology the output of Sokoto Energy Research Centre. Nigerian Journal Solar Energy 7: 183-194.

Research Paper   Open Access

Pixel Based Off-line Signature Verification System

Anik Barua[1], Mohammad Minhazul Hoque[2], A.F.M. Nurul Goni[3],
Md. Ahsan Habib[4]

[1, 2]*(Department of ICT, Mawlana Bhashani Science and Technology University, Bangladesh)*
[3]*(Department of CSE, Mawlana Bhashani Science and Technology University, Bangladesh)*
[4]*(Associate Professor, Department of ICT, Mawlana Bhashani Science and Technology University, Bangladesh)*

ABSTRACT : *The verification of handwritten signatures is one of the oldest and the most popular authentication methods all around the world. As technology improved, different ways of comparing and analyzing signatures become more and more sophisticated. Since the early seventies, people have been exploring how computers can fully take over the task of signature verification and tried different methods. However, none of them is satisfactory enough and time consuming too. Therefore, our proposed pixel based off-line signature verification system is one of the fastest and easiest ways to authenticate any handwritten signature we have ever found. For signature acquisition, we have used scanner. Then we have divided the signature image into 2D array and calculated the hexadecimal RGB value of each pixel. After that, we have calculated the total percentage of matching. If the percentage of matching is more than 90, the signature is considered as valid otherwise invalid. We have experimented on more than 35 signatures and the result of our experiment is quite impressive. We have made the whole system web based so that the signature can be verified from anywhere. The average execution time for signature verification is only 0.00003545 second only.*

Keywords– *off-line signature, signature verification, pixel, execution time, pre-processing*

I.   INTRODUCTION

Signature Verification System (SVS) provides an organization with the ability to deliver a signature or customer image to an operator, enabling identification of the customer. Hand-written signature verification is the most easy-to-use and secure. As signatures continue to play an important role in financial, commercial and legal transactions, truly secured authentication becomes more and more crucial. For instance, financial institutions relay on them for account openings, withdrawals and transaction payments. A signature by an authorized person is considered to be the "seal of approval" and remains the most preferred means of authentication. On the other hand, the threats and monetary losses continue to rise dramatically. In particular check fraud has reached epidemical scope. In this regard, off-line signature verification is the most suited technique for reducing fraud through payment forms such as checks, fax money transactions and remote payment until now.

Handwritten Signature verification is a reliable method of verification since many years. This is natural since mankind has been signing our names as a form of identity verification for thousands of years from the great civilizations of ancient Egypt, China and Mesopotamia through to the current day. The way each individual writes and signs are something very personal and often quite distinctive. With technological advancements, rapid increments in computing power have taken place. This has led to the ability of computer machines performing complex and computationally intensive algorithms at a faster rate.

These developments have made the automated processes increasingly popular, targeted potentially at reducing manpower demands. Accurate and rapid programs for matching can thus be written to use the capabilities of these advancements. Until now, different computer based method have been tried to verify signature, but the results are not satisfactory especially in case of off-line handwritten signature verification

system. Besides this, different algorithms and methods have been tried, but they are very complex to implement and time consuming too. For this reason, we have developed a new and effective system for off-line signature verification. Our proposed pixel by pixel based method therefore a very efficient way which can verify the signature in a very short time. We have made the whole system online accessible with a minimum memory storage requirement with user friendly interfaces.

II. OFF-LINE AND ON-LINE SIGNATURE

Off-line signature is a 2-D image of the signature. Processing off-line is complex due to the absence of stable dynamic characteristics. Difficulty also lies in the fact that it is hard to segment signature strokes due to highly stylish and unconventional writing styles. The non-repetitive nature of variation of the signatures, because of age, illness, geographic location and perhaps to some extent the emotional state of the person, accentuates the problem. All these coupled together cause large intra-personal variation. A robust system has to be designed which should not only be able to consider these factors but also detect various types of forgeries.

On-line data records the motion of the stylus while the signature is produced, and includes location, and possibly velocity, acceleration and pen pressure, as functions of time. Online systems use this information captured during acquisition. These dynamic characteristics are specific to each individual and sufficiently stable as well as repetitive. The signature verification algorithms analyzes the shape, speed, stroke order, off-tablet motion, pen pressure and timing information captured during the act of signing. The technology is easy to explain and trust. The advantage that signature verification systems have over other types of technologies is that signatures are already accepted as the common method of identity verification.
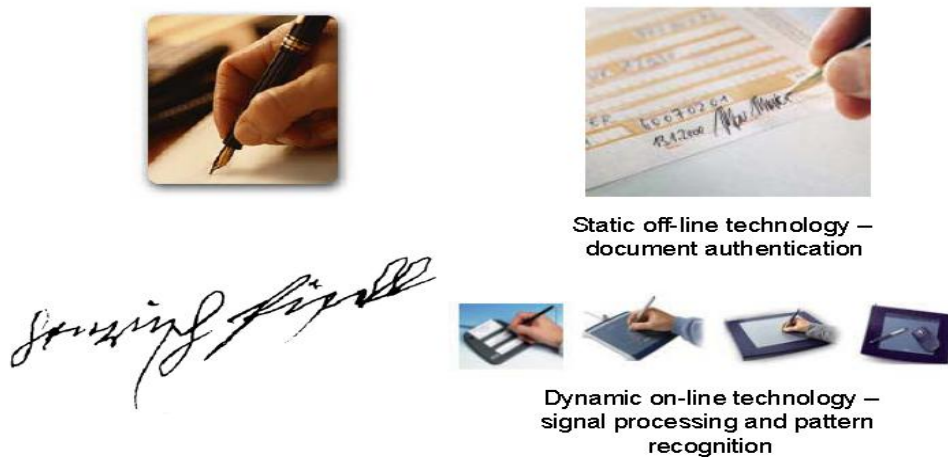

Figure 1: Classification of Signature (Off-line and On-line Signature)

III. EXISTING METHODS OF OFF-LINE SIGNATURE VERIFICATION

The major approaches to off-line signature verification systems are Hidden Markov Models (HMMs), Artificial Neural Networks (ANNs), Weighted Euclidean Distance Classifiers, Statistical Approach, Structural or Syntactic approach and Spectrum Analysis Approach.

In the statistical classifier approach, signature verification system consisted of three steps – the first step is to transform the original signatures using the identity and four Gabor transforms, the second step is to inter correlate the analyzed signature with the similarly transformed signatures of the learning database and then in the third step verification of the authenticity of signatures by fusing the decisions related to each transform. The proposed system allowed the rejection of 62.4% of the forgeries used for the experiments when 99% of genuine signatures were correctly recognized.

The template matching is the simplest and earliest but rigid approach to pattern recognition. Because of its rigidness, in some domains, this approach has a number of disadvantages. It may fail if the patterns are distorted due to the imaging process, viewpoint change or large interclass variations among the patterns as in the

case of signatures. It can detect casual forgeries from genuine signatures successfully. But it is not suitable for the verification between the genuine signature and skilled ones. The template matching method can be categorized into several forms such as graphics matching, stroke analysis and geometric feature extraction, depending on different features.

In the statistical approach, each pattern is represented in terms of the features and is viewed as a point in a d-dimensional space. Features should be chosen such a way that the pattern vectors belonging to different categories occupy compact and disjoint regions in a d-dimensional feature space. The effectiveness of the representation space (feature set) is determined by how well patterns from different classes can be separated. Hidden Markov Model (HMM), Bayesian these are some statistical approach commonly used in pattern recognition. They can detect causal forgeries as well as skilled and traced forgeries from the genuine ones. Hidden Markov Modeling (HMM) technique is to build a reference model for each local feature. The verification phase had three layers of statistical techniques. In the first layer, HMM-based log-likelihood probability match score was computed. In the second layer this score was mapped into soft boundary ranges of acceptance or rejection through the use of z-score analysis and normalization function. Then Bayesian inference technique was used for deciding acceptance or rejection of the given signature sample. For random and skilled forgeries FAR were 22% and 37% respectively.

Structural approaches mainly related to string, graph, and tree matching techniques and are generally used in combination with other techniques. When the signature image is considered as a whole entity, the structural approach is used for the signature verification. It shows good performance detecting genuine signatures and forgeries. But this approach may demand a large training set and very large computational efforts.

Neural networks are massively parallel computing systems consisting of an extremely large number of simple processors with many interconnections. The main characteristics of neural networks are that they have the ability to learn complex nonlinear input-output relationships, use sequential training procedures and adapt themselves to the data. Neural Networks approach offers several advantages such as, unified approaches for feature extraction and classification and flexible procedures for finding good, moderately nonlinear solutions. When it is used in off-line signature verification, it also shows reasonable performance. To improve the efficiency of the signature verification systems, researchers have tried different methods with various approaches. Some of them have employed two or three expert systems that evaluate the signature in two or three different ways and verify whether it is genuine or forgery.

IV. OUR PROPOSED ALGORITHM

In the past decade, there have been ample amount of research in the field of pattern recognition and also in the field of offline signature verification. A bunch of solutions has been introduced, to overcome the limitations of off-line signature verification and to compensate for the loss of accuracy. Among them we have implemented a pixel based matching algorithm for the verification of signature which is an effective way of off-line signature verification.
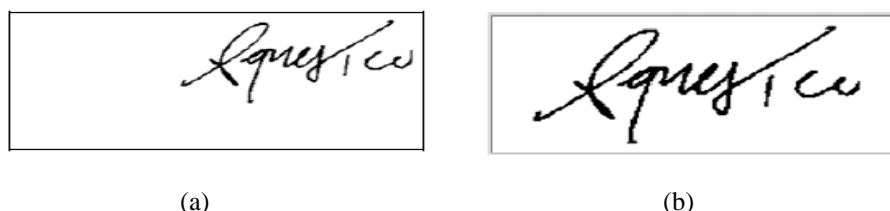

(a)   (b)

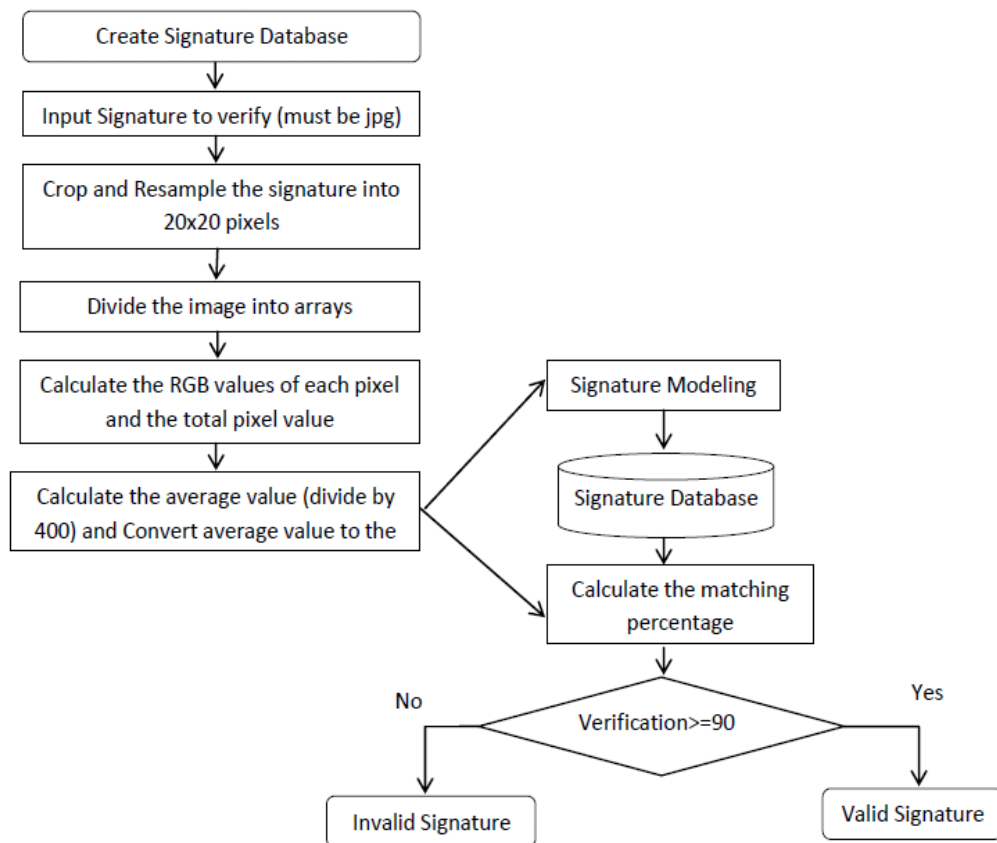Figure 2: (a) Before pre-processing   (b) After pre-processing

Figure 3: Algorithmic Flowchart

V.   SIMULATION AND PERFORMANCE ANALYSIS

For off-line signature verification system we have used PHP for make the whole system accessible online and MySQL for database. The page below is used to insert signatures into the database accessible only by the administrators. They can insert client's valid signature in the database.
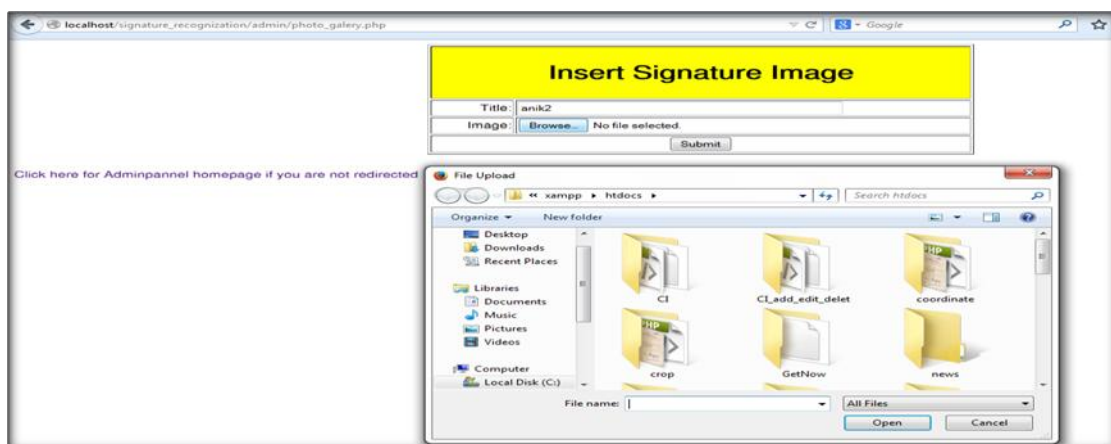

Figure 4: Insert Client's Signature

The page is used to show signatures inside the database. Administrators will get a brief overview about the system and database from this page. They can also delete any signature from database if necessary. Most importantly, this is a part of our data set we have experimented.

Figure 5: Database of Client's Signature

The page is the most important page because we can verify any signature from this page. At first, administrators have to select the signature they want to verify. Then after clicking on the verification button the page will automatically show the verification time with a very short time. The whole process is very easy and effective at the same time.
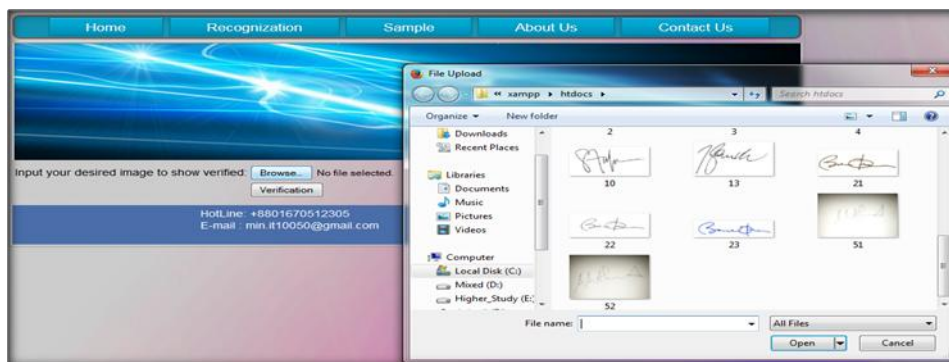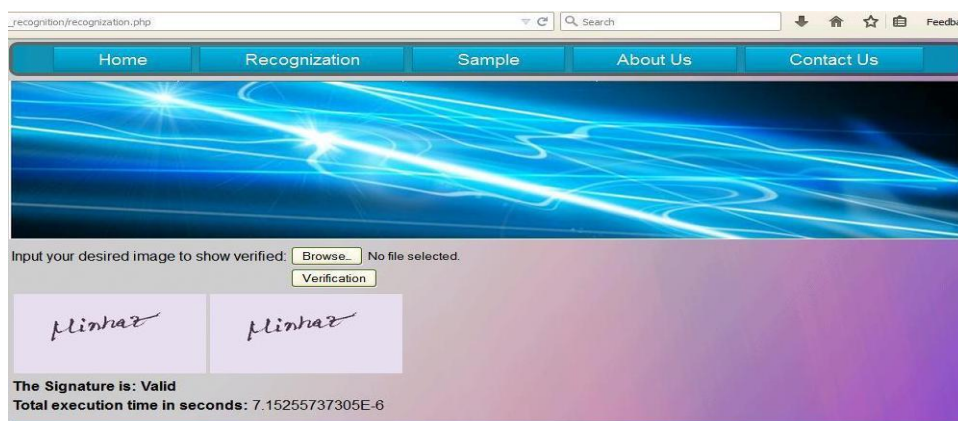

Figure 6: Verification of Signature

Figure 7: Verification Result of Signature

For verification we can compare any signature with any signature from database. We have experiment this method for more than 35 signatures for verification and the result was quite satisfactory. In performance evolution we have given more priority on accuracy and system execution time. Among them, some of the results are shown below. A signature is valid when the matching percentage is at least 90, otherwise it is invalid. Our system average execution time is 0.00003545 second only.

Figure 8: Experimental Result

VI.   CONCLUSION

Handwritten Signature verification is a reliable method of verification. With the technological advancement, researchers are trying to make the result by computer based automated process. Although many techniques have already tried but none of them are fully satisfactory and mostly complex at least in case of off-line signature verification. Therefore, our proposed pixel based signature authentication is an easy and effective way with user friendly interface. Our system execution time of verification is 0.00003545 second only. However, in our present system, the input signature must be scanned and is applicable for some specific format only. Therefore, extra hardware cost is needed and similarity rate may vary for different color of signature. As a solution different algorithmic process may be integrated together.

REFERENCES

[1]   Bence andras kovari, *Models and algorithms in off-line, feature-based, handwritten signature verification*, doctoral diss., Budapest University of Technology and Economics, Budapest, 2013
[2]   Ibrahim S.I. Abuhaiba, Offline Signature Verification Using Graph Matching, Turkish Journal of Electrical Engineering and Computer Sciences, 15(1), 2007, 89-104
[3]   Ashwin C S, Harihar V, Karthick G, Karthik A, Rangarajan K R, PIXBAS "Pixel Based Offline Signature Verification", Advanced in Information Sciences and Service Sciences, 2(3), 2010, 1-4
[4]   R. Sabourin, R. Plamondon, G. Lorette, Offline identification with handwritten signature images: survey and perspectives, Structured Image Analysis, Springer, New York, 1992, pp 219-234
[5]   M. Hanmandlu, K.R. Murali Mohan, S. Chakraborty, G. Garg, Fuzzy modeling based signature verification system, *Proc. 6th International Conference on Document Analysis and Recognition*, USA, 2001, pp.110-114
[6]   M. Ammar, Y. Yochida, T. Fukumura, A new effective approach for offline verification of signature by using pressure features, *Proc. International Conference on Pattern Recognition*, 1986, pp 566-599
[7]   Edson J. R. Justino, Abdenaim El Yacoubi, Flávio Bortolozzi, Robert Sabourin, *An off-line Signature Verification System Using Hidden MarkovModel and Cross-validation*, Pontifícia Universidade Católica do Paraná, Brasil
[8]   A. Vinoth, V. Sujathabai, A Pixel Based Signature Authentication System, International Journal of Innovative Technology and Exploring Engineering, 2(6), 2013
[9]   Madhuri Yadav, Alok Kumar, Tushar Patnaik, Bhupendra Kumar, A Survey on Offline Signature Verification, International Journal of Engineering and Innovative Technology, 2(7), 2013, 337-340
[10]   B. Kovari, G. Kiss, and I. Albert, Stroke Matching for Off-line Signature Verification based on Bounding Rectangles, *Proc. Of the 23rd IEEE International Symposium on Computer and Information Sciences*, 2008
[11]   Abu Shamim Mohammad Arif, Md. Sabbir Hussain, Md. Rafiqul Islam, S. A. Ahsan Rajon And Abdullah, Al Nahid, An Approach for Off-Line Signature Verification System Using Peak And Curve Comparison, International Journal of Computer and Information Technology, 1(1), 2010, 24-29